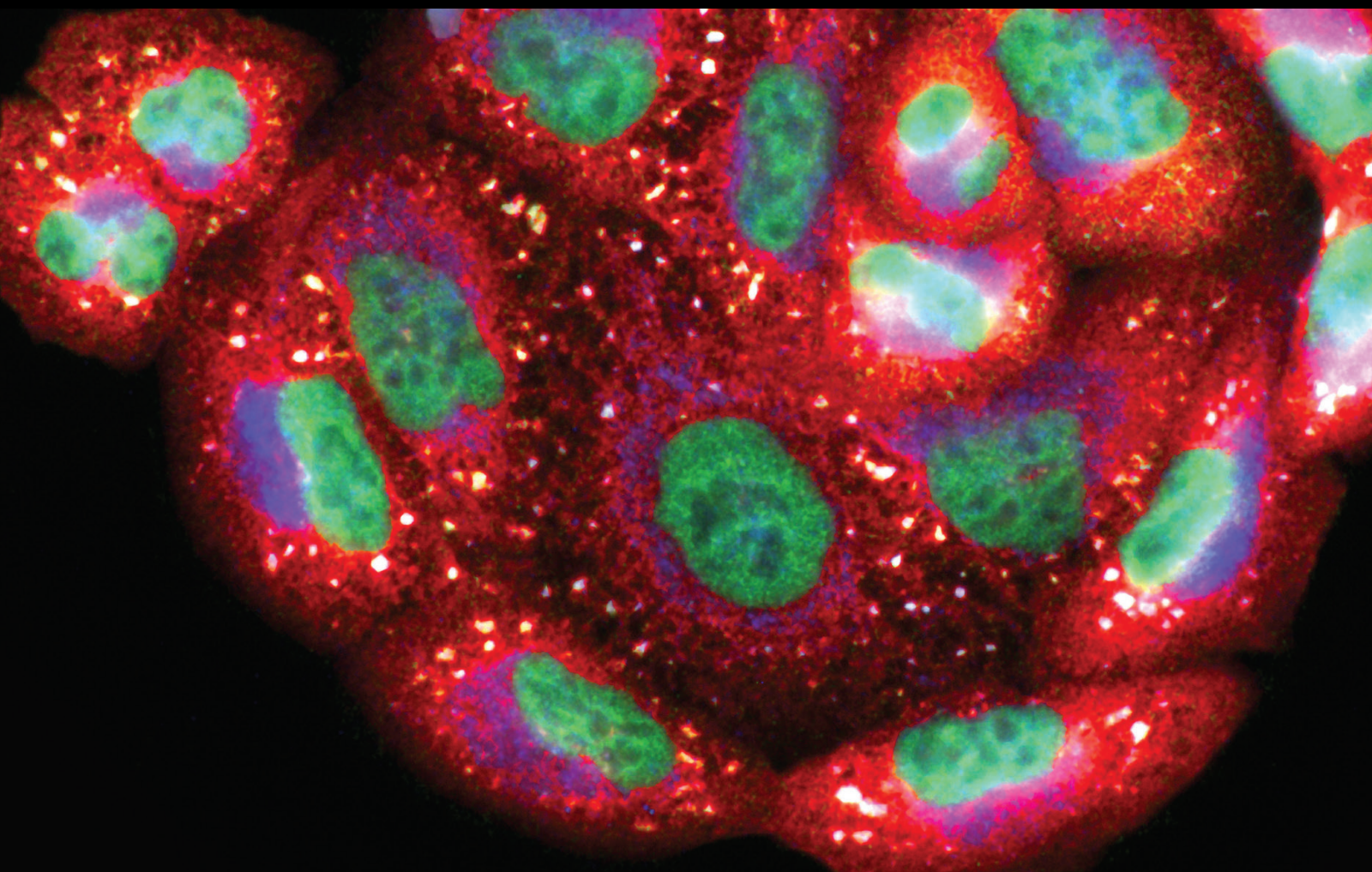


Biochemistry and Biology of Endogenous and Exogenous Sulfur Compounds in the Modulation of Reactive Oxygen Species Metabolism

Lead Guest Editor: Luciana Mosca

Guest Editors: Alessia Baseggio Conrado, Teruo Miyazaki, Kyoung Soo Kim, and Mario Fontana





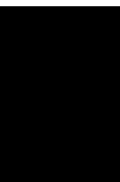
**Biochemistry and Biology of Endogenous
and Exogenous Sulfur Compounds in the
Modulation of Reactive Oxygen Species
Metabolism**

Oxidative Medicine and Cellular Longevity

**Biochemistry and Biology of
Endogenous and Exogenous Sulfur
Compounds in the Modulation of
Reactive Oxygen Species Metabolism**

Lead Guest Editor: Luciana Mosca

Guest Editors: Alessia Baseggio Conrado, Teruo
Miyazaki, Kyoung Soo Kim, and Mario Fontana



Copyright © 2020 Hindawi Limited. All rights reserved.

This is a special issue published in "Oxidative Medicine and Cellular Longevity" All articles are open access articles distributed under the Creative Commons Attribution License, which permits unrestricted use, distribution, and reproduction in any medium, provided the original work is properly cited.

Chief Editor

Jeannette Vasquez-Vivar, USA

Associate Editors

Amjad Islam Aqib, Pakistan
Angel Catalá , Argentina
Cinzia Domenicotti , Italy
Janusz Gebicki , Australia
Aldrin V. Gomes , USA
Vladimir Jakovljevic , Serbia
Thomas Kietzmann , Finland
Juan C. Mayo , Spain
Ryuichi Morishita , Japan
Claudia Penna , Italy
Sachchida Nand Rai , India
Paola Rizzo , Italy
Mithun Sinha , USA
Daniele Vergara , Italy
Victor M. Victor , Spain

Academic Editors

Ammar AL-Farga , Saudi Arabia
Mohd Adnan , Saudi Arabia
Ivanov Alexander , Russia
Fabio Altieri , Italy
Daniel Dias Rufino Arcanjo , Brazil
Peter Backx, Canada
Amira Badr , Egypt
Damian Bailey, United Kingdom
Rengasamy Balakrishnan , Republic of Korea
Jiaolin Bao, China
Ji C. Bihl , USA
Hareram Birla, India
Abdelhakim Bouyahya, Morocco
Ralf Braun , Austria
Laura Bravo , Spain
Matt Brody , USA
Amadou Camara , USA
Marcio Carochio , Portugal
Peter Celec , Slovakia
Giselle Cerchiaro , Brazil
Arpita Chatterjee , USA
Shao-Yu Chen , USA
Yujie Chen, China
Deepak Chhangani , USA
Ferdinando Chiaradonna , Italy

Zhao Zhong Chong, USA
Fabio Ciccarone, Italy
Alin Ciobica , Romania
Ana Cipak Gasparovic , Croatia
Giuseppe Cirillo , Italy
Maria R. Ciriolo , Italy
Massimo Collino , Italy
Manuela Corte-Real , Portugal
Manuela Curcio, Italy
Domenico D'Arca , Italy
Francesca Danesi , Italy
Claudio De Lucia , USA
Damião De Sousa , Brazil
Enrico Desideri, Italy
Francesca Diomede , Italy
Raul Dominguez-Perles, Spain
Joël R. Drevet , France
Grégory Durand , France
Alessandra Durazzo , Italy
Javier Egea , Spain
Pablo A. Evelson , Argentina
Mohd Farhan, USA
Ioannis G. Fatouros , Greece
Gianna Ferretti , Italy
Swaran J. S. Flora , India
Maurizio Forte , Italy
Teresa I. Fortoul, Mexico
Anna Fracassi , USA
Rodrigo Franco , USA
Juan Gambini , Spain
Gerardo García-Rivas , Mexico
Husam Ghanim, USA
Jayeeta Ghose , USA
Rajeshwary Ghosh , USA
Lucia Gimeno-Mallench, Spain
Anna M. Giudetti , Italy
Daniela Giustarini , Italy
José Rodrigo Godoy, USA
Saeid Golbidi , Canada
Guohua Gong , China
Tilman Grune, Germany
Solomon Habtemariam , United Kingdom
Eva-Maria Hanschmann , Germany
Md Saquib Hasnain , India
Md Hassan , India

Tim Hofer , Norway
John D. Horowitz, Australia
Silvana Hrelia , Italy
Dragan Hrnčić, Serbia
Zebo Huang , China
Zhao Huang , China
Tariq Hussain , Pakistan
Stephan Immenschuh , Germany
Norsharina Ismail, Malaysia
Franco J. L. , Brazil
Sedat Kacar , USA
Andleeb Khan , Saudi Arabia
Kum Kum Khanna, Australia
Neelam Khaper , Canada
Ramoji Kosuru , USA
Demetrios Kouretas , Greece
Andrey V. Kozlov , Austria
Chan-Yen Kuo, Taiwan
Gaocai Li , China
Guoping Li , USA
Jin-Long Li , China
Qiangqiang Li , China
Xin-Feng Li , China
Jialiang Liang , China
Adam Lightfoot, United Kingdom
Christopher Horst Lillig , Germany
Paloma B. Liton , USA
Ana Lloret , Spain
Lorenzo Loffredo , Italy
Camilo López-Alarcón , Chile
Daniel Lopez-Malo , Spain
Massimo Lucarini , Italy
Hai-Chun Ma, China
Nageswara Madamanchi , USA
Kenneth Maiese , USA
Marco Malaguti , Italy
Steven McAnulty, USA
Antonio Desmond McCarthy , Argentina
Sonia Medina-Escudero , Spain
Pedro Mena , Italy
V́ctor M. Mendoza-Núñez , Mexico
Lidija Milkovic , Croatia
Alexandra Miller, USA
Sara Missaglia , Italy

Premysl Mladenka , Czech Republic
Sandra Moreno , Italy
Trevor A. Mori , Australia
Fabiana Morroni , Italy
Ange Mouithys-Mickalad, Belgium
Iordanis Mourouzis , Greece
Ryoji Nagai , Japan
Amit Kumar Nayak , India
Abderrahim Nemmar , United Arab Emirates
Xing Niu , China
Cristina Nocella, Italy
Susana Novella , Spain
Hassan Obied , Australia
Pál Pacher, USA
Pasquale Pagliaro , Italy
Dilipkumar Pal , India
Valentina Pallottini , Italy
Swapnil Pandey , USA
Mayur Parmar , USA
Vassilis Paschalis , Greece
Keshav Raj Paudel, Australia
Ilaria Peluso , Italy
Tiziana Persichini , Italy
Shazib Pervaiz , Singapore
Abdul Rehman Phull, Republic of Korea
Vincent Pialoux , France
Alessandro Poggi , Italy
Zsolt Radak , Hungary
Dario C. Ramirez , Argentina
Erika Ramos-Tovar , Mexico
Sid D. Ray , USA
Muneeb Rehman , Saudi Arabia
Hamid Reza Rezvani , France
Alessandra Ricelli, Italy
Francisco J. Romero , Spain
Joan Roselló-Catafau, Spain
Subhadeep Roy , India
Josep V. Rubert , The Netherlands
Sumbal Saba , Brazil
Kunihiro Sakuma, Japan
Gabriele Saretzki , United Kingdom
Luciano Saso , Italy
Nadja Schroder , Brazil



Anwen Shao , China
Iman Sherif, Egypt
Salah A Sheweita, Saudi Arabia
Xiaolei Shi, China
Manjari Singh, India
Giulia Sita , Italy
Ramachandran Srinivasan , India
Adrian Sturza , Romania
Kuo-hui Su , United Kingdom
Eisa Tahmasbpour Marzouni , Iran
Hailiang Tang, China
Carla Tatone , Italy
Shane Thomas , Australia
Carlo Gabriele Tocchetti , Italy
Angela Trovato Salinaro, Italy
Rosa Tundis , Italy
Kai Wang , China
Min-qi Wang , China
Natalie Ward , Australia
Grzegorz Wegrzyn, Poland
Philip Wenzel , Germany
Guangzhen Wu , China
Jianbo Xiao , Spain
Qiongming Xu , China
Liang-Jun Yan , USA
Guillermo Zalba , Spain
Jia Zhang , China
Junmin Zhang , China
Junli Zhao , USA
Chen-he Zhou , China
Yong Zhou , China
Mario Zoratti , Italy

Contents




Chemistry and Biochemistry of Sulfur Natural Compounds: Key Intermediates of Metabolism and Redox Biology

Antonio Francioso , Alessia Baseggio Conrado , Luciana Mosca , and Mario Fontana 
Review Article (27 pages), Article ID 8294158, Volume 2020 (2020)



Allylmethylsulfide, a Sulfur Compound Derived from Garlic, Attenuates Isoproterenol-Induced Cardiac Hypertrophy in Rats

Soheb Anwar Mohammed, Bugga Paramesha, Yashwant Kumar, Ubaid Tariq, Sudheer Kumar Arava , and Sanjay Kumar Banerjee 
Research Article (15 pages), Article ID 7856318, Volume 2020 (2020)



Taurine Attenuates Carcinogenicity in Ulcerative Colitis-Colorectal Cancer Mouse Model

Guifeng Wang, Ning Ma , Feng He, Shosuke Kawanishi , Hatasu Kobayashi, Shinji Oikawa, and Mariko Murata 
Research Article (7 pages), Article ID 7935917, Volume 2020 (2020)

DpdtC-Induced EMT Inhibition in MGC-803 Cells Was Partly through Ferritinophagy-Mediated ROS/p53 Pathway

Jiankang Feng, Cuiping Li, Ruifang Xu, Yongli Li , Qi Hou, Rui Feng, Senye Wang, Lei Zhang, and Changzheng Li 
Research Article (14 pages), Article ID 9762390, Volume 2020 (2020)





Hydrogen Sulfide as a Potential Alternative for the Treatment of Myocardial Fibrosis

Se Chan Kang , Eun-Hwa Sohn, and Sung Ryul Lee 
Review Article (14 pages), Article ID 4105382, Volume 2020 (2020)




Oxidative Modifications in Advanced Atherosclerotic Plaques: A Focus on *In Situ* Protein Sulfhydryl Group Oxidation

Antonio Junior Lepedda , and Marilena Formato 
Review Article (7 pages), Article ID 6169825, Volume 2020 (2020)

Products of Sulfide/Selenite Interaction Possess Antioxidant Properties, Scavenge Superoxide-Derived Radicals, React with DNA, and Modulate Blood Pressure and Tension of Isolated Thoracic Aorta

Marian Grman, Anton Misak, Lucia Kurakova, Vlasta Brezova, Sona Cacanyiova , Andrea Berenyiova, Peter Balis , Lenka Tomasova, Ammar Kharm, Enrique Domínguez-Álvarez, Miroslav Chovanec , and Karol Ondrias 
Research Article (15 pages), Article ID 9847650, Volume 2019 (2019)

L-Cystathionine Protects against Homocysteine-Induced Mitochondria-Dependent Apoptosis of Vascular Endothelial Cells

Xiuli Wang, Yi Wang, Lulu Zhang, Da Zhang, Lu Bai, Wei Kong, Yaqian Huang , Chaoshu Tang, Junbao Du , and Hongfang Jin 
Research Article (13 pages), Article ID 1253289, Volume 2019 (2019)

Review Article

Chemistry and Biochemistry of Sulfur Natural Compounds: Key Intermediates of Metabolism and Redox Biology

Antonio Francioso ^{1,2}, Alessia Baseggio Conrado ¹, Luciana Mosca ¹
and Mario Fontana ¹

¹Department of Biochemical Sciences “A. Rossi Fanelli”, Sapienza University of Rome, 00185 Rome, Italy

²Department of Organic Chemistry, Instituto Universitario de Bio-Organica Antonio González, University of La Laguna, La Laguna, 38296 Tenerife, Spain

Correspondence should be addressed to Luciana Mosca; luciana.mosca@uniroma1.it
and Mario Fontana; mario.fontana@uniroma1.it

Received 10 April 2020; Revised 28 June 2020; Accepted 29 July 2020; Published 30 September 2020

Academic Editor: Giuseppe Cirillo

Copyright © 2020 Antonio Francioso et al. This is an open access article distributed under the Creative Commons Attribution License, which permits unrestricted use, distribution, and reproduction in any medium, provided the original work is properly cited.

Sulfur contributes significantly to nature chemical diversity and thanks to its particular features allows fundamental biological reactions that no other element allows. Sulfur natural compounds are utilized by all living beings and depending on the function are distributed in the different kingdoms. It is no coincidence that marine organisms are one of the most important sources of sulfur natural products since most of the inorganic sulfur is metabolized in ocean environments where this element is abundant. Terrestrial organisms such as plants and microorganisms are also able to incorporate sulfur in organic molecules to produce primary metabolites (e.g., methionine, cysteine) and more complex unique chemical structures with diverse biological roles. Animals are not able to fix inorganic sulfur into biomolecules and are completely dependent on preformed organic sulfur compounds to satisfy their sulfur needs. However, some higher species such as humans are able to build new sulfur-containing chemical entities starting especially from plants' organosulfur precursors. Sulfur metabolism in humans is very complicated and plays a central role in redox biochemistry. The chemical properties, the large number of oxidation states, and the versatile reactivity of the oxygen family chalcogens make sulfur ideal for redox biological reactions and electron transfer processes. This review will explore sulfur metabolism related to redox biochemistry and will describe the various classes of sulfur-containing compounds spread all over the natural kingdoms. We will describe the chemistry and the biochemistry of well-known metabolites and also of the unknown and poorly studied sulfur natural products which are still in search for a biological role.

1. Introduction

In living organisms, sulfur is one of the most fundamental elements and the seventh most abundant mineral in the human body. Sulfur belongs to chalcogens, elements of the 16 group of the periodic table, which display the awesome characteristic of having a variety of redox states and redox potentials allowing them to form interchalcogen bonds and atom exchange reactions, giving rise to a vast number of sulfur species that take part in biological processes. Noteworthy, the bulk of biomolecules consists only of carbon, hydrogen, nitrogen, and oxygen atoms, and the presence of sulfur

accounts for the distinctive properties of sulfur compounds. Actually, sulfur and oxygen belong to the same group in the periodic table; however, Met and Cys analogues with the sulfur atom replaced by oxygen do not serve the same function. Sulfur has unique characteristics that differentiate it from oxygen. The increased atomic size confers to sulfur a lower electronegativity than oxygen. The thioether (R_2S) moiety of Met is more reactive than the analogue ether (R_2O). Thioethers can form sulfonium ions (R_3S^+) by donating electrons to other organic species thanks to their ability to sink electrons and stabilize a negative charge on a neighboring carbon [1]. These compounds undergo sequential oxidation

to sulfoxides (R_2SO) and sulfones (R_2SO_2), conferring to these derivatives novel unexpected roles. In cell metabolism, a sulfonium compound such as S-adenosylmethionine (SAM) mediates most biochemical methylation reactions. It is doubtful whether other amino acid derivatives or other “-onium” compounds could play this role: quaternary ammonium compounds are unable to effectively methylate acceptor compounds, and oxonium compounds, such as a hypothetical oxygen analogue of SAM, would produce such a powerful methylating agent that it would methylate cellular nucleophiles without the need for an enzyme [2, 3]. The sulfur compounds contained in food are amino acids or vitamins including methionine (Met), cysteine (Cys), homocysteine (HCy), cystine (Cys-Cys), taurine (Tau), lipoic acid, thiamine, and biotin as well as the glucosinolates and allylic sulfur compounds that are contained in cabbage and cauliflower (cruciferous vegetables). The amount of sulfur compounds in food greatly varies depending on the type of food: 8% for egg white, 5% for beef as well as for chicken and fish, and 4% for dairy products and plant proteins [4]. The recommended dietary allowance (RDA) for sulfur has been estimated to be 13–14 mg/kg of body weight per day. Considering 70 kg weight for a person, not affected by sex or age, this means 1.1 g of sulfur per day [5–9]. Among the sulfur compounds ingested with food, Met and Cys represent the largest part and are extensively metabolized by the organisms [3]. The Met/Cys ratio in food is 3/1 for dairy products, fish, and meat and 4/3 for eggs and plant products such as soybeans [10, 11]. Met is an essential amino acid assumed by diet and cannot be synthesized contrary to nonessential Cys. Numerous key metabolic intermediates such as HCy, Cys-Cys, and Tau are generated by these sulfur amino acids [4, 12]. Throughout the transsulfuration pathway, Met can be converted to Cys with a yield depending on cell needs. Interestingly, both these two sulfur amino acids cannot be stored as such in the body but cysteine can be stocked as glutathione (GSH) and sulfur excess is promptly excreted in the urine after its oxidation to sulfate or reabsorbed if required [13].

In this review, we will explore the fundamental aspects of sulfur metabolism and redox biochemistry and the large pool of naturally occurring sulfur-containing compounds. We will focus on the chemistry and the biochemistry of exogenous and endogenous sulfur metabolites. We will underline the importance of well-known and widely studied molecules, and we will also focus on unknown and poorly studied sulfur natural products whose biological role is still a mystery and needs to be investigated [14, 15].

2. How Sulfur Comes to “Life”

Sulfur, as well as nitrogen, needs to be fixed in organic molecules with a process part of the so-called biogeochemical “sulfur cycle.” Before being incorporated into the essential organic molecules, sulfur needs to be fixed with carbon in an organic skeleton. A significant part of sulfur fixation starts in the oceans that represent a major reservoir of sulfur on Earth, with large quantities in the form of dissolved sulfate and sedimentary minerals. Inorganic sulfur, mostly SO_4^{2-}

coming from gypsum and from pyrite oxidation, is fixed by algae in the ocean upper water column to dimethylsulfonio-propionate (DMSP) [16]. DMSP produced by algae is utilized by a diverse assemblage of microbes, leading to the production of methanethiol (MeSH) and dimethylsulfide (DMS) [17, 18] (Figure 1). These compounds are highly volatile and represent a significant amount of sulfur transfer from the oceans to the atmosphere and ultimately to land. On the other hand, volcanic emissions are the main natural sources of on-land sulfur release to the atmosphere in which furthermore is oxidized via photochemical processes to various sulfur oxidation state species [19]. SO_4^{2-} , MeSH, and DMS are the most important precursors of sulfur organic compounds synthesized by plants and microorganisms [20] (Figure 1).

Cys is the precursor (thiol-reduced sulfur donor) of most organic sulfur-containing molecules in the plant metabolome. Sulfur fixation is strictly related to Cys biosynthesis in which through different enzymatic steps, oxidized sulfate, alkane sulfates, or thiosulfate are reduced to sulfide and subsequently incorporated to Cys upon Ser activation (O-acetylserine) [21]. Plants are also able to produce a large variety of sulfur-containing products with interesting chemical, biochemical, and pharmacological features [22–25].

One of the principal ways to introduce inorganic sulfur in metabolism is via SO_4^{2-} incorporation in adenosine phosphosulfate (APS). APS is the crucial transporter of inorganic sulfur and serves as a central metabolic route for Cys biosynthesis (Figure 2) [26].

Among plant volatile organic compounds, the class of volatile sulfur compounds (VSCs) represents an important tool for plant physiology. Vegetables are one of the sources in diet for the uptake of Met and Cys, and plants possess specific metabolic pathways for the production of diverse sulfur-containing organic compounds with different important roles (defense, signaling, and communication) [27–29].

In mammals, sulfur occurs mainly in proteins as Cys and Met but also in coenzymes such as Coenzyme A (CoA), biotin, lipoic acid, and thiamine (Figure 3).

It is also common in the form of iron-sulfur clusters in metalloproteins and in bridging ligands as in cytochromes. Animals are completely dependent on preformed organic sulfur compounds to satisfy their sulfur needs [3]. Primary plant metabolism produces Met that is the essential source of sulfur for mammals and higher species such as humans. However, some higher species such as humans are able to build new sulfur-containing chemical entities starting from plants’ sulfur precursors. Sulfur metabolism in humans is very complicated and plays a central role in redox biochemistry. The large number of oxidation states that this element can display makes it ideal for redox biological reaction and electron transfers (e.g., Fe-S clusters in mitochondrial proteins). Also, the biosynthesis of particular sulfur metabolites is a unique feature in some species from the animal kingdom and seems to occur via diverse biochemical pathways evolutionarily far from plant sulfur metabolism [30].

The sulfur cycle, like the nitrogen cycle, is extremely important and promoted by specific prokaryotes. Most of the organic sulfur coming from this cycle is generated in

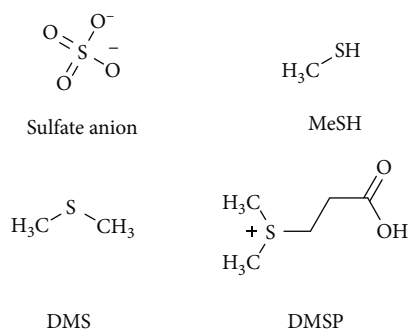


FIGURE 1: Inorganic and organic forms of entry for sulfur into biosynthetic metabolism of plants and microorganisms.

the oceanic environment by microorganisms that can convert and incorporate inorganic sulfur in organic molecules necessary to satisfy the sulfur needs of all the other living beings. The metabolism of organic sulfur is at the same time a key component of the global sulfur cycle. Phototrophic and diazotrophic marine organisms such as particular marine cyanobacteria and red algae are able to use sulfur compounds as electron acceptors or donors in sulfate/sulfur reduction and oxidation [31].

3. Naturally Occurring Organosulfur Compounds in Terrestrial Plants and Marine Organisms

3.1. Natural Products from the Marine World. Marine organisms are a relatively recent successful source of novel natural bioactive compounds due also to the presence of diverse still not explored habitats and ecosystems. Several papers in the last decades reported the pharmacological activities of different compounds such as ziconotide for the management of severe chronic pain and eribulin mesylate, an antimetastatic breast cancer, both successful derivatives of compounds coming from the “marine world” [32].

3.1.1. Sulfurous Amines and Amino Acids. Marine microorganisms and algae are able to produce a wide range of sulfur-containing natural products, also because of the abundance of this element in the marine environment. Most of the biosynthetic routes and the biological significance of these compounds are still unknown [33]. The most ubiquitous group is that of sulfur amines and amino acids. These compounds have been found in a variety of marine organisms including algae, gorgonians, clams, and fishes, and they include Met, Cys, methionine sulfone, methionine N-methyl sulfoxide, and several aliphatic sulfonated amines (Figure 4). Studies performed on deep sea animals have detected also a high level of hypotaurine (Htau) as well as thiotaurine (Ttau) (Figure 4) [34].

These latter two sulfur amino acids seem to act as osmolytes, to balance internal osmotic pressure with that of the ocean. Ttau, in particular, seems to transport and/or to detoxify sulfide and is probably produced by the interaction of the sulfinic group of Htau with H₂S [34–36]. The spontaneous oxidation of sulfide can produce different reactive oxy-

gen and sulfur radical species. The presence of Ttau in these organisms is related to their need to decrease the level of sulfide; consequently, Ttau formation can be included in the mechanisms developed to counteract the presence of oxygen and sulfur radicals in the deep sea organisms. Moreover, Ttau has been proposed as a marker in animals with a sulfide-based symbiosis. This organic thiosulfate has the ability to release hydrogen sulfide (H₂S) in a thiol-dependent reaction [37]. In particular, a thiosulfate reductase activity occurring in various cells uses electrons of thiols, such as GSH, to reduce sulfane sulfur of thiosulfonates, such as Ttau to H₂S [38]. The H₂S gasotransmitter is one of the most important sulfur inorganic compounds whose role is crucial in oxidative stress and inflammation processes. H₂S has important signaling properties but also plays a crucial role in cellular redox homeostasis by modulating GSH concentration and Nrf2 factor transcription [39, 40].

3.1.2. Histidine and Aromatic Derivatives. Other groups of marine sulfur products are represented by the histidine derivatives and the aromatic amine derivatives. The first one includes othiols from echinoderm egg species such as 1-methyl-5-mercapto-L-histidine and their disulfide derivatives (Figure 5) [41], and the second includes one of the precursors of melanin produced by tyrosinase enzymes, such as 2,5-S,S-dicysteinyl-dopa that is part of the red-violet marine pigment, adenochrome, extracted from the branchial heart of the common octopus, *Octopus vulgaris* (Figure 5) [42]. One of the marine natural products belonging to this class of compounds that was recently found to be very promising for its biological activities is ergothioneine (Figure 5), a sulfur histidine compound derived from 2-mercapto-L-histidine by quaternization of the α -amino group and characterized by the presence of the sulfur thione tautomeric form [43–46]. Certain mushrooms (in the Basidiomycetes class), fungi such as *Aspergillus oryzae*, *Streptomyces* species, and cyanobacteria are the only organisms capable of producing this compound that demonstrates to possess a high pharmacological potential mainly due to its thione moiety that confers to the compound high stability and activity against ROS [47, 48].

3.1.3. Indolic Compounds and Thiazolic Peptides. Besides, indole compounds derived from tryptophan metabolism were found in marine species (Figure 6). Among this group, the occurrence of simple brominated methylthioindoles has been reported from a Taiwanese collection of the red alga *Laurencia brongniarti* (2,4,6-tribromo-3-methylthioindole and derivatives). Simple brominated methylthioindoles are encountered in the molluscan families Muricidae and Thaisidae as the precursors of the pigment Tyrian purple, used since ancient times as a valuable coloring matter. Another important indole (or guanidine) alkaloid is dendrodione, the first identified naturally occurring 1,2,4-thiadiazole ring system extracted from a tunicate *Dendrodia grossularia* with cytotoxic properties [49, 50]. The thiazoles and thiazolidinones group includes also dysidenin and isodysidenin pseudopeptides isolated from a collection of the marine sponge *Dysidea herbacea*. Furthermore, the tunicate *Lissoclinum patella* collected from Palau, Western Caroline Islands, gave

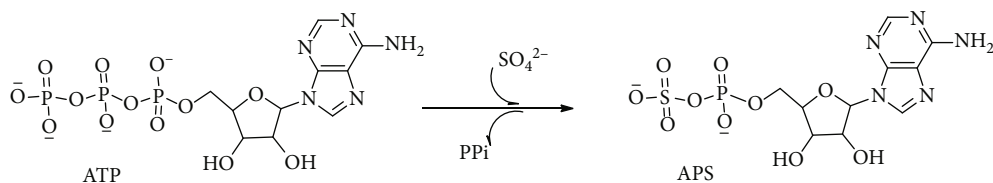


FIGURE 2: Sulfate anion incorporation in adenosine phosphosulfate (APS) from ATP.

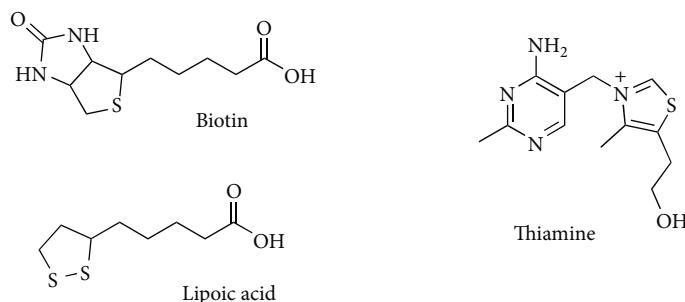


FIGURE 3: Important sulfur-containing cofactors and vitamins.

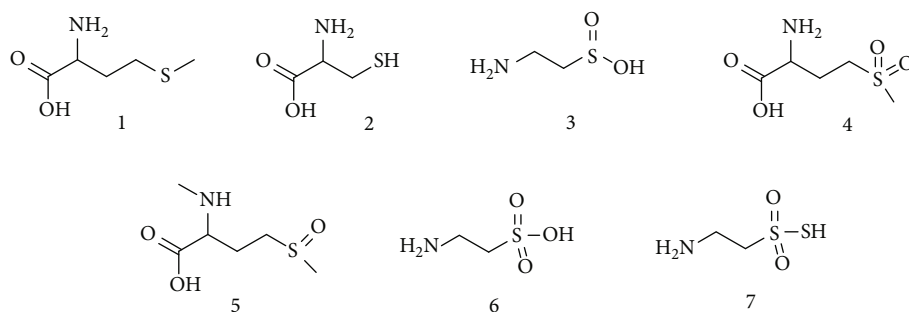


FIGURE 4: Organosulfur amines. (1) Methionine. (2) Cysteine. (3) Hypotaurine. (4) Methionine sulfone. (5) Methionine N-methyl sulfoxide. (6) Taurine. (7) Thiotaaurine.

the first two examples of thiazole-containing macrocyclic peptides, ulicyclamide and ulithiacyclamide [51].

3.2. Terrestrial Products. Terrestrial organisms such as plants and fungi are also able to produce an interesting pool of sulfur organic compounds.

3.2.1. Alkyl and Allyl-S-Oxides. Forms of sulfur compounds relevant to human nutrition are present in foods such as garlic, onion, and broccoli. Yet, the ingestion of these forms of sulfur compounds is very important for human health since it provides many antioxidants and immunomodulating substances that are useful to maintain an adequate physiological function of most body organs [52]. Garlic (*Allium sativum*) is the perfect example of bioactive sulfur compound (antioxidant and antibacterial molecules) intake with the diet. *Allium* species have a characteristic flavor that is due to the production of particular compounds when fresh garlic is crushed. When garlic is chopped, the precursors allin, isoallin, and other S-alk(en)yl-L-cysteine-S-oxides are converted via an enzymatic process mediated by allinase enzyme into the respective thiosulfonates such as allicin, isoallicin, and allsulfonates, which are also responsible for the aroma of fresh gar-

lic and its antiseptic activity (Figure 7). Also, in onions, a series of VSCs is formed by cleavage of S-alk(en)yl cysteine sulfoxides catalyzed by allinase and lachrymatory factor synthase [53].

3.2.2. Glucosinolates and Isothiocyanates. Glucosinolates are another important class of organosulfur plant secondary metabolites and are present mostly in species of the *Brassicaceae* family, such as cabbage, broccoli, and horseradish, and are derived from glucose and thiohydroxamic acids starting from different amino acids [54]. Nonaromatic glucosinolates are derived mainly from Met and aliphatic amino acids, while aromatic glucosinolates, such as glucobrassicin, are derived from tryptophan as an amino acid donor. As for garlic S-alk(en)yl-L-cysteine-S-oxides, also glucosinolates represent inactive precursors that release the biologically active sulfur species when the plant material is cut, chewed, or crushed. When the enzyme myrosinase enters in contact with the glucosinolates, substrates cleave off the glucose moiety and release isothiocyanates (commonly known as mustard oil), which are responsible for pungency and defense mechanism (Figure 8) [55].

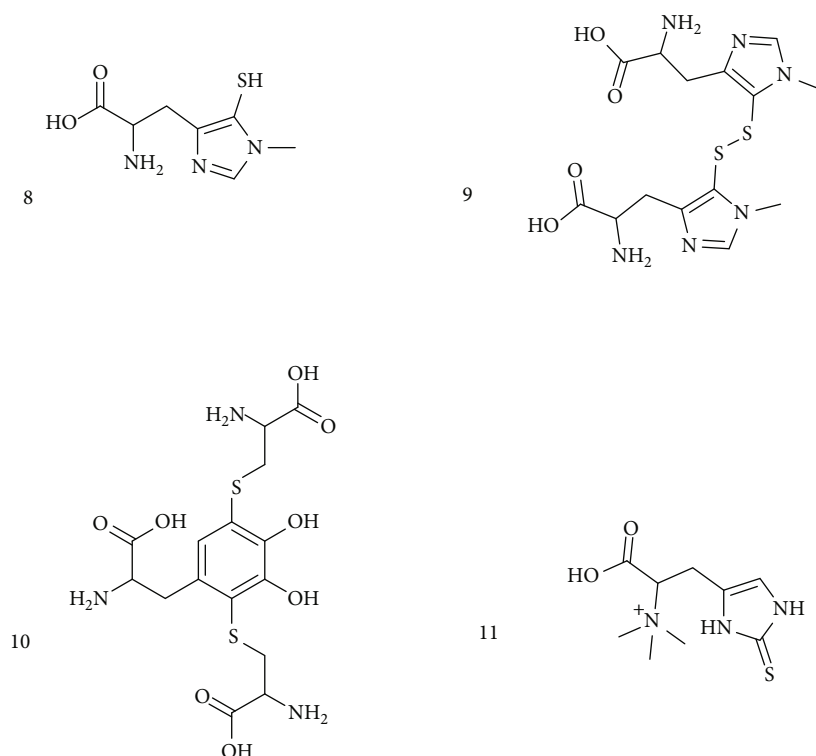


FIGURE 5: Histidine and aromatic amine organosulfur derivatives. (8) 1-Methyl-5-mercapto-L-histidine. (9) 1-Methyl-5-mercapto-L-histidine disulfide derivatives. (10) 2,5-S,S-dicysteinyl-dopa. (11) Ergothioneine.

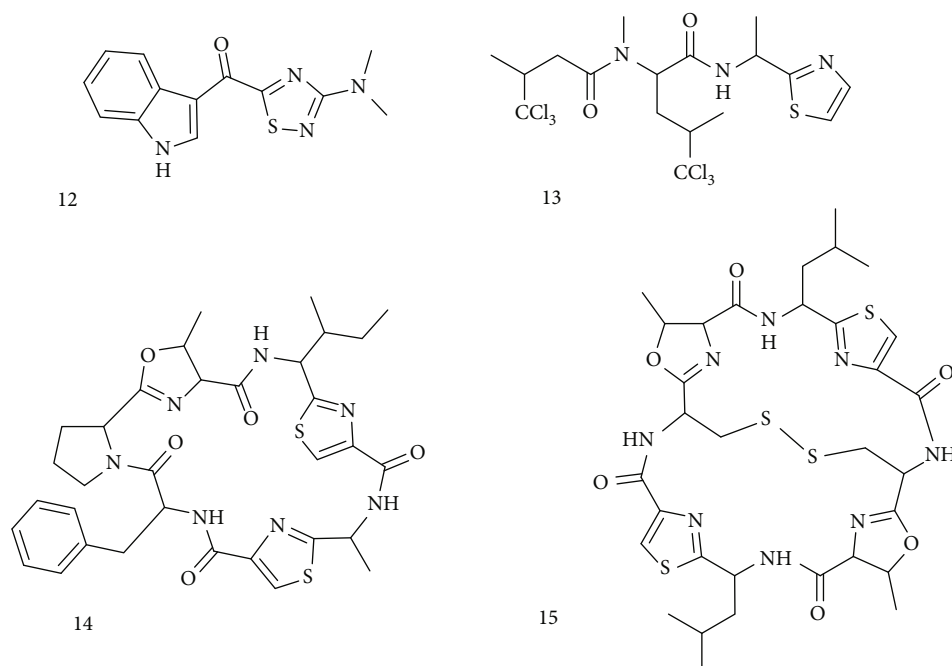


FIGURE 6: Sulfur-containing indole derivatives. (12) Dendrodoine. (13) Dysidenins. (14) Ulicyclamide. (15) Ulithiacyclamide.

When the plant is attacked or damaged, the organism is already prepared with this two-component system (enzyme-precursor) and immediately starts the enzymatic hydrolysis of glucosinolates and the subsequent formation of the bioactive isothiocyanates [56]. Allyl isothiocyanates

(Figure 9) from radish, horseradish, and wasabi are well-recognized VSCs for strong repellent activity against various arthropods, nematodes, and microorganisms and possess a good chemopreventive activity [57]. An important part of the beneficial effect of the Mediterranean diet is related to

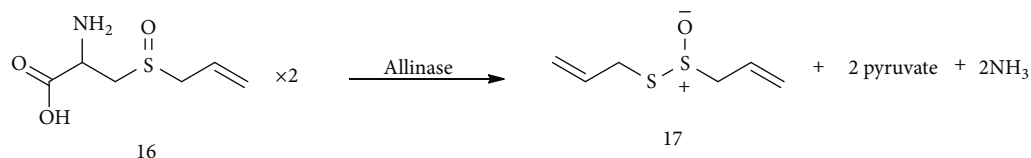


FIGURE 7: Allin (16) enzymatic conversion into allicin (17) in crushed fresh garlic.

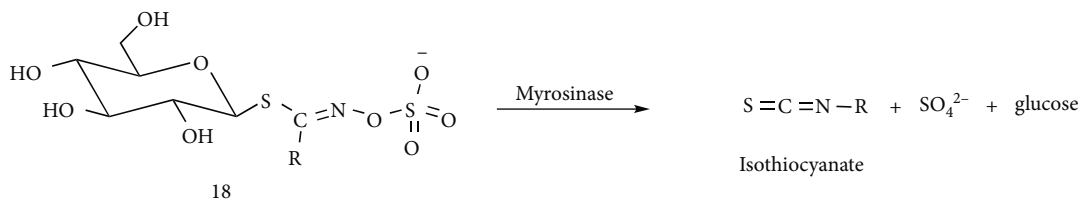


FIGURE 8: Glucosinolate (18) hydrolysis and isothiocyanate formation.

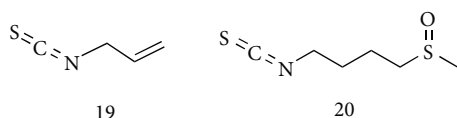


FIGURE 9: Bioactive isothiocyanates. (19) Allyl isothiocyanates. (20) Sulforaphane.

isothiocyanate intake such as sulforaphane (Figure 9). Sulforaphane, an isothiocyanate compound that occurs in high concentration as its precursor glucoraphanin, is abundant in broccoli, Brussels sprouts, and cabbages and many biological effects such as anti-inflammatory, antidiabetic, anticancer, and neuroprotective effects were recently ascribed to this compound [58].

3.2.3. Polysulfides and Phytochelatins. Other two important classes of nonaromatic sulfur derivatives are cyclic methylene-sulfur compounds (polysulfides) and phytochelatin polymers. The most famous molecule belonging to cyclic polysulfides is lenthionine. Lenthionine (Figure 10) and 1,2,4,6-tetrathiepane were earlier isolated from an extract of the edible “shiitake” mushroom (*Lentinus edodes*) and are partly responsible for its flavor. Lenthionine biosynthesis was not completely elucidated, but it seems also in this case as for garlic thiosulfonates that catalytic cleavage of C-S lyase enzyme is the crucial step for the formation of the final product [59, 60]. Phytochelatins (Figure 10) are a class of sulfur derivatives which are polymeric peptides. They are synthesized by plants, fungi, and cyanobacteria when the cellular environment is rich in metal ions. Structurally, they are polymers of GSH and their principal role is the environmental detoxification exerted by their strong activity as chelating agents [61].

4. Biochemical Aspects of Endogenous Sulfurous Metabolites

The metabolism of sulfur-containing amino acids consists of a variety of reactions and pathways with several intermedi-

ates and products whose biochemical significance still needs to be fully elucidated [62–66]. Crucial functions for cell survival are served by some of these metabolites. Met and Cys are the two main sulfur amino acids. They are incorporated into proteins and have important catalytic roles in the active sites of many enzymes [67, 68]. Dietary proteins normally supply Met and Cys. In addition to the intake of dietary protein, turnover of body proteins releases free Met and Cys into the body pools [69, 70].

Met serves as the source of sulfur for Cys biosynthesis in a one-way transsulfuration pathway that links metabolically Met and Cys. In mammals, Met is an essential amino acid as it cannot be synthesized in amounts sufficient to maintain the normal growth, whereas Cys is considered a semiessential amino acid because it can be produced from Met sulfur and serine via transsulfuration. Cys and Met oxidation and catabolism yield a considerable amount of energy. This was originally believed to be wasted, as the oxidation of this sulfur to sulfate ($-2 \rightarrow +6$) was not thought to be coupled to ATP synthesis [71]. However, recent findings suggest that H_2S derived from Cys and Met metabolism can stimulate oxidative phosphorylation via sulfide:quinone oxidoreductase (SQR) and sulfite oxidase [72–76]. Beyond this energetic potential of Cys and Met, these sulfur amino acids exert crucial functions through their well-known metabolites, such as SAM, Tau, and GSH.

4.1. Transmethylation/Transsulfuration Pathway. In mammalian cells, the transmethylation/transsulfuration pathway is central for sulfur amino acid metabolism and the regulation of redox balance. The pathway involves the transfer of sulfur from Hcy to Cys via cystathionine and is the only route for biosynthesis of Cys. This pathway is intimately linked to the transmethylation pathway via Hcy, which can be remethylated to generate Met or be irreversibly converted to Cys (Figure 11).

Met metabolism begins with the activation of Met to SAM by Met adenosyltransferase (MAT). The reaction requires ATP and the sequential cleavage of all its high-energy phosphate groups. SAM as a methyl group donor generates S-adenosylhomocysteine (SAHcy) by cellular

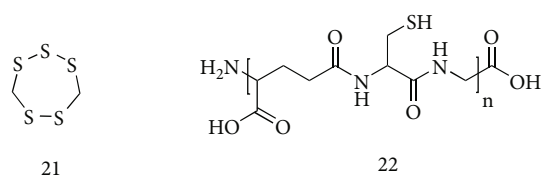


FIGURE 10: Cyclic polysulfide (21) lenthionine and (22) phytochelatins.

methyltransferases. SAHCy is hydrolyzed to yield Hcy and adenosine by SAHCy hydrolase (SAH). This sequential reaction route is present in all cell types and is referred to as the transmethylation pathway. Hcy is methylated back to Met by the Met synthase (MS) and, only in the liver and the kidney of some species, by betaine:homocysteine methyltransferase (BHMT) [77]. The Hcy remethylation is catalyzed by both MS and BHMT, and the combination of transmethylation and remethylation comprises the Met cycle.

The transsulfuration pathway diverts Hcy from the Met cycle, converting Hcy to Cys by the sequential action of two pyridoxal 5'-phosphate- (PLP-) dependent enzymes, cystathionine β -synthase (CBS) and cystathionine γ -lyase (CSE). Hcy, which is derived from dietary Met, is converted to cystathionine by CBS, which is acted on by CSE to generate Cys. The transmethylation and remethylation pathway occurs in all cells, whereas the transsulfuration pathway is restricted to certain tissues. An exogenous source of Cys is required in conditions where transsulfuration reactions do not occur at a sufficient rate [78–80]. These tissues accumulate Hcy (or cystathionine) which must be exported to other tissues for further metabolism/removal. The transsulfuration pathway occurs in tissues that contain both CBS and CSE [81]. CBS activity is widely present in mammalian organs including the liver, adipose tissue, kidney, and brain [82]. Conversely, it is widely assumed that a high level of CSE is present in the liver, kidney, and pancreas, whereas CSE activity is absent in the brain [83]. However, recent studies have demonstrated that also CSE is both present and active in the brain [84, 85]. Both CSE and CBS occupy a central role in the cell redox regulation. It has been reported that approximately half of the intracellular GSH pool in the human liver is derived from Cys generated from Hcy via the transsulfuration pathway [86]. In the mouse brain, the activity of the pathway is lower as compared to that in the liver, but the flux can be regulated by oxidative stress [84, 85]. It has been observed that CSE undergoes inactivation under oxidative stress condition in mice [65]. In this regard, an intact transsulfuration pathway plays a key role in maintaining GSH homeostasis and affords an effective neuroprotection.

4.2. S-Adenosylmethionine. SAM is a high-energy sulfonium compound which acts primarily as a methyl donor in reactions catalyzed by a vast array of methyltransferases. Given its high energy, the molecule is not so stable in vitro and can be degraded rapidly even at room temperature, giving rise to SAHCy, homoserine (HSer), 5'-methylthioadenosine

(MTA), and S-5'-adenosyl-(5')-3-methylpropylamine (dSAM) (Figure 12) [87–90].

These SAM-dependent methylations are essential for biosynthesis of various biomolecules including creatine, epinephrine, melatonin, carnitine, and choline. An alternative fate of SAM is decarboxylation to form dSAM, which is the donor of aminopropyl groups for synthesis of spermidine and spermine [63, 91]. As a result of polyamine synthesis, MTA forms from dSAM. Alternatively, SAM provides amino groups in biotin synthesis and 5'-deoxyadenosyl radicals and also sulfur atoms in the synthesis of biotin and lipoic acid [92–97].

SAM is also a potent allosteric regulator of the transmethylation/transsulfuration pathways. SAM promotes Met catabolism through the transsulfuration pathway and inhibits the remethylation of Hcy to Met [98–101]. As a result, SAM increases the activity of CBS which is the primary enzyme in transsulfuration and contributes to the synthesis of Cys, thereby increasing the GSH level. The attenuation of oxidative stress by SAM administration has been evidenced by several studies. For example, Li et al. [102] showed that cells can be protected from oxidative stress induced by β -amyloid peptide after SAM administration; indeed, SAM actually increases endogenous antioxidant defense by restoring the normal GSH/GSSG ratio and inducing antioxidant enzyme activities.

4.3. Nontranssulfuration Pathway. The SAM-independent catabolic pathway of Met also occurs, involving an initial transamination reaction [62]. The transamination of Met forms α -keto- γ -methylbutyrate, the α -keto acid analogue of Met, which may be further catabolized via oxidative decarboxylation to 3-methylthiopropionate, MeSH, and additional catabolites [103, 104]. This is considered a minor pathway under normal circumstances, but it becomes more significant at high Met concentrations. Because it produces powerful toxins such as MeSH, it has been considered to be responsible for Met toxicity [105]. Indeed, Met has been regarded as a toxic amino acid, whether large amounts are taken up from the diet or it accumulates from metabolic dysfunction of the transsulfuration pathway. Excessive dietary Met causes acute liver injury and erythrocyte membrane damage through mechanisms that are not still fully elucidated [104–107]. The toxic effect has been observed especially in rodent tissues where Met transamination occurs and appears to play a crucial role in Met toxicity [106]. In humans, the physiological and toxicological significance of the Met transamination pathway remains unclear [108, 109]. Interestingly, not only Met but also other thioether metabolites undergo transamination generating a class of sulfur-containing heterocyclic compounds called ketimines (described below) [110, 111].

4.4. Cysteine Metabolism. Cys, whether formed from Met and serine via transsulfuration or supplied preformed in the diet, serves as a precursor for synthesis of proteins and several other essential molecules. These metabolites include GSH, CoA, and Tau. These fates of Cys, except GSH, involve loss of the Cys moiety as such. Cys is a substrate for CoA

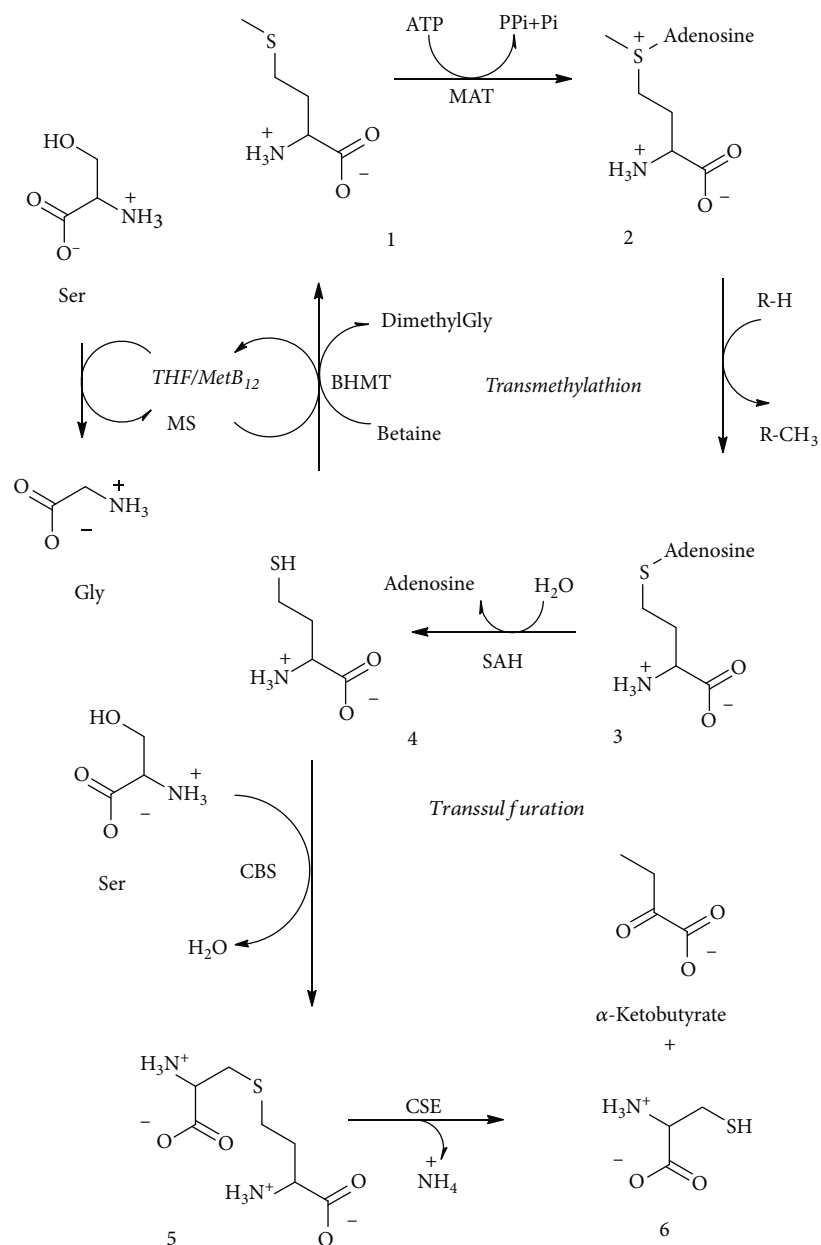


FIGURE 11: Transsulfuration/transmethylation pathway. Methionine (1), SAM (2), S-adenosylhomocysteine (3), homocysteine (4), cystathionine (5), and cysteine (6). MAT: Met adenosyltransferase; SAH: SAHCy hydrolase; MS: Met synthase; BHMT: betaine:homocysteine methyltransferase; CBS: cystathionine β -synthase; CSE: cystathionine γ -lyase.

synthesis in that it is used to form the cysteamine (decarboxylated Cys) moiety of the CoA molecule and, hence, contributes to the reactive sulfhydryl group. Cys is also the precursor of the gaseous signaling molecule H₂S [112–114].

Cys is metabolized via two distinct routes. The first one, called the cysteine sulfinate- (CSA-) dependent (aerobic) pathway, is a series of oxidative steps leading to Htaur. The second one, a transsulfuration (anaerobic) pathway, is a source of sulfane sulfur-containing compounds as well as H₂S [115]. The enzymes involved in the H₂S production include pyridoxal 5'-phosphate- (PLP-) dependent CSE

and CBS as well as cysteine aminotransferase (CAT) in conjunction with PLP-independent mercaptopyruvate sulfurtransferase (MST) (Figure 13) [112, 116, 117].

Cys is readily oxidized to Cys-Cys and exists in oxidized form in plasma and in the extracellular milieu, thus representing the major transport form of non-protein-bound Cys [118]. Across membranes, Cys and Cys-Cys are transported by different membrane carriers. In the CNS, glial cells mainly import Cys-Cys via the cystine-glutamate antiporter providing the major route for GSH synthesis in the brain [119]. Cys-Cys undergoes β -elimination reaction by

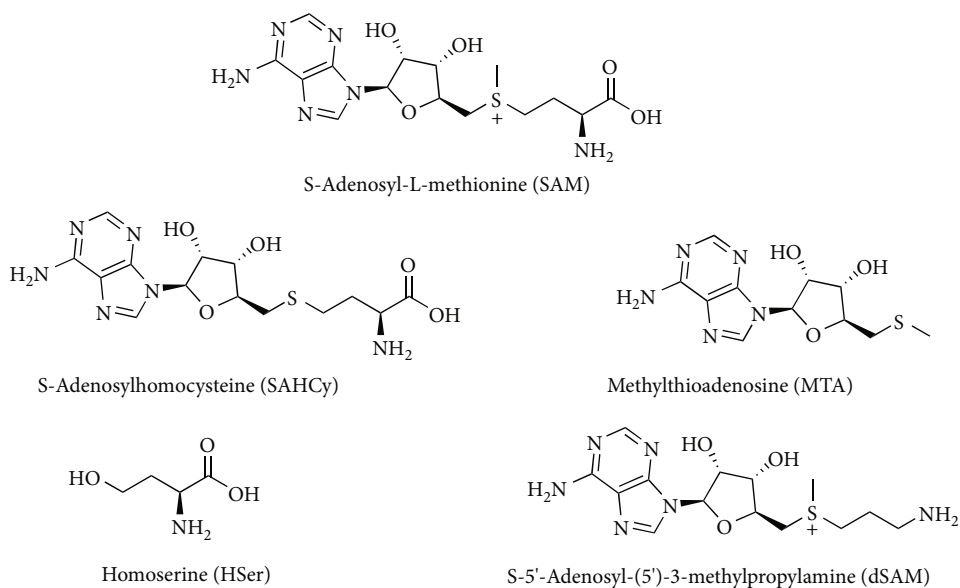


FIGURE 12: S-Adenosyl-L-methionine (SAM) degradation products.

transsulfuration enzymes, CBS and CSE, yielding thiocysteine, the persulfide analogue of Cys (RSSH) [120–123].

4.5. Glutathione. The GSH tripeptide is derived from Cys, glutamate, and glycine present in all mammalian cells at mM concentration level (1–10 mM) with the highest amount in the liver. GSH has an unusual γ -glutamyl bond linking glutamate and Cys. This unconventional peptide bond through the γ -carboxyl group of glutamate rather than the α -carboxyl group confers stability to hydrolysis by cellular peptidases, requiring a specific enzyme for GSH degradation. The first step in the GSH synthesis is catalyzed by the enzyme glutamate-cysteine ligase (GCL) which forms γ -glutamylcysteine in an ATP-dependent reaction [124]. This conjugation reaction between glutamate and Cys is considered the rate-limiting step in GSH synthesis, whereas Cys the limiting substrate [125]. The addition of Gly to γ -glutamylcysteine is catalyzed by the ATP-dependent enzyme glutathione synthase (GS) which results in the formation of the mature GSH tripeptide [126, 127]. The enzyme that accounts for the hydrolysis of the γ -glutamyl bond is γ -glutamyltranspeptidase (γ GT), which localizes on the luminal surfaces of cells lining the glands and ducts of various organs particularly the kidney, pancreas, and liver [128] (Figure 14).

As consequence, GSH is resistant to intracellular degradation and is mainly metabolized extracellularly by cells that express γ GT. However, recently, cytosolic breakdown pathways for GSH have been described [129]. GSH breakdown by γ GT produces glutamate and cysteinylglycine which can be taken up by cells where the released amino acids are reused for the synthesis of GSH (so-called the γ -glutamyl cycle) [130]. In addition to the several vital functions of GSH, GSH serves as a reservoir of Cys and as a means for transporting Cys to extrahepatic tissues. An association between Cys and GSH metabolism disruption and aberrant

redox homeostasis and neurodegeneration has been frequently observed [131, 132].

4.6. Coenzyme A, Pantetheine, and Cysteamine. CoA (Figure 15) is synthesized starting from pantothenate and cysteine in five reaction steps (Figure 16). 4'-Phosphopantetheine (cysteamine-pantothenate conjugate) is the moiety bearing the reactive thiol for the formation of the high-energy thioester bond in acetyl CoA [133].

CoA breakdown generates pantetheine which is hydrolyzed by the vanin family of pantetheinase enzymes to pantothenate and the aminothiols, cysteamine [134, 135]. Cysteamine is the decarboxylated derivative of Cys. However, in mammals, cysteamine is not formed from Cys directly by decarboxylation. Rather, it is produced mainly by the pantetheinase activity during CoA breakdown (Figure 16). An alternative route to cysteamine from lantionine has been described, where lantionine undergoes first decarboxylation to S-2-aminoethyl-L-cysteine (also called thialysine); subsequently, this latter compound is converted to cysteamine by a β -elimination reaction [136]. In humans, cysteamine undergoes different metabolic degradations such as conversion to volatile sulfur compounds, i.e., methanethiol and dimethylsulfide, which have been detected in cystinosis patients treated with this aminothiol [137, 138]. Cysteamine is highly reactive, and it readily oxidizes in solution to form the disulfide cystamine. Cysteamine readily forms mixed disulfides with susceptible Cys thiol groups in a process called cysteaminylation which is key for many reported biological activities [139]. At low concentrations, cysteamine can form a mixed disulfide with Cys, promoting Cys transport into cells. Recently, the complex role of cysteamine and cystamine as oxidative stress sensors has been illustrated by experiments using vanin 1-deficient mice [140, 141]. Interestingly, cysteamine has been used to treat cystinosis and

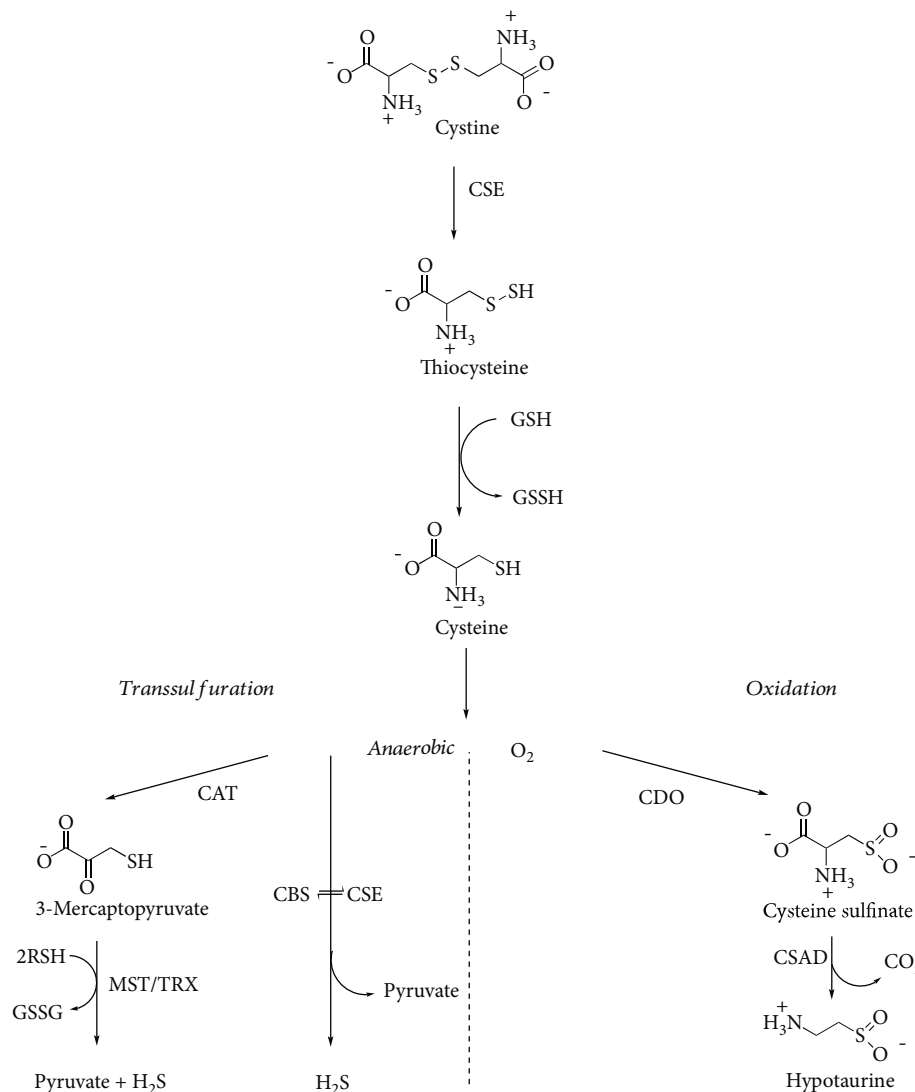


FIGURE 13: Cystine metabolism by transsulfuration enzymes. CAT: cysteine aminotransferase; CBS: cystathionine β -synthase; CDO: cysteine dioxygenase; CSAD: cysteine sulfinate decarboxylase; CSE: cystathionine γ -lyase; MST: mercaptopyruvate sulfurtransferase; TRX: thioredoxin.

neurodegenerative disorders [142, 143]. A recent review recapitulates the use of cysteamine as a mutation-tailored drug. This aminothiols has been proposed to repair Arg to Cys missense mutations in genetic disorders. Upon binding of cysteamine to the Cys residue by a disulfide bond, a mimic structure resembling the original arginine residue is created on the mutated protein [144].

4.7. Taurine. In the mammalian pathway leading from Cys to Tau, Htau is the main metabolic precursor of Tau. Htau is synthesized by the CSA-dependent (aerobic) pathway of Cys metabolism (Figure 13). The production of Htau is dependent upon the sequential action of cysteine dioxygenase (CDO) that adds molecular oxygen to the thiol group of Cys to form CSA and of cysteine sulfinate decarboxylase (CSAD) that finally generates Htau [115]. In a minor pathway, CSA can also undergo oxidation to produce cysteic acid (CA) and, through subsequent decarboxylation, forms Tau

[115, 145]. Another pathway involves the production of Htau from cysteamine via the action of cysteamine dioxygenase (2-aminoethanethiol dioxygenase, ADO) (Figure 17) [146].

CDO and ADO are the only two mammalian thiol oxygenases capable of specifically oxidizing free sulfhydryl groups [147]. The activities for these two proteins were first reported in mammalian tissues almost 60 years ago [148, 149].

The importance of the cysteamine/Htau/Tau pathway has been largely regarded as minor relative to the Cys/CSA/Htau/Tau pathway. Indeed, it is the reaction catalyzed by CDO that has been implicated as the major rate-determining step in the synthesis of Htau and Tau [150]. Interestingly, the brain is capable of synthesizing Tau and yet expresses relatively little CDO [151], and it is, thus, possible that the ADO-mediated pathway is largely responsible for Htau/Tau synthesis in the brain [146].

Noteworthy, the oxidation of the sulfinic group of both Htau and CSA with production of the respective sulfonate

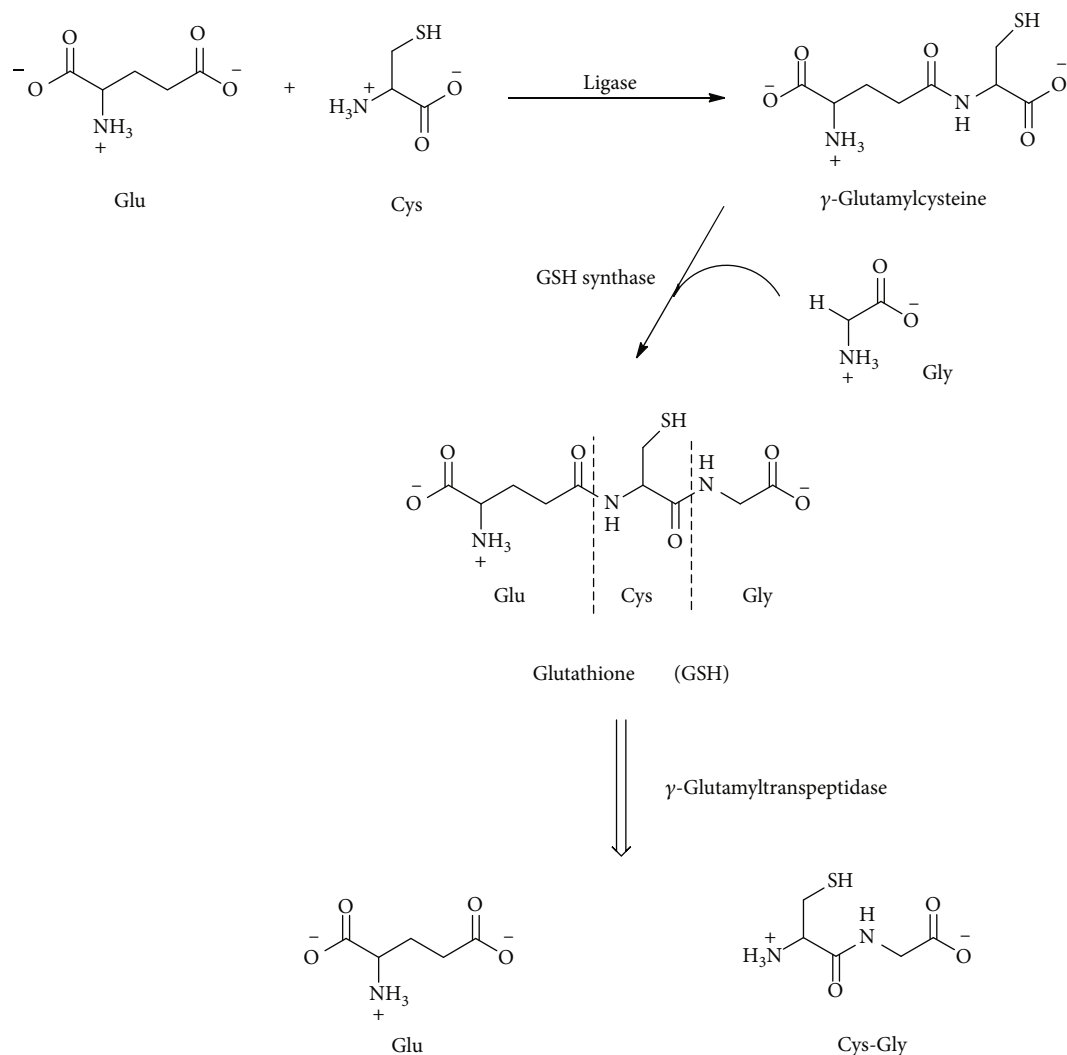


FIGURE 14: Glutathione (GSH) and its enzymatic degradation products, glutamate (Glu) and cysteinylglycine (Cys-Gly).

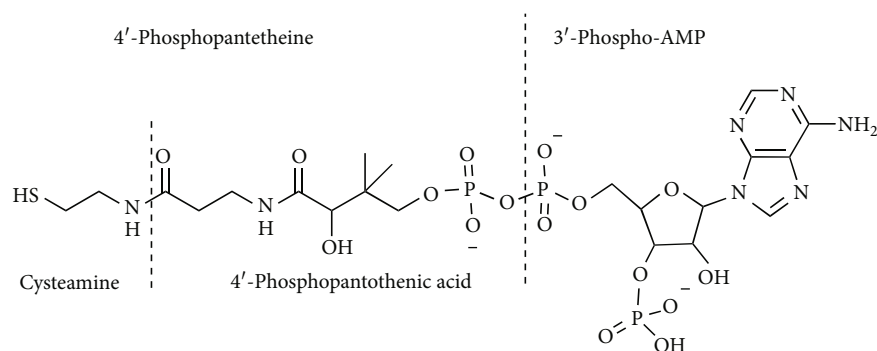


FIGURE 15: Coenzyme A. Chemical structure of CoA and its components.

(RSO_3^-), Tau and CA, is a crucial point for the generation of Tau in mammalian tissues [145, 152]. However, no specific enzymatic activity has been detected for this oxidation. Conversely, there is strong evidence that *in vivo* formation of Tau and CA is the result of sulfinate (RSO_2^-) interaction with a variety of biologically relevant oxidizing agents [153–156].

The relevance of both CO_3^{2-} and NO_2^- in the oxidation of Htau has been recently evidenced by the peroxidase activity of Cu-Zn superoxide dismutase and horseradish peroxidase [157–159]. Recently, it has been shown that a wide substrate range enzyme such as flavin monooxygenase 1 (FMO1) is able to catalyze the oxidation of Htau to Tau [160].

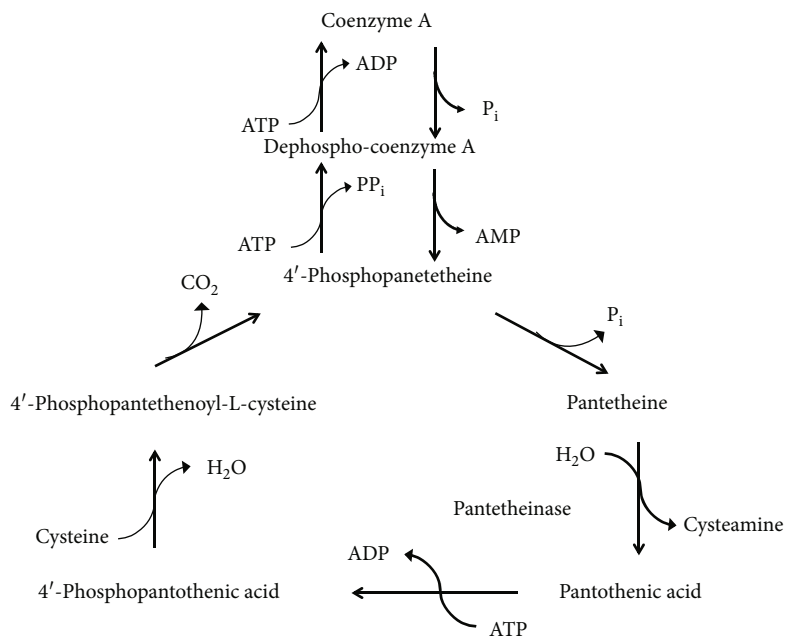


FIGURE 16: CoA biosynthesis and degradation.

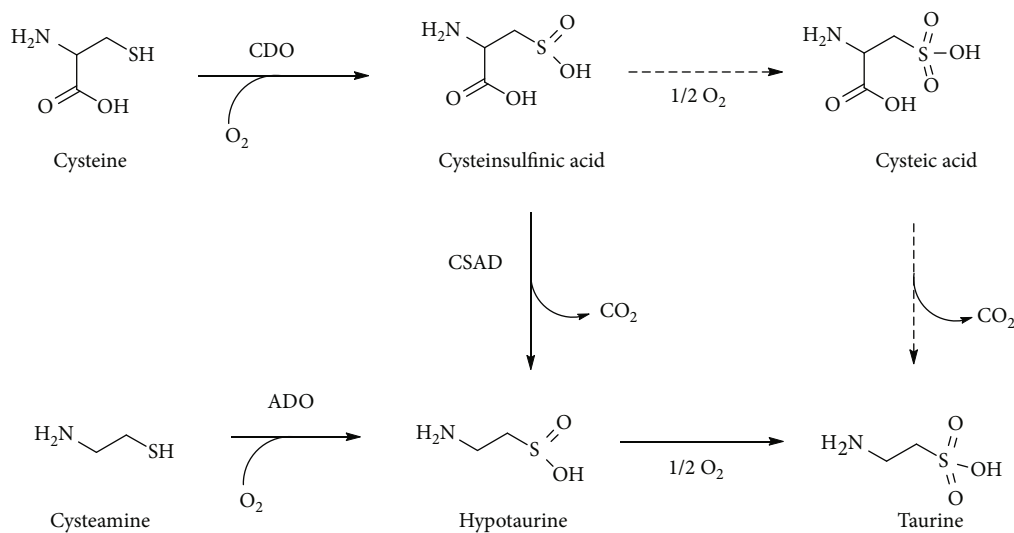


FIGURE 17: Taurine biosynthesis. Alternative routes for taurine biosynthesis from cysteine or cysteamine. ADO: cysteamine dioxygenase; CDO: cysteine dioxygenase; CSAD: cysteine sulfinatase decarboxylase.

Tau is the most abundant free amino acid in animal tissues and is present especially in excitable tissues such as the brain, retina, muscle, and heart, whereas circulating levels are, in comparison, much lower [2, 161–163]. The Tau content differs between species such that taurine levels have been reported lower in primates than in rodents. The amounts range from 2 $\mu\text{mol/g}$ wet weight in the human brain to 40 $\mu\text{mol/g}$ in the mouse heart, with even higher concentrations in the eye retina and in the developing brain of mice [164, 165]. In the muscle, retina, and neurons, the Na⁺-dependent transport through the Tau transport accumulates Tau at high levels [166]. Tau is capable of regulating osmolarity through exchange with the extracellular space without

altering membrane potential. This role of Tau as a critical regulator of osmolarity is particularly important in maintaining neuronal function [167]. Both Tau and Htau exhibit neurotransmitter activity reminiscent of γ -aminobutyric acid (GABA) and β -alanine. According to this chemical structure similarity, Tau can mimic some effects provoked by GABA release [168]. In the CNS, where Tau is highly concentrated, this β -amino acid exhibits neuromodulator and neuroprotector activity, also preserving the homeostasis of retinal functions [169]. Tau plays a role also in bile salt formation.

Similarly, Htau is a unique amino sulfinatase with a powerful antioxidant capacity [170–172]. Htau achieves a millimolar concentration in tissues and biological fluids typically

subjected to high oxidative stress, such as the regenerating liver, human neutrophils, and human semen [173–175]. Noteworthy, Htau is capable of protecting SOD by the H_2O_2 -mediated inactivation, thus reinforcing the cell defense against oxidative damage [176]. However, the one-electron oxidative reaction between Htau and various biologically relevant oxidants is accompanied by generation of reactive intermediates, such as sulfonyl radicals, which could promote oxidative chain reactions [156, 157].

4.8. Sulfane Sulfur: Persulfides and Thiosulfonates. Low-molecular weight RSSH such as thiocysteine and glutathione persulfides (GSSH) are present at μM concentration inside the cells. Due to highly reducing and nucleophilic properties, RSSH can act as scavenging oxidants and intracellular electrophiles. RSSH are considered the major source of sulfane sulfur in biological systems. One proposed mechanism for sulfane sulfur biological effect is the modification of protein Cys residues by persulfidation [113, 177, 178]. Noteworthy, biological effects attributed to H_2S as a signaling molecule may also be partially caused by sulfane sulfur, such as Cys-based persulfides as the actual signaling species [179–181]. H_2S , indeed, can react with oxidized thiols, such as sulfenates (RSOH), in biological systems to give persulfides [182]. Thiocysteine can be directly generated by transsulfuration enzymes CBS and CSE from Cys-Cys, whereas GSSH is produced in the mitochondrial sulfide oxidation by SQR [40, 120, 183–185]. Recently, the *in vivo* formation of thiocysteine by the transsulfuration pathway has been questioned [186]. Sulfane sulfur species such as thiocysteine, GSSH, and protein-Cys persulfides are also generated by MST [187, 188]. Furthermore, a recent report revealed that a mitochondrial enzyme, cysteinyl-tRNA synthetase (CARS2), plays a major role in converting Cys into Cys per/polysulfide species [189].

The sulfane sulfur of thiocysteine can be transferred by sulfurtransferases to various acceptors, including sulfite and Htau [120, 190]. The transfer of sulfur to Htau produces Ttau, a component of the Tau family characterized by the presence of a sulfane sulfur in the thiosulfonate group ($-S_2O_2^-$). The biological occurrence of Ttau in mammals as a metabolic product of Cys-Cys *in vivo* was reported initially by Cavallini and coworkers [191] by demonstrating that rats fed with a diet supplemented in Cys-Cys excreted a newly unknown compound identified as the thiosulfonate analogue of Tau, Ttau. Furthermore, Ttau is formed by a sulfurtransferase catalyzing sulfur transfer from mercaptopyruvate to Htau [192, 193]. Structurally, Ttau carries a hypotaurine moiety and a sulfane sulfur moiety generated, respectively, by aerobic and anaerobic metabolism of cysteine. Consequently, Ttau can represent a linking intermediate of the cysteine metabolic paths (Figure 18).

Interestingly, Ttau is capable of releasing H_2S in a thiol-dependent reaction. In particular, thiols, such as GSH, and other reducing agents reduce sulfane sulfur of thiosulfonates to H_2S [38, 117, 193]. Accordingly, in human neutrophils, GSH acts as a catalyst in the generation of H_2S and Htau from Ttau [194].

Overall, Ttau formed as a result of the reaction between Htau and RSSH may be converted back to H_2S and Htau

(Figure 18). It is likely that Ttau, due to its peculiar biochemical properties, takes part in the modulation and control of H_2S signal as suggested by the effect of Ttau on human neutrophil functional responses [37, 195–197].

4.9. Lanthionines, Cyclic Ketimine, and Imino Acid Derivatives: Sulfur-Containing Metabolites Still in Search for a Role. Lanthionines are a class of sulfur organic compounds that are extremely interesting but still remain a mystery. From a chemical point of view, lanthionines are thioethers derived from the condensation of aminothiols or amino acids. Cystathionine probably represents one of the most important biological thioethers for humans. This molecule is essential for the transsulfuration pathway in which HCy is converted to Cys in relation to the folate cycle and SAM-mediated methylation pathway [15]. The four most important thioethers involved in this metabolism and other mammalian metabolic disorders are lanthionine, cystathionine, S-2-aminoethyl-L-cysteine (thialysine), and homolanthionine (Figure 19).

The biosynthesis of these compounds in mammals is mediated by the transsulfuration enzymes, CBS and CSE, starting from Cys, cysteamine, and HCy to produce lanthionine, thialysine, and cystathionine, respectively. CBS enzyme can use serine or Cys as the substrate and releases H_2O or H_2S (Figure 20).

The catabolism of cystathionine involves CSE releasing Cys and α -ketobutyric acid in a reaction that catalyzes a PLP-mediated α - γ elimination. The role of linear thioethers such as lanthionine and thialysine is still unknown from a metabolic point of view, also because they are poor substrates of CSE enzyme and then they should be addressed to different metabolic routes. Some of them such as thialysine can be used as substrates for decarboxylases giving rise to different thioether polyamines (e.g., thiocadaverine). In most of the cases, the fate and significance of lanthionine compounds is unclear and difficult to understand. In this contest, it is important to underline the fundamental contribution of professor Cavallini and coworkers in the study and discovery of some sulfur-containing cyclic ketimines as products of the linear thioethers discussed above [14]. Lanthionine, cystathionine, and thialysine can undergo an oxidative deamination to produce the respective α -keto acids that subsequently cyclize to give rise to their sulfur-containing cyclic ketimine, lanthionine ketimine (LK), cystathionine ketimine (CK), and thialysine ketimine (TK) [110, 198, 199] (Figure 21).

LK, CK, and TK can also be obtained via a chemical reaction in aqueous solutions of Cys, HCy, and cysteamine with bromopyruvic acid [200, 201]. In the case of CK, a seven-membered asymmetric ring, the ketimine could also exist in the isomeric form with the double bond located in the longer carbon chain moiety of the ring. This isomer has been prepared by reacting β -chloro-L-alanine with 2-oxo-4-thiobutyrate obtained enzymatically. One common feature of this class of compounds is their reducing power. Reduced saturated cycles can be obtained by the reduction of the imine bond ($C=N$) with $NaBH_4$ [202]. TK yields 1,4-thiomorpholine-3-carboxylic acid (TMA), LK gives 1,4-thiomorpholine-3,5-dicarboxylic acid (TMDA), and CK produces 1,4-

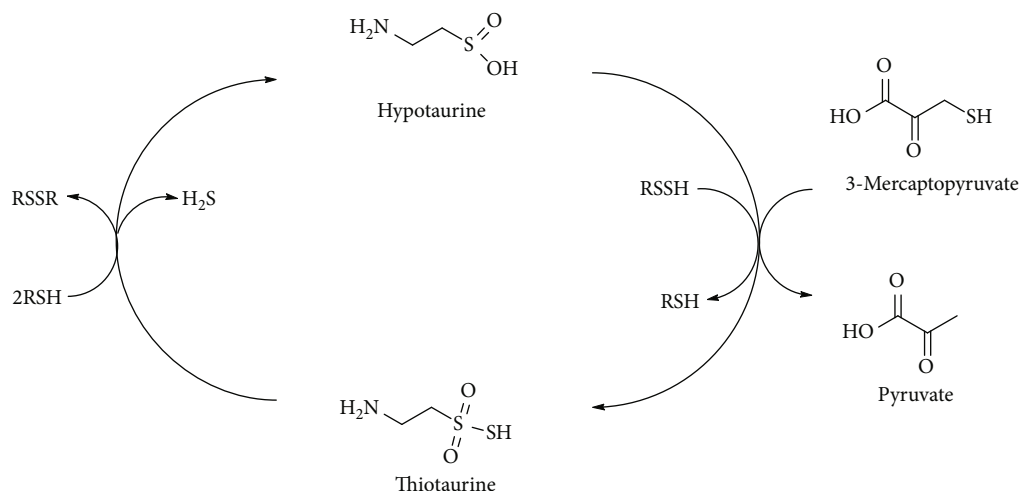


FIGURE 18: Thiotaurine transsulfuration pathway.

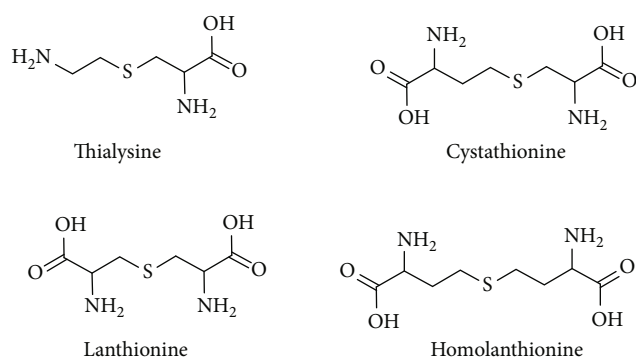


FIGURE 19: Biological thioethers belonging to the class of lanthionines

hexahydrothiazepine-3,5-dicarboxylic acid (cyclothionine) [203]. The reduced products are much more stable than the parent ketimines and can be produced also biochemically by a NADP(H) reductase enzyme [204] (Figure 22).

All of these cyclic derivatives (LK, CK, TK, and their reduced products TMDA, cyclothionine, and TMA) were detected in human urines and mammalian brains [205–208]. LK and CK were also directly detected for the first time in the human brain in 1991 by Fontana and coworkers [209]. The very unusual and particular issue is that lanthionine differently from the other linear precursors was never found in human urines and brain tissues [208].

Lanthionines and sulfur cyclic ketimines are a very interesting class of compounds that may play an important physiological role. In degenerative processes, thiol redox biochemistry is crucial and in some neuronal disorders such as Alzheimer's disease may represent an important diagnostic marker [131]. The metabolism of organic sulfur in many organisms is still not completely understood, and there are many evidences of an emerging role of some of sulfurous ketimines in inflammation and neuronal associated disorders [15]. The brain contains a functional transsulfuration pathway able to generate H₂S and several unusual amino acids,

such as LK and other sulfur-containing cyclic ketimines and imino acids (Figure 20), whose biological role and significance are still unknown [14, 15, 210]. Among these compounds, LK demonstrated potent antioxidant, neuroprotective, and neurotrophic actions [211], properties that have made this compound a candidate for studies that focus on neurodegenerative diseases and processes including ischemia, amyotrophic lateral sclerosis, multiple sclerosis, and Alzheimer's and Batten's diseases [15, 210, 212–214].

The group of natural heterocyclic sulfur compounds includes not only the six-membered ring cyclic ketimines such as CK, LK, and TK but also the class of five-membered ring heterocycles like terrestrial and marine thiazolidine and thiazoline derivatives such as thioproline, ovolthiols, and thiazoline carboxylic acids (e.g., 2-amino-2-thiazoline-4-carboxylic acid (ATCA)) [41, 215–218] (Figure 23).

All of these compounds demonstrated to possess different and in some cases convergent biological activities such as oxygen and nitrogen-free radical scavenging capacity, detoxification of cyanide, and antioxidant activity [41, 217, 219–222].

4.10. Substrate Flexibility in the Enzymology of Sulfur-Containing Compounds. Many of the enzymes responsible of the metabolic pathways involving sulfur-containing compounds show a relaxed substrate specificity, and at the same time, many reactions involving sulfur-containing molecules are carried out by enzymes also used for different purposes.

This fact came to the attention of Cavallini and colleagues more than sixty years ago, when cystamine and lanthionamine, the R₂S analogue of cystamine, were assayed as substrates of diamine oxidase [223, 224]. The interest of this finding was increased by the observation that the rate of the oxidation was in the range of that of traditional substrates and the product of the reaction was a cyclic cystaldimine (1,2-dehydrodithiomorpholine), which was then cleaved giving rise to a variety of products such as thiocysteamine, Htau, Ttau, and Tau.

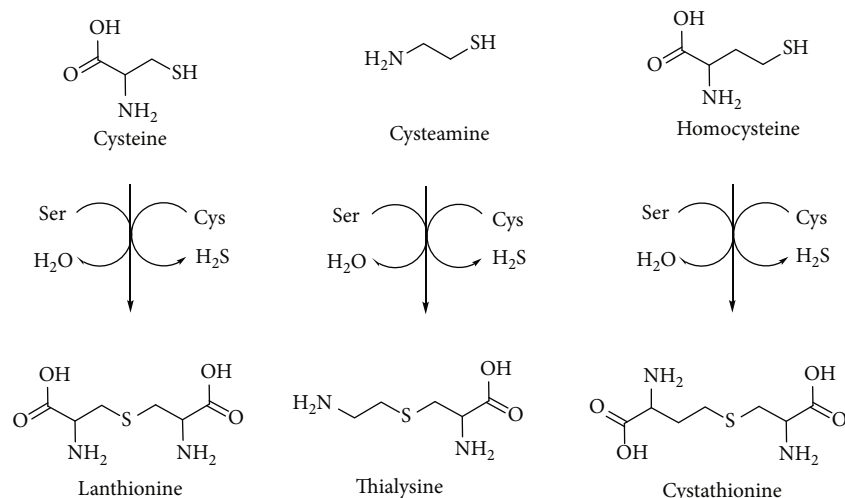


FIGURE 20: Cystathionine β -synthase (CBS) catalyzed synthesis of lanthionines.

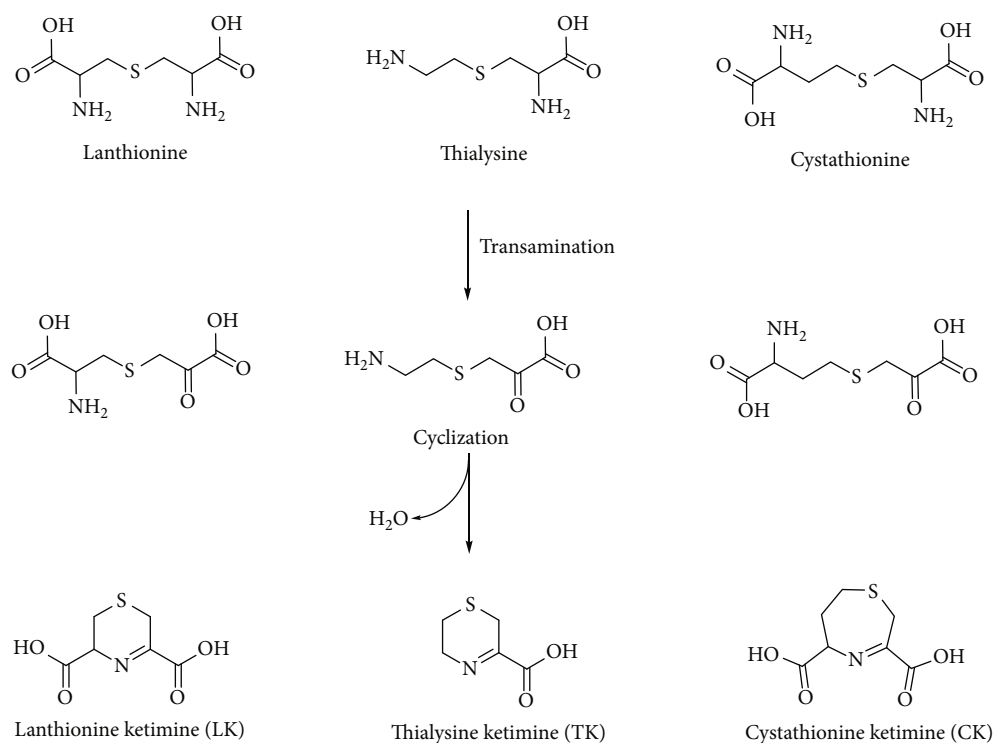


FIGURE 21: Lanthionines and related sulfur-containing cyclic ketimines generated by the brain alternative transsulfuration pathway.

CSA and CA, but also their homologues, homocysteine sulfinic acid (HCSA) and homocysteic acid (HCA), are also known to take profit from a number of enzymes used for other purposes. In this case, the sulfinic and sulfonic groups can mimic the carboxyl group of the carbon analogues aspartate and glutamate. All these sulfur compounds can substitute glutamate and aspartate in the common amino acid transamination and decarboxylation reaction. The decarboxylation reaction converts the sulfinates, CSA/HCSA, and the sulfonates, CA/HCA, in Htau/homoHtau and Tau/homoTau, respectively [225]. In addition to enzyme reactions, these metabolic derivatives interact with molecular targets

such as neurotransmitter receptors, channels, or transporters. Due to structure similarity, HCSA/HCA and their decarboxylated derivatives, homoHtau/homoTau, can represent natural mimetics as neuroactive agents for glutamate and GABA, respectively (Figure 24) [226, 227].

Interestingly, the Hcy derivatives can attain a major biological relevance during hyperhomocysteinemia [228]. Mild hyperhomocysteinemia is a common clinical condition associated with an increased risk for cardiovascular and neurodegenerative diseases [229, 230]. Noteworthy, in Down syndrome, or trisomy 21, the overexpression of CBS removes homocysteine from the transmethylation pathway leading to

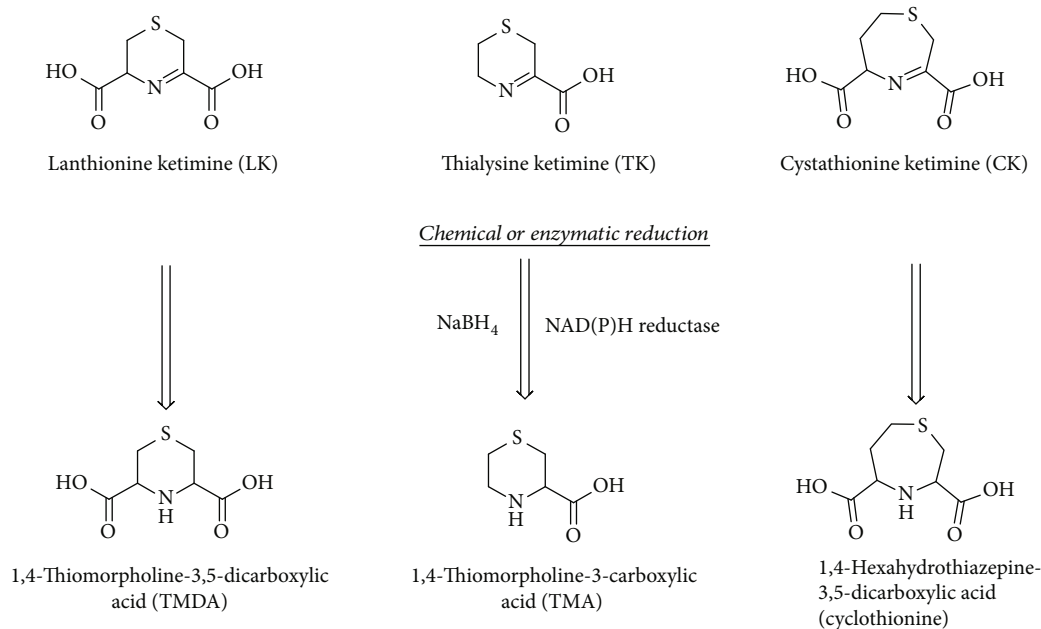


FIGURE 22: Reduced lanthionine ketimines. These compounds as their precursors were found to be produced enzymatically in specific human tissues.

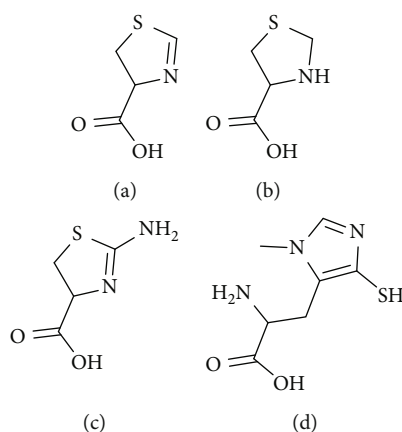


FIGURE 23: Natural heterocyclic five-membered ring compounds. (a) Thiiazolin-4-carboxylic acid (derivative of formylcysteine). (b) Thiazolidine-4-carboxylic acid (thioproline). (c) 2-Amino-2-thiazoline-4-carboxylic acid (ATCA). (d) 2-Amino-3-methyl-5-sulfanylimidazol-4-yl propanoic acid (ovothiol A).

decreased plasma levels of homocysteine and a low incidence of atherosclerosis in these subjects [231, 232]. Consequently, cystathionine, cysteine, and H_2S levels are increased, consistent with an increased CBS activity [233, 234].

In mammals, the relaxed substrate specificity makes the two transsulfuration enzymes, CBS and CSE, chiefly responsible for H_2S biogenesis [122, 235]. These human enzymes afford H_2S generation by a multiplicity of routes involving Cys and/or HCy as substrates. In addition to H_2S , a variety of products is generated in these reactions, including lanthionine and homolanthionine [122]. These thioethers have been proposed as markers of H_2S production in homocystinurias [236]. CBS is also involved in the formation of thialysine by replacing HCy with cysteamine [237]. Thialysine has been actually detected in brain tissues following gavage feeding

of cysteamine in rats [238] and in urine of normal human adults, suggesting thialysine may even be a natural occurring metabolite [208].

According to this substrate flexibility in the enzymology of sulfur amino acid, a vast array of sulfur compounds occurs and can be detected in living organisms, whose biological and metabolic role is worth to be explored.

5. Sulfur-Containing Compounds and Redox Biochemistry

The electronic configuration of sulfur allows it to occur in numerous oxidation states, both negative and positive, ranging from -2 to +6 and possibly including fractional oxidation states [239]. Apart from the well-known ROS and RNS, the

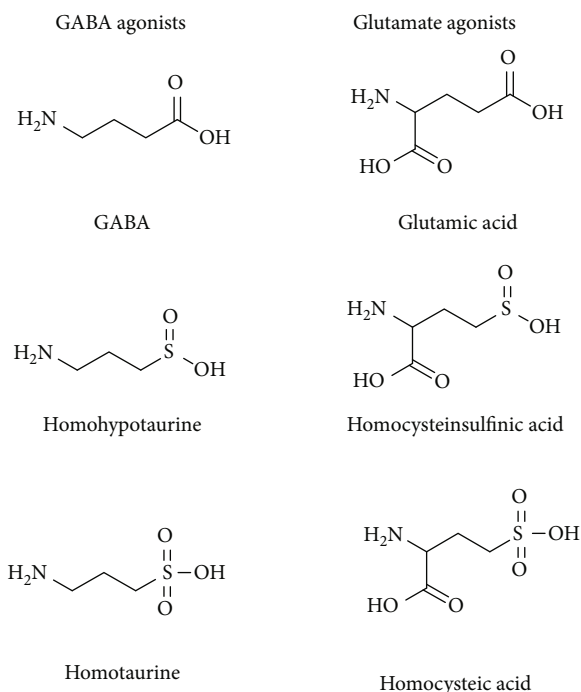


FIGURE 24: Structural relation of neuroactive sulfur amines and amino acids. These compounds can act as GABA or glutamate agonists.

existence of reactive sulfur species (RSS) is well documented [240–242]. RSS include species such as sulfur-centered radicals (RS[•]), disulfides (RSSR), disulfide-S-oxides, and sulfenic acids (RSOH) and can easily be formed *in vitro* from thiols by reaction with oxidizing agents such as hydrogen peroxide, singlet oxygen, peroxyxynitrite, and superoxide. However, the redox potential of RSS is considerably less positive than that of ROS; their biochemical importance is not to be undervalued. For instance, the thiyl radical is an oxidative stressor whereas the disulfide can be a mild oxidative stressor [239]. All of these RSS could in principle oxidize and subsequently inhibit redox-sensitive proteins. Furthermore, thiols could store nitric oxide via the formation of nitrosothiols, which could release nitroxyl ions [243] or nitric oxide in physiological conditions or in the presence of transition metal chelators [244–246].

The best-known RSS is thiyl radical (RS[•]), which is formed by the one-electron oxidation of Cys and is unstable in physiological conditions. If not adequately quenched by ascorbate or GSH, the thiyl radical undergoes a rather efficient intramolecular hydrogen transfer processes, and in oxidative stress conditions, the extent of irreversible protein thiyl radical-dependent protein modification increases [247]. Thiyl radical can be formed in physiological conditions via three major routes: hydrogen donation, enzymatic oxidation, and reaction with ROS. Particularly, formation of this radical has been documented for the reaction of hydrogen peroxide either with hemin or with heme proteins, such as hemoglobin [248, 249]. Many other sulfur-centered radicals could be theoretically formed, but those species are extremely unstable and can only be studied by EPR at very

low temperatures; hence, their pathophysiological role, if ever, is still unclear [250]. Sulfinyl and sulfonyl radicals have also been observed as free radical metabolites of Cys oxidation, which are formed during the interaction of thiols with ROS. These species can be further oxidized to highly reactive radical species, which could lead to dimerization or oxidation [239].

Due to its high reactivity, the reduced thiol group of cysteinyl side chains in proteins plays a major role in many biological processes, and its redox state is of paramount importance in maintaining physiological functions such as catalysis, metal binding, and signal transduction. Hence, the redox regulation of the intracellular environment is a critical factor in cellular homeostasis. Particularly, the regulation of thiol redox balance is fundamental for the maintenance of many different cellular processes such as signal transduction, cell proliferation, and protein integrity and function.

The cellular thiol groups are protected by the “thiol redox buffering system,” whose key components are GSH, either reduced (GSH) or oxidized (GSSG), and the families of enzymes glutaredoxins, thioredoxins, and peroxiredoxins. GSH is the major intracellular thiol antioxidant. Apart from the antioxidant activity, GSH has also a role in the detoxification of xenobiotics and heavy metals [251]. Its concentration is in the mM range, up to 10 mM in certain cells making this compound the most concentrated antioxidant in the cells [251]. However, rather than the absolute concentration of GSH, a better index of redox state is represented by the [GSH]/[GSSG] ratio which also reflects changes in redox signaling and control of cell functions [131]. During acute oxidative stress, GSH concentration decreases and the associated increase in GSSG concentration results in an increased turnover of the GSH/GSSG cycle, but GSSG is also actively extruded from the cell; thus, the intracellular turnover of GSH is affected [251]. Under normal conditions, the ratio of GSH/GSSG is around 50:1 to 100:1, whereas in oxidative stress condition, it can drop to 10:1 and even to 1:1 [252].

Some disulfides may be strongly oxidizing and cause oxidative damage to cell components. For instance, under conditions of oxidative stress, GSSG could reach toxic concentration in the cells and oxidize proteins like metallothioneins [253]. GSSG is formed from GSH when enzymes like glutathione peroxidase (GSHPx) use GSH as a reducing species to detoxify peroxides or other ROS to prevent oxidative damage. GSH is then regenerated by the aid of NADPH in the presence of glutathione reductase (GR).

Reversible reduction of disulfide bonds can be mediated by a variety of thiol redox enzymes such as the thioredoxins (TRXs) and the glutaredoxins (GRXs). The TRX and GRX systems control cellular redox potential, keeping a reduced intracellular environment, by utilizing reducing equivalents from NADPH. These proteins are expressed in all organisms, tissues, cell types, and organelles, and some of them can shuttle between cellular compartments and the extracellular space [254].

TRXs were first identified as hydrogen donors for ribonucleotide reductase, the essential enzyme providing deoxyribonucleotides for DNA replication. The paramount

importance of TRXs in the cell is witnessed by the evidence that TRX knockout is embryonically lethal [254]. There are two main forms of TRXs, TRX-1 which is present in the cytosol and TRX-2 localized in the mitochondria. TRXs are induced by oxidative stress and act as antioxidants by catalyzing the reversible reduction of disulfides utilizing both cysteinyl residues present in the active site, whose motif is Cys-Gly-Pro-Cys. Oxidized TRX is then reduced via TrxR (TRX reductase) using electrons from NADPH. As for TRXs, there are two main forms of TrxRs, one in the cytosol (TrxR-1) and one in the mitochondria (TrxR-2). Due to the easily accessible C-terminal catalytic center, TrxRs can reduce a broad range of substrates including hydrogen peroxide, selenite, lipoic acid, ascorbate, and ubiquinone, and TrxR-2 was demonstrated to act on cytochrome c [255], but the main substrates remain TRXs. In response to oxidative stress, TRXs can be secreted by the cells and exert an anti-inflammatory action by inhibiting neutrophil extravasation into the inflammatory sites, opening to the possibility of using these proteins as therapeutic tools [256, 257].

GRXs are a group of thiol redox enzymes whose active site contains the sequence motif CXXC, same as in TRXs and protein disulfide isomerases. In the GRX system, electrons flow from NADPH to GSH via GR and are then transferred to one of the three up-to-date identified GRXs. Akin TRXs, GRXs are able to reduce protein disulfides but are also able to act on mixed disulfides for which TRXs display low or no activity [258]. GRXs can act via a dithiol or monothiol mechanism, respectively, on protein disulfides or mixed disulfides, particularly on glutathionylated proteins [258]. Protein glutathionylation does not only occur in oxidative stress conditions but rather seems to be a fundamental regulatory mechanism by reversible modification of protein thiols. Hence, deglutathionylation by GRXs could represent a more general mechanism of protein activity control by GRXs than the simple regeneration of protein thiols.

6. Conclusions

Biomolecules consist principally of carbon, hydrogen, and the heteroatoms oxygen and nitrogen. As sulfur and oxygen belong to the same group in the periodic table, the group of chalcogens, the question that arises is as follows: “why analogue compounds with the sulfur atom replaced by oxygen do not serve the same function?”

Sulfur actually has unique characteristics that differentiate it from oxygen, such as increased atomic size that confers to sulfur a lower electronegativity. This leads to bond formation that is less ionic and weaker than bonds between carbon and sulfur. There are also important differences in primary organosulfur metabolites with respect to oxygenated analogues, such as polarity and reactivity. In particular, thiols and thioether moieties (R_2S) can be oxidized to sulfoxides (R_2SO) and sulfones (R_2SO_2) and can form stable sulfonium cations (i.e., SAM) that allow unique carbon alkyl-transfer reactions in biology (e.g., substrates methylation). It is doubtful whether other compounds or other “-onium” compounds could adequately serve this role: quaternary ammonium

compounds are too thermodynamically stable to effectively methylate most acceptors, and oxonium compounds are too strong alkylating agents for most of the biological environments with subsequent toxic effects.

Sulfur metabolites are utilized by all living beings and depending on the function are distributed in the different kingdoms from marine organisms to terrestrial plants and animals. Mammals, such as humans, are not able to fix inorganic sulfur in biomolecules and are completely dependent on preformed organic sulfur compounds to satisfy their sulfur needs. However, some higher species such as humans are able to build new sulfur-containing chemical entities starting especially from plants' organosulfur precursors. Sulfur metabolism in humans is very complicated and plays a central role in redox biochemistry. In this review, we explored sulfur metabolism in relation to redox biochemistry and the large pool of naturally occurring sulfur-containing compounds in the marine and terrestrial “world.” We focused on the chemistry and the biochemistry of exogenous and endogenous sulfur metabolites underlining the importance of well-known and studied molecules and also of the unknown and poorly studied sulfur natural products whose biological role is still a mystery and needs to be investigated.

It is worth investigating the role of these and other still unknown natural sulfur compounds also in view of the extremely promising beneficial activity that the molecules could exert in different pathophysiological conditions.

The biosynthesis of particular sulfur metabolites is a unique feature in some species from the animal kingdom and seems to occur via diverse biochemical pathways evolutionally far from microorganisms and plants' sulfur metabolism. It is also important to underline the somehow paradoxical situation beyond sulfur biochemistry, probably the oldest redox metabolic form of “life” on Earth and at the same time a continuously newly uncovered field with still more and more opened scientific questions.

Acronyms

ADO:	Cysteamine dioxygenase
APS:	Adenosine phosphosulfate
ATCA:	2-Amino-2-thiazoline-4-carboxylic acid
BHMT:	Betaine:homocysteine methyltransferase
CA:	Cysteic acid
CARS2:	Cysteinyl-tRNA synthetase
CAT:	Cysteine aminotransferase
CBS:	Cystathionine β -synthase
CDO:	Cysteine dioxygenase
CoA:	Coenzyme A
CSA:	Cysteine sulfinat
CSAD:	Cysteine sulfinat decarboxylase
CSE:	Cystathionine γ -lyase
Cys:	Cysteine
Cys-Cys:	Cystine
DMS:	Dimethylsulfide
DMSP:	Dimethylsulfoniopropionate
dSAM:	S-5'-Adenosyl-(5')-3-methylpropylamine
GABA:	γ -Aminobutyric acid

GR:	Glutathione reductase
GRXs :	Glutaredoxins
GSH:	Glutathione
GSHPx:	Glutathione peroxidase
GSSH:	Glutathione persulfides
H ₂ S:	Hydrogen sulfide
HCA:	Homocysteic acid
HCSA :	Homocysteine sulfinic acid
HCy:	Homocysteine
Htau:	Hypotaurine
MAT:	Met adenosyltransferase
MeSH :	Methanethiol
Met:	Methionine
MS:	Met synthase
MST:	Mercaptopyruvate sulfurtransferase
MTA:	5'-Methylthioadenosine
R ₂ O:	Ether
R ₂ S:	Thioether
R ₂ SO :	Sulfoxides
R ₂ SO ₂ :	Sulfones
R ₃ S ⁺ :	Sulfonium ion
RDA:	Recommended dietary allowance
RNS :	Reactive nitrogen species
ROS:	Reactive oxygen species
RS·:	Sulfur-centered radicals
RSO ₂ ⁻ :	Sulfinate
RSO ₃ ⁻ :	Sulfonate
RSOH:	Sulfenic acids
RSS:	Reactive sulfur species
RSSR:	Disulfides
-S ₂ O ₂ ⁻ :	Thiosulfonate group
SAH:	S-Adenosylhomocysteine hydrolase
SAHCy:	S-Adenosylhomocysteine
SAM:	S-Adenosylmethionine
SQR:	Sulfide:quinone oxidoreductase
Tau:	Taurine
TMA:	1,4-Thiomorpholine-3-carboxylic acid
TMDA:	1,4-Thiomorpholine-3,5-dicarboxylic acid
TRXs:	Thioredoxins
Ttau:	Thiotaurine
VSCs:	Volatile sulfur compounds
γGT:	γ-Glutamyltranspeptidase.

Conflicts of Interest

The authors declare no conflict of interest.

Authors' Contributions

Antonio Francioso and Alessia Baseggio Conrado equally contributed to this work and co-first authors.

Acknowledgments

This work was supported by funds from MIUR Ateneo 2018 and 2019.

References

- [1] N. P. Ward and G. M. DeNicola, "Sulfur metabolism and its contribution to malignancy," *Cellular Nutrient Utilization and Cancer*, vol. 347, pp. 39–103, 2019.
- [2] J. T. Brosnan and M. E. Brosnan, "The sulfur-containing amino acids: an overview," *The Journal of Nutrition*, vol. 136, no. 6, pp. 1636S–1640S, 2006.
- [3] O. W. Griffith, "Mammalian sulfur amino acid metabolism: an overview," *Methods Enzymology*, vol. 143, pp. 366–376, 1987.
- [4] M. E. Nimni, B. Han, and F. Cordoba, "Are we getting enough sulfur in our diet?," *Nutrition & Metabolism*, vol. 4, no. 1, p. 24, 2007.
- [5] W. ROSE, M. COON, H. LOCKHART, and G. LAMBERT, "The amino acid requirements of man. 11. The threonine and methionine requirements," *Journal of Biological Chemistry*, vol. 215, no. 1, pp. 101–110, 1955.
- [6] W. Rose and R. Wixom, "The amino acid requirements of man. 13. The sparing effect of cystine on the methionine requirement," *Journal of Biological Chemistry*, vol. 216, no. 2, pp. 753–773, 1955.
- [7] M. I. Irwin and D. M. Hegsted, "A conspectus of research on amino acid requirements of man," *The Journal of Nutrition*, vol. 101, no. 4, pp. 539–566, 1971.
- [8] W. W. Campbell, M. C. Crim, G. E. Dallal, V. R. Young, and W. J. Evans, "Increased protein requirements in elderly people: new data and retrospective reassessments," *The American Journal of Clinical Nutrition*, vol. 60, no. 4, pp. 501–509, 1994.
- [9] K. WRETLIND and W. ROSE, "Methionine requirement for growth and utilization of its optical isomers," *Journal of Biological Chemistry*, vol. 187, no. 2, pp. 697–703, 1950.
- [10] J. O. Anderson, R. E. Warnick, and R. K. Dalai, "Replacing dietary methionine and cystine in chick diets with sulfate or other sulfur compounds," *Poultry Science*, vol. 54, no. 4, pp. 1122–1128, 1975.
- [11] J. B. Schutte and M. Pack, "Effects of dietary sulphur-containing amino acids on performance and breast meat deposition of broiler chicks during the growing and finishing phases," *British Poultry Science*, vol. 36, no. 5, pp. 747–762, 1995.
- [12] M. C. H. Gruhlke and A. J. Slusarenko, "The biology of reactive sulfur species (RSS)," *Plant Physiology and Biochemistry*, vol. 59, pp. 98–107, 2012.
- [13] N. Tateishi, T. Higashi, A. Naruse, K. Hikita, and Y. Sakamoto, "Relative contributions of sulfur atoms of dietary cysteine and methionine to rat liver glutathione and proteins," *The Journal of Biochemistry*, vol. 90, no. 6, pp. 1603–1610, 1981.
- [14] D. Cavallini, G. Ricci, S. Dupre et al., "Sulfur-containing cyclic ketimines and imino acids. A novel family of endogenous products in the search for a role," *European Journal of Biochemistry*, vol. 202, no. 2, pp. 217–223, 1991.
- [15] K. Hensley and T. T. Denton, "Alternative functions of the brain transsulfuration pathway represent an underappreciated aspect of brain redox biochemistry with significant potential for therapeutic engagement," *Free Radical Biology and Medicine*, vol. 78, pp. 123–134, 2015.
- [16] D. C. Yoch, "Dimethylsulfoniopropionate: its sources, role in the marine food web, and biological degradation to

- dimethylsulfide,” *Applied and Environmental Microbiology*, vol. 68, no. 12, pp. 5804–5815, 2002.
- [17] R. P. Kiene, “Production of methanethiol from dimethylsulfoniopropionate in marine surface waters,” *Marine Chemistry*, vol. 54, no. 1–2, pp. 69–83, 1996.
- [18] U. Alcolombri, S. Ben-Dor, E. Feldmesser, Y. Levin, D. S. Tawfik, and A. Vardi, “Identification of the algal dimethyl sulfide-releasing enzyme: A missing link in the marine sulfur cycle,” *Science*, vol. 348, no. 6242, pp. 1466–1469, 2015.
- [19] A. O. Meinrat, “Ocean-atmosphere interactions in the global biogeochemical sulfur cycle,” *Marine Chemistry*, vol. 30, pp. 1–29, 1990.
- [20] R. P. Kiene, L. J. Linn, J. González, M. A. Moran, and J. A. Bruton, “Dimethylsulfoniopropionate and methanethiol are important precursors of methionine and protein-sulfur in marine bacterioplankton,” *Applied and environmental microbiology*, vol. 65, no. 10, pp. 4549–4558, 1999.
- [21] N. M. Kredich, “Biosynthesis of cysteine,” *EcoSal Plus*, vol. 3, no. 1, 2008.
- [22] D. Cavallini, G. E. Gaull, and V. Zappia, Eds., *Natural sulfur compounds: novel biochemical and structural aspects*, Plenum Press, New York, 1980.
- [23] M. Iranshahi, “A review of volatile sulfur-containing compounds from terrestrial plants: biosynthesis, distribution and analytical methods,” *Journal of Essential Oil Research*, vol. 24, no. 4, pp. 393–434, 2012.
- [24] L. W. Wattenberg, V. L. Sporn, and G. Barany, “Inhibition of Af-nitrosodiethylamine carcinogenesis in mice by naturally occurring organosulfur compounds and monoterpenes,” *Cancer Research*, vol. 49, 1989.
- [25] S. C. Sahu, “Dual role of organosulfur compounds in foods: a review,” *Journal of Environmental Science and Health, Part C*, vol. 20, no. 1, pp. 61–76, 2002.
- [26] A. Schmidt, W. R. Abrams, and J. A. Schiff, “Reduction of adenosine 5'-phosphosulfate to cysteine in extracts from chlorella and mutants blocked for sulfate reduction,” *European Journal of Biochemistry*, vol. 47, no. 3, pp. 423–434, 1974.
- [27] E. Bloem, S. Haneklaus, and E. Schnug, “Significance of sulfur compounds in the protection of plants against pests and diseases,” *Journal of Plant Nutrition*, vol. 28, no. 5, pp. 763–784, 2005.
- [28] M. Burow, U. Wittstock, and J. Gershenzon, “Sulfur-Containing Secondary Metabolites and Their Role in Plant Defense,” in *Sulfur Metabolism in Phototrophic Organisms*, pp. 201–222, Springer, 2008.
- [29] C. Jacob, “A scent of therapy: pharmacological implications of natural products containing redox-active sulfur atoms,” *Natural Product Reports*, vol. 23, no. 6, pp. 851–863, 2006.
- [30] T. K. Korendyaseva, D. N. Kuvatov, V. A. Volkov et al., “An allosteric mechanism for switching between parallel tracks in mammalian sulfur metabolism,” *PLoS Computational Biology*, vol. 4, no. 5, article e1000076, 2008.
- [31] M. Giordano and L. Prioretti, “Sulphur and algae: metabolism, ecology and evolution,” in *The Physiology of Microalgae*, pp. 185–209, Springer, Cham, 2016.
- [32] R. Montaser and H. Luesch, “Marine natural products: a new wave of drugs?,” *Future Medicinal Chemistry*, vol. 3, no. 12, pp. 1475–1489, 2011.
- [33] M. R. Prinsep, “Sulfur-containing natural products from marine invertebrates,” in *Studies in Natural Products Chemistry*, A. Rahman, Ed., vol. 28, pp. 617–751, Elsevier, 2003.
- [34] P. H. Yancey, J. Ishikawa, B. Meyer, P. R. Girguis, and R. W. Lee, “Thiourine and hypotaourine contents in hydrothermal-vent polychaetes without thiotrophic endosymbionts: correlation with sulfide exposure,” *Journal of Experimental Zoology Part A: Ecological Genetics and Physiology*, vol. 311A, no. 6, pp. 439–447, 2009.
- [35] N. K. Rosenberg, R. W. Lee, and P. H. Yancey, “High contents of hypotaourine and thiourine in hydrothermal-vent gastropods without thiotrophic endosymbionts,” *Journal of Experimental Zoology Part A: Comparative Experimental Biology*, vol. 305A, no. 8, pp. 655–662, 2006.
- [36] J. A. Ortega, J. M. Ortega, and D. Julian, “Hypotaourine and sulfhydryl-containing antioxidants reduce H₂S toxicity in erythrocytes from a marine invertebrate,” *Journal of Experimental Biology*, vol. 211, no. 24, pp. 3816–3825, 2008.
- [37] A. Baseggio Conrado, E. Capuozzo, L. Mosca, A. Francioso, and M. Fontana, “Thiourine: from chemical and biological properties to role in H₂S signaling,” in *Advances in Experimental Medicine and Biology*, pp. 755–771, Springer, 2019.
- [38] T. M. Hildebrandt and M. K. Grieshaber, “Three enzymatic activities catalyze the oxidation of sulfide to thiosulfate in mammalian and invertebrate mitochondria,” *FEBS Journal*, vol. 275, no. 13, pp. 3352–3361, 2008.
- [39] T. Corsello, N. Komaravelli, and A. Casola, “Role of hydrogen sulfide in NRF2- and sirtuin-dependent maintenance of cellular redox balance,” *Antioxidants*, vol. 7, no. 10, p. 129, 2018.
- [40] O. Kabil and R. Banerjee, “Redox biochemistry of hydrogen sulfide,” *Journal of Biological Chemistry*, vol. 285, no. 29, pp. 21903–21907, 2010.
- [41] I. Castellano and F. P. Seebeck, “On ovothiol biosynthesis and biological roles: from life in the ocean to therapeutic potential,” *Natural Product Reports*, vol. 35, no. 12, pp. 1241–1250, 2018.
- [42] G. Nardi and H. Steinberg, “Isolation and distribution of adenochrome (s) in *Octopus vulgaris* Lam,” *Comparative Biochemistry and Physiology Part B: Comparative Biochemistry*, vol. 48, no. 3, pp. 453–461, 1974.
- [43] F. P. Seebeck, “In vitro reconstitution of mycobacterial ergothioneine biosynthesis,” *Journal of the American Chemical Society*, vol. 132, no. 19, pp. 6632–6633, 2010.
- [44] F. Leisinger, R. Burn, M. Meury, P. Lukat, and F. P. Seebeck, “Structural and mechanistic basis for anaerobic ergothioneine biosynthesis,” *Journal of the American Chemical Society*, vol. 141, no. 17, pp. 6906–6914, 2019.
- [45] R. Burn, L. Misson, M. Meury, and F. P. Seebeck, “Anaerobic origin of ergothioneine,” *Angewandte Chemie*, vol. 129, no. 41, pp. 12682–12685, 2017.
- [46] K. V. Goncharenko, A. Vit, W. Blankenfeldt, and F. P. Seebeck, “Structure of the sulfoxide synthase EgtB from the ergothioneine biosynthetic pathway,” *Angewandte Chemie International Edition*, vol. 54, no. 9, pp. 2821–2824, 2015.
- [47] S. Nachimuthu, R. Kandasamy, R. Ponnusamy, J. Deruiter, M. Dhanasekaran, and S. Thilagar, “L-Ergothioneine: a potential bioactive compound from edible mushrooms,” in *Medicinal Mushrooms*, pp. 391–407, Springer, 2019.
- [48] B. Halliwell, I. K. Cheah, and R. M. Y. Tang, “Ergothioneine – a diet-derived antioxidant with therapeutic potential,” *FEBS Letters*, vol. 592, no. 20, pp. 3357–3366, 2018.
- [49] S. De, T. P. A. Devasagayam, S. Adhikari, and V. P. Menon, “Antioxidant properties of a novel marine analogue of dendroine,” *BARC Newsletter*, vol. 273, pp. 123–133, 2006.

- [50] N. Helbecque, C. Moquin, J. L. Bernier, E. Morel, M. Guyot, and J. P. Henichart, "Grossularine-1 and grossularine-2, alpha carbolines from *Dendrodoa grossularia*, as possible intercalative agents," *Cancer Biochemistry Biophysics*, vol. 9, no. 3, pp. 271–279, 1987.
- [51] C. Ireland and P. J. Scheuer, "Ulicyclamide and ulithiacyclamide, two new small peptides from a marine tunicate," *Journal of the American Chemical Society*, vol. 102, no. 17, pp. 5688–5691, 1980.
- [52] P. Rose, P. K. Moore, M. Whiteman, and Y. Z. Zhu, "An appraisal of developments in allium sulfur chemistry: expanding the pharmacopeia of garlic," *Molecules*, vol. 24, no. 21, p. 4006, 2019.
- [53] C. Shang, S.-Y. Cao, X.-Y. Xu et al., "Bioactive compounds and biological functions of garlic (*Allium sativum* L.)," *Foods*, vol. 8, no. 7, p. 246, 2019.
- [54] N. Baenas, D. Villaño, C. García-Viguera, and D. A. Moreno, "Optimizing elicitation and seed priming to enrich broccoli and radish sprouts in glucosinolates," *Food Chemistry*, vol. 204, pp. 314–319, 2016.
- [55] E. Glawischnig, M. D. Mikkelsen, and B. A. Halkier, "Glucosinolates: biosynthesis and metabolism," in *Sulphur in Plants*, pp. 145–162, Springer Netherlands, 2003.
- [56] H. Zikalova and D. B. J. Vasak, "Glucosinolates—secondary plant products as important complex interaction in our biosphere," *Current Nutrition & Food Science*, vol. 6, no. 4, pp. 281–289, 2010.
- [57] Y. Zhang, "Allyl isothiocyanate as a cancer chemopreventive phytochemical," *Molecular Nutrition and Food Research*, vol. 54, no. 1, pp. 127–135, 2010.
- [58] A. Alfieri, S. Srivastava, R. C. M. Siow et al., "Sulforaphane preconditioning of the Nrf 2/HO-1 defense pathway protects the cerebral vasculature against blood-brain barrier disruption and neurological deficits in stroke," *Free Radical Biology and Medicine*, vol. 65, pp. 1012–1022, 2013.
- [59] K. Morita and S. Kobayashi, "Isolation, structure, and synthesis of lenthionine and its Analogs," *Chemical & Pharmaceutical Bulletin*, vol. 15, no. 7, pp. 988–993, 1967.
- [60] E. Block and R. Deorazio, "Chemistry in a salad bowl: comparative organosulfur chemistry of garlic, onion and shiitake mushrooms," *Pure and Applied Chemistry*, vol. 66, no. 10–11, pp. 2205–2206, 1994.
- [61] J. Luis Gómez-Ariza, T. García-Barrera, F. Lorenzo, and A. Arias, "Analytical characterization of bioactive metal species in the cellular domain (metallomics) to simplify environmental and biological proteomics," *International Journal of Environmental Analytical Chemistry*, vol. 85, no. 4–5, pp. 255–266, 2005.
- [62] A. J. L. Cooper, "Biochemistry of sulfur-containing amino acids," *Annual Review of Biochemistry*, vol. 52, no. 1, pp. 187–222, 1983.
- [63] M. H. Stipanuk, "Metabolism of sulfur-containing amino acids," *Annual Review of Nutrition*, vol. 6, no. 1, pp. 179–209, 1986.
- [64] L. P. Laura Betti, "Sulfur metabolism and sulfur-containing amino acids: I-molecular effectors," *Biochemistry & Pharmacology: Open Access*, vol. 4, no. 1, 2015.
- [65] O. Kabil, V. Vitvitsky, and R. Banerjee, "Sulfur as a signaling nutrient through hydrogen sulfide," *Annual Review of Nutrition*, vol. 34, no. 1, pp. 171–205, 2014.
- [66] M. A. Pajares and D. Pérez-Sala, "Mammalian sulfur amino acid metabolism: a nexus between redox regulation, nutrition, epigenetics, and detoxification," *Antioxidants and Redox Signaling*, vol. 29, no. 4, pp. 408–452, 2018.
- [67] G. Kim, S. J. Weiss, and R. L. Levine, "Methionine oxidation and reduction in proteins," *Biochimica et Biophysica Acta (BBA) - General Subjects*, vol. 1840, no. 2, pp. 901–905, 2014.
- [68] Y.-M. Go, J. D. Chandler, and D. P. Jones, "The cysteine proteome," *Free Radical Biology and Medicine*, vol. 84, pp. 227–245, 2015.
- [69] M. H. Stipanuk, "SULFUR AMINO ACID METABOLISM: Pathways for production and removal of homocysteine and cysteine," *Annual Review of Nutrition*, vol. 24, no. 1, pp. 539–577, 2004.
- [70] M. J. MacCoss, N. K. Fukagawa, and D. E. Matthews, "Measurement of intracellular sulfur amino acid metabolism in humans," *American Journal of Physiology-Endocrinology And Metabolism*, vol. 280, no. 6, pp. E947–E955, 2001.
- [71] R. J. Huxtable, "The Chemistry of sulfur," in *Biochemistry of Sulfur*, Springer US, Boston, MA, 1986.
- [72] M. Velayutham, C. F. Hemann, A. J. Cardounel, and J. L. Zweier, "Sulfite oxidase activity of cytochrome c: role of hydrogen peroxide," *Biochemistry and Biophysics Reports*, vol. 5, pp. 96–104, 2016.
- [73] A. P. Landry, D. P. Ballou, and R. Banerjee, "H₂S oxidation by nanodisc-embedded human sulfide quinone oxidoreductase," *Journal of Biological Chemistry*, vol. 292, no. 28, pp. 11641–11649, 2017.
- [74] E. Lagoutte, S. Mimoun, M. Andriamihaja, C. Chaumontet, F. Blachier, and F. Bouillaud, "Oxidation of hydrogen sulfide remains a priority in mammalian cells and causes reverse electron transfer in colonocytes," *Biochimica et Biophysica Acta (BBA) - Bioenergetics*, vol. 1797, no. 8, pp. 1500–1511, 2010.
- [75] K. Módis, C. Coletta, K. Erdélyi, A. Papapetropoulos, and C. Szabo, "Intramitochondrial hydrogen sulfide production by 3-mercaptopyruvate sulfurtransferase maintains mitochondrial electron flow and supports cellular bioenergetics," *The FASEB Journal*, vol. 27, no. 2, pp. 601–611, 2012.
- [76] M. Goubern, M. Andriamihaja, T. Nübel, F. Blachier, and F. Bouillaud, "Sulfide, the first inorganic substrate for human cells," *The FASEB Journal*, vol. 21, no. 8, pp. 1699–1706, 2007.
- [77] L. M. Stead, J. T. Brosnan, M. E. Brosnan, D. E. Vance, and R. L. Jacobs, "Is it time to reevaluate methyl balance in humans?," *American Journal of Clinical Nutrition*, vol. 83, no. 1, pp. 5–10, 2006.
- [78] I. Ishii, N. Akahoshi, H. Yamada, S. Nakano, T. Izumi, and M. Suematsu, "Cystathionine γ -lyase-deficient mice require dietary cysteine to protect against acute lethal myopathy and oxidative injury," *Journal of Biological Chemistry*, vol. 285, no. 34, pp. 26358–26368, 2010.
- [79] S. Mani, G. Yang, and R. Wang, "A critical life-supporting role for cystathionine γ -lyase in the absence of dietary cysteine supply," *Free Radical Biology and Medicine*, vol. 50, no. 10, pp. 1280–1287, 2011.
- [80] J. A. Martin, J. Sastre, J. G. de la Asunción, F. V. Pallardó, and J. Viña, "Hepatic γ -cystathionase deficiency in patients with AIDS," *Journal of the American Medical Association*, vol. 285, no. 11, pp. 1444–1445, 2001.
- [81] I. Quéré, V. Paul, C. Rouillac et al., "Spatial and temporal expression of the cystathionine β -synthase gene during early

- human development," *Biochemical and Biophysical Research Communications*, vol. 254, no. 1, pp. 127–137, 1999.
- [82] S. H. Mudd, J. D. Finkelstein, F. Irreverre, and L. Laster, "Transsulfuration in mammals. Microassays and tissue distributions of three enzymes of the pathway," *Journal of Biological Chemistry*, vol. 240, no. 11, pp. 4382–4392, 1965.
- [83] I. Ishii, N. Akahoshi, X.-N. Yu et al., "Murine cystathionine γ -lyase: complete cDNA and genomic sequences, promoter activity, tissue distribution and developmental expression," *Biochemical Journal*, vol. 381, no. 1, pp. 113–123, 2004.
- [84] V. Vitvitsky, M. Thomas, A. Ghorpade, H. E. Gendelman, and R. Banerjee, "A functional transsulfuration pathway in the brain links to glutathione homeostasis," *Journal of Biological Chemistry*, vol. 281, no. 47, pp. 35785–35793, 2006.
- [85] L. Diwakar and V. Ravindranath, "Inhibition of cystathionine- γ -lyase leads to loss of glutathione and aggravation of mitochondrial dysfunction mediated by excitatory amino acid in the CNS," *Neurochemistry International*, vol. 50, no. 2, pp. 418–426, 2007.
- [86] E. Mosharov, M. R. Cranford, and R. Banerjee, "The Quantitatively Important Relationship between Homocysteine Metabolism and Glutathione Synthesis by the Transsulfuration Pathway and Its Regulation by Redox Changes†," *Biochemistry*, vol. 39, no. 42, pp. 13005–13011, 2000.
- [87] C. Desiderio, R. A. Cavallaro, A. De Rossi, F. D'Anselmi, A. Fuso, and S. Scarpa, "Evaluation of chemical and diastereoisomeric stability of S-adenosylmethionine in aqueous solution by capillary electrophoresis," *Journal of Pharmaceutical and Biomedical Analysis*, vol. 38, no. 3, pp. 449–456, 2005.
- [88] J. L. Hoffman, "Chromatographic analysis of the chiral and covalent instability of S-adenosyl-L-methionine," *Biochemistry*, vol. 25, no. 15, pp. 4444–4449, 1986.
- [89] S. H. MUDD, "Enzymatic cleavage of S-adenosylmethionine," *Journal of Biological Chemistry*, vol. 34, no. 1, pp. 87–92, 1959.
- [90] P. Laurino and D. S. Tawfik, "Spontaneous emergence of S-adenosylmethionine and the evolution of methylation," *Angewandte Chemie International Edition*, vol. 56, no. 1, pp. 343–345, 2017.
- [91] A. E. Pegg, H. Xiong, D. J. Feith, and L. M. Shantz, "S-Adenosylmethionine decarboxylase: structure, function and regulation by polyamines," *Biochemical Society Transactions*, vol. 26, no. 4, pp. 580–586, 1998.
- [92] B. J. Landgraf, E. L. McCarthy, and S. J. Booker, "Radical S-Adenosylmethionine enzymes in human health and disease," *Annual Review of Biochemistry*, vol. 85, no. 1, pp. 485–514, 2016.
- [93] J. E. Cronan, "Advances in synthesis of biotin and assembly of lipoic acid," *Current Opinion in Chemical Biology*, vol. 47, pp. 60–66, 2018.
- [94] M. Lotierzo, B. Tse Sum Bui, D. Florentin, F. Escalettes, and A. Marquet, "Biotin synthase mechanism: an overview," *Biochemical Society Transactions*, vol. 33, no. 4, pp. 820–823, 2005.
- [95] A. Marquet, B. Tse Sum Bui, and D. Florentin, "Biosynthesis of biotin and lipoic acid," *Vitamins and Hormones*, vol. 61, pp. 51–101, 2001.
- [96] J. T. Jarrett, "The generation of 5'-deoxyadenosyl radicals by adenosylmethionine-dependent radical enzymes," *Current Opinion in Chemical Biology*, vol. 7, no. 2, pp. 174–182, 2003.
- [97] S. Ollagnier, E. Mulliez, P. P. Schmidt et al., "Activation of the anaerobic ribonucleotide reductase from *Escherichia coli*. The essential role of the iron-sulfur center for S-adenosylmethionine reduction," *Journal of Biological Chemistry*, vol. 272, no. 39, pp. 24216–24223, 1997.
- [98] C. CABRERO, J. PUERTA, and S. ALEMANY, "Purification and comparison of two forms of S-adenosyl-L-methionine synthetase from rat liver," *European Journal of Biochemistry*, vol. 170, no. 1–2, pp. 299–304, 1987.
- [99] J. D. Finkelstein, "Pathways and regulation of homocysteine metabolism in mammals," *Seminars in Thrombosis and Hemostasis*, vol. 26, no. 3, pp. 219–226, 2000.
- [100] A. L. Pey, T. Majtan, J. M. Sanchez-Ruiz, and J. P. Kraus, "Human cystathionine β -synthase (CBS) contains two classes of binding sites for S-adenosylmethionine (SAM): complex regulation of CBS activity and stability by SAM," *Biochemical Journal*, vol. 449, no. 1, pp. 109–121, 2013.
- [101] T. Majtan, A. L. Pey, and J. P. Kraus, "Kinetic stability of cystathionine beta-synthase can be modulated by structural analogs of S-adenosylmethionine: potential approach to pharmacological chaperone therapy for homocystinuria," *Biochimie*, vol. 126, pp. 6–13, 2016.
- [102] Q. Li, J. Cui, C. Fang, M. Liu, G. Min, and L. Li, "S-Adenosylmethionine Attenuates Oxidative Stress and Neuroinflammation Induced by Amyloid- β Through Modulation of Glutathione Metabolism," *Journal of Alzheimer's Disease*, vol. 58, no. 2, pp. 549–558, 2017.
- [103] G. L. Case and N. J. Benevenga, "Significance of formate as an intermediate in the oxidation of the methionine, S-methyl-L-cysteine and sarcosine methyl carbons to CO₂ in the rat," *The Journal of Nutrition*, vol. 107, no. 9, pp. 1665–1676, 1977.
- [104] R. D. Steele and N. J. Benevenga, "Identification of 3-methylthiopropionic acid as an intermediate in mammalian methionine metabolism in vitro," *Journal of Biological Chemistry*, vol. 253, no. 21, pp. 7844–7850, 1978.
- [105] A. Finkelstein and N. J. Benevenga, "The effect of methanethiol and methionine toxicity on the activities of cytochrome c oxidase and enzymes involved in protection from peroxidative damage," *The Journal of Nutrition*, vol. 116, no. 2, pp. 204–215, 1986.
- [106] J. T. Dever and A. A. Elfarra, "L-Methionine toxicity in freshly isolated mouse hepatocytes is gender-dependent and mediated in part by transamination," *Journal of Pharmacology and Experimental Therapeutics*, vol. 326, no. 3, pp. 809–817, 2008.
- [107] H. Yamada, N. Akahoshi, S. Kamata et al., "Methionine excess in diet induces acute lethal hepatitis in mice lacking cystathionine γ -lyase, an animal model of cystathioninuria," *Free Radical Biology and Medicine*, vol. 52, no. 9, pp. 1716–1726, 2012.
- [108] P. G. Marchesini, E. Bugianesi, G. Bianchi et al., "Defective methionine metabolism in cirrhosis: relation to severity of liver disease. Hepatology," vol. 16, no. 1, pp. 149–155, 1992.
- [109] P. J. Garlick, "Toxicity of methionine in humans," *The Journal of Nutrition*, vol. 136, pp. 1722S–1725S, 2006.
- [110] M. Costa, B. Pensa, M. Fontana, C. Foppoli, and D. Cavallini, "Transamination of L-cystathionine and related compounds by a bovine liver enzyme. Possible identification with glutamine transaminase," *Biochimica et Biophysica Acta (BBA) - General Subjects*, vol. 881, no. 3, pp. 314–320, 1986.
- [111] B. Pensa, M. Achilli, M. Fontana, A. M. Caccuri, and D. Cavallini, "S-Aminoethyl-L-cysteine transaminase from

- bovine brain: purification to homogeneity and assay of activity in different regions of the brain," *Neurochemistry International*, vol. 15, no. 3, pp. 285–291, 1989.
- [112] M. H. Stipanuk and P. W. Beck, "Characterization of the enzymic capacity for cysteine desulphhydration in liver and kidney of the rat," *Biochemical Journal*, vol. 206, no. 2, pp. 267–277, 1982.
- [113] B. D. Paul and S. H. Snyder, "H₂S signalling through protein sulfhydration and beyond," *Nature Reviews Molecular Cell Biology*, vol. 13, no. 8, pp. 499–507, 2012.
- [114] B. D. Paul and S. H. Snyder, "Gasotransmitter hydrogen sulfide signaling in neuronal health and disease," *Biochemical Pharmacology*, vol. 149, pp. 101–109, 2018.
- [115] M. H. Stipanuk and I. Ueki, "Dealing with methionine/homocysteine sulfur: cysteine metabolism to taurine and inorganic sulfur," *Journal of Inherited Metabolic Disease*, vol. 34, no. 1, pp. 17–32, 2011.
- [116] N. Shibuya, M. Tanaka, M. Yoshida et al., "3-Mercaptopyruvate sulfurtransferase produces hydrogen sulfide and bound sulfane sulfur in the brain," *Antioxidants & Redox Signaling*, vol. 11, no. 4, pp. 703–714, 2009.
- [117] Y. Mikami, N. Shibuya, Y. Kimura, N. Nagahara, Y. Ogasawara, and H. Kimura, "Thioredoxin and dihydrolipoic acid are required for 3-mercaptopyruvate sulfurtransferase to produce hydrogen sulfide," *Biochemical Journal*, vol. 439, no. 3, pp. 479–485, 2011.
- [118] P. M. Ueland, M. A. Mansoor, A. B. Guttormsen et al., "Reduced, oxidized and protein-bound forms of homocysteine and other aminothiols in plasma comprise the redox thiol status—a possible element of the extracellular antioxidant defense system," *The Journal of Nutrition*, vol. 126, Supplement 4, pp. 1281S–1284S, 1996.
- [119] H. Sato, A. Shiiya, M. Kimata et al., "Redox imbalance in cystine/glutamate transporter-deficient mice," *Journal of Biological Chemistry*, vol. 280, no. 45, pp. 37423–37429, 2005.
- [120] D. Cavallini, C. De Marco, B. Mondovì, and B. G. Mori, "The cleavage of cystine by cystathionase and the transulfuration of hypotaurine," *Enzymologia*, vol. 22, pp. 161–173, 1960.
- [121] D. Cavallini, B. Mondovì, C. De Marco, and A. Scioscia-Santoro, "The mechanism of desulphhydration of cysteine," *Enzymologia*, vol. 24, pp. 253–266, 1962.
- [122] T. Chiku, D. Padovani, W. Zhu, S. Singh, V. Vitvitsky, and R. Banerjee, "H₂S biogenesis by human cystathionine γ -lyase leads to the novel sulfur metabolites lanthionine and homolanthionine and is responsive to the grade of hyperhomocysteinemia," *Journal of Biological Chemistry*, vol. 284, no. 17, pp. 11601–11612, 2009.
- [123] T. Yamanishi and S. Tuboi, "The mechanism of the L-cystine cleavage reaction catalyzed by rat liver γ -cystathionase1," *The Journal of Biochemistry*, vol. 89, no. 6, pp. 1913–1921, 1981.
- [124] M. Orłowski and A. Meister, "Isolation of highly purified γ -glutamylcysteine synthetase from rat kidney," *Biochemistry*, vol. 10, no. 3, pp. 372–380, 1971.
- [125] R. Dringen, B. Pfeiffer, and B. Hamprecht, "Synthesis of the antioxidant glutathione in neurons: supply by astrocytes of Cys Gly as precursor for neuronal glutathione," *The Journal of Neuroscience*, vol. 19, no. 2, pp. 562–569, 1999.
- [126] J. E. Snoke, "Isolation and properties of yeast glutathione synthetase," *Journal of Biological Chemistry*, vol. 213, no. 2, pp. 813–824, 1955.
- [127] S. C. Lu, "Regulation of glutathione synthesis," *Molecular Aspects of Medicine*, vol. 30, no. 1–2, pp. 42–59, 2009.
- [128] M. H. Hanigan, "Gamma-glutamyl transpeptidase: redox regulation and drug resistance," in *Advances in Cancer Research*, vol. 122, pp. 103–141, Academic Press, 2014.
- [129] A. K. Bachhawat and A. Kaur, "Glutathione degradation," *Antioxidants & Redox Signaling*, vol. 27, no. 15, pp. 1200–1216, 2017.
- [130] M. Inoue, "Glutathionists in the battlefield of gamma-glutamyl cycle," *Archives of Biochemistry and Biophysics*, vol. 595, pp. 61–63, 2016.
- [131] G. J. McBean, M. Aslan, H. R. Griffiths, and R. C. Torrão, "Thiol redox homeostasis in neurodegenerative disease," *Redox Biology*, vol. 5, pp. 186–194, 2015.
- [132] B. D. Paul, J. I. Sbdio, and S. H. Snyder, "Cysteine metabolism in neuronal redox homeostasis," *Trends in Pharmacological Sciences*, vol. 39, no. 5, pp. 513–524, 2018.
- [133] R. Leonardi, Y. M. Zhang, C. O. Rock, and S. Jackowski, "Coenzyme A: back in action," *Progress in Lipid Research*, vol. 44, no. 2–3, pp. 125–153, 2005.
- [134] D. Cavallini, S. Dupre, M. T. Graziani, and M. G. Tinti, "Identification of pantethinase in horse kidney extract," *FEBS Letters*, vol. 1, no. 2, pp. 119–121, 1968.
- [135] B. Maras, D. Barra, S. Duprè, and G. Pitari, "Is pantetheinase the actual identity of mouse and human vanin-1 proteins?," *FEBS Letters*, vol. 461, no. 3, pp. 149–152, 1999.
- [136] R. Scandurra, V. Consalvi, C. De Marco, L. Politi, and D. Cavallini, "Lanthionine decarboxylation by animal tissues," *Life Sciences*, vol. 24, no. 21, pp. 1925–1930, 1979.
- [137] M. Besouw, H. Blom, A. Tangerman, A. de Graaf-Hess, and E. Levchenko, "The origin of halitosis in cystinotic patients due to cysteamine treatment," *Molecular Genetics and Metabolism*, vol. 91, no. 3, pp. 228–233, 2007.
- [138] M. Besouw and E. Levchenko, "Pharmacokinetics of cysteamine in a cystinosis patient treated with hemodialysis," *Pediatric Nephrology*, vol. 26, pp. 639–640, 2011.
- [139] C. A. O'Brian and F. Chu, "Post-translational disulfide modifications in cell signaling - role of inter-protein, intra-protein, S-glutathionyl, and S-cysteaminyll disulfide modifications in signal transmission," *Free Radical Research*, vol. 39, no. 5, pp. 471–480, 2005.
- [140] G. Pitari, F. Malergue, F. Martin et al., "Pantetheinase activity of membrane-bound Vanin-1: lack of free cysteamine in tissues of Vanin-1 deficient mice," *FEBS Letters*, vol. 483, no. 2–3, pp. 149–154, 2000.
- [141] L. Di Leandro, B. Maras, M. E. Schininà et al., "Cystamine restores GSTA3 levels in Vanin-1 null mice," *Free Radical Biology and Medicine*, vol. 44, no. 6, pp. 1088–1096, 2008.
- [142] M. Besouw, R. Masereeuw, L. Van Den Heuvel, and E. Levchenko, "Cysteamine: an old drug with new potential," *Drug Discovery Today*, vol. 18, no. 15–16, pp. 785–792, 2013.
- [143] C. Gibrat and F. Cicchetti, "Potential of cystamine and cysteamine in the treatment of neurodegenerative diseases," *Progress in Neuro-Psychopharmacology and Biological Psychiatry*, vol. 35, no. 2, pp. 380–389, 2011.
- [144] L. Gallego-Villar, L. Hannibal, J. Häberle et al., "Cysteamine revisited: repair of arginine to cysteine mutations," *Journal of Inherited Metabolic Disease*, vol. 40, no. 4, pp. 555–567, 2017.
- [145] R. J. Huxtable, "Physiological actions of taurine," *Physiological Reviews*, vol. 72, no. 1, pp. 101–164, 1992.

- [146] J. E. Dominy, C. R. Simmons, L. L. Hirschberger, J. Hwang, R. M. Coloso, and M. H. Stipanuk, "Discovery and characterization of a second mammalian thiol dioxygenase, cysteamine dioxygenase," *Journal of Biological Chemistry*, vol. 282, no. 35, pp. 25189–25198, 2007.
- [147] B. Sarkar, M. Kulharia, and A. K. Mantha, "Understanding human thiol dioxygenase enzymes: structure to function, and biology to pathology," *International Journal of Experimental Pathology*, vol. 98, no. 2, pp. 52–66, 2017.
- [148] L. Ewetz and B. Sörbo, "Characteristics of the cysteinesulfinate-forming enzyme system in rat liver," *Biochimica et Biophysica Acta (BBA) - Enzymology and Biological Oxidation*, vol. 128, no. 2, pp. 296–305, 1966.
- [149] D. Cavallini, R. Scandurra, and C. De Marco, "The enzymatic oxidation of cysteamine to hypotaurine in the presence of," *Journal of Biological Chemistry*, vol. 238, pp. 2999–3005, 1963.
- [150] M. H. Stipanuk, J. E. Dominy, J.-I. Lee, and R. M. Coloso, "Mammalian cysteine metabolism: new insights into regulation of cysteine metabolism," *The Journal of Nutrition*, vol. 136, no. 6, pp. 1652S–1659S, 2006.
- [151] J. Dominy, S. Eller, and R. Dawson, "Building biosynthetic schools: reviewing compartmentation of CNS taurine synthesis," *Neurochemical Research*, vol. 29, pp. 97–103, 2004.
- [152] C. E. Wright, H. H. Tallan, and Y. Y. Lin, "Taurine: biological update," *Annual Review of Biochemistry*, vol. 55, no. 1, pp. 427–453, 1986.
- [153] L. Pecci, M. Costa, G. Montefoschi, A. Antonucci, and D. Cavallini, "Oxidation of hypotaurine to taurine with photochemically generated singlet oxygen: the effect of azide," *Biochemical and Biophysical Research Communications*, vol. 254, no. 3, pp. 661–665, 1999.
- [154] M. Fontana, D. Amendola, E. Orsini, A. Boffi, and L. Pecci, "Oxidation of hypotaurine and cysteine sulphinic acid by peroxynitrite," *Biochemical Journal*, vol. 389, no. 1, pp. 233–240, 2005.
- [155] M. Fontana, S. Duprè, and L. Pecci, "The reactivity of hypotaurine and cysteine sulfinic acid with peroxynitrite," in *Taurine 6*, vol. 583, pp. 15–24, Springer, 2006.
- [156] A. Baseggio Conrado, M. D'Angelantonio, M. D'Erme, L. Pecci, and M. Fontana, "The interaction of hypotaurine and other sulfinates with reactive oxygen and nitrogen species: a survey of reaction mechanisms," in *Advances in Experimental Medicine and Biology*, vol. 975, pp. 573–583, Springer, 2017.
- [157] A. Baseggio Conrado, M. D'Angelantonio, A. Torreggiani, L. Pecci, and M. Fontana, "Reactivity of hypotaurine and cysteine sulfinic acid toward carbonate radical anion and nitrogen dioxide as explored by the peroxidase activity of Cu, Zn superoxide dismutase and by pulse radiolysis," *Free Radical Research*, vol. 48, no. 11, pp. 1300–1310, 2014.
- [158] A. Baseggio Conrado, L. Pecci, E. Capuozzo, and M. Fontana, "Oxidation of hypotaurine and cysteine sulfinic acid by peroxidase-generated reactive species," in *Taurine 9*, vol. 803, pp. 41–51, Springer, 2015.
- [159] A. Baseggio Conrado, L. Pecci, and M. Fontana, "Effects of hypotaurine on carbonate radical anion and nitrogen dioxide radical generated by peroxidase activity of Cu, Zn-superoxide dismutase," *Free Radical Biology and Medicine*, vol. 65, pp. S23–S24, 2013.
- [160] S. Veeravalli, I. R. Phillips, R. T. Freire, D. Varshavi, J. R. Everett, and E. A. Shephard, "Flavin-containing monooxygenase 1 catalyzes the production of taurine from hypotaurine," *Drug Metabolism and Disposition*, vol. 48, pp. 378–385, 2020.
- [161] J. T. Brosnan, K. C. Man, D. E. Hall, S. A. Colbourne, and M. E. Brosnan, "Interorgan metabolism of amino acids in streptozotocin-diabetic ketoacidotic rat," *American Journal of Physiology-Endocrinology and Metabolism*, vol. 244, no. 2, pp. E151–E158, 1983.
- [162] A. Francioso, S. Fanelli, D. Vigli et al., "HPLC determination of bioactive sulfur compounds, amino acids and biogenic amines in biological specimens," *Advances in Experimental Medicine and Biology*, vol. 975, pp. 535–549, 2017.
- [163] H. Ripps and W. Shen, "Review: taurine: a "very essential" amino acid," *Molecular Vision*, vol. 18, pp. 2673–2686, 2012.
- [164] K. C. Hayes and J. A. Sturman, "Taurine in metabolism," *Annual Review of Nutrition*, vol. 1, pp. 401–425, 1981.
- [165] N. Froger, R. R. Sahel, and S. Picaud, "Taurine deficiency and the eye," *Handbook of Nutrition, Diet and the Eye*, S. Victor, Ed., pp. 505–512, Preedy Academic Press Inc, 2014.
- [166] V. Vitvitsky, S. K. Garg, and R. Banerjee, "Taurine biosynthesis by neurons and astrocytes," *Journal of Biological Chemistry*, vol. 286, no. 37, pp. 32002–32010, 2011.
- [167] R. Banerjee, V. Vitvitsky, and S. K. Garg, "The undertow of sulfur metabolism on glutamatergic neurotransmission," *Trends in Biochemical Sciences*, vol. 33, no. 9, pp. 413–419, 2008.
- [168] M. F. Olive, "Interactions between taurine and ethanol in the central nervous system," *Amino Acids*, vol. 23, no. 4, pp. 345–357, 2002.
- [169] A. El Idrissi, "Taurine increases mitochondrial buffering of calcium: role in neuroprotection," *Amino Acids*, vol. 34, no. 2, pp. 321–328, 2008.
- [170] O. I. Aruoma, B. Halliwell, B. M. Hoey, and J. Butler, "The antioxidant action of taurine, hypotaurine and their metabolic precursors," *Biochemical Journal*, vol. 256, no. 1, pp. 251–255, 1988.
- [171] M. Fontana, F. Giovannitti, and L. Pecci, "The protective effect of hypotaurine and cysteine sulphinic acid on peroxynitrite-mediated oxidative reactions," *Free Radical Research*, vol. 42, no. 4, pp. 320–330, 2008.
- [172] M. Fontana, L. Pecci, S. Duprè, and D. Cavallini, "Antioxidant properties of sulfinates: protective effect of hypotaurine on peroxynitrite-dependent damage," *Neurochemical Research*, vol. 29, no. 1, pp. 111–116, 2004.
- [173] J. A. Sturman, "Formation and accumulating of hypotaurine in rat liver regenerating after partial hepatectomy," *Life Sciences*, vol. 26, no. 4, pp. 267–272, 1980.
- [174] D. B. Learn, V. A. Fried, and E. L. Thomas, "Taurine and hypotaurine content of human leukocytes," *Journal of Leukocyte Biology*, vol. 48, no. 2, pp. 174–182, 1990.
- [175] R. P. Holmes, H. O. Goodman, Z. K. Shihabi, and J. Jarow, "The taurine and hypotaurine content of human semen," *Journal of Andrology*, vol. 13, no. 3, pp. 289–292, 1992.
- [176] A. B. Conrado, S. Maina, H. Moseley et al., "Carbonate anion radical generated by the peroxidase activity of copper-zinc superoxide dismutase: scavenging of radical and protection of enzyme by hypotaurine and cysteine sulfinic acid," in *Advances in Experimental Medicine and Biology*, vol. 975, pp. 551–561, Springer, 2017.
- [177] A. K. Mustafa, M. M. Gadalla, N. Sen et al., "H2S signals through protein S-sulhydration," *Science Signaling*, vol. 2, no. 96, article ra72, 2009.

- [178] M. R. Filipovic, J. Zivanovic, B. Alvarez, and R. Banerjee, "Chemical biology of H₂S signaling through persulfidation," *Chemical Reviews*, vol. 118, pp. 1253–1337, 2018.
- [179] T. Ida, T. Sawa, H. Ihara et al., "Reactive cysteine persulfides and S-polythiolation regulate oxidative stress and redox signaling," *Proceedings of the National Academy of Sciences*, vol. 111, no. 21, pp. 7606–7611, 2014.
- [180] T. V. Mishanina, M. Libiad, and R. Banerjee, "Biogenesis of reactive sulfur species for signaling by hydrogen sulfide oxidation pathways," *Nature Chemical Biology*, vol. 11, pp. 457–464, 2015.
- [181] J. I. Toohey, "Sulfur signaling: is the agent sulfide or sulfane?," *Analytical Biochemistry*, vol. 413, no. 1, pp. 1–7, 2011.
- [182] N. E. Franconeri, S. J. Carrington, and J. M. Fukuto, "The reaction of H₂S with oxidized thiols: generation of persulfides and implications to H₂S biology," *Archives of Biochemistry and Biophysics*, vol. 516, pp. 146–153, 2011.
- [183] M. R. Jackson, S. L. Melideo, and M. S. Jorns, "Human sulfide: quinone oxidoreductase catalyzes the first step in hydrogen sulfide metabolism and produces a sulfane sulfur metabolite," *Biochemistry*, vol. 51, no. 34, pp. 6804–6815, 2012.
- [184] M. Libiad, P. K. Yadav, V. Vitvitsky, M. Martinov, and R. Banerjee, "Organization of the human mitochondrial hydrogen sulfide oxidation pathway," *Journal of Biological Chemistry*, vol. 289, no. 45, pp. 30901–30910, 2014.
- [185] O. Kabil and R. Banerjee, "Enzymology of H₂S biogenesis, decay and signaling," *Antioxidants & Redox Signaling*, vol. 20, no. 5, pp. 770–782, 2014.
- [186] P. K. Yadav, M. Martinov, V. Vitvitsky et al., "Biosynthesis and reactivity of cysteine persulfides in signaling," *Journal of the American Chemical Society*, vol. 138, no. 1, pp. 289–299, 2016.
- [187] P. K. Yadav, K. Yamada, T. Chiku, M. Koutmos, and R. Banerjee, "Structure and kinetic analysis of H₂S production by human mercaptopyruvate sulfurtransferase," *Journal of Biological Chemistry*, vol. 288, no. 27, pp. 20002–20013, 2013.
- [188] Y. Kimura, S. Koike, N. Shibuya, D. Lefer, Y. Ogasawara, and H. Kimura, "3-Mercaptopyruvate sulfurtransferase produces potential redox regulators cysteine- and glutathione-persulfide (Cys-SSH and GSSH) together with signaling molecules H₂S₂, H₂S₃ and H₂S," *Scientific Reports*, vol. 7, 2017.
- [189] T. Akaike, T. Ida, F.-Y. Wei et al., "CysteinyI-tRNA synthetase governs cysteine polysulfidation and mitochondrial bioenergetics," *Nature Communications*, vol. 8, no. 1, p. 1177, 2017.
- [190] G. X. Luo and P. M. Horowitz, "The sulfurtransferase activity and structure of rhodanese are affected by site-directed replacement of Arg-186 or Lys-249," *Journal of Biological Chemistry*, vol. 269, no. 11, pp. 8220–8225, 1994.
- [191] D. Cavallini, C. De Marco, and B. Mondovì, "Chromatographic evidence on the occurrence of thiotaurine in the urine of rats fed with cystine," *Journal of Biological Chemistry*, vol. 234, no. 4, pp. 854–857, 1959.
- [192] B. Sörbo, "Enzymic transfer of sulfur from mercaptopyruvate to sulfite or sulfates," *Biochimica et Biophysica Acta*, vol. 24, no. C, pp. 324–329, 1957.
- [193] T. R. Chauncey and J. Westley, "The catalytic mechanism of yeast thiosulfate reductase," *Journal of Biological Chemistry*, vol. 258, no. 24, pp. 15037–15045, 1983.
- [194] E. Capuozzo, L. Pecci, A. Baseggio Conrado, and M. Fontana, "Thiotaurine prevents apoptosis of human neutrophils: a putative role in inflammation," in *Advances in Experimental Medicine and Biology*, vol. 775, pp. 227–236, Springer, 2013.
- [195] E. Capuozzo, A. Baseggio Conrado, and M. Fontana, "Thiotaurine modulates human neutrophil activation," in *Advances in Experimental Medicine and Biology*, vol. 803, pp. 145–155, Springer, 2015.
- [196] E. Capuozzo, A. Giorgi, S. Canterini et al., "A proteomic approach to study the effect of thiotaurine on human neutrophil activation," in *Advances in Experimental Medicine and Biology*, vol. 975, pp. 563–571, Springer, 2017.
- [197] J. Dragotto, E. Capuozzo, M. Fontana, A. Curci, M. T. Fiorenza, and S. Canterini, "Thiotaurine protects mouse cerebellar granule neurons from potassium deprivation-induced apoptosis by inhibiting the activation of caspase-3," in *Advances in Experimental Medicine and Biology*, vol. 803, pp. 513–523, Springer, 2015.
- [198] M. Costa, B. Pensa, B. Di Costanzo, R. Coccia, and D. Cavallini, "Transamination of l-cystathionine and related compounds by bovine brain glutamine transaminase," *Neurochemistry International*, vol. 10, no. 3, pp. 377–382, 1987.
- [199] M. Costa, B. Pensa, C. Blarmino, and D. Cavallini, "New enzymatic changes of L-cystathionine catalyzed by bovine tissue extracts," *Physiological Chemistry and Physics and Medical NMR*, vol. 17, no. 1, pp. 107–111, 1985.
- [200] T. S. Soper and J. M. Manning, "β Elimination of β-halo substrates by d-amino acid transaminase associated with inactivation of the enzyme. Trapping of a key intermediate in the reaction," *Biochemistry*, vol. 17, no. 16, pp. 3377–3384, 1978.
- [201] G. Ricci, L. Santoro, M. Achilli, R. M. Matarese, M. Nardini, and D. Cavallini, "Similarity of the oxidation products of L-cystathionine by L-amino acid oxidase to those excreted by cystathioninuric patients," *Journal of Biological Chemistry*, vol. 258, no. 17, pp. 10511–10517, 1983.
- [202] D. Cavallini, G. Ricci, and G. Federici, "The ketamine derivatives of thialysine, lanthionine, cystathionine, cystine: preparation and properties," *Progress in Clinical and Biological Research*, vol. 125, pp. 355–363, 1983.
- [203] L. Pecci, M. Costa, F. Pinnen, A. Antonucci, and D. Cavallini, "Properties of the phenylthiohydantoin derivatives of some sulfur-containing cyclic amino acids," *Physiological Chemistry and Physics and Medical NMR*, vol. 20, no. 3, pp. 199–203, 1988.
- [204] M. Nardini, G. Ricci, L. Vesci, L. Pecci, and D. Cavallini, "Bovine brain ketimine reductase," *Biochimica et Biophysica Acta (BBA) - Protein Structure and Molecular Enzymology*, vol. 957, no. 2, pp. 286–292, 1988.
- [205] R. M. Matarese, S. P. Solinas, G. Montefoschi, G. Ricci, and D. Cavallini, "Identification of 1, 4-thiomorpholine-3-carboxylic acid (TMA) in normal human urine," *FEBS Letters*, vol. 250, no. 1, pp. 75–77, 1989.
- [206] D. Cavallini, R. M. Matarese, L. Pecci, and G. Ricci, "1, 4-Thiomorpholine-3, 5-dicarboxylic acid, a novel cyclic imino acid detected in bovine brain," *FEBS Letters*, vol. 192, no. 2, pp. 247–250, 1985.
- [207] M. Nardini, R. M. Matarese, L. Pecci, A. Antonucci, G. Ricci, and D. Cavallini, "Detection of 2H-1, 4-thiazine-5, 6-dihydro-3-carboxylic acid (aminoethylcysteine ketimine) in the bovine brain," *Biochemical and Biophysical Research Communications*, vol. 166, no. 3, pp. 1251–1256, 1990.
- [208] S. Yu, K. Sugahara, J. Zhang et al., "Simultaneous determination of urinary cystathionine, lanthionine, S-(2-aminoethyl)-

- L-cysteine and their cyclic compounds using liquid chromatography-mass spectrometry with atmospheric pressure chemical ionization," *Journal of Chromatography B: Biomedical Sciences and Applications*, vol. 698, no. 1–2, pp. 301–307, 1997.
- [209] M. Fontana, A. Brunori, M. Costa, and A. Antonucci, "Detection of cystathionine ketimine and lanthionine ketimine in human brain," *Neurochemical Research*, vol. 22, no. 7, pp. 821–824, 1997.
- [210] K. Hensley, K. Venkova, and A. Christov, "Emerging biological importance of central nervous system lanthionines," *Molecules*, vol. 15, no. 8, pp. 5581–5594, 2010.
- [211] N. Marangoni, K. Kowal, Z. Deliu, K. Hensley, and D. L. Feinstein, "Neuroprotective and neurotrophic effects of lanthionine ketimine ester," *Neuroscience Letters*, vol. 664, pp. 28–33, 2018.
- [212] J. L. Dupree, P. E. Polak, K. Hensley, D. Pelligrino, and D. L. Feinstein, "Lanthionine ketimine ester provides benefit in a mouse model of multiple sclerosis," *Journal of Neurochemistry*, vol. 134, no. 2, pp. 302–314, 2015.
- [213] K. Hensley, S. P. Gabbita, K. Venkova et al., "A derivative of the brain metabolite lanthionine ketimine improves cognition and diminishes pathology in the 3×Tg-AD mouse model of Alzheimer disease," *Journal of Neuropathology & Experimental Neurology*, vol. 72, no. 10, pp. 955–969, 2013.
- [214] A. C. Hensley, S. Kamat, X. C. Zhang, K. W. Jackson, S. Snow, and J. Post, "Proteomic identification of binding partners for the brain metabolite lanthionine ketimine (LK) and documentation of LK effects on microglia and motoneuron cell cultures," *Journal of Neuroscience*, vol. 30, no. 8, pp. 2979–2988, 2010.
- [215] C. J. Bataille, M. B. Brennan, S. Byrne et al., "Thiazolidine derivatives as potent and selective inhibitors of the PIM kinase family," *Bioorganic & Medicinal Chemistry*, vol. 25, no. 9, pp. 2657–2665, 2017.
- [216] A. Ahmad, A. Ahmad, R. Sudhakar et al., "Designing, synthesis, and antimicrobial action of oxazoline and thiazoline derivatives of fatty acid esters," *Journal of Biomolecular Structure and Dynamics*, vol. 35, no. 15, pp. 3412–3431, 2017.
- [217] W. Suvachittanont, Y. Kurashima, H. Esumi, and M. Tsuda, "Formation of thiazolidine-4-carboxylic acid (thioprolin), an effective nitrite-trapping agent in human body, in *Parkia speciosa* seeds and other edible leguminous seeds in Thailand," *Food Chemistry*, vol. 55, no. 4, pp. 359–363, 1996.
- [218] D. Cavallini, B. Mondovi, and C. De Marco, "Thiazoline carboxylic acid from formylcysteine," *Experientia*, vol. 13, no. 11, pp. 436–438, 1957.
- [219] H. Kumagai, K. I. Mukaisho, H. Sugihara, K. Miwa, G. Yamamoto, and T. Hattori, "Thioprolin inhibits development of esophageal adenocarcinoma induced by gastro-duodenal reflux in rats," *Carcinogenesis*, vol. 25, no. 5, pp. 723–727, 2004.
- [220] H. U. Weber, J. F. Fleming, and J. Miquel, "Thiazolidine-4-carboxylic acid, a physiologic sulfhydryl antioxidant with potential value in geriatric medicine," *Archives of Gerontology and Geriatrics*, vol. 1, pp. 299–310, 1982.
- [221] K. R. Martin, "The bioactive agent ergothioneine, a key component of dietary mushrooms, inhibits monocyte binding to endothelial cells characteristic of early cardiovascular disease," *Journal of Medicinal Food*, vol. 13, no. 6, pp. 1340–1346, 2010.
- [222] I. Petrikovics, D. E. Thompson, G. A. Rockwood et al., "Organ-distribution of the metabolite 2-aminothiazoline-4-carboxylic acid in a rat model following cyanide exposure," *Biomarkers*, vol. 16, no. 8, pp. 686–690, 2011.
- [223] D. Cavallini, C. De Marco, and B. Mondovi, "The oxidation of cystamine and other sulfur-diamines by diamine-oxidase preparations," *Experientia*, vol. 12, no. 10, pp. 377–379, 1956.
- [224] D. Cavallini, G. Federici, S. Dupre, C. Cannella, and R. Scandurra, "Ambiguities in the enzymology of sulfur-containing compounds," *Pure and Applied Chemistry*, vol. 52, no. 1, pp. 147–155, 1980.
- [225] I. Winge, K. Teigen, A. Fossbakk et al., "Mammalian CSAD and GADL1 have distinct biochemical properties and patterns of brain expression," *Neurochemistry International*, vol. 90, pp. 173–184, 2015.
- [226] Q. Shi, J. E. Savage, S. J. Hufeisen et al., "L-Homocysteine sulfonic acid and other acidic homocysteine derivatives are potent and selective metabotropic glutamate receptor agonists," *Journal of Pharmacology and Experimental Therapeutics*, vol. 305, no. 1, pp. 131–142, 2003.
- [227] M. Costa, L. Vesci, M. Fontana, S. P. Solinas, S. Dupre, and D. Cavallini, "Displacement of [3H] GABA binding to bovine brain receptors by sulfur-containing analogues," *Neurochemistry International*, vol. 17, no. 4, pp. 547–551, 1990.
- [228] A. Khan, Y. Choi, J. H. Back, S. Lee, S. H. Jee, and Y. H. Park, "High-resolution metabolomics study revealing l-homocysteine sulfonic acid, cysteic acid, and carnitine as novel biomarkers for high acute myocardial infarction risk," *Metabolism*, vol. 104, article 154051, 2020.
- [229] K. S. McCully, "Homocysteine, vitamins, and vascular disease prevention," *The American Journal of Clinical Nutrition*, vol. 86, no. 5, pp. 1563S–1568S, 2007.
- [230] S. Seshadri, A. Beiser, J. Selhub et al., "Plasma homocysteine as a risk factor for dementia and Alzheimer's disease," *New England Journal of Medicine*, vol. 346, no. 7, pp. 476–483, 2002.
- [231] N. Fillon-Emery, A. Chango, C. Mircher et al., "Homocysteine concentrations in adults with trisomy 21: effect of B vitamins and genetic polymorphisms," *The American Journal of Clinical Nutrition*, vol. 80, pp. 1551–1557, 2004.
- [232] B. Chadeaux, I. Ceballos, M. Hamet et al., "Is absence of atheroma in Down syndrome due to decreased homocysteine levels?," *The Lancet*, vol. 332, no. 8613, p. 741, 1988.
- [233] P. Kamoun, M.-C. Belardinelli, A. Chabli, K. Lallouchi, and B. Chadeaux-Vekemans, "Endogenous hydrogen sulfide overproduction in Down syndrome," *American Journal of Medical Genetics*, vol. 116A, no. 3, pp. 310–311, 2003.
- [234] M. Pogribna, S. Melnyk, I. Pogribny, A. Chango, P. Yi, and S. J. James, "Homocysteine metabolism in children with down syndrome: in vitro modulation," *The American Journal of Human Genetics*, vol. 69, no. 1, pp. 88–95, 2001.
- [235] T. Majtan, J. Krijt, J. Sokolová et al., "Biogenesis of hydrogen sulfide and thioethers by cystathionine beta-synthase," *Antioxidants & Redox Signaling*, vol. 28, no. 4, pp. 311–323, 2018.
- [236] V. Kožich, J. Krijt, J. Sokolová et al., "Thioethers as markers of hydrogen sulfide production in homocystinurias," *Biochimie*, vol. 126, pp. 14–20, 2016.
- [237] W. Shen, M. K. McGath, R. Evande, and D. B. Berkowitz, "A continuous spectrophotometric assay for human cystathionine beta-synthase," *Analytical Biochemistry*, vol. 342, no. 1, pp. 103–110, 2005.

- [238] J. T. Pinto, T. Khomenko, S. Szabo et al., "Measurement of sulfur-containing compounds involved in the metabolism and transport of cysteamine and cystamine. Regional differences in cerebral metabolism," *Journal of Chromatography B*, vol. 877, no. 28, pp. 3434–3441, 2009.
- [239] G. I. Giles and C. Jacob, "Reactive sulfur species: an emerging concept in oxidative stress," *Biological Chemistry*, vol. 383, no. 3–4, pp. 375–388, 2002.
- [240] G. I. Giles, K. M. Tasker, and C. Jacob, "Hypothesis: the role of reactive sulfur species in oxidative stress," *Free Radical Biology and Medicine*, vol. 31, no. 10, pp. 1279–1283, 2001.
- [241] J. Li, F. L. Huang, and K. P. Huang, "Glutathiolation of proteins by glutathione disulfide S-oxide derived from S-nitrosoglutathione. Modifications of rat brain neurogranin/RC3 and neuromodulin/GAP-43," *Journal of Biological Chemistry*, vol. 276, no. 5, p. 3098, 2001.
- [242] T. Okamoto, T. Akaike, T. Sawa, Y. Miyamoto, A. Van der Vliet, and H. Maeda, "Activation of matrix metalloproteinases by peroxynitrite-induced protein S-glutathiolation via disulfide S-oxide formation," *Journal of Biological Chemistry*, vol. 276, no. 31, pp. 29596–29602, 2001.
- [243] B. C. Smith and M. A. Marletta, "Mechanisms of S-nitrosothiol formation and selectivity in nitric oxide signaling," *Current Opinion in Chemical Biology*, vol. 16, pp. 498–506, 2012.
- [244] R. J. Singh, N. Hogg, J. Joseph, and B. Kalyanaraman, "Mechanism of nitric oxide release from S-nitrosothiols," *Chemical Communications*, vol. 271, no. 31, pp. 18596–18603, 1996.
- [245] H. AL-SA'DONI and A. FERRO, "S-Nitrosothiols: a class of nitric oxide-donor drugs," *Clinical Science*, vol. 98, no. 5, pp. 507–520, 2000.
- [246] D. R. Arnelle and J. S. Stamler, "NO⁺, NO, and NO⁻ donation by S-nitrosothiols: implications for regulation of physiological functions by S-nitrosylation and acceleration of disulfide formation," *Archives of Biochemistry and Biophysics*, vol. 318, no. 2, pp. 279–285, 1995.
- [247] T. Nauser, W. H. Koppenol, and C. Schöneich, "Protein thiyl radical reactions and product formation: a kinetic simulation," *Free Radical Biology and Medicine*, vol. 80, pp. 158–163, 2015.
- [248] H. D. Venters, L. E. Bonilla, T. Jensen et al., "Heme from Alzheimer's brain inhibits muscarinic receptor binding via thiyl radical generation," *Brain Research*, vol. 764, no. 1–2, pp. 93–100, 1997.
- [249] K. R. Maples, C. H. Kennedy, S. J. Jordan, and R. P. Mason, "In vivo thiyl free radical formation from hemoglobin following administration of hydroperoxides," *Archives of Biochemistry and Biophysics*, vol. 277, no. 2, pp. 402–409, 1990.
- [250] M. D. Sevilla, D. Becker, and M. Yan, "The formation and structure of the sulfoxyl radicals RSO·, RSOO·, RSO₂·, and RSO₂OO· from the reaction of cysteine, glutathione and penicillamine thiyl radicals with molecular oxygen," *International Journal of Radiation Biology*, vol. 57, no. 1, pp. 65–81, 1990.
- [251] D. P. Jones, "Redox potential of GSH/GSSG couple: assay and biological significance," *Methods in Enzymology*, vol. 348, pp. 93–112, 2002.
- [252] O. Zitka, S. Skalickova, J. Gumulec et al., "Redox status expressed as GSH: GSSG ratio as a marker for oxidative stress in paediatric tumour patients," *Oncology Letters*, vol. 4, no. 6, pp. 1247–1253, 2012.
- [253] W. Maret, C. Jacob, B. L. Vallee, and E. H. Fischer, "Inhibitory sites in enzymes: zinc removal and reactivation by thioinein," *Proceedings of the National Academy of Sciences*, vol. 96, no. 5, pp. 1936–1940, 1999.
- [254] E. M. Hanschmann, J. R. Godoy, C. Berndt, C. Hudemann, and C. H. Lillig, "Thioredoxins, glutaredoxins, and peroxiredoxins-molecular mechanisms and health significance: from cofactors to antioxidants to redox signaling," *Antioxidants and Redox Signaling*, vol. 19, no. 13, pp. 1539–1605, 2013.
- [255] M. Conrad, G. W. Bornkamm, and M. Brielmeier, "Mitochondrial and cytosolic thioredoxin reductase knockout mice," in *Selenium: Its Molecular Biology and Role in Human Health*, pp. 195–206, Springer US, Boston, MA, 2nd edition, 2006.
- [256] H. Nakamura, "Extracellular functions of thioredoxin," in *The Biology of Extracellular Molecular Chaperones*, pp. 184–195, Wiley, 2008.
- [257] Y. Matsuo and J. Yodoi, "Extracellular thioredoxin: a therapeutic tool to combat inflammation," *Cytokine and Growth Factor Reviews*, vol. 24, pp. 345–353, 2013.
- [258] A. P. Fernandes and A. Holmgren, "Glutaredoxins: glutathione-dependent redox enzymes with functions far beyond a simple thioredoxin backup system," *Antioxidants and Redox Signaling*, vol. 6, pp. 63–74, 2004.

Research Article

Allylmethylsulfide, a Sulfur Compound Derived from Garlic, Attenuates Isoproterenol-Induced Cardiac Hypertrophy in Rats

Soheb Anwar Mohammed,¹ Bugga Paramesha,¹ Yashwant Kumar,¹ Ubaid Tariq,¹ Sudheer Kumar Arava ,² and Sanjay Kumar Banerjee ^{1,3}

¹Non-Communicable Diseases Group, Translational Health Science and Technology Institute (THSTI), 121001, Faridabad, India

²Department of Pathology, All India Institute of Medical Sciences, New Delhi 110029, India

³Department of Biotechnology, National Institute of Pharmaceutical Education and Research (NIPER), Guwahati, Assam 781101, India

Correspondence should be addressed to Sanjay Kumar Banerjee; skbanerjee@thsti.res.in

Received 30 January 2020; Accepted 25 March 2020; Published 12 June 2020

Academic Editor: Luciana Mosca

Copyright © 2020 Soheb Anwar Mohammed et al. This is an open access article distributed under the Creative Commons Attribution License, which permits unrestricted use, distribution, and reproduction in any medium, provided the original work is properly cited.

Allylmethylsulfide (AMS) is a novel sulfur metabolite found in the garlic-fed serum of humans and animals. In the present study, we have observed that AMS is safe on chronic administration and has a potential antihypertrophic effect. Chronic administration of AMS for 30 days did not cause any significant differences in the body weight, electrocardiogram, food intake, serum biochemical parameters, and histopathology of vital organs. Single-dose pharmacokinetics of AMS suggests that AMS is rapidly metabolized into Allylmethylsulfoxide (AMSO) and Allylmethylsulfone (AMSO₂). To evaluate the efficacy of AMS, cardiac hypertrophy was induced by subcutaneous implantation of ALZET[®] osmotic minipump containing isoproterenol (~5 mg/kg/day), cotreated with AMS (25 and 50 mg/kg/day) and enalapril (10 mg/kg/day) for 2 weeks. AMS and enalapril significantly reduced cardiac hypertrophy as studied by the heart weight to body weight ratio and mRNA expression of fetal genes (ANP and β -MHC). We have observed that TBARS, a parameter of lipid peroxidation, was reduced and the antioxidant enzymes (glutathione, catalase, and superoxide dismutase) were improved in the AMS and enalapril-cotreated hypertrophic hearts. The extracellular matrix (ECM) components such as matrix metalloproteinases (MMP2 and MMP9) were significantly upregulated in the diseased hearts; however, with the AMS and enalapril, it was preserved. Similarly, caspases 3, 7, and 9 were upregulated in hypertrophic hearts, and with the AMS and enalapril treatment, they were reduced. Further to corroborate this finding with *in vitro* data, we have checked the nuclear expression of caspase 3/7 in the H9c2 cells treated with isoproterenol and observed that AMS cotreatment reduced it significantly. Histopathological investigation of myocardium suggests AMS and enalapril treatment reduced fibrosis in hypertrophied hearts. Based on our experimental results, we conclude that AMS, an active metabolite of garlic, could reduce isoproterenol-induced cardiac hypertrophy by reducing oxidative stress, apoptosis, and stabilizing ECM components.

1. Introduction

Cardiovascular diseases (CVDs) contribute the highest among the noncommunicable disease's deaths globally; nearly 17.8 million deaths were reported due to CVDs alone in the year 2017 [1]. Cardiac hypertrophy (CH) is a compensatory phase of the heart against various underlying pathophysiological stimuli. If untreated, CH progresses into the decompensatory phase, and which ultimately results in the

irreversible heart failure. During this transition phase, an increase in myocardial mass, sarcomeric reorganization, expression of fetal genes, and remodeling of extracellular matrix take place [2].

The extracellular matrix (ECM) of the adult myocardium hosts both cardiomyocytes and interstitial cells in a complex three-dimensional orientation. ECM in addition to mechanical support also serves as a reservoir of growth factors to maintain basal physiology. During myocardial stress, homeostasis

of the ECM is perturbed, resulting in systolic and diastolic dysfunctions due to compromised signal transduction [3]. In myocardial remodeling, a fine balance between synthesis and breakdown of ECM components is perturbed. Specifically, matrix metalloproteinase (MMP) activation was reported in various cardiovascular complications [4]. Cardiac fibrosis, an underlying pathophysiological stage in many cardiovascular complications, results due to abnormal ECM deposition [5]. Activation of MMPs and inhibition of tissue inhibitor of matrix metalloproteinases (TIMPs) favors ECM degradation and its accumulation in the myocardium [6].

Several attempts have been made to inhibit ECM remodeling by inhibiting MMPs in the diseased heart and thereby reduce heart failure [7]. But none of the matrix metalloproteinase inhibitors succeed as a drug for heart failure [8]. Therefore, researchers are more interested to explore natural compounds or nutraceutical agents to inhibit ECM remodeling and thus prevent or delay the disease progression. Evidence-based studies in the past have shown the pivotal role of gaseous signaling molecules such as hydrogen sulfide (H_2S) and sulfur dioxide in mitigating cardiovascular complications [9, 10]. Hence, there is a pressing need to identify novel sulfur molecules to reverse the remodeling of cardiovascular complications. Among all the kinds of vegetables and fruits that are enriched with sulfur-rich compounds, garlic is more promising to show a cardioprotective effect.

Nutraceutical properties of the garlic against various complications are documented in ancient scriptures. Both prophylactic and therapeutic effects of garlic were promising in cardiometabolic complications [11]. Despite having myriad beneficial effects of raw garlic, largely, people avoid it because of the gastric disturbing property of garlic due to the presence of allicin.

Earlier, we have reported the promising cardiometabolic properties of garlic [12–14]. During the LC-MS investigation of sulfur compounds in garlic-fed rat serum, we have identified Allylmethylsulfide (AMS) as one of the major garlic-derived metabolites [15]. Similarly, in clinical studies, serum, breast milk, and urine samples also showed the presence of AMS [16, 17]. Pretreatment of AMS ameliorated X-ray-induced inflammation in mouse kidney [18]. It is reported that garlic intervention in various forms ultimately results in the formation of AMS in the physiological system. Therefore, it could be hypothesized that the beneficial effects of garlic such as lipid-lowering, antiatherosclerotic, antidiabetic, antihypertensive, antioxidant, and anticancer are attributed to its active metabolite AMS [19, 20].

Isoproterenol (isoprenaline) is a synthetic nonspecific beta-adrenergic receptor agonist. Sustained release of isoproterenol induces cardiac hypertrophy followed by myocardial remodeling and ultimately leading to heart failure [21]. Biochemical and pathophysiological perturbations due to isoproterenol are very similar to human disease settings and mimic anxiety- and stress-induced cardiac hypertrophy [22]. Hence, isoproterenol-induced cardiac hypertrophy in rodents is considered a suitable model to test the efficacy of novel molecules.

In our previous study, we have reported the antihypertrophic effect of AMS on cardio myoblast [15]. However,

the *in vivo* effect of AMS in cardiac hypertrophy and molecular mechanism underlying the beneficial effect, if any, is not explored yet. Therefore, the present study was designed to find the effect of AMS on isoproterenol-induced cardiac hypertrophy and to explore its molecular mechanism mostly focusing on oxidative stress, apoptosis, and alteration of ECM components.

2. Material and Methods

2.1. Animals and Study Design. Male Sprague Dawley Rats of 200–250-gram weight were procured from the National Institute of Pharmaceutical Education and Research (Mohali, India). All animal studies were performed in accordance with the standard operating procedures of the Translational Health Science and Technology Institute (THSTI) and with Institutional Animal Ethical Committee (IAEC/THSTI/2015-4) approval, Faridabad. Animals were housed in a small animal facility of THSTI, maintained at a $22 \pm 2^\circ C$ temperature, $50 \pm 15\%$ relative humidity, and 12 hrs of dark and light cycle.

2.1.1. Safety Study. Fifty-six animals were randomly divided into seven groups ($n = 8$): Group 1 (control), Group 2 (corn oil/vehicle control), Group 3 (garlic 250 mg/kg), Group 4 (AMS 25 mg/kg/day), Group 5 (AMS 50 mg/kg/day), Group 6 (AMS 100 mg/kg/day), and Group 7 (AMS 200 mg/kg/day).

2.1.2. Efficacy Study. Forty animals were randomly divided into five groups ($n = 8$): Group 1 (control), Group 2 (hypertrophy), Group 3 (hypertrophy+25 mg/kg/day), Group 4 (hypertrophy+AMS 50 mg/kg/day), and Group 5 (hypertrophy+enalapril 10 mg/kg/day).

2.2. Dosage Information. For safety study, 0.5 ml of virgin corn oil (Group 2), freshly prepared garlic homogenate 250 mg/kg/day along with 0.5 ml of corn oil (Group 3), and AMS 25, 50, 100, and 200 mg/kg (Groups 4, 5, 6, and 7) dissolved in 0.5 ml of corn oil were administered orally for 30 days. For efficacy study, 0.5 ml of corn oil was orally administered as vehicle in three groups (Group 1, Group 2, and Group 5) while AMS (25 and 50 mg/kg/day) dissolved in 0.5 ml was orally administered in two groups (Groups 3 and 4). Group 5 received 10 mg/kg of enalapril orally.

2.3. Electrocardiography. Rats were anesthetized in supine position by gaseous anesthesia (isoflurane 2%) coupled with a 100% oxygen supply. The core body temperature of the animal was maintained at $37^\circ C$ by a controlled heating pad (Homeothermic Blanket Control unit, Harvard Apparatus®). As per the manufacturer's instructions, 15 minutes of ECG was recorded to each animal on Power Lab 26T (ADInstruments, Australia) and the acquired data was analyzed on LabChart 8 software.

2.4. Serum Biochemical Parameters. Safety study animals were subjected to retroorbital bleeding under gaseous anesthesia. Blood samples were kept at room temperature for 1 hr followed by centrifugation at 3,000 g for 30 minutes at $4^\circ C$. Serum glutamic oxaloacetic transaminase (SGOT),

serum glutamic pyruvic transaminase (SGPT), creatinine kinase-myocardium bound (CK-MB), and alkaline phosphatase were measured by a semi autoanalyzer.

2.5. Single-Dose Pharmacokinetics of Allylmethylsulfide. To study the pharmacokinetics of AMS, SD rats were used. AMS 100 mg/kg single dose was administered orally, and subsequently, blood samples were collected at 0, 0.25, 0.5, 1, 2, 4, 8, 12, 24, 36, and 48 hrs. Post 30 minutes of sample collection, serum was separated by centrifugation at 600 g for 20 minutes at 4°C and stored at -80°C for further analysis.

2.5.1. Metabolite Extraction. For sample preparation, 100 μ l of serum was mixed with 100 μ l of LC-MS grade methanol and vortexed for 10 min at room temperature. Further, the sample was incubated on ice for 15 min and centrifuged at 16000 g for 20 min at 4°C. The resultant supernatant was filtered with a 0.2 μ m filter.

2.5.2. Metabolomics Measurement. For standard curve, AMS (Cas. No. 10152-76-8, Sigma-Aldrich), AMSO (Cas. No. 21892-75-1, EPTES, Food and Flavor Analytical), and AMSO₂ (Cas. No. 16215-14-8, Sigma-Aldrich) were spiked in control serum and the earlier mentioned extraction procedure was followed. All data were acquired on the orbitrap fusion mass spectrometer equipped with a heated electrospray ionization (HESI) source. Data were acquired on a positive mode at 120,000 resolution in full-scan MS1. We used a spray voltage of 4000 for positive. Sheath gas and auxiliary gas were set to 42 and 11, respectively. The mass scan range was 50-500 m/z, AGC (automatic gain control) target at 400000 ions, and the maximum injection time was 200 ms for MS. Extracted metabolites were separated on UPLC ultimate 3000 using an HSST3 column (100 \times 2.1 mm i.d., 1.9 micrometer, Waters Corporation) maintained at 40°C temperature. Mobile phase A was methanol with 0.1% formic acid, and mobile phase B was water with 0.1% formic acid. The elution gradient is used as follows: 0 min, 1% B; 1 min, 15% B; 4 min, 35% B; 7 min, 95% B; 9 min, 85% B; 10 min, 1% B; and 14 min, 1% B. The flow rate of 0.3 ml/min, and the sample injection volume were 5 microliters.

2.5.3. Data Processing. All acquired data has been processed using Progenesis QI for metabolomics (Waters Corporation) software using the default setting. The untargeted metabolomics workflow of Progenesis QI was used to perform retention time alignment, feature detection, deconvolution, and elemental composition prediction. Identification of metabolites has been done based on the match of accurate mass and the retention time of purchased standards. Relative intensity of the corresponding metabolites has been used for quantification. PKSolver a freely available add-in program for Microsoft Excel was used for pharmacokinetic parameters as mentioned [23].

2.6. In Vivo Cardiac Hypertrophy Model. Isoproterenol (~5 mg/kg/day) prepared in 0.001% ascorbic acid solution was delivered by ALZET® osmotic minipump (model #2002) as per the manufacturer's instructions. Briefly, rats were anesthetized with gaseous anesthesia (isoflurane 2%)

coupled with a 100% oxygen supply. The core body temperature of the animal was maintained at 37°C by a controlled heating pad (Homeothermic Blanket Control unit, Harvard Apparatus®). Hairs on the dorsal side below the neck are removed by depilatory cream, and a small incision is made to accommodate the sterile minipump charged with isoproterenol solution subcutaneously. Finally, 4-0 silk sutures are used to close the incision. Control animals received osmotic minipump filled with 0.001% ascorbic acid alone. Finally, povidone-iodine ointment was applied until complete wound healing is achieved. Minipump (model 2002) dispenses 0.5 μ l per hour for 14 days.

2.7. Biochemical Estimation

2.7.1. Lipid Peroxidation. Lipid peroxidation in the myocardium was measured by the protocol described by Ohkawa et al. [24]. Briefly, an equal amount of tissue is homogenized in 10% (w/v) of ice-cold 0.05 M potassium phosphate buffer (pH 7.4). Each homogenate (0.2 ml) was added to 0.2 ml of 8.1% SDS, 1.5 ml of 20% acetic acid, and 1.5 ml of 0.8% thiobarbituric acid (TBA). Distilled water was added to make up the volume to 4.0 ml, and the solution was kept on water bath maintained at 95°C for 1 hr. Finally, the supernatant was mixed with an equal volume of butanol: pyridine (15:1) and centrifuged and the optical density of the organic layer was measured at 532 nm. For quantification of malondialdehyde (MDA) formed in the myocardium, we make a standard curve after putting 1,1,3,3-tetraethoxypropane in different concentrations and mixed with the TBARS as mentioned above.

2.7.2. Reduced Glutathione. Reduced glutathione in the myocardium was measured by Ellman's method [25]. Briefly, an equal amount of heart tissue was homogenized in 10% (w/v) of ice-cold 0.05 M potassium phosphate buffer (pH 7.4). The resultant homogenate was centrifuged at 15,800 g for 30 minutes at 4°C. To deproteinize, 0.5 ml of the above supernatant was mixed with 0.5 ml of 5% trichloroacetic acid (TCA) and centrifuged at 2,300 g for 10 minutes. The deproteinized 0.5 ml sample is mixed with 0.25 ml of dithio-nitro-benzoic-acid (DTNB) and 1.5 ml of 0.3 M disodium hydrogen phosphate. Finally, the optical density of the mixture was measured at 412 nm. The readout of the sample was normalized by total protein present as measured by the bicinchoninic acid assay method (Thermo Scientific).

2.7.3. Catalase Estimation. Myocardial catalase was estimated by the method as described by Aebi [26]. Briefly, tissue samples were homogenized as mentioned earlier. About 20 μ l of tissue supernatant was mixed with 0.5 ml of 50 mM phosphate buffer (pH 7.0), and finally, 0.25 ml of 30 mM H₂O₂ is added, and change in the absorbance at 240 nm was recorded for 1.5 minutes with a 15-second interval. Catalase activity is expressed as the decomposition of H₂O₂/min/mg of protein.

2.7.4. Superoxide Dismutase. Total superoxide dismutase activity is measured as per the manufacturer's protocol using the Sigma-Aldrich (19160-1KT-F) kit.

TABLE 1: Primers used in RT-PCR analysis.

Gene	Forward primer	Reverse primer
ANP	AGCGAGCAGACCGATGAAGG	AGCCCTCAGTTTGCTTTTCA
Beta MHC	TGGAGCTGATGCACCTGTAG	ACTTCGTCTCATTGGGGATG
RPL32	AGATTCAAGGGCCAGATCCT	CGATGGCTTTTCGGTTCTTA

2.8. Immunoblotting. Approximately 50 mg of myocardial tissue is homogenized in 1 ml of RIPA buffer containing (1x) protease and phosphatase inhibitors. The homogenate is centrifuged at 13,500 g for 20 min at 4°C. Protein concentration in the supernatant is measured by the bicinchoninic acid assay method (Thermo Scientific). Sample preparation is done in Laemmli buffer using an equal amount of protein. For electrophoresis, protein is resolved on 10% SDS-polyacrylamide gel prepared by the TGX stain-free kit (Bio-Rad). Methanol-activated 0.2 μ m pore size (Thermo Scientific) polyvinylidene difluoride (PVDF) membrane is used for protein transfer after electrophoresis. To avoid non-specific binding of antibodies, membranes are blocked with 5% bovine serum albumin (BSA) prepared in tris-buffered saline (TBS) containing 0.1% Tween 20 for 60 min at room temperature. Primary antibody incubation is done overnight at 4°C. To remove the unbound primary antibody, the membrane is washed with 1x TBST thrice with 5 min interval each.

The specific HRP-labelled secondary antibody is incubated at room temperature for 60 min. Further, the membrane is washed with TBST thrice and finally, the signal is recorded using the Gel Doc XR system (Bio-Rad) with West Dura Pico kit (Thermo Scientific). The following antibodies were used in the study: beta MHC (Abcam; ab50967), MnSOD (Abcam; ab137037), catalase (Abcam; ab52477), caspase 3 (Cell Signaling; 9665), caspase 7 (Cell Signaling; 12827), caspase 9 (Cell Signaling; 9508), MMP2 (Abcam; ab86607), MMP9 (Abcam; ab38898), TIMP3 (Cell Signaling; 5673), and GAPDH antibody (Cell Signaling; 2118). Measured protein expression was normalized to GAPDH as a housekeeping protein.

2.9. Gene Expression. Total RNA was isolated from the left ventricular tissue by TRI reagent (Sigma-Aldrich) as per the manufacturer's protocol. The purity and concentration of RNA were measured by a NanoDrop spectrophotometer (Thermo Scientific). Following DNase treatment, reverse transcriptase reaction was performed by SuperScript-III Reverse Transcriptase (Takara, USA) for cDNA synthesis from 2 μ g of RNA. Primer sequences for real-time polymerase chain reaction (RT-PCR) were designed from the published sequences available in the public domain. RT-PCR was performed on Roche Light Cycler using the SYBR Green mix (Takara, USA). The data obtained were normalized to RPL32 expression as a reference gene. The following primer sequences were used in the study as mentioned in Table 1.

2.10. Histopathology. Immediately after sacrifice of the whole heart, kidney and liver tissues were excised and cleaned with

ice-cold PBS to remove blood clot. Histopathology samples were stored in freshly prepared 10% phosphate-buffered formalin. Masson's trichrome and haematoxylin-eosin stains were used to stain 5 μ m thick sections prepared from the paraffin block. To examine the histopathological changes, the Nikon Eclipse Ti microscope was used.

2.11. Cell Culture and Treatments. The rat cardio myoblast (H9c2) cell line was procured from ATCC® (USA) and was cultured in Dulbecco's Modified Eagle Media, (Cat. No. SH30243.01, HyClone™, GE Life Sciences) containing (4 mM L-glutamine and 45000 mg/L glucose and sodium pyruvate) and supplemented with 10% Fetal Bovine Serum (Cat. No. SH30071.03, HyClone™, GE Life Sciences). Cell culture was maintained at 37°C in a 5% CO₂ incubator (HER-ACELL VIOS 160I, Thermo Scientific). For flow cytometry and confocal imaging, 0.2% ethanol was added to the control group. The hypertrophy group was treated with 10 μ m isoproterenol (Sigma-Aldrich) along with 0.2% ethanol, and the treatment group received 50 μ m AMS along with 10 μ m isoproterenol. In every experiment, it is made sure that the final volume of ethanol did not exceed 0.2%. During 72 hrs of the abovementioned treatments, H9c2 cells were grown in DMEM containing 1% FBS with intermittent medium rechange at every 24 hrs.

2.12. ROS Detection by Flow Cytometry and Immunostaining. Intracellular ROS is measured by BD FACSCanto™ II (BD Biosciences, US). Briefly, following 72 hrs of earlier mentioned treatments, 10 μ m dichlorodihydrofluorescein diacetate (Cat. No. D399, Invitrogen, San Diego, CA) is incubated for 30 minutes at 37°C. Cells were trypsinized with 1x Trypsin-EDTA (Cat. No. CC5027.010L, Cell Clone™) and centrifuged at 210 g for 10 minutes with two times of PBS washing. The results were analyzed by FlowJo™ software for Windows Version V10, Ashland.

For immunostaining, we followed the previously described protocol [27], Briefly, following 72 hrs of earlier mentioned treatment, 10 μ m DCFDA was incubated for 30 minutes at 37°C and washed twice with 1x PBS. H9c2 cells on coverslip are fixed with 10% menthol prepared in 1x PBS for 5 minutes at room temperature. Finally, after two times of PBS washing, the coverslips were mounted on a glass slide with mounting media (Cat. No. H-1200, VECTA-SHIELD, Vector Laboratories, Inc., Burlingame, CA) containing DAPI. Fluorescent images were captured with a FV 3000 (OLYMPUS, Life Science Solutions) laser scanning confocal microscope. The images were analyzed by FIJI (NIH-Image J) software.

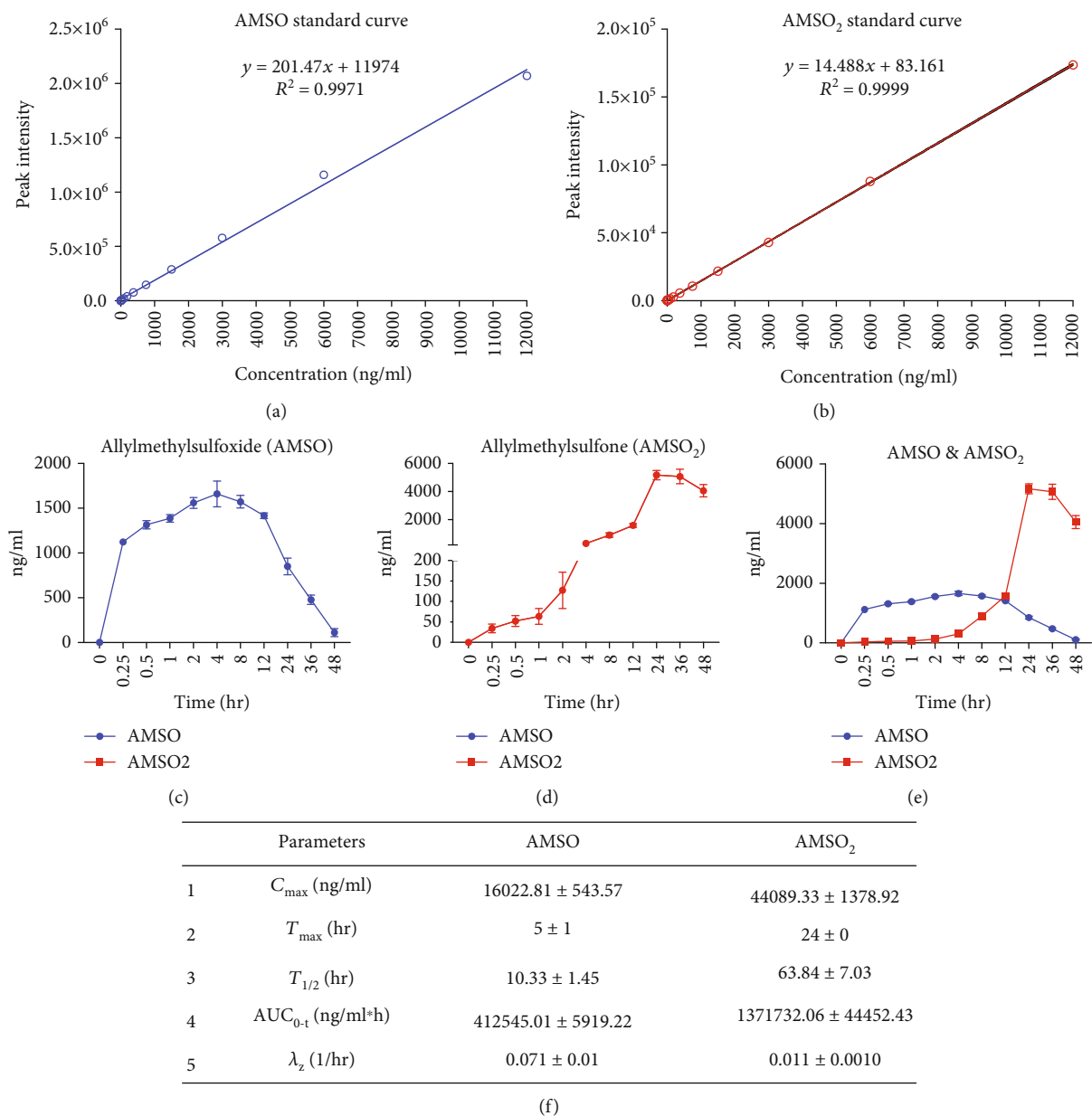


FIGURE 1: Effect of Allylmethylsulfide on pharmacokinetic parameters. (a) Standard curve of Allylmethylsulfoxide (AMSO). (b) Standard curve of Allylmethylsulfone (AMSO₂). (c, d) Concentration vs time graph of AMSO and AMSO₂. (e) Cumulative representation of graphs c and d. (f) Pharmacokinetic parameters of AMSO and AMSO₂. Maximum serum concentration (C_{max}), time taken to reach maximum serum concentration (T_{max}), elimination half-life ($T_{1/2}$), area under curve from time “0” to time “t” (AUC_{0-t}), and terminal elimination rate constant (λ_z). Data were represented as mean ± SEM ($n = 4$).

2.13. Caspase 3/7 Assay in H9c2 Cell. H9c2 cardio myoblasts were grown on a glass coverslip and treated with the above-mentioned doses for 72 hrs. Caspase 3/7 green fluorescent reagent (Cat. No. C10423, CellEvent™, Invitrogen) is a four-amino acid peptide (DEVD) attached to a nucleic acid-binding dye with absorption/emission maxima of ~502/530 nm. Activated caspase 3/7 will cleave the DEVD peptide sequence and allow it to bind with the nucleic acid and produce a green signal. Following treatments, 5 μ m of caspase 3/7 green detection reagent in complete media is incubated for 30 minutes at 37°C. Finally, the media is

removed and washed with 1x PBS. Further, to fix the cells, 4% paraformaldehyde was used for 15 minutes. Coverslips are mounted on a glass slide with mounting media added with nuclei counter stain DAPI and imaged using a FV 3000 machine. For analysis, mean fluorescence in the nuclei region was considered by FIJI software.

2.14. MTT Assay. In vitro AMS toxicity is determined by methyl thiazolyl tetrazolium (MTT) assay. Briefly, cardio myoblasts (10,000 cells/well) were seeded in each 96 well plate to attain a 60-70% confluency. Further, AMS dose range

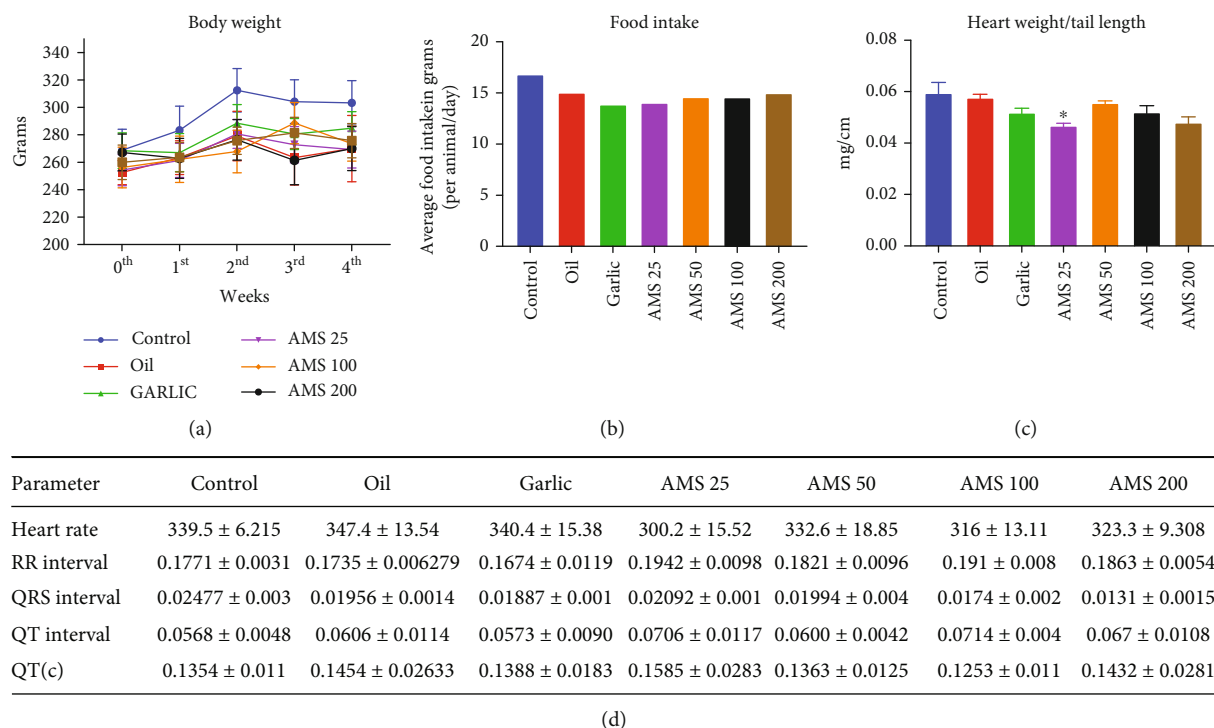


FIGURE 2: Effect of Allylmethylsulfide on the (a) body weight, (b) food intake, (c) heart weight to tail length ratio, and (d) electrocardiogram (ECG) parameters. Data were represented as mean ± SEM, $n = 5$ for ECG and $n = 8$ for other parameters. * $p < 0.05$ vs control.

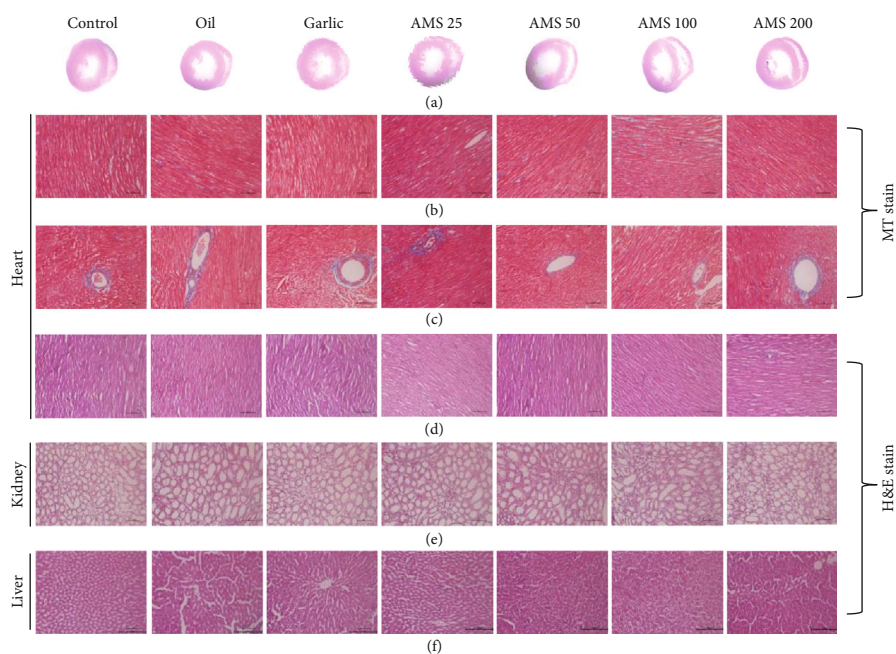


FIGURE 3: Effect of AMS on histopathology. (a) Transverse section of the heart representing the ventricular diameter. (b, c) Masson's trichrome staining of the heart tissue representing interstitial and perivascular fibrosis, respectively. (d–f) Haematoxylin and eosin stain of the heart, kidney, and liver.

(100 nm to 500 μm) in ethanol was treated for 24 hrs and then incubated with 1 mg/ml of MTT for 4 hrs in complete media. During MTT incubation, live cells form purple-colored formazan crystals. Unused MTT in the supernatant

was removed, and media was replaced with 50 μl of dimethyl sulfoxide (DMSO), and then incubated for 30 minutes at 37°C to dissolve the crystals. Finally, absorbance at 570 nm was recorded on a microplate reader (Molecular Devices).

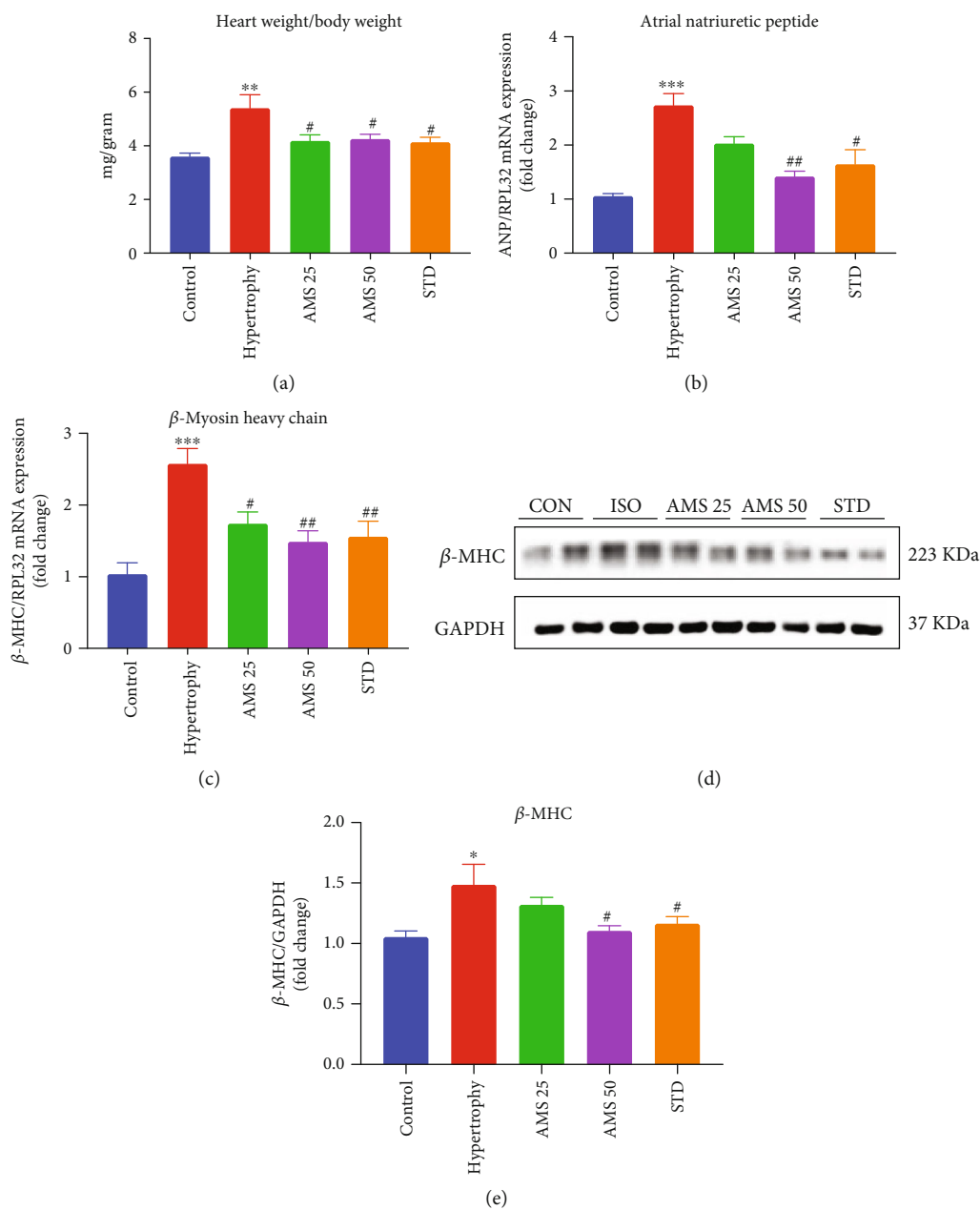


FIGURE 4: Effect of AMS on cardiac hypertrophy markers. (a) Heart weight to body weight ratio. (b) mRNA expression of atrial natriuretic peptide (ANP). (c) mRNA expression of beta myosin heavy chain (β -MHC). (d) Representative western blot images of β -MHC and GAPDH. (e) Densitometric analysis of β -MHC. mRNA expression data were normalized to the expression of the reference gene, RPL32. Protein expression data were normalized with the reference protein expression, GAPDH. Data were expressed as mean \pm SEM, ($n = 5$ for mRNA expression and $n = 4$ for protein expression). * $p < 0.05$, ** $p < 0.01$, *** $p < 0.001$ vs control and # $p < 0.05$, ## $p < 0.01$ vs hypertrophy.

The effect of AMS on H9c2 proliferation was expressed as relative percentage viability. Percent viability = (OD of treatment/OD of control) * 100.

2.15. Statistical Analysis. Data in the present study is reported as the mean \pm standard error of the mean (S.E.M). Mean differences among the study group were analyzed by one-way analysis of variance (ANOVA), followed by the Bonferroni multiple comparison test. A significance level is assumed if $p < 0.05$. Statistical analysis was performed in GraphPad

Prism 8.2.1 (279) (Graph Pad Software Inc., San Diego, CA, USA).

3. Results

3.1. Allylmethylsulfide Is Rapidly Metabolized into Allylmethylsulfoxide and Allylmethylsulfone. To study the pharmacokinetics of AMS, a single dose of 100 mg/kg was administered orally. We have observed that AMS is rapidly metabolized into AMSO and AMSO₂ in the physiological

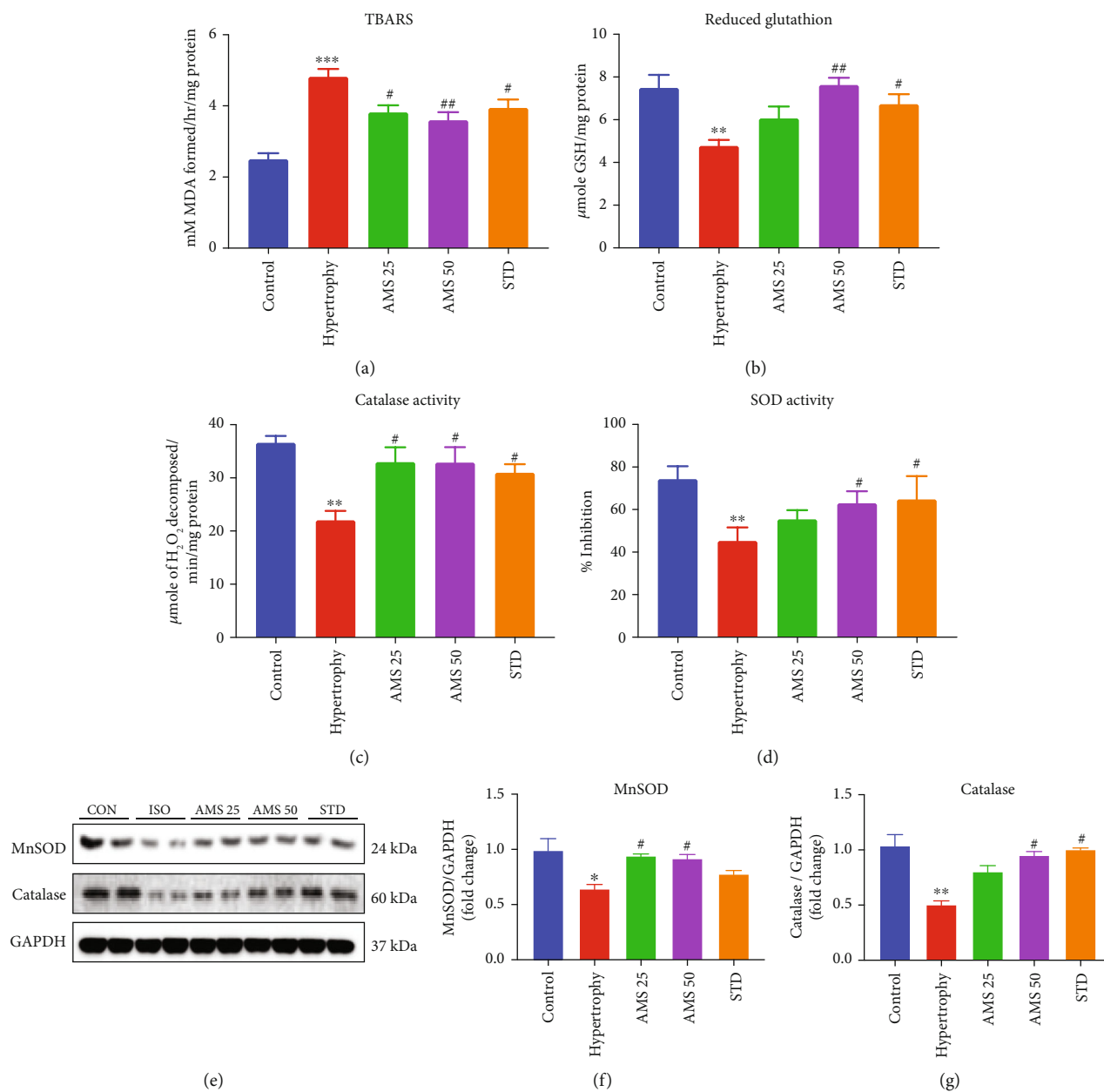


FIGURE 5: Effect of AMS on biochemical parameters and endogenous antioxidants. (a) Thiobarbituric acid reactive substances (TBARS). (b) Reduced glutathione (GSH). (c) Catalase activity. (d) Super oxide dismutase activity (SOD). (e) Representative western blot images of MnSOD, catalase, and GAPDH. (f) Densitometric analysis of manganese superoxide dismutase (MnSOD). (g) Densitometric analysis of catalase expression. Protein expression data were normalized with the reference protein expression, GAPDH. Data were expressed as mean \pm SEM, ($n = 5$ for biochemical parameters and $n = 4$ for protein expression). * $p < 0.05$, ** $p < 0.01$, and *** $p < 0.001$ vs control group and # $p < 0.05$, ## $p < 0.01$ vs hypertrophy.

system. To measure the exact concentration of AMSO and AMSO₂ in the serum, peak intensity of the metabolites was extrapolated to the standard curve of the same, respectively (Figures 1(a) and 1(b)). With time, the concentration of AMSO and AMSO₂ is gradually increased and showed peak at 5 hrs and 24 hrs, respectively (Figures 1(c)–1(e)). Pharmacokinetic parameters, derived from concentration vs time curve by PKsolver, suggests that half-life of AMSO is less (10.33 hrs) compared to AMSO₂ (63.84 hrs) (Figure 1(f)).

The C_{max} for AMSO and AMSO₂ are 16022.81 and 44089.33 ng/ml, respectively (Figure 1(f)).

3.2. Allylmethylsulfide Is Safe in Rats on Chronic Administration. To evaluate the effect of chronic administration of AMS, we have measured the body weight of the animals at every week from the beginning of AMS intervention till 4 weeks. We did not observe any significant change in the body weight in any of our treatment groups

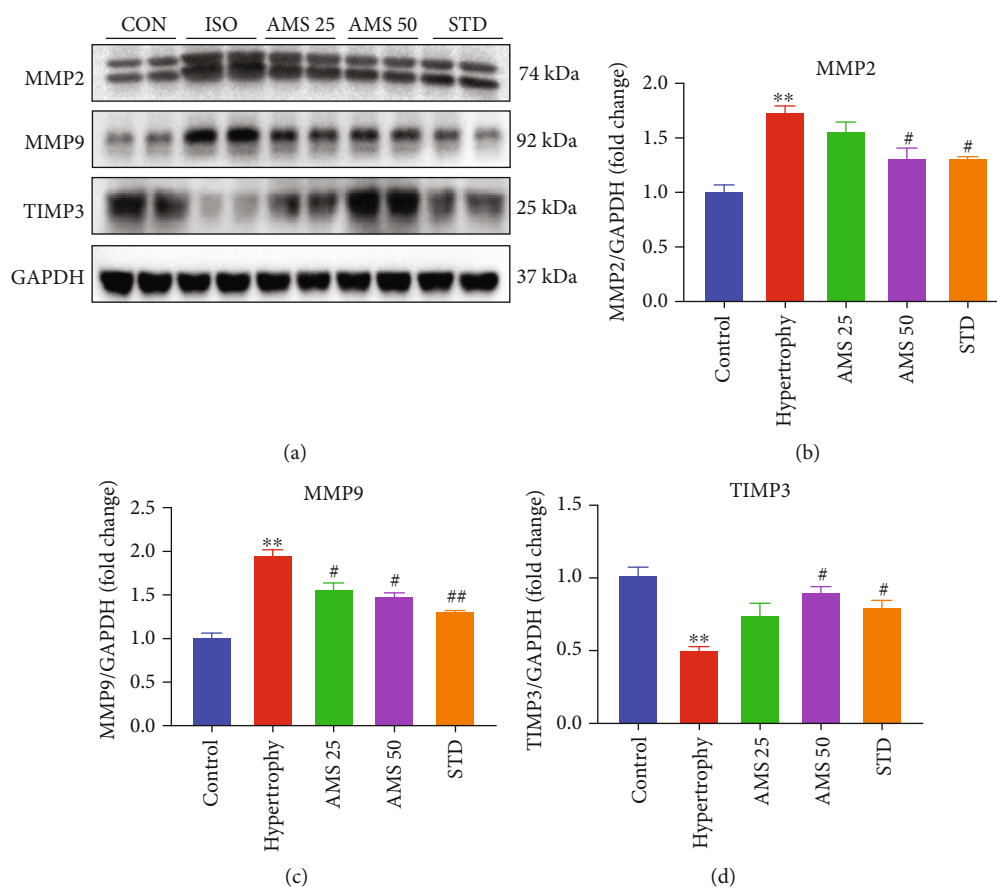


FIGURE 6: Effect of AMS on extracellular matrix components. (a) Representative western blot images of caspase matrix metalloproteinases (MMPs 2 and 9), tissue inhibitor of matrix metalloproteinase 3 (TIMP3), and GAPDH. (b, c) Densitometric analysis of MMPs 2 and 9. (d) Densitometric analysis of TIMP3. Protein expression data were normalized with the reference protein expression, GAPDH. Data expressed as mean \pm SEM, ($n = 4$). ** $p < 0.01$, *** $p < 0.001$ vs control group and # $p < 0.05$, ## $p < 0.01$ vs hypertrophy.

(Figure 2(a)). Similarly, food consumed by each rat per day (normalized with the number of animals per cage) did not show a major difference between the groups (Figure 2(b)). Except for AMS 25 mg/kg dose, there was no significant decrease in the heart weigh to tail length ratio compared with other doses (Figure 2(c)). Further, to study the impact to AMS on electrical conduction of the myocardium, we have performed electrocardiogram (ECG), at the end of 30 days of the treatment. We did not observe significant differences in any of the ECG parameters (Figures 2(d)).

3.3. Histopathology and Serum Biomarkers of Vital Organs Remained Normal on Chronic Administration of Allylmethylsulfide. To study the effect of AMS on histopathology of vital organs such as the heart, liver, and kidney, we have stored the tissues immediately after the euthanasia and stained it with MT and H&E stain. We did not observe any structural difference between any of the treatment groups (Figures 3(a)-3(f)). Before sacrifice, we have collected the serum and measured biomarkers for liver and heart injury. Here, we did not observe a significant difference in serum glutamic oxaloacetic transaminase (SGOT) (Figure S1 (a)), serum glutamic pyruvic transaminase (SGPT) (Figures S1

(b)), creatinine kinase-myocardium bound (CK-MB) (Figure S1 (c)), and alkaline phosphatase (Figure S1 (d)) levels among any of the AMS treatment groups.

3.4. Allylmethylsulfide Ameliorates Isoproterenol-Induced Cardiac Hypertrophy. Isoproterenol-induced cardiac hypertrophy was measured by the heart weight to body weight (HW/BW) ratio at the end of 14 days of AMS cotreatment. We have noticed there is a significant increase in the HW/BW ratio in the diseased group, while with the AMS and enalapril treatment, it was reduced (Figure 4(a)). mRNA expression of the fetal genes such as atrial natriuretic peptide (ANP) (Figure 4(b)) and beta myosin heavy chain (β -MHC) (Figure 4(c)) was significantly reduced with the AMS and enalapril treatment in the myocardium. Further, we have measured the protein expression of β -MHC and noticed that AMS (50 mg/kg/day) and enalapril significantly reduced it in the hypertrophied heart (Figure 4(e)).

3.5. Allylmethylsulfide Reduced Lipid Peroxidation and Improved Endogenous Antioxidants in Cardiac Hypertrophy. We next decided to study the effect of AMS on lipid peroxidation and endogenous antioxidants. Isoproterenol induced a significant increase in the MDA levels as measured by

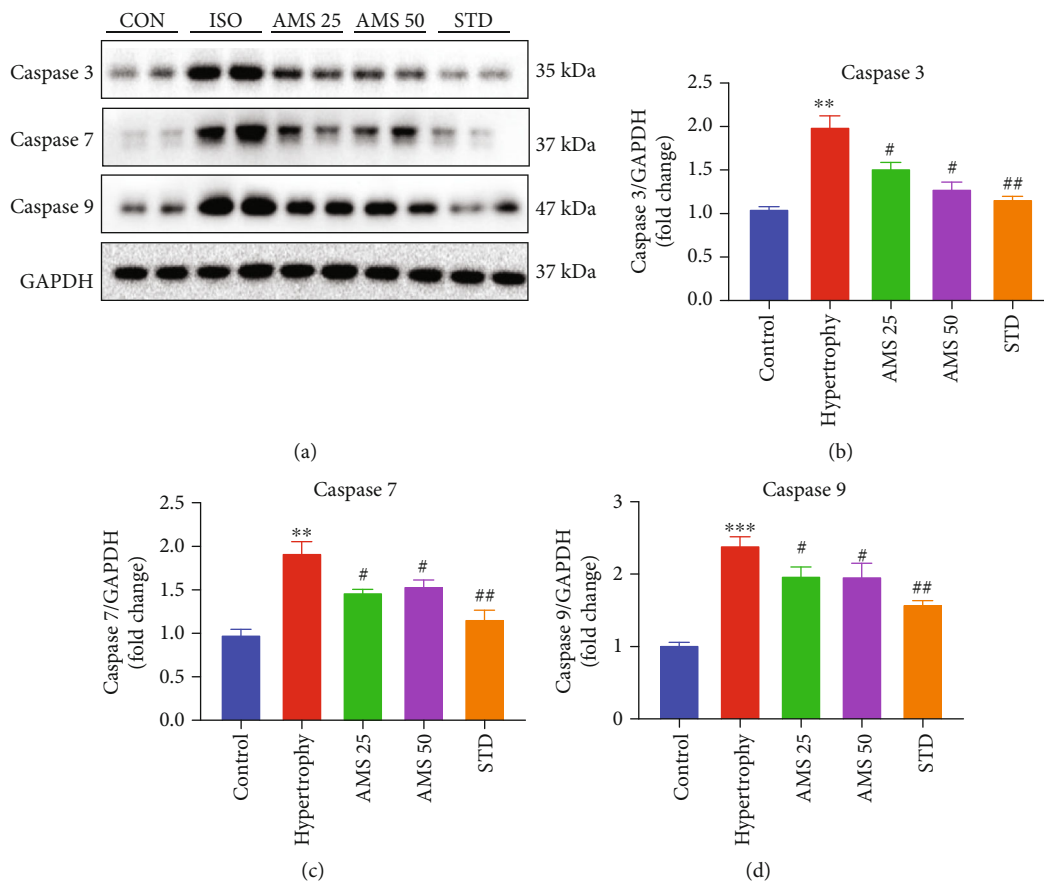


FIGURE 7: Effect of AMS on caspases. (a) Representative western blot images of caspase 3, caspase 7, caspase 9, and GAPDH. (b–d) Densitometric analysis of caspases 3, 7, and 9. Protein expression data were normalized with the reference protein expression, GAPDH. Data were expressed as mean \pm SEM, ($n = 4$). ** $p < 0.01$, *** $p < 0.001$ vs control group and # $p < 0.05$, ## $p < 0.01$ vs hypertrophy.

TBARS, and with the AMS (25 and 50 mg/kg/day) and enalapril treatment, it was reduced significantly (Figure 5(a)). The enzyme levels of endogenous antioxidant such as glutathione (GSH) were reduced with the isoproterenol treatment, and with AMS (50 mg/kg/day) and enalapril, it was preserved (Figure 5(b)). Similarly, decreased catalase and superoxide dismutase (SOD) activity in isoproterenol-treated hearts was improved with the AMS and enalapril treatment (Figures 5(c) and 5(d)). To further check the protein expression of catalase and MnSOD, we did immunoblot analysis. We observed that AMS and enalapril treatment increased both of their protein levels in the hypertrophic heart (Figures 5(f) and 5(g)).

3.6. Allylmethylsulfide Ameliorated Reactive Oxygen Species in Isoproterenol-Treated Cardio Myoblast. To corroborate the results of the *in vivo* study, we have treated H9c2 cardio myoblast for 72 hrs. With isoproterenol (10 μ m) and cotreated with AMS (50 μ m). Further, we have measured the ROS generation by flow cytometry (Figures S3 (A–D)) and immunofluorescence (Figures S4 (a)–S4(d)). Similar to our *in vivo* study, we have observed that AMS cotreatment reduced the isoproterenol-induced ROS generation. These two independent experiments confirmed that AMS has a property to reduce the ROS production. We have also checked the viability of the H9c2 cells post 24 hrs treatment

with AMS and did not find any significant cytotoxicity (Figure S2).

3.7. Allylmethylsulfide Prevented Extracellular Matrix Damage by Matrix Metalloproteinases. During isoproterenol-induced cardiac hypertrophy, homeostasis of extracellular matrix is perturbed and may result in the activation of matrix metalloproteinases (MMPs). We have observed a significant increase in the protein expression of MMP2 in the hypertrophic group, and with AMS (50 mg/kg/day) and enalapril treatment, it was reduced significantly (Figures 6(b)). Similarly, MMP9 expression was also reduced with the AMS (25 and 50 mg/kg/day) and enalapril treatment (Figure 6(c)). Tissue inhibitor of matrix metalloproteinases (TIMP) modulates the activity of MMPs. We have noticed a reduction of TIMP3 in the isoproterenol-treated heart. However, AMS (50 mg/kg/day) and enalapril pretreatment preserved the TIMP3 expression in the isoproterenol-treated heart (Figure 6(d)).

3.8. Allylmethylsulfide Reduced Apoptosis in the Isoproterenol-Induced Hypertrophic Heart. We have studied the protein expression of proapoptotic caspases in the hypertrophic heart. We have observed that isoproterenol-induced hypertrophic hearts showed increased expression of caspase 3 (Figure 7(b)), caspase 7 (Figure 7(c)), and caspase 9

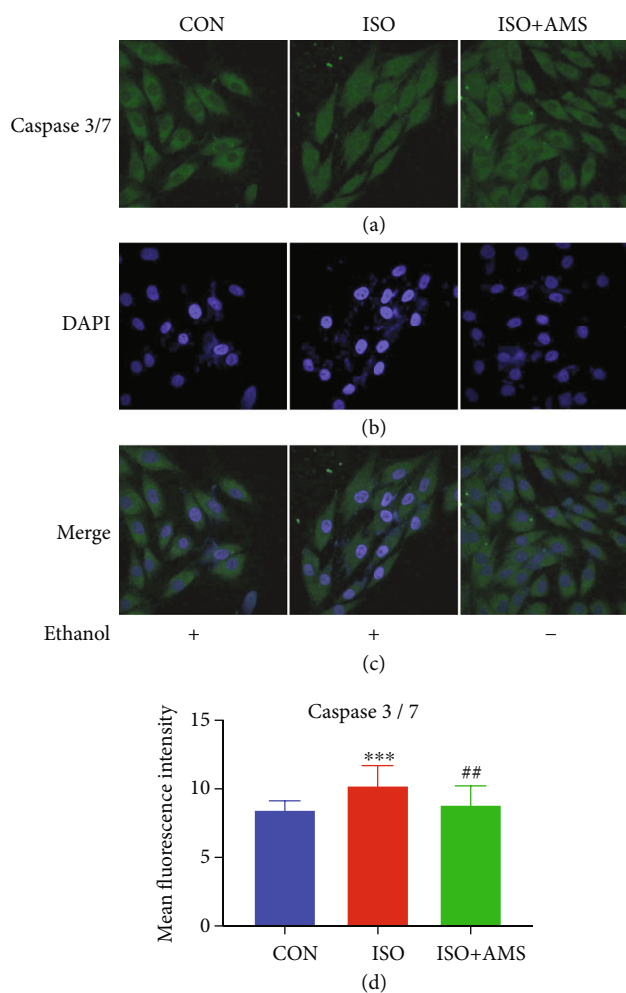


FIGURE 8: Effect of AMS on caspase 3/7 expression in H9c2 cardio myoblast (a) Representative confocal images of caspase 3/7 expression in the nucleus. (b) Nuclear staining by DAPI. (c) Merged images of DAPI and caspase 3/7. (d) Representative bar graph of mean fluorescence intensity. Data were expressed as mean \pm SEM, ($n = 100$ cells/group). *** $p < 0.001$ vs control (CON) group and ## $p < 0.01$ vs isoproterenol (ISO).

(Figure 7(d)), and the same were significantly reduced with the AMS (25 and 50 mg/kg/day) and enalapril treatment.

3.9. Allylmethylsulfide Reduced Apoptosis Signal in Isoproterenol-Treated Cardio Myoblast. To corroborate our *in vivo* finding, we decided to check the effect of AMS on the nuclear expression of caspase 3/7 in isoproterenol-treated H9c2 cells. We have noticed that there was a significant increase in the green fluorescence of caspase 3/7 in the nuclear portion of isoproterenol-treated cells. However, these signals were reduced in the AMS-cotreated isoproterenol cells (Figures 8(a)-8(d))

3.10. Allylmethylsulfide Reduced Fibrosis in the Hypertrophic Heart. We did histopathology study to check the effect of increased protein expression of matrix metalloproteinases on fibrosis. Gross investigation of the left ventricular diameter showed the presence of hypertrophy in the iso-

proterenol group; however, with AMS treatment, we have seen a decrease in the diameter and muscle thickness (Figure 9(a)). To check the fibrosis, we have stained the heart sections with MT staining. Interstitial and perivascular fibrosis were prominent in the isoproterenol-treated heart. However, a reduction of fibrosis was observed with AMS and enalapril treatment (Figures 9(d) and 9(e)). H&E staining showed a presence of high neutrophil infiltration in the isoproterenol-treated heart. However, AMS and enalapril treatment reduced the extent of neutrophil infiltration (Figures 9(b) and 9(c)).

4. Discussion

Both prophylactic and therapeutic effects of garlic in the past have documented numerous promising results. Previously, we have identified that AMS is an active metabolite of garlic and showed a reduction in the cell size *in vitro* [15]. Pretreatment of AMS ameliorated inflammation in mouse kidney by downregulation of NF- κ B signaling [18]. However, the safety and efficacy dose of the AMS, particularly in the cardiac hypertrophy model, are not explored yet. In the current study, we have explored the safety of chronic administration of AMS in rats, single-dose pharmacokinetics, and efficacy of AMS in an isoproterenol-induced cardiac hypertrophy model. Chronic intervention of AMS for 30 days did not show any significant difference in the body weight and food intake. However, the heart weight to tail length ratio was slightly lower with only an AMS 25 mg/kg dose. Although, at present, we do not know the reason for this change, we have performed ECG to further evaluate any cardiac abnormalities. ECG parameters did not show any significant difference within the dose range. QT prolongation, an important parameter of drug toxicity, did not alter with any of the doses. Next, we checked the effect of AMS on tissue biomarkers in the blood. We have measured SGOT, SGPT, CK-MB, and alkaline phosphatase in the serum at the end of the study. Any damage in the liver can be diagnosed by high SGOT and SGPT levels in the blood [28]. Alkaline phosphatase is present in most of the tissues; however, the bones and liver have the highest amount. The estimation of CK-MB provides information on cardiac muscles [29]. These biomarkers are leaked out from their respective localization into the blood during tissue damage. We did not observe any significant difference in these biomarkers with our treatments. To corroborate these results, we have checked for the histopathology of the heart, liver, and kidney. However, we did not observe any structural differences in the morphology of these vital organs. Single-dose pharmacokinetics suggest that AMS is well-absorbed through an oral route and rapidly metabolized into AMSO and then subsequently to AMSO₂. Presence of AMSO and AMSO₂ in the serum for a longer duration may allow a single dose of AMS for an efficacy purpose. Interestingly, we did not observe mortality in any of our treatment groups, these results proved that AMS is a safe molecule in rats. Further, in a concentration range from 0.1 to 500 μ m of AMS, we did not observe cytotoxicity in rat cardio myoblast (H9c2) cells.

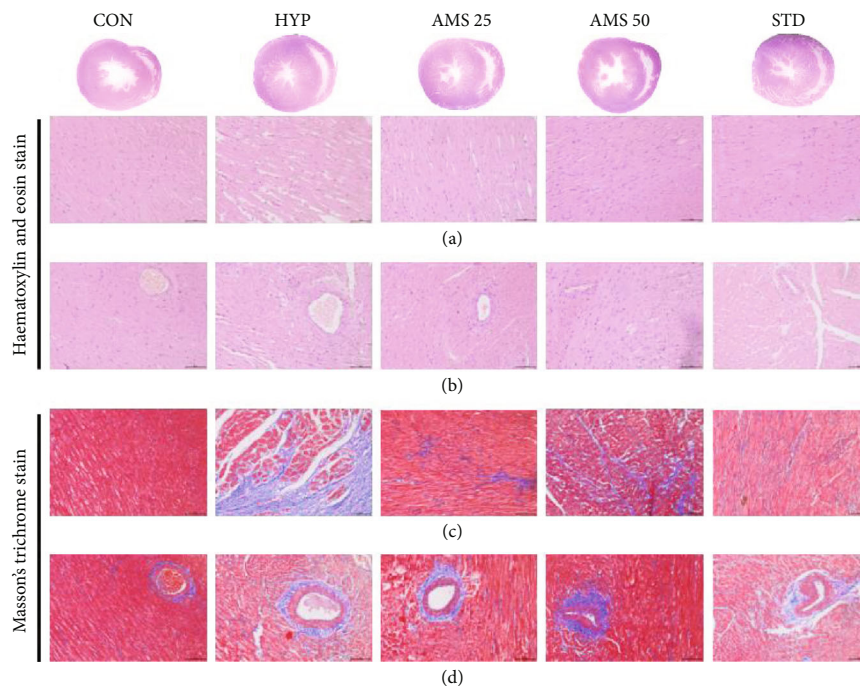


FIGURE 9: Effect of AMS on isoproterenol-induced hypertrophic heart. (a) Gross transverse section of the heart representing ventricular diameters. (b, c) Haematoxylin and eosin staining of the heart representing neutrophil infiltration in interstitial and perivascular, respectively. (d, e) Masson's trichrome staining of the heart representing interstitial and perivascular fibrosis.

Furthermore, after safety and pharmacokinetic studies, we looked the effect of AMS in the rodent model of cardiac hypertrophy. Isoproterenol-induced cardiac hypertrophy upregulates mRNA expression of fetal genes (ANP and β -MHC) [30]. In general, they are highly expressed during the early stages of heart development and later remain constitutively expressed in the mature heart. We have observed that the heart weight to body weight ratio, an important parameter of cardiac hypertrophy in animals, and fetal gene expression in heart were significantly reduced in the AMS and enalapril-treated animals. Isoproterenol-induced cardiac hypertrophy is associated with reduced antioxidants and excessive ROS generation. ROS interacts with cellular components and results in lipid peroxidation [31]. Our data showed that there is a significant increase of malondialdehyde (MDA) in hypertrophic hearts, and however, with AMS and enalapril treatment, it was reduced. Antioxidants such as superoxide dismutase (SOD), catalase, glutathione, and glutathione peroxidase play an important role in maintaining the physiological levels of ROS [32]. We have observed decreased activity of antioxidant enzymes in hypertrophic hearts, and however, with AMS and enalapril intervention, it was significantly preserved. We have also found similar results in the protein expression of MnSOD and catalase with AMS and enalapril treatment.

We next thought to corroborate the *in vivo* findings of oxidative stress with the cellular hypertrophy model. To explore the underlying protective effect of AMS, we have studied the ROS generation in H9c2 cells. During myocardial stress, excessive ROS production and a compromised antioxidant effect leads to pathological cardiac hypertrophy and ultimately progresses into heart failure [33]. Recent reports

suggest that targeting ROS generation could be a better alternative to ameliorate cardiac hypertrophy [34]. In our study, the immunofluorescence and flow cytometric analysis suggest that AMS cotreatment significantly reduced ROS generation in isoproterenol-treated cardio myoblast.

Fibrosis develops due to excessive accumulation of collagen and other ECM components by the differentiation of fibroblast into myofibroblast. Based on the nature of pathological insult, the three types of cardiac fibrosis that develop are reactive interstitial fibrosis, infiltrative interstitial fibrosis, and replacement fibrosis [35]. In our study, the replacement of the myocardium with the fibrous scar was observed in the isoproterenol-induced hypertrophy hearts. However, we have observed a significant reduction of cardiac fibrosis with the treatment of both AMS and enalapril.

Cardiac fibroblast plays a pivotal role in the ECM homeostasis. The major components of ECM include collagen I, collagen III, fibronectin, laminin, and elastin. ECM maintains the structural integrity of cardio myocytes, fibroblast, and coronary arteries within the myocardium and also maintains the electrical signal conduction for rhythmic contractility of the heart. The integrity of the ECM components is mainly regulated by matrix metalloproteinases (MMPs) and their tissue inhibitors (TIMPs) produced by fibroblasts [36]. MMP2 and MMP9 are the important enzymes involved in the degradation of ECM and are involved in various cardiac complications [37]. AMS and enalapril treatment preserved a significant increase in the protein expression of MMP2 and MMP9 in the isoproterenol-induced hypertrophic heart. TIMPs have an important role in preventing the proteolytic degradation of ECM by MMPs. The lack of TIMP3 has resulted in many cardiovascular complications [38]. In our

study, we have noticed AMS and enalapril improved the protein expression of TIMP3 in hypertrophied hearts.

Cardiac fibrosis resulting from MMP expression was observed in the isoproterenol-induced hypertrophic heart and may lead to cardiomyocyte death, i.e., apoptosis. To investigate the effect of AMS on apoptosis, we have studied the protein expression of caspases. Pathological enlargement of the myocardium with isoproterenol results in activation of programmed cell death, compromised contractile function, and eventually heart failure [39]. Besides apoptosis, caspases play an important role in cardiac inflammation. There are evidence-based studies suggesting the role of caspase 3 and caspase 9 in both cellular and animal models of cardiac hypertrophy [40]. The use of caspase 3 inhibitors holds a promising role in reducing cardiac remodeling [41]. We have observed that caspase 3, caspase 7, and caspase 9 protein expressions were significantly increased in hypertrophic hearts; however, with AMS and enalapril, these expressions were reduced. Nuclear expression of caspase 3/7 is a sign of apoptotic induction in cells due to various underlying pathological insults [42]. We have noticed a significant increase in the nuclear expression of caspase 3/7 in isoproterenol-treated H9c2 cells. However, it was reduced with the AMS cotreatment. The data obtained from *in vitro* and *in vivo* studies confirmed that AMS showed some of its beneficial effects in hypertrophic conditions through protection from apoptosis.

5. Conclusion

In the present study, we have demonstrated that AMS is a safe molecule in rats. The pharmacokinetic study showed that AMS results into two stable metabolites, i.e., AMSO and AMSO₂ in the physiological system. AMS reduced cardiac hypertrophy markers such as fetal gene expression and improved endogenous antioxidants. Isoproterenol-induced cardiac fibrosis and dysregulated ECM deposition in the myocardium were reduced with AMS and enalapril treatment. The only limitation of the efficacy study is that we could not measure the functional parameters of the heart by echocardiography. Overall, our study confirms that AMS is a safe and efficacious molecule for the prevention of cardiac hypertrophy and associated remodeling.

Data Availability

The data used to support the findings of this study are available from the corresponding author upon request.

Ethical Approval

All animal studies were approved by the Institutional Animal Ethical Committee (IAEC) of the Translational Health Science and Technology Institute, Faridabad (IAEC/TH-STI/2015-4).

Conflicts of Interest

The authors declare no conflict of interest.

Authors' Contributions

S.A.M and B.P have performed the animal studies. S.A.M and B.P carried out dosing, biochemical, gene and protein estimation, and analysis of results. U.T performed *in vitro* studies and analysis of results. S.A.M and Y.K performed the pharmacokinetic study and analyzed the results. S.K.A investigated the histopathology samples. S.A.M and S.K.B conceived and designed the study, interpreted the results, and drafted the manuscript.

Acknowledgments

The authors are grateful to the Indian Council of Medical Research (ICMR) and Council of Scientific and Industrial Research (CSIR) for providing research fellowship to S.A.M and B.P, respectively. This study was supported by the Translational Health Science and Technology Institute core fund. The authors are thankful to Dr. Md. Jahangir Alam and Mr. Sonu for their assistance in the pharmacokinetic study.

Supplementary Materials

Figure S1: effect of Allylmethylsulfide on serum biochemical parameters. (a) Serum glutamic oxaloacetic transaminase (SGOT). (b) Serum glutamic pyruvic transaminase (SGPT). (c) Creatinine kinase-myocardium bound (CK-MB). (d) Alkaline phosphatase. Data are represented as mean \pm SEM ($n = 4$). Figure S2: effect of Allylmethylsulfide on cardio myoblast viability. Post 24 hrs of AMS treatment with a dose range from 0.1 to 500 μ m, the fluorescence was analyzed. Figure S3: effect of Allylmethylsulfide on reactive oxygen species (ROS) production in H9c2 cardio myoblast. (a) Representative histogram of control. (b) Representative histogram of isoproterenol. (c) Representative histogram of isoproterenol cotreated with AMS. (d) Representative bar graph of percentage of Alexa Fluor 488-positive cells. Data are expressed as mean \pm SEM, *** $p < 0.001$ vs control (CON) group and ** $p < 0.01$ vs isoproterenol (ISO). Figure S4: effect of Allylmethylsulfide on reactive oxygen species (ROS) production in H9c2 cardio myoblast. (a) Representative confocal images of DCFDA. (b) Nuclear staining by DAPI. (c) Merged images of DAPI and DCFDA. (d) Representative bar graph of mean fluorescence intensity. Data are expressed as mean \pm SEM, ($n = 100$ cells/group). **** $p < 0.0001$ vs control (CON) group and *** $p < 0.001$ vs isoproterenol (ISO). (*Supplementary Materials*)

References

- [1] GBD 2017 Causes of Death Collaborators, "Global, regional, and national age-sex-specific mortality for 282 causes of death in 195 countries and territories, 1980-2017: A systematic analysis for the global burden of disease study 2017," *Lancet*, vol. 392, no. 10159, pp. 1736-1788, 2018.
- [2] M. Nakamura and J. Sadoshima, "Mechanisms of physiological and pathological cardiac hypertrophy," *Nature Reviews Cardiology*, vol. 15, no. 7, pp. 387-407, 2018.

- [3] N. G. Frangogiannis, "The extracellular matrix in myocardial injury, repair, and remodeling," *The Journal of Clinical Investigation*, vol. 127, no. 5, pp. 1600–1612, 2017.
- [4] K. Y. DeLeon-Pennell, C. A. Meschiari, M. Jung, and M. L. Lindsey, "Matrix metalloproteinases in myocardial infarction and heart failure," *Progress in Molecular Biology and Translational Science*, vol. 147, pp. 75–100, 2017.
- [5] L. Li, Q. Zhao, and W. Kong, "Extracellular matrix remodeling and cardiac fibrosis," *Matrix Biology*, vol. 68–69, pp. 490–506, 2018.
- [6] X. Wang and R. A. Khalil, "Matrix metalloproteinases, vascular remodeling, and vascular disease," *Advances in Pharmacology*, vol. 81, pp. 241–330, 2018.
- [7] F. G. Spinale and N. M. Wilbur, "Matrix metalloproteinase therapy in heart failure," *Current Treatment Options in Cardiovascular Medicine*, vol. 11, no. 4, pp. 339–346, 2009.
- [8] A. Yabluchanskiy, Y. Li, R. J. Chilton, and M. L. Lindsey, "Matrix metalloproteinases: drug targets for myocardial infarction," *Current Drug Targets*, vol. 14, no. 3, pp. 276–286, 2013.
- [9] G. Meng, J. Liu, S. Liu et al., "Hydrogen sulfide pretreatment improves mitochondrial function in myocardial hypertrophy via a SIRT3-dependent manner," *British Journal of Pharmacology*, vol. 175, no. 8, pp. 1126–1145, 2018.
- [10] G. Meng, S. Zhao, L. Xie, Y. Han, and Y. Ji, "Protein S-sulfhydration by hydrogen sulfide in cardiovascular system," *British Journal of Pharmacology*, vol. 175, no. 8, pp. 1146–1156, 2018.
- [11] I. A. Sobenin, V. A. Myasoedova, M. I. Iltchuk, D. W. Zhang, and A. N. Orekhov, "Therapeutic effects of garlic in cardiovascular atherosclerotic disease," *Chinese Journal of Natural Medicines*, vol. 17, no. 10, pp. 721–728, 2019.
- [12] R. Padiya, D. Chowdhury, R. Borkar, R. Srinivas, M. Pal Bhadra, and S. K. Banerjee, "Garlic attenuates cardiac oxidative stress via activation of PI3K/AKT/Nrf2-Keap1 pathway in fructose-fed diabetic rat," *PLoS One*, vol. 9, no. 5, 2014.
- [13] G. Kaur, R. Padiya, R. Adela et al., "Garlic and resveratrol attenuate diabetic complications, loss of β -Cells, pancreatic and hepatic oxidative stress in streptozotocin-induced diabetic rats," *Frontiers in Pharmacology*, vol. 7, 2016.
- [14] M. R. Sultana, P. K. Bagul, P. B. Katore, S. Anwar Mohammed, R. Padiya, and S. K. Banerjee, "Garlic activates SIRT-3 to prevent cardiac oxidative stress and mitochondrial dysfunction in diabetes," *Life Sciences*, vol. 164, pp. 42–51, 2016.
- [15] T. N. Khatua, R. M. Borkar, S. A. Mohammed, A. K. Dinda, R. Srinivas, and S. K. Banerjee, "Novel sulfur metabolites of garlic attenuate cardiac hypertrophy and remodeling through induction of Na(+)/K(+)-ATPase expression," *Frontiers in Pharmacology*, vol. 8, 2017.
- [16] L. Scheffler, Y. Saueremann, A. Heinlein, C. Sharapa, and A. Buettner, "Detection of volatile metabolites derived from garlic (*Allium sativum*) in human urine," *Metabolites*, vol. 6, no. 4, p. 43, 2016.
- [17] L. Scheffler, Y. Saueremann, G. Zeh et al., "Detection of volatile metabolites of garlic in human breast milk," *Metabolites*, vol. 6, no. 2, p. 18, 2016.
- [18] E. K. Lee, S. W. Chung, J. Y. Kim et al., "Allylmethylsulfide Down-Regulates X-Ray Irradiation-Induced Nuclear Factor- κ B Signaling in C57/BL6 Mouse Kidney," *Journal of Medicinal Food*, vol. 12, no. 3, pp. 542–551, 2009.
- [19] L. D. Lawson and Z. J. Wang, "Allicin and allicin-derived garlic compounds increase breath acetone through allyl methyl sulfide: use in measuring allicin bioavailability," *Journal of Agricultural and Food Chemistry*, vol. 53, no. 6, pp. 1974–1983, 2005.
- [20] L. Lawson and S. Hunsaker, "Allicin bioavailability and bioequivalence from garlic supplements and garlic foods," *Nutrients*, vol. 10, no. 7, p. 812, 2018.
- [21] J. D'Ambrosi and N. Amin, "Hyperinflation of isoproterenol," *Journal of Pharmacy Practice*, vol. 31, no. 4, pp. 390–394, 2018.
- [22] A. I. Othman, M. M. Elkomy, M. A. el-Missiry, and M. Dardor, "Epigallocatechin-3-gallate prevents cardiac apoptosis by modulating the intrinsic apoptotic pathway in isoproterenol-induced myocardial infarction," *European Journal of Pharmacology*, vol. 794, pp. 27–36, 2017.
- [23] Y. Zhang, M. Huo, J. Zhou, and S. Xie, "PKSolver: an add-in program for pharmacokinetic and pharmacodynamic data analysis in Microsoft Excel," *Computer Methods and Programs in Biomedicine*, vol. 99, no. 3, pp. 306–314, 2010.
- [24] H. Ohkawa, N. Ohishi, and K. Yagi, "Assay for lipid peroxides in animal tissues by thiobarbituric acid reaction," *Analytical Biochemistry*, vol. 95, no. 2, pp. 351–358, 1979.
- [25] G. L. Ellman, "Tissue sulfhydryl groups," *Archives of Biochemistry and Biophysics*, vol. 82, no. 1, pp. 70–77, 1959.
- [26] H. Aebi, *Catalase A2*, in *methods of enzymatic analysis*, Academic Press, Second edition, 1974.
- [27] W. J. Shen, C. Y. Hsieh, C. L. Chen et al., "A modified fixed staining method for the simultaneous measurement of reactive oxygen species and oxidative responses," *Biochemical and Biophysical Research Communications*, vol. 430, no. 1, pp. 442–447, 2013.
- [28] R. Hegarty and A. Dhawan, "Fifteen-minute consultation: the child with an incidental finding of elevated aminotransferases," *Archives of disease in childhood - Education & practice edition*, vol. 103, no. 5, pp. 228–230, 2018.
- [29] Y. Saidu, M. J. Usman, S. A. Isa et al., "Biochemical and histological changes in the heart of post-partum rats exposed to Natron," *Indian Heart Journal*, vol. 70, no. 6, pp. 887–893, 2018.
- [30] S. A. Bageghni, K. E. Hemmings, N. Zava et al., "Cardiac fibroblast-specific p38 α MAP kinase promotes cardiac hypertrophy via a putative paracrine interleukin-6 signaling mechanism," *The FASEB Journal*, vol. 32, no. 9, pp. 4941–4954, 2018.
- [31] S. Panda, A. Kar, and S. Biswas, "Preventive effect of Agnucastolide C against isoproterenol-induced myocardial injury," *Scientific Reports*, vol. 7, no. 1, p. 16146, 2017.
- [32] T. Zhou, E. Prather, D. Garrison, and L. Zuo, "Interplay between ROS and antioxidants during ischemia-reperfusion injuries in cardiac and skeletal muscle," *International Journal of Molecular Sciences*, vol. 19, no. 2, p. 417, 2018.
- [33] K. Huynh, B. C. Bernardo, J. McMullen, and R. H. Ritchie, "Diabetic cardiomyopathy: mechanisms and new treatment strategies targeting antioxidant signaling pathways," *Pharmacology & Therapeutics*, vol. 142, no. 3, pp. 375–415, 2014.
- [34] J. Farías, V. Molina, R. Carrasco et al., "Antioxidant therapeutic strategies for cardiovascular conditions associated with oxidative stress," *Nutrients*, vol. 9, no. 9, p. 966, 2017.
- [35] S. Hinderer and K. Schenke-Layland, "Cardiac fibrosis – A short review of causes and therapeutic strategies," *Advanced Drug Delivery Reviews*, vol. 146, pp. 77–82, 2019.

- [36] N. Cui, M. Hu, and R. A. Khalil, "Biochemical and biological attributes of matrix metalloproteinases," *Progress in Molecular Biology and Translational Science*, vol. 147, pp. 1–73, 2017.
- [37] J. Radosinska, M. Barancik, and N. Vrbjar, "Heart failure and role of circulating MMP-2 and MMP-9," *Panminerva Medica*, vol. 59, no. 3, pp. 241–253, 2017.
- [38] H. Tian, M. Cimini, P. W. M. Fedak et al., "TIMP-3 deficiency accelerates cardiac remodeling after myocardial infarction," *Journal of Molecular and Cellular Cardiology*, vol. 43, no. 6, pp. 733–743, 2007.
- [39] W. Yao, N. Wang, J. Qian et al., "Renal sympathetic denervation improves myocardial apoptosis in rats with isoproterenol-induced heart failure by downregulation of tumor necrosis factor- α and nuclear factor- κ B," *Experimental and Therapeutic Medicine*, vol. 14, no. 5, pp. 4104–4110, 2017.
- [40] B. Ouyang, Z. Li, X. Ji, J. Huang, H. Zhang, and C. Jiang, "The protective role of lutein on isoproterenol-induced cardiac failure rat model through improving cardiac morphology, antioxidant status via positively regulating Nrf2/HO-1 signalling pathway," *Pharmaceutical Biology*, vol. 57, no. 1, pp. 529–535, 2019.
- [41] B. Yang, D. Ye, and Y. Wang, "Caspase-3 as a therapeutic target for heart failure," *Expert Opinion on Therapeutic Targets*, vol. 17, no. 3, pp. 255–263, 2013.
- [42] S. Kamada, U. Kikkawa, Y. Tsujimoto, and T. Hunter, "Nuclear translocation of caspase-3 is dependent on its proteolytic activation and recognition of a substrate-like protein(s)," *The Journal of Biological Chemistry*, vol. 280, no. 2, pp. 857–860, 2005.

Research Article

Taurine Attenuates Carcinogenicity in Ulcerative Colitis-Colorectal Cancer Mouse Model

Guifeng Wang,^{1,2} Ning Ma ,^{3,4} Feng He,¹ Shosuke Kawanishi ,⁵ Hatasu Kobayashi,¹ Shinji Oikawa,¹ and Mariko Murata ¹

¹Department of Environmental and Molecular Medicine, Mie University Graduate School of Medicine, Tsu, Mie 514-8507, Japan
²Sakuranomori Shiroko Home, Social Service Elderly Facilities, Suzuka University of Medical Science, Suzuka, Mie 513-0816, Japan
³Graduate School of Health Science, Suzuka University of Medical Science, Suzuka, Mie 513-8670, Japan
⁴Institute of Traditional Chinese Medicine, Suzuka University of Medical Science, Suzuka, Mie 510-0226, Japan
⁵Graduate School of Pharmaceutical Sciences, Suzuka University of Medical Science, Suzuka, Mie 513-8670, Japan

Correspondence should be addressed to Mariko Murata; mmurata@doc.medic.mie-u.ac.jp

Received 2 April 2020; Accepted 9 May 2020; Published 21 May 2020

Guest Editor: Mario Fontana

Copyright © 2020 Guifeng Wang et al. This is an open access article distributed under the Creative Commons Attribution License, which permits unrestricted use, distribution, and reproduction in any medium, provided the original work is properly cited.

Taurine (2-aminoethane-sulfonic acid) is a type of amino acids and has numerous physiological and therapeutic functions, including anti-inflammation. However, there are few studies on the anticancer action of taurine. Our previous studies have demonstrated that taurine exhibits an apoptosis-inducing effect on human nasopharyngeal carcinoma cells *in vitro*. In this study, we have investigated whether taurine has an anticancer effect, using azoxymethane (AOM)/sulfate sodium (DSS)-induced mouse model for colon carcinogenesis. All mice, except those in control group, received a single intraperitoneal injection of AOM and DSS in the drinking water for 7 days twice, with 1-week interval. After the first DSS treatment, mice were given distilled water (model group) or taurine in the drinking water (taurine group) *ad libitum*. No tumor was observed in the control group. Taurine significantly suppressed AOM+DSS-induced tumor formation. Histopathological examination revealed AOM/DSS treatment induced colon cancer in all mice (8/8, 100%), and taurine significantly inhibited the progression of colon cancer (4/9, 44.4%). Taurine significantly attenuated cell proliferation in cancer tissues detected by Ki-67 staining. Taurine significantly increased the levels of an apoptosis marker cleaved caspase-9 and tumor suppressor protein PTEN. This is the first study that demonstrated that taurine significantly reduced carcinogenicity *in vivo* using AOM/DSS-induced colon cancer mouse model.

1. Introduction

Taurine (2-aminoethane-sulfonic acid) is a special amino acid containing sulfonate group and lacking carboxyl group and is found in high concentrations in many cells. Humans can endogenously synthesize taurine, but primarily depend on their diet for taurine, mostly found in seafood [1]. Therefore, it is considered a conditionally essential nutrient. Taurine has numerous physiological functions, including bile salt conjugation, osmoregulation, membrane stabilization, calcium modulation, antioxidation, and anti-inflammation [2–4]. Taurine has different biological effects in various systems or organs, such as the cardiovascular system, skeletal muscle, retina, liver, kidney, and nervous system [3, 5, 6].

Taurine is used in the treatment of congestive heart failure, liver disease [7], and recently, for the suppression of stroke-like seizures in mitochondrial encephalomyopathy, lactic acidosis, and stroke-like seizures (MELAS) syndrome [8]. Taurine is also used as an ingredient of dietary supplements for energy drink ingested prior to exercise and revitalizing beverage for recovery from fatigue. Although many useful effects of taurine intake are reported, there are few studies about the anticancer action of taurine. We proposed the mechanism for crosstalk between DNA damage and inflammation in the multiple steps of carcinogenesis [9]. Our previous studies have demonstrated that taurine exhibits an apoptosis-inducing effect on human nasopharyngeal carcinoma cells *in vitro* [10, 11]. Suzuki et al. [12] demonstrated

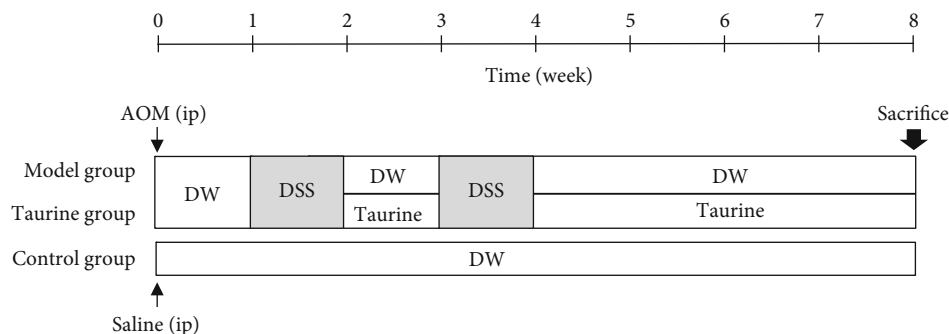


FIGURE 1: Experimental protocol.

that azoxymethane (AOM) and subsequent severe inflammation induced by sulfate sodium (DSS) resulted in a high incidence of colonic epithelial malignancy, which is a useful mouse model for inflammation-related carcinogenesis. The proposed mechanism may raise the possibility of the cancer prevention by taurine because of its anti-inflammatory activity. In this study, we investigated whether taurine has an anticancer effect, using AOM/DSS-induced mouse model for colorectal cancer.

2. Materials and Methods

2.1. Animals and Chemicals. In this study, 4-week-old male C57BL/6J mice were purchased from Japan SLC Inc. (Hamamatsu, Japan). All protocols for animal studies were approved by the committee of animal center of Mie University, Mie, Japan (approval no. 26-19-sai2-hen1). They were acclimated for 1 week with tap water and a pelleted diet, ad libitum, before the start of the experimentation. They were housed under controlled conditions of humidity ($50 \pm 10\%$), light (12/12 h light/dark cycle), and temperature ($22 \pm 2^\circ\text{C}$). A colonic carcinogen AOM and taurine (>99%) were purchased from Sigma Chemical Co. (St. Louis, MO). DSS with a molecular weight of 40,000 was purchased from ICN Biomedicals, Inc. (Aurora, OH).

2.2. Experimental Procedure. Figure 1 shows the experimental protocol. All mice for AOM-DSS model received a single intraperitoneal injection (ip) of AOM at a dose level of 10 mg/kg body weight. One week and 3 weeks after the AOM injection, animals were exposed to 1.0% DSS (W/V) in the drinking water for 7 days twice, with one-week interval. After the first DSS treatment, the mice were randomly divided into two groups ($n=9$, each) for DW and 0.5% (W/V) taurine in drinking water (model group and taurine group, respectively), ad libitum. The mice for control group ($n=3$) were intraperitoneally injected saline and given distilled water. Body weight and stool status were checked twice a week after DSS treatment. Then, they were then sacrificed by ether overdose at week 8. At autopsy, their large bowel was flushed with saline, and excised. The large bowel (from the ileocecal junction to the anal verge) was measured, cut open longitudinally along the main axis, and then washed with saline. Tumor lesions were counted micropathologically, by two investigators.

2.3. Fecal Blood Score. For scoring fecal blood status, the presence or absence of fecal blood was indicated as follows: 0 = negative hemocult test, 1 = positive hemocult test, and 2 = gross bleeding. Fecal occult blood of mice was detected by using a forensic luminol reaction kit (Luminol Reaction Experiment Kit, Wako Pure Chemical, Osaka, Japan), according to the instruction of the company and a study of Park and Tsunoda [13] in which they presented a simple protocol to detect fecal occult blood in mice, using this kit.

2.4. Histopathological and Immunohistochemical Studies. Colon tissue samples were fixed with 4% formaldehyde in phosphate buffered saline (PBS) for one day. Following dehydration and paraffin infiltration, the tumors were embedded in paraffin blocks and then sectioned to $5 \mu\text{m}$ thickness using Leica Microsystems (Wetzlar, Germany) by routine procedures. Histopathological appearance of mouse tumors was evaluated by staining with hematoxylin and eosin (H&E) staining. Benign and malignant lesions were histopathologically distinguished using H&E staining samples by two investigators.

For immunohistochemistry (IHC) analysis, the paraffin-embedded mouse tumor sections were deparaffinized in xylene and series of alcohol. After the retrieval of heat-induced epitopes and blocking with 1% skim milk, sections were incubated overnight with primary antibodies (phosphatase and tensin homolog deleted on chromosome 10 (PTEN), Cell Signaling Technology, Inc., Danvers, MA #9188, 1:400), Ki-67 (Proteintech Group Inc., Chicago, IL, 27309-1-AP, 1:10,000), followed by incubation with biotinylated secondary antibodies (Vector Laboratories Burlingame, California, CA) for 2 h. The immunoreaction was visualized by a peroxidase stain DAB kit (Nacalai Tesque Inc., Kyoto, Japan). Nuclear counterstaining for PTEN staining samples was performed with hematoxylin, and tissues were observed and photographed under microscope (BX51, Olympus, Tokyo, Japan). The semiquantitative analysis of staining intensity was graded by an IHC score between 0 and 4 by two investigators as follows: no staining (0), weak staining (1+), moderate staining (2+), strong staining (3+), and very strong staining (4+) in all IHC studies.

2.5. Western Blot Analysis. A part of colon tissue samples (model group, $n=4$; taurine group, $n=4$; control group, $n=3$) were immediately stored at -80°C until use. They

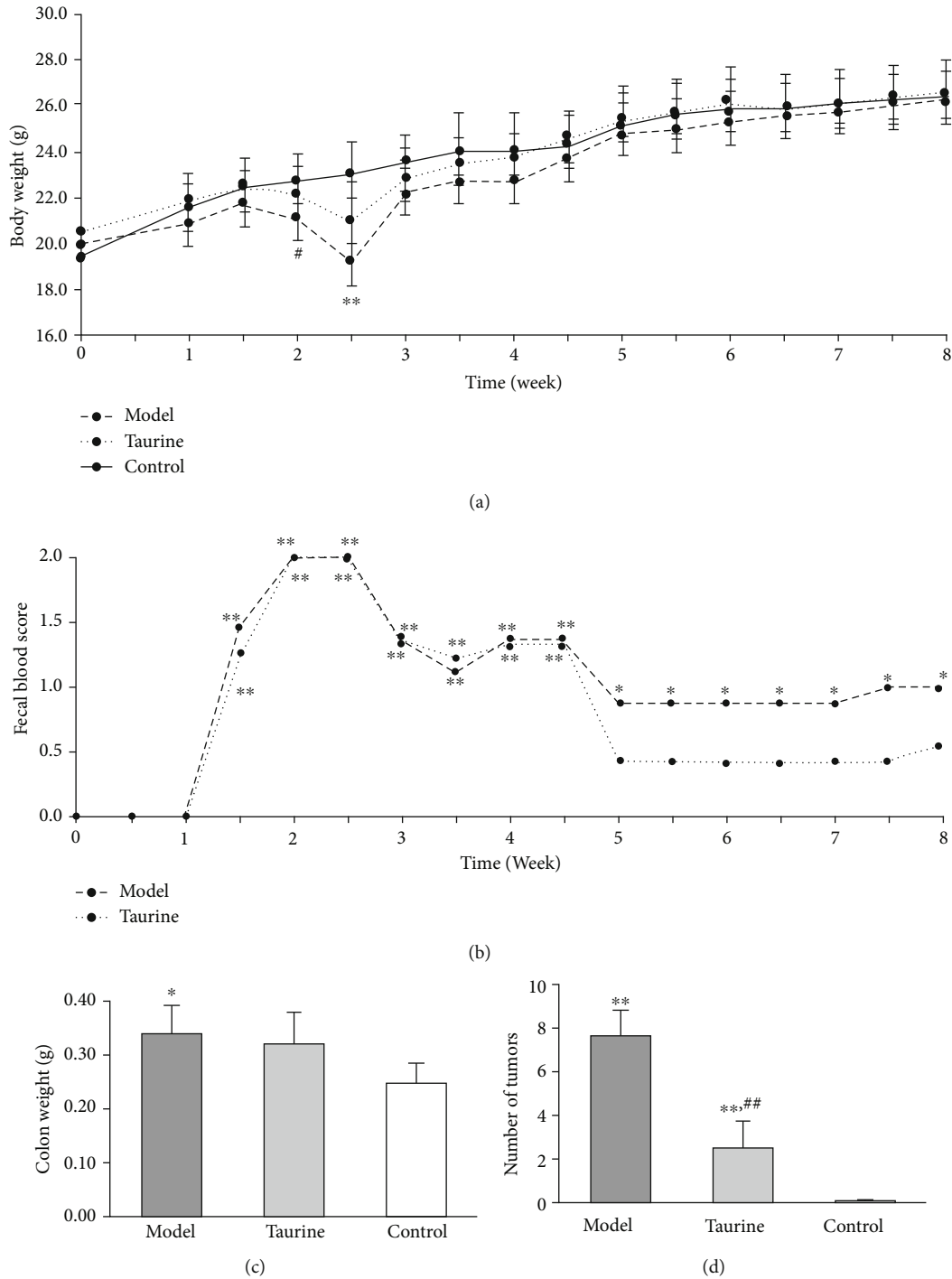


FIGURE 2: Changes in (a) body weight and (b) fecal blood scores of mice and averages of (c) colon weight and (d) number of tumors. * $P < 0.05$, ** $P < 0.01$ vs. control group, # $P < 0.05$, ## $P < 0.01$ vs. model group by (a, c, d) Student's t -test and (b) Mann-Whitney U test.

were homogenized and lysed using RIPA buffer (Cell Signaling Technology Inc.) supplemented with phenylmethylsulfonyl fluoride (PMSF, Nacalai Tesque Inc.). Equal amounts of protein were separated by SDS-PAGE and transferred to polyvinylidene fluoride (PVDF) membranes (0.45 μm , Millipore). The membranes were blocked with Tris-buffered saline (TBST) containing 0.1% Tween-20 (Nacalai Tesque Inc.) and 5% Difco Skim Milk (232100, BD Biosciences, Franklin

Lakes, NJ) and incubated overnight at 4°C with primary antibodies. Rabbit anti-cleaved caspase-9 antibody (20750S, 1: 1,000) and rabbit anti- β -actin antibody (#4967S, 1: 1,000) were obtained from Cell Signaling Technology, Inc. After washing with TBST, the membranes were further incubated with horseradish peroxidase (HRP)- conjugated secondary antibody (1: 10,000, Santa Cruz Biotechnology Inc.) for 1 h at room temperature and finally developed with an

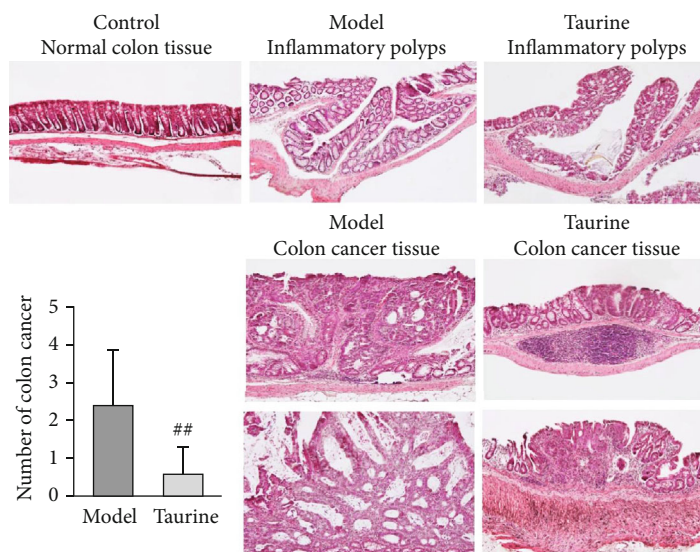


FIGURE 3: Microscopic examination of colon tissues using H&E staining. Representative images of the normal tissue from the control group, and inflammatory polyps and colon cancer from model and taurine groups. Magnification; 100–200x. Graph represents the average number of colon cancer per mouse (bar; SD). ## $P < 0.01$ between the model and taurine groups by Student's t -test.

electrochemiluminescence system (ECL) (GE Healthcare, Little Chalfont, UK). The bands were detected using a LAS4000 Mini (Fujifilm, Tokyo, Japan), and the intensities were quantitatively measured by calculating integrated grayscale densities in consistently sized windows incorporating each band using ImageJ software (version 1.48).

2.6. Statistical Analysis. Comparisons of data between groups were analyzed using Student's t -test. In the case of score values, Mann–Whitney U test was used. Fisher's exact test was used for the difference of distribution. A P value of less than 0.05 was considered statistically significant.

3. Results

3.1. Taurine Ameliorates Tumor Load in AOM/DSS Mice. The AOM+DSS mouse model was induced by intraperitoneal injection of AOM followed by two cycles of DSS exposure (Figure 1). One mouse died at week 3 in the model group ($n = 9$ to be $n = 8$) before the termination of the experiment, while no mouse died from taurine group ($n = 9$) and control group ($n = 3$).

Figure 2(a) shows the body weight change. Mice in the control group gradually gained body weight. Mice receiving DSS lost some body weight during and after the first DSS cycle, and then, the body weight was restored within the interval period. The second DSS also affected the body weight, but lesser than the effect in the first exposure. Mice in the taurine group showed less body weight loss than those in the model group.

Mice in the control group had no fecal blood during the experiment (score = 0 at all time points). All mice receiving DSS showed gross bleeding (score = 2) in feces at the end of the first cycle (week 2, Figure 2(b)). Then, mice were randomly divided into two groups (model group and taurine group). The fecal blood score decreased during the interval

period and then slightly increased during the second exposure of DSS. After two cycles of DSS, the mean scores decreased until week 5 and later plateaued (score 1 in the model group and 0.5 in the taurine group). The model group showed significantly higher fecal blood scores than the control group ($P < 0.05$ at least) during and after DSS treatment until the sacrifice. In contrast, the taurine group exhibited no significant differences after week 5. Colon weight (Figure 2(c)) was significantly greater in the model group than in the control group. There was no significant difference between the taurine and control groups, and also between the taurine and model groups. The mean number of tumors (standard deviation, SD) was 7.6 (1.2) in the model group and 2.4 (1.3) in the taurine group (Figure 2(d)). No tumor was observed in the control group. Taurine significantly suppressed AOM+DSS-induced tumor formation ($P < 0.01$). The treatment of AOM, a mutagenic agent, and DSS-induced inflammation for the mouse model of colon cancer is valuable in the understanding of the mechanisms of inflammation in tumorigenesis. In DSS treatment, colitis occurred as observed in the data of gross/occult bleeding and body weight loss. As shown here, taurine alleviated these outcomes.

3.2. Taurine Attenuates AOM-DSS-Induced Colon Carcinogenesis. H&E staining (Figure 3) showed that no inflammation and cancer lesion were observed in the control group. Many inflammatory polyps were observed in both model and taurine groups, but cancer lesions in the taurine group were smaller than those in the model group. Microscopic examination revealed that AOM/DSS treatment induced colon cancer in all mice (8/8, 100%), and taurine inhibited the progression of colon cancer (4/9, 44.4%, $P < 0.05$ by Fisher's exact test). Taurine significantly suppressed the average number of colon cancer compared to that of the model group ($P < 0.01$, Figure 3, graph).

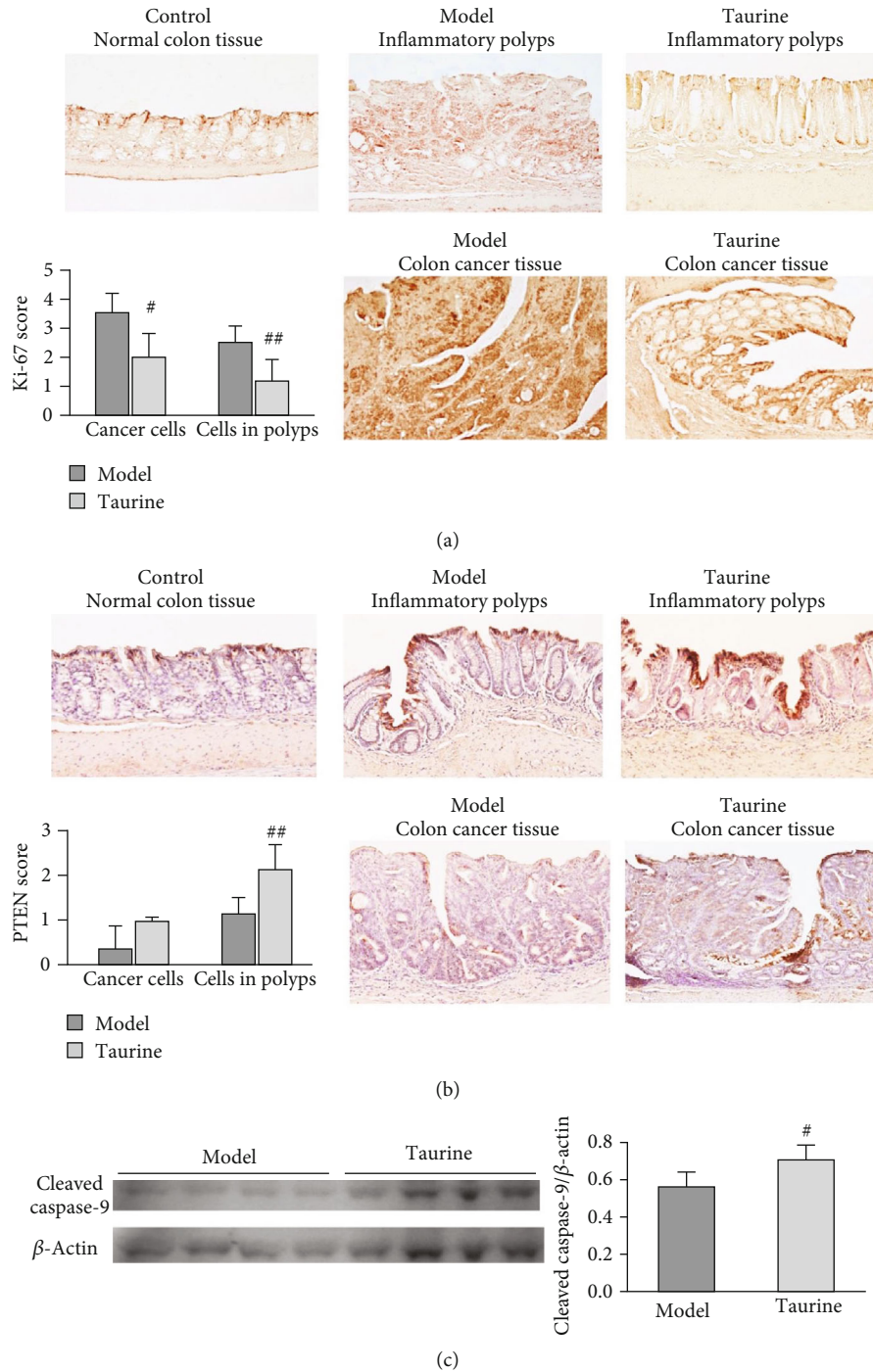


FIGURE 4: Immunohistochemistry of (a) Ki-67 and (b) PTEN and western blot analysis of (c) cleaved caspase-9. The expression of Ki-67 and PTEN was assessed by avidin-biotin kits with peroxidase-based detection (brown). Nuclei were counterstained with hematoxylin. Original magnifications 100x. (c) Western blot image and relative intensity of cleaved caspase-9 adjusted by β -actin. Graphs represent the average score (bar; SD) of (a) Ki-67 score, (b) PTEN score, (c) cleaved caspase-9. $\#P < 0.05$, $\#\#P < 0.01$ between model and taurine groups by Mann-Whitney U test for score values and Student's t -test for the intensities in the western blot analysis.

3.3. Taurine Inhibits Cell Proliferation and Induces Apoptosis through Activation of PTEN. Figure 4(a) shows levels of a marker of cell proliferation, Ki-67, in the colon tissues. The intensive Ki-67 immunoreactivities were observed in a large proportion of colon cancer cells in the model group. Ki-67 was expressed in the nuclei of cancer cells and also showed

strong immunoreactivities in the epithelial cells adjacent to inflammation polyps in the model group. In the taurine group, the cancer cells showed relatively weak Ki-67 staining in the nuclei. Normal control colon epithelial cells showed a weak immunoreactivity of Ki-67. There were significant decreases in Ki-67 immunoreactivities in both cancer and

polyp tissues of taurine-treated mice compared with those of the model mice (Figure 4(a), graph).

Figure 4(b) shows the levels of PTEN, a tumor suppressor. PTEN expression was scarcely detected in the tumor area of colon cancer tissues in the model group, compared to that in the taurine group. The PTEN expression was intensively expressed in the cytoplasm and colon mucosal epithelial cells adjacent to colon cancer tumor area of the taurine group compared to that of the model group. In contrast, normal control epithelial cells showed relatively weak immunoreactivity for PTEN expression. There was a significant increase in PTEN immunoreactivities in polyp tissues of taurine-treated mice, compared with those of model mice (Figure 4(b), graph).

Western blot analysis (Figure 4(c)) showed that taurine increased cleaved caspase-9 level, suggesting taurine-induced apoptosis.

4. Discussion

The present study demonstrated that taurine attenuated carcinogenesis in AOM-DSS model mice. At the first time, we had performed a single intraperitoneal injection of AOM at a dose level of 10 mg/kg body weight, and on the 7th day after the injection of AOM, mice received 2% DSS in drinking water for one week, according to the protocol of Suzuki et al. [12]. In our primary experiment, the high mortality of mice was observed after drinking 2% DSS, provably due to the difference of mouse species and age. So, we changed the protocol of 2% DSS into 1% DSS twice with one-week interval. The treatment of AOM and DSS induced colon cancer in all mice (8/8, 100%) of the model group, although one mouse died at week 3. Therefore, it is suggested that our protocol is an adequate method for AOM/DSS-induced mouse model for colon carcinogenesis. Interestingly, we found that taurine reduced the number of colon cancer with lower fecal blood score. Zhang et al. [14] showed antitumor properties of taurine to inhibit cell proliferation and induce apoptosis in colorectal cancer cells *in vitro*. The present *in vivo* study indicates that taurine exhibits an anticancer effect in ulcerative colitis-colorectal cancer mouse model.

In the present study, we observed the increase in cleaved caspase-9 level and decrease of Ki-67 level in mouse colon tissues of the taurine group compared to those of AOM-DSS model group. Takano et al. indicated that apoptosis in colon cancer is related to proliferative activity that can be assessed using Ki-67 labeling [15]. Moreover, several studies showed that taurine induced cell apoptosis in the colon [14], lung [16], and breast cancer cells [17]. This study demonstrated that taurine can significantly enhance the cleaved form of caspase-9, suggesting that the mitochondrial pathway of apoptosis [18] is involved in taurine-induced apoptosis in colon cancer. Our previous *in vitro* studies demonstrated that taurine increased the PTEN level in human nasopharyngeal carcinoma cells, as its anticancer mechanism [10, 11]. PTEN regulates cell division and apoptosis and helps to prevent uncontrolled cell growth, which can suppress tumor formation. PTEN interacts with p53 and enhances p53 stability, resulting in cell cycle arrest and apoptosis [19]. The present

study demonstrated that PTEN increased in mouse colon tissues of the taurine group compared to that of the AOM-DSS model group. Taurine-induced PTEN may function as a tumor suppressor, leading to reduction in colon cancer in the mouse model.

Inflammation promotes various pathogeneses, including cancer [20]. Marcinkiewicz and Kontny [2] reviewed a possible contribution of taurine to protect against the pathogenesis of inflammatory diseases. Sun et al. [21] showed that taurine suppressed the inflammatory reaction related to NF- κ B in ischemic rat brain damage. Our results suggested that taurine reduced DSS-induced inflammation as observed in lower fecal blood scores. In addition to its anti-inflammation activity, PTEN activation is one of the anticancer mechanisms of taurine.

5. Conclusions

This is the first study that demonstrated that taurine significantly reduced carcinogenicity *in vivo* using AOM/DSS-induced colon cancer mouse model. It is suggested that taurine attenuates cell proliferation and induces apoptosis via PTEN induction. Taurine could contribute to the suppression of inflammation-related carcinogenesis.

Data Availability

All data are available on request to the corresponding author.

Conflicts of Interest

The authors declare that there is no conflict of interest regarding the publication of this paper.

Acknowledgments

This work was partly supported by JSPS KAKENHI (Grant numbers JP19H03884 and JP19K22757).

References

- [1] Y. Yamori, T. Taguchi, A. Hamada, K. Kunimasa, H. Mori, and M. Mori, "Taurine in health and diseases: consistent evidence from experimental and epidemiological studies," *Journal of Biomedical Science*, vol. 17, Supplement 1, p. S6, 2010.
- [2] J. Marcinkiewicz and E. Kontny, "Taurine and inflammatory diseases," *Amino Acids*, vol. 46, no. 1, pp. 7–20, 2014.
- [3] K. Pandya, G. J. Clark, and C. A. Lau-Cam, "Investigation of the role of a supplementation with taurine on the effects of hypoglycemic-hypotensive therapy against diabetes-induced nephrotoxicity in rats," *Advances in Experimental Medicine and Biology*, vol. 975, pp. 371–400, 2017.
- [4] K. Shimada, C. J. Jong, K. Takahashi, and S. W. Schaffer, "Role of ROS production and turnover in the antioxidant activity of taurine," *Advances in Experimental Medicine and Biology*, vol. 803, pp. 581–596, 2015.
- [5] C. Chen, S. F. Xia, J. He, G. Lu, Z. Xie, and H. Han, "Roles of taurine in cognitive function of physiology, pathologies and toxication," *Life Sciences*, vol. 231, p. 116584, 2019.

- [6] H. Kaneko, M. Kobayashi, Y. Mizunoe et al., "Taurine is an amino acid with the ability to activate autophagy in adipocytes," *Amino Acids*, vol. 50, no. 5, pp. 527–535, 2018.
- [7] A. A. Makhova, E. V. Shikh, T. V. Bulko, Z. M. Sizova, and V. V. Shumyantseva, "The influence of taurine and L-carnitine on 6 β -hydroxycortisol/cortisol ratio in human urine of healthy volunteers," *Drug Metabolism and Personalized Therapy*, vol. 34, no. 3, 2019.
- [8] Y. Ohsawa, H. Hagiwara, S. I. Nishimatsu et al., "Taurine supplementation for prevention of stroke-like episodes in MELAS: a multicentre, open-label, 52-week phase III trial," *Journal of Neurology, Neurosurgery, and Psychiatry*, vol. 90, no. 5, pp. 529–536, 2019.
- [9] S. Kawanishi, S. Ohnishi, N. Ma, Y. Hiraku, and M. Murata, "Crosstalk between DNA damage and inflammation in the multiple steps of carcinogenesis," *International Journal of Molecular Sciences*, vol. 18, no. 8, p. 1808, 2017.
- [10] F. He, N. Ma, K. Midorikawa et al., "Anti-cancer mechanisms of taurine in human nasopharyngeal carcinoma cells," *Advances in Experimental Medicine and Biology*, vol. 1155, pp. 533–541, 2019.
- [11] F. He, N. Ma, K. Midorikawa et al., "Taurine exhibits an apoptosis-inducing effect on human nasopharyngeal carcinoma cells through PTEN/Akt pathways in vitro," *Amino Acids*, vol. 50, no. 12, pp. 1749–1758, 2018.
- [12] R. Suzuki, H. Kohno, S. Sugie, and T. Tanaka, "Sequential observations on the occurrence of preneoplastic and neoplastic lesions in mouse colon treated with azoxymethane and dextran sodium sulfate," *Cancer Science*, vol. 95, no. 9, pp. 721–727, 2004.
- [13] A. M. Park and I. Tsunoda, "Forensic luminol reaction for detecting fecal occult blood in experimental mice," *BioTechniques*, vol. 65, no. 4, pp. 227–230, 2018.
- [14] X. Zhang, S. Tu, Y. Wang, B. Xu, and F. Wan, "Mechanism of taurine-induced apoptosis in human colon cancer cells," *Acta Biochimica et Biophysica Sinica*, vol. 46, no. 4, pp. 261–272, 2014.
- [15] Y. Takano, M. Saegusa, M. Ikenaga, H. Mitomi, and I. Okayasu, "Apoptosis of colon cancer: comparison with Ki-67 proliferative activity and expression of p53," *Journal of Cancer Research and Clinical Oncology*, vol. 122, no. 3, pp. 166–170, 1996.
- [16] S. Tu, X.-L. Zhang, H.-F. Wan et al., "Effect of taurine on cell proliferation and apoptosis human lung cancer A549 cells," *Oncology Letters*, vol. 15, no. 4, pp. 5473–5480, 2018.
- [17] X. Zhang, H. Lu, Y. Wang et al., "Taurine induces the apoptosis of breast cancer cells by regulating apoptosis-related proteins of mitochondria," *International Journal of Molecular Medicine*, vol. 35, no. 1, pp. 218–226, 2015.
- [18] Y. Luu, J. Bush, K. J. Cheung Jr., and G. Li, "The p53 stabilizing compound CP-31398 induces apoptosis by activating the intrinsic Bax/mitochondrial/caspase-9 pathway," *Experimental Cell Research*, vol. 276, no. 2, pp. 214–222, 2002.
- [19] L. Salvatore, M. A. Calegari, F. Loupakis et al., "PTEN in colorectal cancer: shedding light on its role as predictor and target," *Cancers*, vol. 11, no. 11, p. 1765, 2019.
- [20] M. Murata, "Inflammation and cancer," *Environmental Health Preventive Medicine*, vol. 23, 2018.
- [21] M. Sun, Y. Zhao, Y. Gu, and C. Xu, "Anti-inflammatory mechanism of taurine against ischemic stroke is related to down-regulation of PARP and NF- κ B," *Amino Acids*, vol. 42, no. 5, pp. 1735–1747, 2012.

Research Article

DpdtC-Induced EMT Inhibition in MGC-803 Cells Was Partly through Ferritinophagy-Mediated ROS/p53 Pathway

Jiankang Feng,¹ Cuiping Li,¹ Ruifang Xu,² Yongli Li ,³ Qi Hou,³ Rui Feng,² Senye Wang,² Lei Zhang,² and Changzheng Li ^{1,2,4}

¹Department of Molecular Biology and Biochemistry, Xinxiang Medical University, Xinxiang, Henan, China 453003

²Experimental Teaching Center of Biology and Basic Medical Sciences, Sanquan College of Xinxiang Medical University, Xinxiang, Henan, China 453003

³Department of Histology and Embryology, Sanquan College of Xinxiang Medical University, Xinxiang, Henan, China 453003

⁴Laboratory of Molecular Medicine, Xinxiang Medical University, Xinxiang, Henan, China 453003

Correspondence should be addressed to Yongli Li; liyongli@sqmc.edu.cn and Changzheng Li; changzhenl@yahoo.com

Received 24 November 2019; Accepted 14 February 2020; Published 12 March 2020

Guest Editor: Teruo Miyazaki

Copyright © 2020 Jiankang Feng et al. This is an open access article distributed under the Creative Commons Attribution License, which permits unrestricted use, distribution, and reproduction in any medium, provided the original work is properly cited.

Epithelial-mesenchymal transition (EMT) is a cellular process in which epithelial cells are partially transformed into stromal cells, which endows the polarized epithelium cells more invasive feature and contributes cancer metastasis and drug resistance. Ferritinophagy is an event of ferritin degradation in lysosomes, which contributes Fenton-mediated ROS production. In addition, some studies have shown that ROS participates in EMT process, but the effect of ROS stemmed from ferritin degradation on EMT has not been fully established. A novel iron chelator, DpdtC (2,2'-di-pyridylketone dithiocarbamate), which could induce ferritinophagy in HepG2 cell in our previous study, was used to investigate its effect on EMT in gastric cancer cells. The proliferation assay showed that DpdtC treatment resulted in growth inhibition and morphologic alteration in MGC-803 cell ($IC_{50} = 3.1 \pm 0.3 \mu M$), and its action involved ROS production that was due to the occurrence of ferritinophagy. More interestingly, DpdtC could also inhibit EMT, leading to the upregulation of E-cadherin and the downregulation of vimentin; however, the addition of NAC and 3-MA could attenuate (or neutralize) the action of DpdtC on ferritinophagy induction and EMT inhibition, supporting that the enhanced ferritinophagic flux contributed to the EMT inhibition. Since the degradation of ferritin may trigger the production of ROS and induce the response of p53, we next studied the role of p53 in the above two-cell events. As expected, an upregulation of p53 was observed after DpdtC insulting; however, the addition of a p53 inhibitor, PFT- α , could significantly attenuate the action of DpdtC on ferritinophagy induction and EMT inhibition. In addition, autophagy inhibitors or NAC could counteract the effect of DpdtC and restore the level of p53 to the control group, indicating that the upregulation of p53 was caused by ferritinophagy-mediated ROS production. In conclusion, our data demonstrated that the inhibition of EMT induced by DpdtC was realized through ferritinophagy-mediated ROS/p53 pathway, which supported that the activation of ferritinophagic flux was the main driving force in EMT inhibition in gastric cancer cells, and further strengthening the concept that NCOA4 participates in EMT process.

1. Introduction

Gastric cancer (GC) is the second highest mortality among cancers worldwide, and higher cases of it occur in East Asia [1, 2]. Although significant improvement in both diagnosis and treatment was achieved, the overall survival rate is still poor. Therefore, more efforts to clarify the underlying mechanisms of this deadly cancer are urgently needed. Clinically,

the chemotherapy is still the main treatment for advanced GC [3]; however, attenuating the side effects and resistance of chemotherapeutic agents requires a different strategy. Iron is an essential element for cell growth, and it has been demonstrated that cancer cells have higher iron demand compared to normal cells; disturbing homeostasis of iron may achieve growth inhibition of cancer cells, thus chelation therapy was proposed in clinical practice. Dithiocarbamate is

an important class of sulfur-containing compounds, showing their potent applications on disease treatment, the treatment of bacterial, fungal infections, AIDS, and cancer [4, 5]. Dithiocarbamate has strong affinity toward metal ions; however, the underlying mechanism remains obscure.

Epithelial-to-mesenchymal transition (EMT) is a cellular process that epithelial cells will undergo several biochemical alterations, such as the suppression of epithelial markers and the upregulation of mesenchymal markers, endowing the polarized epithelium cells more invasive feature [6–8]. EMT is considered as a crucial step in cancer metastasis, and transforming growth factor (TGF), the cytokine, and nuclear receptor, receptor tyrosine kinase (RTK), the Wnt, Notch, hedgehog, hippo, and pathways have all been implicated in the onset of EMT [9, 10]. In addition, it has shown that the cells underwent EMT have an ability to resist conventional treatments [10]. Therefore, to develop new diagnostic and therapeutic strategies in treatment of metastases, the details in EMT required to be revealed.

ROS are constantly generated inside cells through a serial of dedicated enzyme complexes or as by-products of redox reactions, such as mitochondrial respiration [10–12]. In addition, the iron either in lysosome due to the occurrence of ferritinophagy or in labile iron pool (LIP) catalyzes Fenton reaction, yielding extremely reactive hydroxyl radicals [13]. Furthermore, the compelling evidence reveals reactive oxygen species (ROS) engage EMT process [14], but the functions of ROS remains to be determined. Recently a series of small molecular compounds exhibit the ability in EMT reversal, different signal pathway were proposed [15–18].

p53 is one of most important transcription factor, regulating proliferation, apoptosis, cell cycle and autophagy that maintain normal cellular homeostasis, controlling cell fates [19]. However, the tumor suppressor gene p53 is the most commonly mutated gene in all human cancers [20–22], such as hepatocellular carcinoma, colorectal cancer, lymphoma, mucosal melanoma, and stomach cancer [23–27]. High invasion and metastasis is the hallmark of cancer cells, EMT is prerequisite for primary cancer metastasizing to blood, and other organs [28, 29]. p53 mutation is essential to EMT process and also plays role in EMT [19, 30]. Since mutant p53 alleles may exhibit certain unique characteristics in cancer development and progression, therefore, reactivation or degradation of mutant p53 may be another strategy in cancer therapy [31]. Wild-type p53 is maintained at a low level by continuous degradation via proteasome through E3 ubiquitin ligase [30, 32], but mut-p53 degradation is diversified [33–35].

Ferritin is a highly conserved iron storage protein which is composed of two subunits, H-ferritin and L-ferritin, and the twelve pairs of subunits binding head to foot form the 24 subunit ferritin cages [36]. Ferritin degradation results in the release of iron for either use by the cell or enhancing labile iron pool; therefore, ferritin also regulates cellular redox balance. Iron chelator can lead to ferritin degradation either through ubiquitination or autophagy; the latter requires participation of microtubule-associated protein light chain 3 (LC3) and NCOA4, termed “ferritinophagy [37]. Iron depletion by some iron chelators resulted in the occurrence of fer-

ritinophagy has been reported [37, 38], but the correlation between EMT and ferritinophagy induced by iron chelator remains to be determined. In our previous work, we reported that activating ferritinophagic flux (NCOA4/ferritin) could inhibit EMT in DpdtP treated CT26 cell, firstly revealing that NCOA4 also involves in EMT process. To verify if this phenomenon is restricted to CT26 cells or if it represents a more general phenomenon, the gastric cancer cell line and a novel iron chelator, DpdtC were chosen in the present study. As expected, the DpdtC as DpdtP acted also displayed EMT inhibition. The mechanistic study further supported that ferritinophagy-mediated EMT inhibition was through by activation of ROS/p53 pathway.

2. Results

2.1. The DpdtC-Induced Growth Inhibition Involved ROS Production. In our previous study, 2,2'-di-pyridineketone hydrazone dithiocarbamate (DpdtC, Figure 1(a)) displayed significant antitumor activity against HepG2 cell [38]. To expand our understanding of the agent, we further studied its growth inhibitory effect on gastric cancer cells. The dose-response curve is depicted in Figure 1(b). As expected, DpdtC displayed significant growth inhibition for gastric cells (IC₅₀: 3.1 ± 0.3 μM for MGC-803). Furthermore, to determine whether the growth inhibition involved ROS production, the cellular ROS level was measured by flow cytometry as described previously [38]. As shown in Figure 1(c), the populations in higher fluorescence intensities significantly increased by ~30% after exposure of DpdtC to the cells for 24 h, but the addition of NAC, a ROS scavenger, significantly decreased ROS production (~14%), hinting that the antiproliferative action involved ROS production. Furthermore, the role of ROS production in the growth inhibition was further determined. As showed in Figure S1, the addition of NAC (0.15 mM) could attenuate the inhibitory ability of DpdtC on proliferation of gastric cancer cells, indicating that DpdtC-induced growth inhibition was related to ROS production.

2.2. DpdtC-Induced ROS Was Partly due to the Occurrence of Ferritinophagy. Previous work revealed that the DpdtC induced ferritinophagy in hepatocellular carcinoma cells [38], which led to ROS generation. DpdtC treatment in gastric cancer cells also resulted in ROS production, we hypothesized that the ROS production might be due to the occurrence of ferritinophagy. To this end, the levels of ferritin and NCOA4, a specific carrier for ferritinophagy, was evaluated via immunofluorescence technique. As shown in Figure 2, DpdtC exposure indeed resulted in upregulated NCOA4 (compare Figure 2(f) to Figure 2(b)) and downregulated ferritin (compare Figure 2(g) to Figure 2(c)), indicating that the ferritin degradation was through autophagic proteolysis. Furthermore, the addition of 3-MA, an autophagy inhibitor, could abolish the ferritinophagy, i.e., leading to a significant upregulation of ferritin (compare Figure 2(k) to Figure 2(g)). The merged photographs (Figures 2(d), 2(h), and 2(l)) clearly showed the alterations

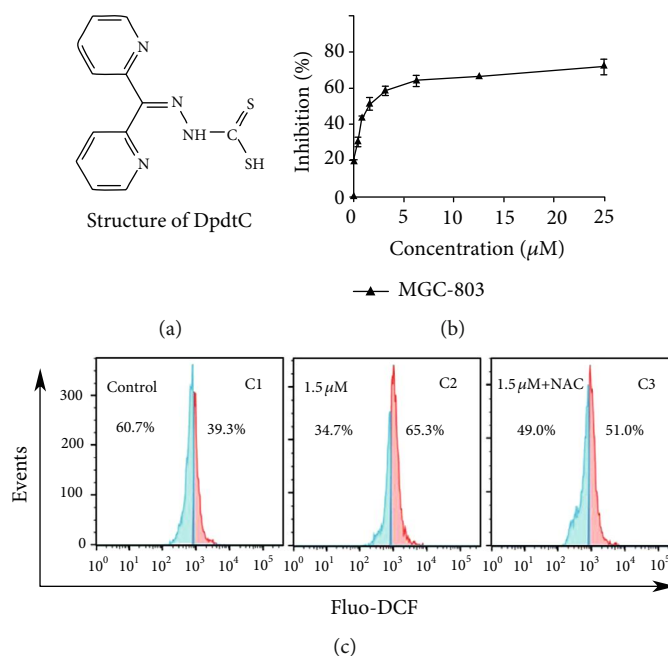


FIGURE 1: DpdtC-induced growth inhibition involved ROS generation. (a) Structure of DpdtC; (b) the effect of DpdtC on proliferation of gastric cancer cell; (c) DpdtC-induced ROS production in MGC-803 cell line: C1, control (H_2O); C2, $1.5 \mu M$ DpdtC; C3, $1.5 \mu M$ DpdtC +NAC ($1.5 mM$). The data from MTT assay were from five measurements; and ROS assays were conducted twice.

in NCOA4 and ferritin. To corroborate the occurrence of ferritinophagy, the levels of ferritin, NCOA4, and autophagy-related proteins before and after DpdtC treatment were further determined by Western blotting. As shown in Figure 3, concomitant to the decrease of ferritin, the upregulated autophagic markers (LC3-II, beclin) and NCOA4 were observed upon DpdtC treatment; however, the addition of 3-MA or DFO, as well as NAC, could markedly attenuate the levels of those upregulated proteins. Accordingly, a quantitative comparison in ratios of NCOA4/ferritin that termed “ferritinophagic flux” [39], LC3-II/ferritin and beclin/ferritin is shown in Figure 3(b), clearly DpdtC treatment resulted in activation of autophagy, i.e., increase of ferritinophagic flux and ferritin degradation. In addition, the occurrence of ferritinophagy would result in the change of cellular iron; thus, the total iron content before and after DpdtC exposure to the gastric cells was determined by atomic absorbance spectrometry. As shown in Figure S2, DpdtC treatment indeed resulted in markedly decrease of iron abundance, in accordance with results from immunofluorescence and Western blotting analysis.

2.3. The DpdtC Induced an EMT Inhibition. In addition to growth inhibition, DpdtC also had effect on cellular morphology of gastric cancer cells. Figures 4(a)–4(c) showed the alteration in morphology when exposure of DpdtC to the cells, which encouraged us to consider whether its action involved EMT transformation, inhibiting metastasis of cancers [40]. Thus, the molecular markers in EMT transformation were labeled by immunofluorescence technique before and after DpdtC treatment. As shown in Figure 4, the green fluorescence of E-cadherin was increased (compare

Figure 4(j) to Figure 4(f)), while the red fluorescence which represented vimentin was decreased (compare Figure 4(g) to Figure 4(k)). The merged photographs (Figures 4(h) and 4(l)) clearly showed the alterations in E-cadherin and vimentin, the proportion of red fluorescence (vimentin) in Figure 4(h) was much higher than that in Figure 4(l), indicating that DpdtC could inhibit the EMT transition. Furthermore, Western blotting analysis also demonstrated that DpdtC could downregulate mesenchymal marker, vimentin, contrarily upregulate epithelial marker, E-cadherin (Figure 4(d)), in consistent with that from immunofluorescence analysis, supporting that DpdtC had inhibitory effect on EMT transformation.

2.4. DpdtC-Suppressed TGF- β 1-Induced EMT through Ferritinophagy Pathway. To validate the ability of DpdtC in EMT modulation, a model that was undergoing EMT required to be established. Thus, the MGC-803 cells were pretreated with TGF- β 1, the most powerful EMT inducer for 48 h, which resulted in obviously morphological alteration. As shown in Figures 5(g) and 5(h), the MGC-803 cells became more spindle-shaped, fibroblast-like cells compared to control (Figures 5(c) and 5(d)), which was considered cells undergoing the EMT [41]. Next, the undergoing EMT cells were further treated by DpdtC, as shown in Figure 5(j), DpdtC could significantly increase the level of E-cadherin and neutralize the action of TGF- β 1 on vimentin modulation (Figure 5(k)). The alterations in E-cadherin and vimentin before and after treatment of DpdtC could be clearly observed in the merged photographs (Figures 5(h) and 5(l)), corroborating that DpdtC was able to resist TGF- β 1-induced EMT.

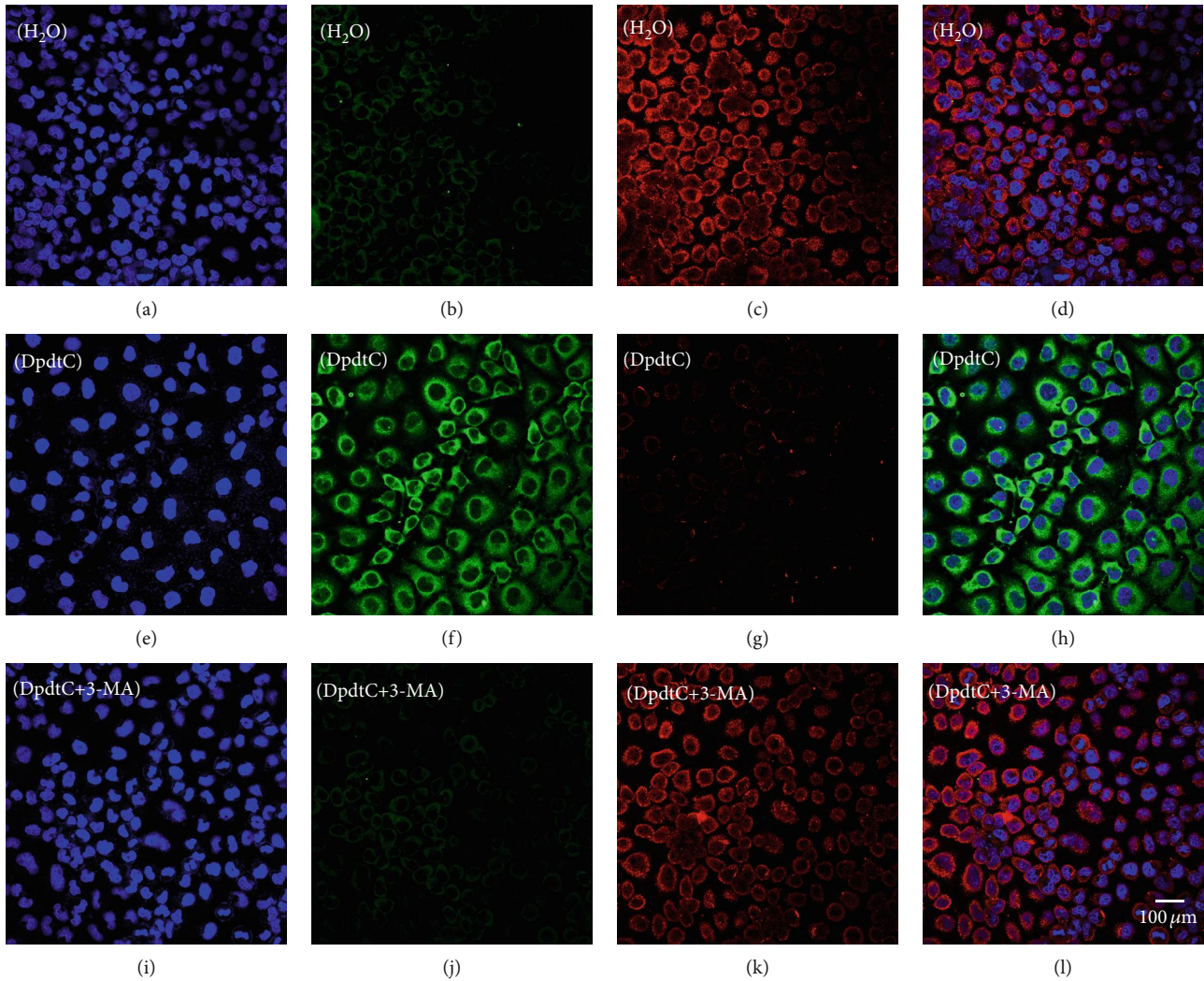


FIGURE 2: DpdtC-induced ferritin autophagy (ferritinophagy). The nuclei stained by DAPI in blue, ferritin labeled in red; NCOA4 labeled in green. (a–d) Control group: (a) nuclei in blue; (b) NCOA4 in green; (c) ferritin in red; and (d) merge of ferritin with NCOA4. (e–h) DpdtC-treated group: (e) nuclei in blue; (f) NCOA4 in green; (g) ferritin in red; and (h) merge of ferritin with NCOA4. (i–l) DpdtC combined with 3-MA group: (i) nuclei in blue; (j) NCOA4 in green; (k) ferritin in red; and (l) merge of ferritin with NCOA4. The experiments were performed thrice. Objective size: 40×10 ; scale bar: $100 \mu\text{m}$.

Since DpdtC could resist the action of TGF- β 1 on EMT modulation, was there an occurrence of ferritinophagy in above experimental condition? Thus, the levels of cellular NCOA4 and ferritin in the presence of TGF- β 1 were further evaluated by immunofluorescence. As shown in Figure 6, TGF- β 1 slightly increased the level of ferritin compared to control (Figures 6(g) and 6(c)); however, the addition of DpdtC significantly attenuated the action of TGF- β 1 on ferritin modulation (Figure 6(k)), leading to marked increase of NCOA4, indicating that DpdtC still induced ferritinophagy in gastric cancer cells even the cells were undergoing EMT. The knockdown of NCOA4 by interfering RNA resulted in increase in vimentin, slug, and snail and also neutralized the action of DpdtC on those genes modulation (Figure S3), indicating that NCOA4 indeed modulated EMT progress, in accordance with previous observation in CT26 cells [39].

To strengthen the relationship between EMT inhibition and ferritinophagy induction, a correlation analysis between ferritinophagic flux (NCOA4/ferritinophagy) and levels of epithelial-mesenchymal markers were performed. As shown in Figure 7, TGF- β 1 boosted EMT (upregulated vimentin and downregulated E-cadherin) through lowering ferritinophagic flux, contrarily EMT inhibition induced by DpdtC was through elevating ferritinophagic flux (Figure 7(b)). Those indicated that the status of EMT may depend on strength of ferritinophagic flux.

2.5. DpdtC-Suppressed EMT Was p53 Dependent. Since mutant p53 exhibits certain unique characteristics in cancer development, p53 mutation is essential to EMT process [19, 30]. The observation that DpdtC could inhibit EMT promoted us to consider that the action of DpdtC may involve the alteration of p53 in gastric cancer cells. To this

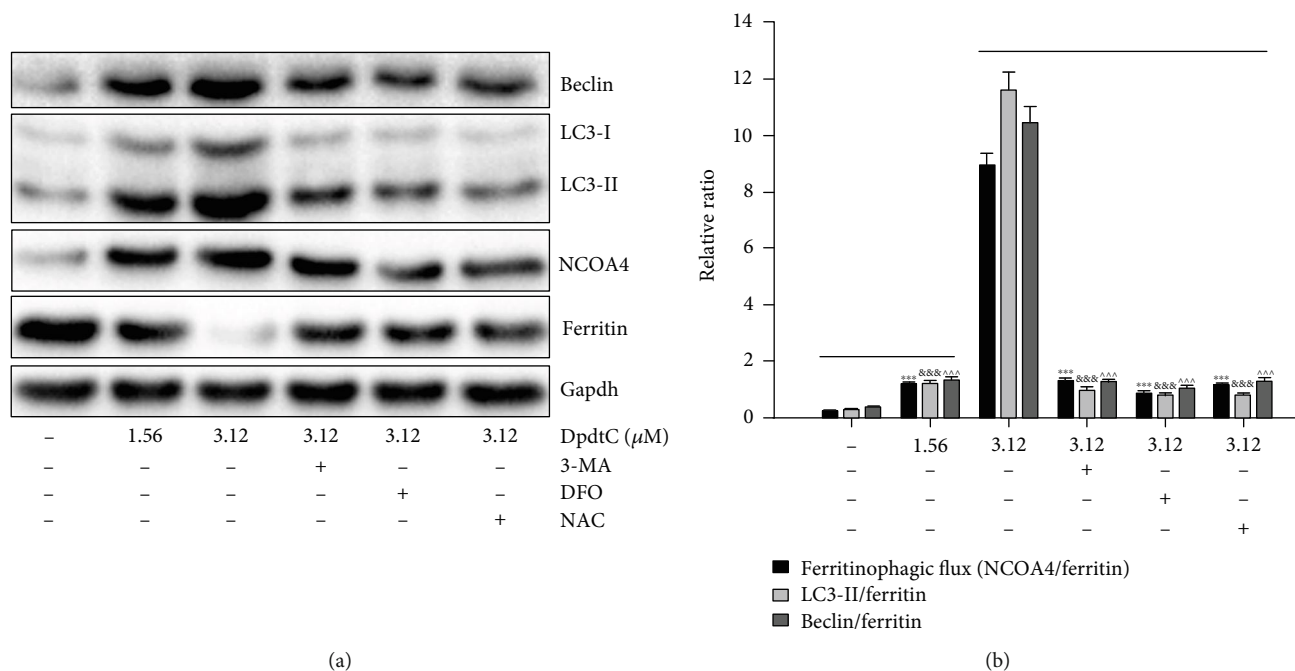


FIGURE 3: DpdtC exposure resulted in the alterations of ferritinophagy- and autophagy-related proteins. (a) Western blotting analysis of autophagic and ferritinophagic proteins; (b) the quantitative analyses of ratio of NCOA4/ferritin, LC3-II/ferritin, and beclin/ferritin at protein level from (a). The quantification analysis of indicated ratio was from two experiments. ***,↑, →, ↓ $p < 0.01$.

end, the PFT- α , a p53 inhibitor, was used to determine whether p53 involved the EMT inhibition. As shown in Figure 8, DpdtC treatment resulted in an upregulated E-cadherin (compare Figure 8(b) with Figure 8(f)) and a downregulated vimentin (compare Figure 8(c) with Figure 8(g)); however, the addition of PFT- α attenuated the upregulation of E-cadherin induced by DpdtC (Figure 8(f) and Figure 8(j)), accordingly enhancing vimentin expression (Figure 8(g) and Figure 8(k)), indicating that p53 indeed involved the action of DpdtC on EMT modulation. The alterations in E-cadherin and vimentin at different conditions could be clearly observed in the merged photographs (Figures 8(d), 8(h), and 5(l)). The additional evidence from Western blotting analysis supported the above conclusion. Figure S4 showed that DpdtC significantly upregulated p53 and E-cadherin expression and downregulated EMT-related genes expression, such as snail, slug, and vimentin; however, a p53 inhibitor, PFT- α , markedly attenuated action of DpdtC on those genes modulation, which was in accordance with result from immunofluorescence.

2.6. DpdtC Triggered Ferritinophagy Was p53 Dependent. Since DpdtC-induced EMT inhibition was p53 dependent, the ferritinophagy induction might be in similar manner. Thus cell were treated with DpdtC alone or combined with PFT- α for 24h, then the level of ferritinophagy-related protein was investigated by immunofluorescence technique. As shown in Figure 9, the addition of PFT- α indeed reversed the action of DpdtC in ferritinophagy induction (Figure 9

H and 9L), indicating that the action of DpdtC involved p53 response. To seek additional evidence, the expressions of EMT and ferritinophagy-related proteins were detected further by Western blotting. As shown in Figure S5, DpdtC could upregulate NCOA4 and downregulate ferritin; however, this action could significantly attenuate PFT- α , indicating that the upregulation of NCOA4 correlated with the upregulation of p53.

2.7. Ferritinophagy-Mediated ROS Resulted in the Upregulation of p53 and Growth Inhibition. As showed in Figure 3, DpdtC could induce autophagy, which led to the upregulation of beclin and LC3-II, with a concomitant accumulation of ferritinophagic flux (the ratio of NCOA4/ferritin increased). The occurrence of ferritinophagy undoubtedly generated excessive ROS due to ferric iron release triggering Fenton reaction, accordingly leading to p53 response to initiate either protect the cell from death or death program. Figure S6 showed that DpdtC-induced ROS production could be attenuated by the addition of a p53 inhibitor, PFT- α , indicating that p53 responded ferritinophagy-mediated ROS production. Additional evidence was from Figure 10; the DpdtC-induced upregulation of p53 could be attenuated by autophagy inhibitor, 3-MA, and chloroquine (conversely the level of MDM2 was enhanced), indicating that the occurrence of autophagy responded the rising of p53. Both knockdown of NCOA4 by interfering RNA and addition of NAC all neutralized upregulation of p53 induced by DpdtC, further supporting that ferritinophagy-mediated ROS triggered p53 activation. Similarly, situation

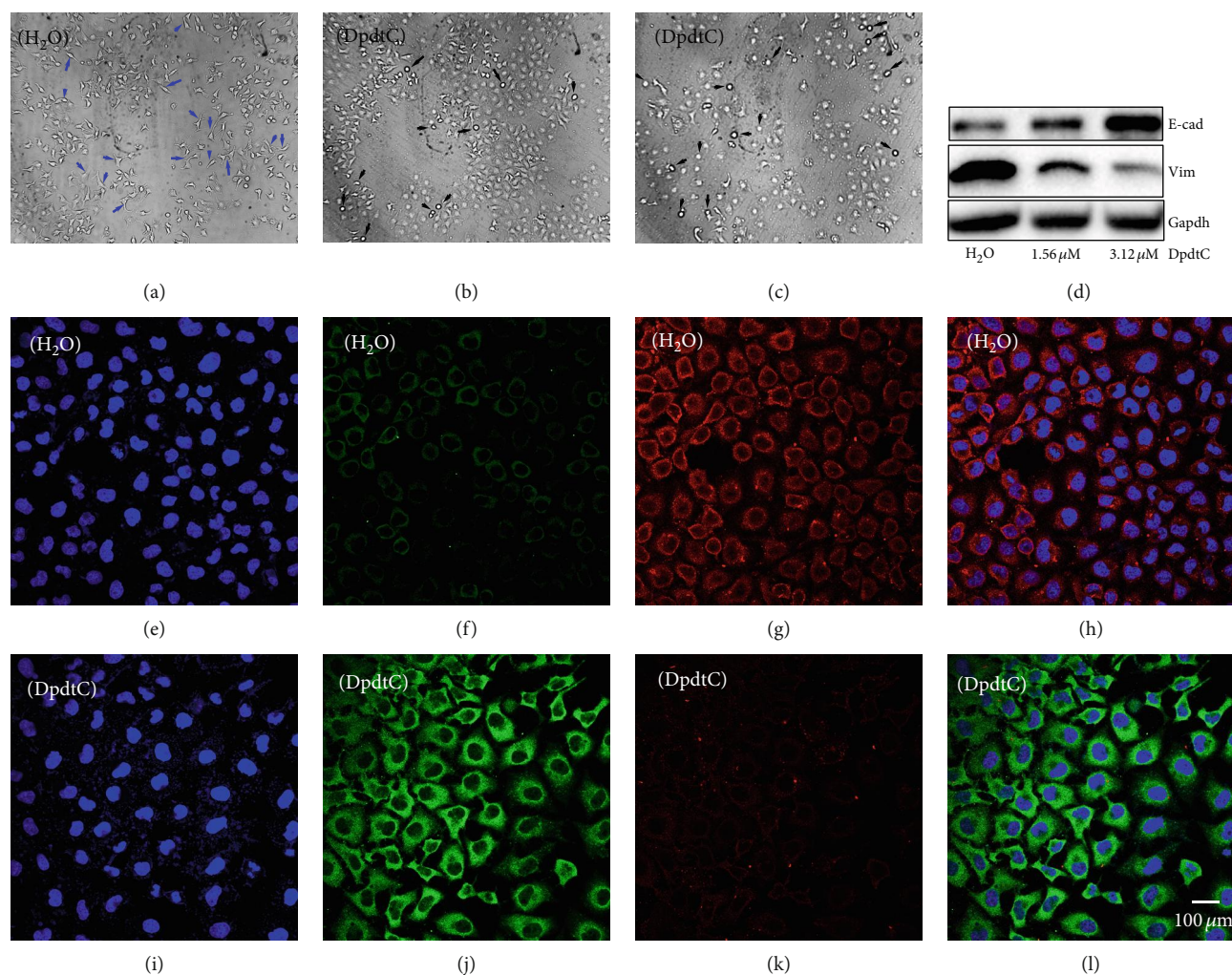


FIGURE 4: DpdtC-induced morphologic change correlated with EMT modulation. (a–c) Morphologic change upon exposure DpdtC to MGC-803 cells for 48 h. The blue arrow: spindle-shaped cells, black arrow: retracted and rounded cells; (a) H_2O , (b) $0.31 \mu M$ DpdtC, and (c) $0.62 \mu M$ DpdtC; objective size: 20×10 ; scale bar: $200 \mu m$. (d) Western blotting analysis. (e–l) immunofluorescence analysis of epithelial-mesenchymal markers. (e–h) Control group (H_2O): (e) nuclei in blue; (f) E-cadherin in green; (g) vimentin in red; and (h) merge of nuclei, E-cadherin, and vimentin in control group. (i–l) DpdtC-treated group: (i) nuclei in blue; (j) E-cadherin in green; (k) vimentin in red; and (l) merge of nuclei, E-cadherin, and vimentin in DpdtC-treated group. Objective size: 40×10 (fluorescence); scale bar: $100 \mu m$.

occurred in growth inhibition induced by DpdtC (Figure S1). Taken together, those supported that ROS (originated from ferritinophagy)/p53 involved EMT inhibition induced by DpdtC.

3. Discussion

Tumor metastasis undergoes epithelial-mesenchymal transition (EMT), which endows cells with invasive ability [40]. Therefore, EMT inhibition may be helpful for tumor therapy. A number of transcription factors, such as ZEB 1 and ZEB 2, snail, slug, and twist, regulate EMT [41]. Furthermore, the growth factors and cytokines, ECM components, hypoxia, ROS, and other factors also observed to be involved in EMT process [42]; therefore, the regulation of EMT is diversified and remains to be elucidated. In previous study, we observed that DpdtA could both inhibit proliferation and

EMT in CT26 cells. DpdtC, an analogue of DpdtA, may have similar function in gastric cancer line. Thus, the current study was focused on the alteration of the MGC-803 cells upon DpdtC treatment. Similar to DpdtA, DpdtC displayed a significant growth inhibition that was attenuated by the addition of NAC, indicating that the induced growth inhibition was ROS dependent (Figures 1 and S1); similar situations were observed in others studies [39, 43]. ROS production may stem from lysosomes, mitochondria, and imbalance between cellular oxidants and antioxidants; thus, the possible origin of ROS generation in DpdtC-induced growth inhibition needed to be determined. Generally, the main types of ROS from mitochondria are superoxide and peroxide [44], while the hydroxyl radical is mainly due to Fenton reaction occurred in lysosomes or labile iron pool. In our study, DpdtC caused marked decrease of ferritin, accompanied by increasing of NCOA4 and autophagy-

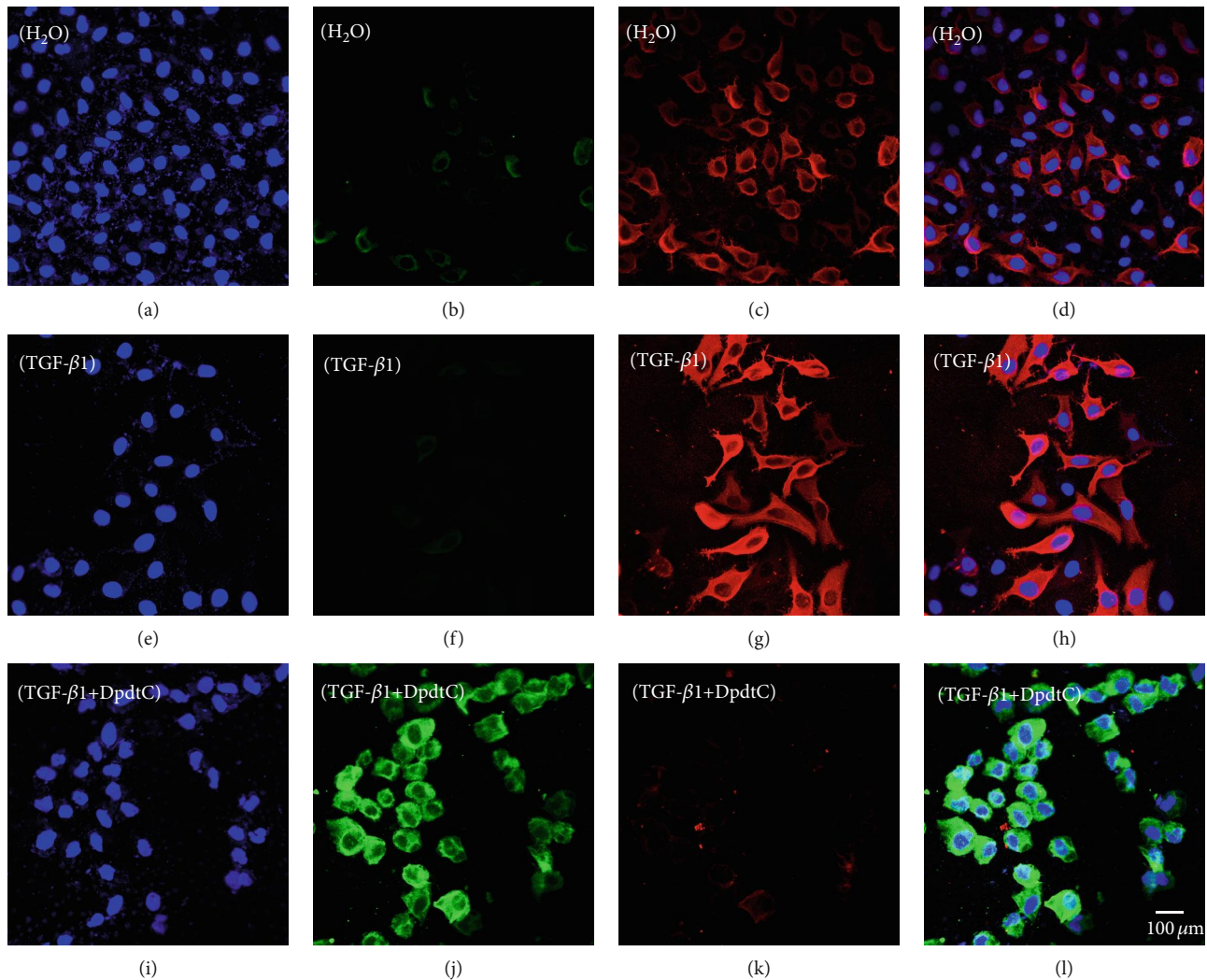


FIGURE 5: DpdtC-resisted TGF- β 1-induced EMT. (a–d) Control: (a) nuclei stained by DAPI in blue (DMSO); (b) E-cadherin in green; (c) vimentin in red; and (d) merge of nuclei, E-cadherin, and vimentin. (e–h) TGF- β 1 treated: (e) nuclei in blue; (f) E-cadherin in green; (g) vimentin in red; and (h) merge of nuclei, E-cadherin, and vimentin. (i–l) TGF- β 1 treatment plus DpdtC: (i) nuclei stained by DAPI in blue (DMSO); (j) E-cadherin in green; (k) vimentin in red; and (l) merge of nuclei, E-cadherin, and vimentin. The measurements were performed thrice from different field of view. Objective size: 40×10 ; scale bar: $100 \mu\text{m}$.

related proteins, revealing that the ROS production partly stemmed from the occurrence of ferritinophagy (Figures 2, 3, and S2), in accordance with observation in HepG2 cells reported previously [38]. The morphologic alteration of MGC-803 induced by DpdtC happened in similar way in CT26 cells caused by DpdtA, which implied that the action of DpdtC might involve EMT regulation. The immunofluorescence and Western blotting analysis confirmed our speculation because of the alteration in epithelial-mesenchymal markers after DpdtC treatment (Figure 4), in accordance with others observation [45]. To corroborate the ability of DpdtC in induction, the EMT model that induced by TGF- β 1 needed to be established for this method has been widely accepted in molecular biology [46]. It was interesting that DpdtC abolished the action of TGF- β 1 on EMT induction in the present study (Figure 5), demonstrating that DpdtC was able to inhibit EMT, which was in accordance with the

action of the iron chelator reported previously [47]. Next, we questioned whether DpdtC could still trigger ferritinophagy in the presence of TGF- β 1. Figure 6 showed that an upregulation of NCOA4 and a downregulation of ferritin occurred as in absence of TGF- β 1, supporting that ferritinophagy induced by DpdtC was independent of EMT process. DpdtC induced the upregulation of NCOA4, leading to EMT inhibition, and the knockdown of NCOA4 by interfering RNA resulted in the upregulation of mesenchyma-related proteins (vimentin, slug, and snail) (Figure 7 and Figure S3), indicating that NCOA4 participated in EMT. We speculated that there could be a correlation between ferritinophagy and EMT inhibition; thus, “ferritinophagic flux” (defined as ratio of NCOA4/ferritin) was used to correlate with the change in EMT. As shown in Figure 7, DpdtC and TGF- β 1 treatment resulted in adverse variation in ferritinophagic flux, the former increase, and the later decrease, so we may also

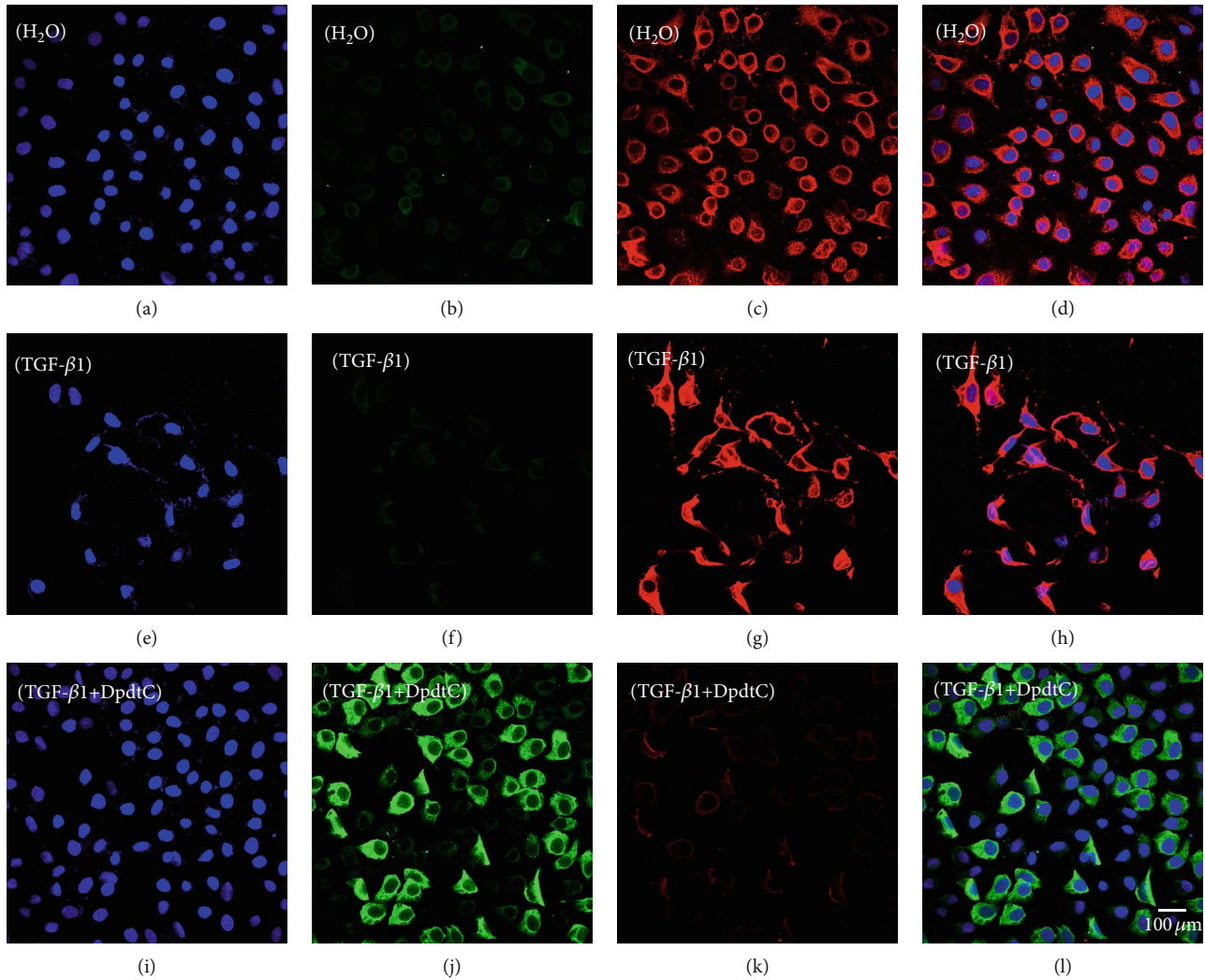


FIGURE 6: DpdtC-induced ferritinophagy in the presence of TGF- β 1. The nuclei stained by DAPI in blue, NCOA4 in green, and ferritin in red. (a–d) Control: (a) nuclei in blue; (b) NCOA4 in green; (c) ferritin in red; and (d) merge of nuclei, ferritin, and NCOA4. (e–h) TGF- β 1 treatment only: TGF- β 1 treatment: (e) nuclei in blue; (f) NCOA4 in green; (g) ferritin in red; (h) merge of nuclei, ferritin, and NCOA4; (i–l) TGF- β 1 combined with DpdtC: (i) nuclei in blue; (j) NCOA4 in green; (k) ferritin in red; and (l) merge of nuclei, ferritin, and NCOA4. The measurements were performed thrice from different field of view. Objective size: 40×10 ; scale bar: $100 \mu\text{m}$.

describe that the EMT status is related to ferritinophagic flux, i.e., ferritinophagic flux was a dominating force in determination of EMT state in gastric cancer cells. This also provided additional evidence that NCOA4 played role in EMT modulation. Normally, NCOA4 acts as a transcriptional coactivator of several nuclear receptors, and its additional function was recently identified as an inhibitor in the activation of DNA replication origins [48]; the downregulation of snail, slug, and vimentin in DpdtC-treated cells might be due to the upregulation of NCOA4. In addition, it has been shown that ROS involved TGF- β 1-induced EMT, and the decrease of ferritin heavy chain (FHC) contributed to EMT transition [49–51]. However, the ferritin degradation induced by DpdtC achieved EMT inhibition in our study; the difference might be attributed to a difference in manner of ferritin downregulation achieved; the knockdown of ferritin by sh-RNA was at

translation level, while induced ferritinophagy by DpdtC at posttranslation modification. On the other hand, the cell specific was also a crucial factor to be considered. Importantly, DpdtC treatment resulted in the downregulation of snail, an EMT transcription factor, implying EMT inhibition achieved was complex for DpdtC. The ferritin degradation led to cellular ROS production on account of the ferric iron liberated from digested ferritin would reduce by the endosomal ferrireductase Steap3 in the acidified lysosome [52], the resulting ferrous ion triggered Fenton reaction. As a stress responder, p53 may respond to the alteration in redox environment; therefore, the p53 response was further determined. Cell growth and proliferation require checkpoint controls, while p53 as a major checkpoint protein in mammalian cells is normally kept at a low level as a result of a negative feedback regulation between p53 and Mdm2 [53, 54]. Our data

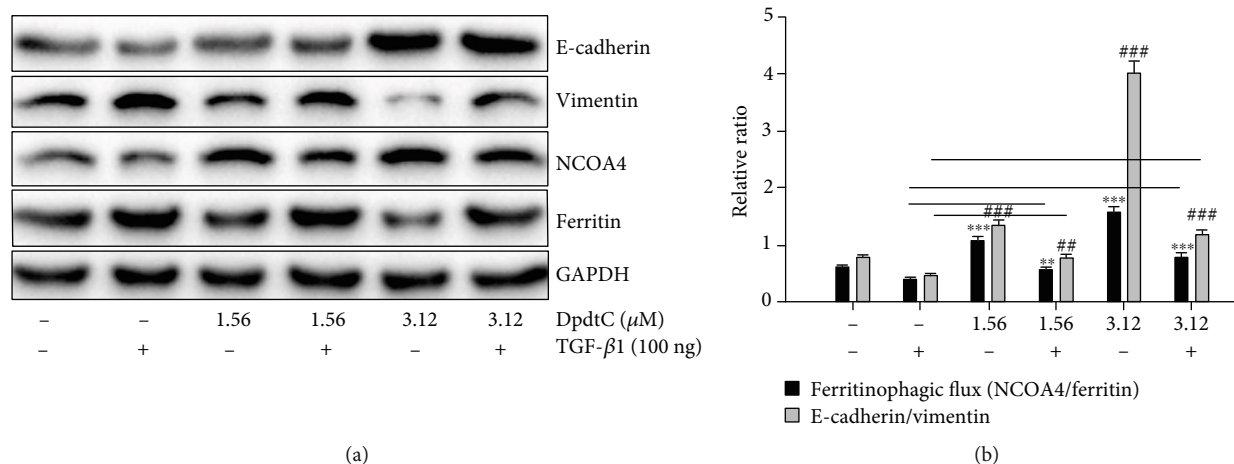


FIGURE 7: Ferritinophagic flux played an important role in EMT process. (a) The alterations in ferritinophagy- and EMT-related proteins when either TGF- β 1 or combined with DpdtC treatment; (b) quantitative analysis of the ferritinophagic flux in the indicated conditions. The quantification analysis of related proteins was from three experiments (**,## $p < 0.05$; ***,### $p < 0.01$).

showed that DpdtC-induced ferritinophagy and EMT inhibition along with the upregulation of p53, and inhibition of p53 could significantly attenuate the effects of DpdtC (Figures 8 and 9), indicating that p53 indeed responded the stress (ROS insulting). It was reported that p53 was regulated by metal ions, and pyrrolidine dithiocarbamate (PDTC) downregulated p53 due to increasing intracellular level of copper [55]. As an analogue of PDTC, but DpdtC has distinct effect on p53 regulation, the difference in p53 regulation may be strictly dependent on the cell type for there were differences in the status of p53 mutation of the cell line used and in the resulting redox environment upon treatment of the agents [56, 57]. Indeed, we also observed that the DpdtbA (a dithiocarbamate derivative) inactivated p53 in esophageal cancer cell lines as PDTC did [58]. In addition, whether the EMT inhibition induced by DpdtC (including its analogues) is related to the degradation of ferritin, and the state of p53 determines whether it occurs or not, which needs further study.

Taken all together, DpdtC induced the growth inhibition in gastric cancer cells that was ROS dependent, which mechanistically was due to the occurrence of ferritinophagy that contributed to ROS production. In addition, DpdtC was also able to inhibit EMT; the correlation analysis further demonstrated that the ferritinophagic flux was a dominating driving force during EMT development, decrease of the ferritinophagic flux resulted in EMT enhancement, while increase of ferritinophagic flux favored to inhibit EMT (reversing EMT). In addition, the p53 also played role in DpdtC-induced EMT inhibition and ferritinophagy induction; the downregulation of p53 would significantly attenuate (or abolish) the action of DpdtC. However, the correlation between ferritinophagic flux and EMT in other cell lines *in vivo* and *in vitro* requires more studies in the future, because the diversity of iron chelators in structure and cell specific influences the effect of iron chelator.

4. Materials and Methods

4.1. Materials. All chemicals used were analytical reagents (AR) grade. 3-(4,5-Dimethylthiazol-2-yl)-2,5-diphenyltetrazolium bromide (MTT), pifithrin- α (PFT- α), 3-methyladenine (3-MA), chloroquine (CQ), dichlorofluorescein (H_2DCF -DA), desferoxamine (DFO), 4',6-diamidino-2-phenylindole (DAPI), Roswell Park Memorial Institute (RPMI)-1640, and other chemicals were purchased from Sigma-Aldrich. Antibodies of vimentin (60330-1-Ig, 10366-1-AP), NCOA4 (E11-17114C), LC3 (14600-1-AP), beclin (66665-1-Ig), and gadp (E12-052) for Western blotting were obtained from Proteintech Group Inc (Wuhan, China). Antibodies of E-cadherin (3195), ferritin (H chain, 3998S), and secondary antibodies (fluorescence labeled for immunofluorescence, 8890S, 4412S) were purchased from Cell Signaling Technology (USA). Ferritin antibody (SC-376594) for immunofluorescence was obtained from Santa Cruz Biotechnology (Santa Cruz, USA). NCOA4 antibody (HPA0512) for immunofluorescence was purchased from Atlas Antibody (Sweden). Secondary antibodies for Western blotting were obtained from EarthOx, LLC (San Francisco, USA).

4.2. Cytotoxicity Assay (MTT Assay). The stock solution of DpdtC (10 mM) was prepared in water and diluted to the required concentration with culture medium when used. The MTT assay was based on reported previously [39]. Briefly, MGC-803 cells were cultured in RPMI 1640 medium supplemented with 10% fetal calf serum (FCS) and antibiotics. The cells in exponential phase were collected and seeded equivalently into a 96-well plate; next, the varied concentration of DpdtC (or other agents) was added after the cells adhered. Following 48 h incubation at 37°C in a humidified atmosphere of 5% CO_2 , 10 μ l MTT solution (5 mg/ml) was added and further incubated for 4 h; next, 100 μ l DMSO was added in each well to dissolve the formazan crystals after removing cell culture. The measurement of absorbance of the solution was performed on a microplate reader (MK3, Thermo Scientific) at 570 nm. Percent growth inhibition

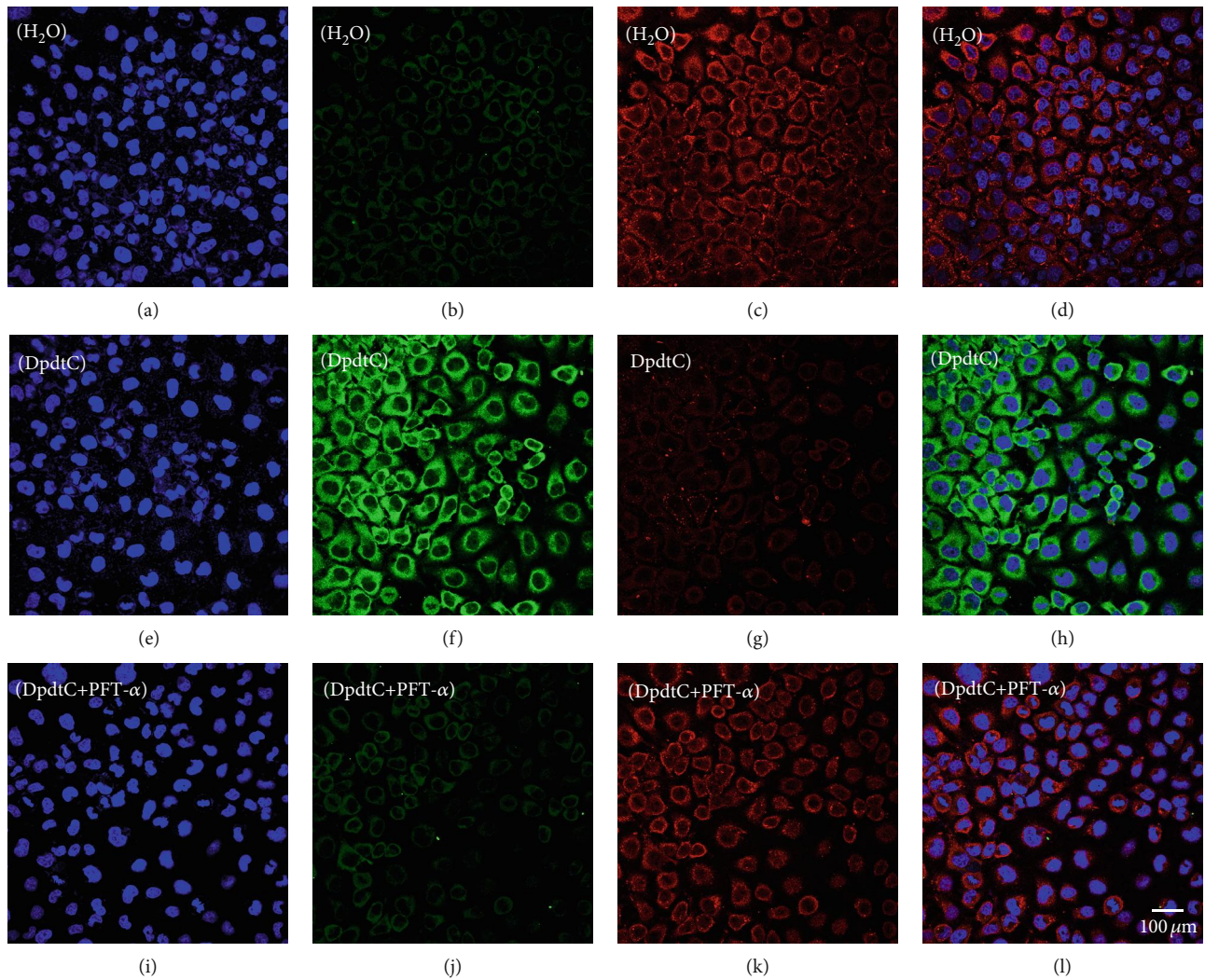


FIGURE 8: DpdtC-induced EMT modulation was p53 dependent. (a–d) Control (H_2O): (a) nuclei in blue; (b) E-cadherin in green; (c) vimentin in red; and (d) merge of nuclei, E-cadherin, and vimentin in control group. (e–h): DpdtC-treated group: (e) nuclei in blue; (f) E-cadherin in green; (g) vimentin in red; and (h) merge of nuclei, E-cadherin, and vimentin in DpdtC-treated group. (i–l): DpdtC combined with PFT- α -treated group: (i) nuclei in blue; (j) E-cadherin in green; (k) vimentin in red; and (l) merge of nuclei, E-cadherin, and vimentin in DpdtC combined with PFT- α -treated group. The measurements were performed thrice from different field of view. Objective size: 40×10 (fluorescence); scale bar: $100\ \mu m$.

was defined as percent absorbance inhibition within appropriate absorbance in each cell line. The same assay was performed in triplet.

4.3. Flow Cytometric Analysis of Cellular ROS. MGC-803 cells were seeded into a 6-well plate and treated as described in the section of cytotoxicity assay. The cells were treated with different concentrations of the agent (1.56 and $3.12\ \mu M$ DpdtC) for 24 h. Then, the cell culture was removed, following PBS washing and trypsin digestion; finally, the cells were resuspended in H_2DCF -DA containing serum-free culture medium and incubated for 30 min. Next, after removing the H_2DCF -DA-contained medium by centrifugation and washing with PBS, the intracellular ROS assay was performed on a flow cytometer (Becton-Dickinson, USA).

4.4. Immunofluorescence Analysis. The immunofluorescence analysis was performed as described previously [39]. Briefly, MGC-803 cells were first cultured in a 6-well plate with cover glass overnight. The cells were treated by DpdtC for 24 h, fixed with 4% paraformaldehyde in PBS for 15 min at $37^\circ C$, and then permeabilized with 0.2% triton-X-100 in PBS for 10 min. After blocking with 1% BSA in PBS for 30 min, the cells on the cover glass were incubated with either ferritin (H chain, Santa Cruz Biotechnology), or combined with LC3 (or NCOA4 (Altas Antibodies)), or vimentin combined with E-cadherin (Cell Signaling Technology) primary antibody at $4^\circ C$ for overnight. Next, removing the primary antibodies and washing with PBS, the cover glasses were further incubated with fluorescence-labeled secondary antibody for 3 h at

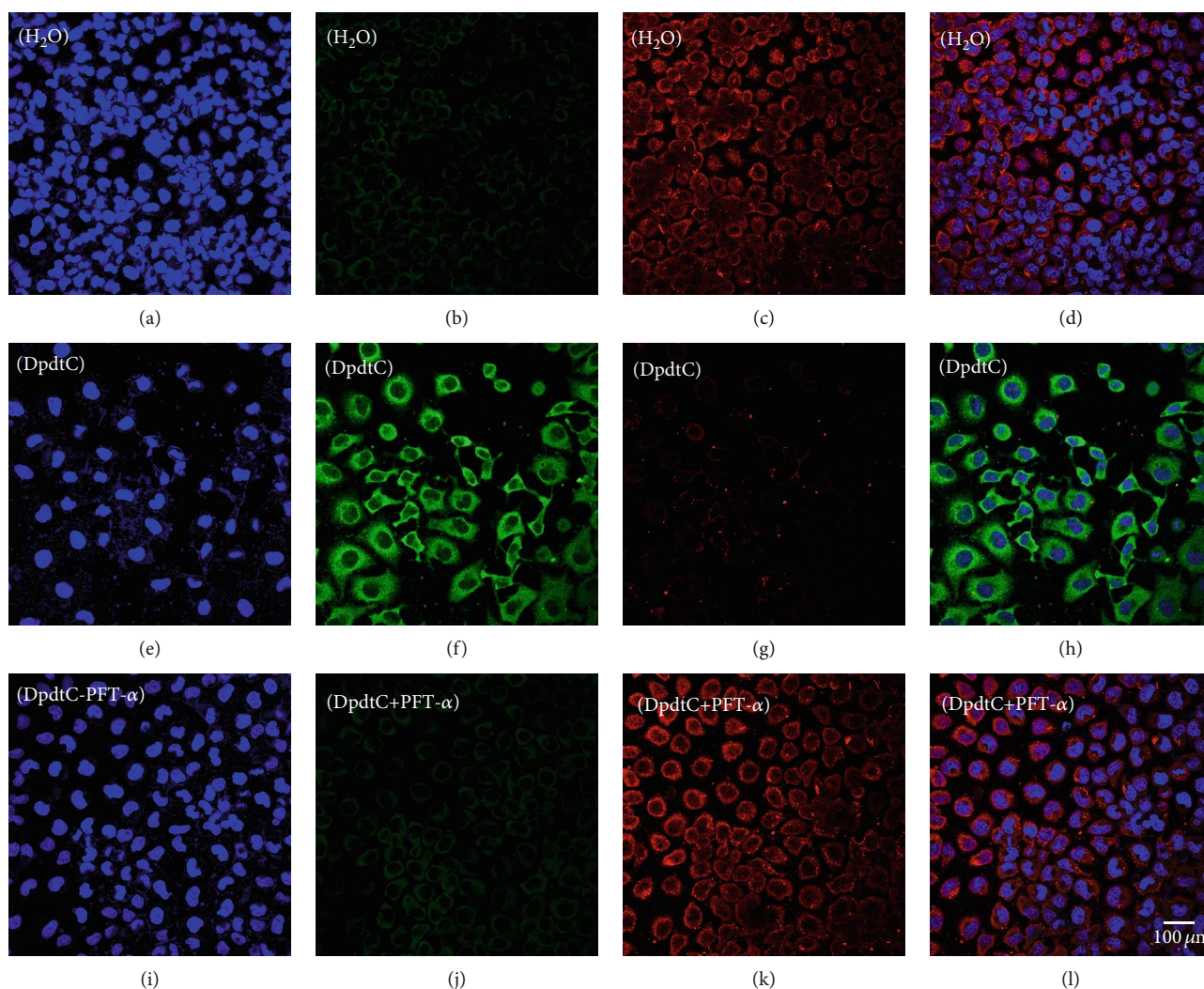


FIGURE 9: DpdtC-induced ferritinophagy involved p53. The nuclei stained by DAPI in blue, ferritin labeled in red, and NCOA4 labeled in green. (a–d) Control group: (a) nuclei in blue; (b) NCOA4 in green; (c) ferritin in red; and (d) merge of ferritin with NCOA4. (e–h) DpdtC-treated group: (e) nuclei in blue; (f) NCOA4 in green; (g) ferritin in red; and (h) merge of ferritin with NCOA4. (i–l) DpdtC combined with PFT- α group: (i) nuclei in blue; (j) NCOA4 in green; (k) ferritin in red; and (l) merge of ferritin with NCOA4. The measurements were performed thrice from different field of view. Scale bar: 100 μ m.

room temperature. After removing the secondary antibody, the cells on the cover glass were further counterstained with DAPI. Finally, a confocal laser scanning microscope (Nikon eclipse Ts2, Japan) was used to visualize the cells, and the representative cells were selected and photographed.

4.5. Western Blotting Analysis. The Western blotting was conducted as described previously [39]; briefly, 1×10^7 MGC-803 cells that treated with or without DpdtC were scraped in lysis buffer (50 mM Tris-HCl, pH 8.0, 150 mM NaCl, 1.0% NP-40, 10% glycerol, and protease inhibitors) on ice for 30 min, and the clear supernatant was stored at -80°C after centrifugation at $14,000 \times g$. Protein concentration was determined using a colorimetric Bio-Rad DC protein assay as recommended by the company (Life Science Research, USA). Proteins (30 μ g) were separated on a 13–

15% sodium dodecyl sulfate-polyacrylamide gel at 200 V for 3 h. Next, the separated proteins on the gel were subsequently transferred onto a PVDF membrane at 60 V for 2 h, followed by washing with Tris-buffered saline (TBS), and the membrane was then blocked for 2 h in TBS containing 0.1% Tween-20 and 5% nonfat skimmed milk. The membrane was further incubated at 4°C overnight with the appropriate primary antibody and with the appropriate HRP-conjugated secondary antibody (1:2,000 in TBST) for 1 h at room temperature after removing primary antibody and washing. Finally, the membrane was washed with TBST, and the protein bands were detected using a super sensitive ECL solution (Boster Biological Technology Co. Ltd.) and visualized using a Syngene G: BOX imager (Cambridge, United Kingdom). Quantifications of protein bands intensities and fluorescence intensity were performed using ImageJ software.

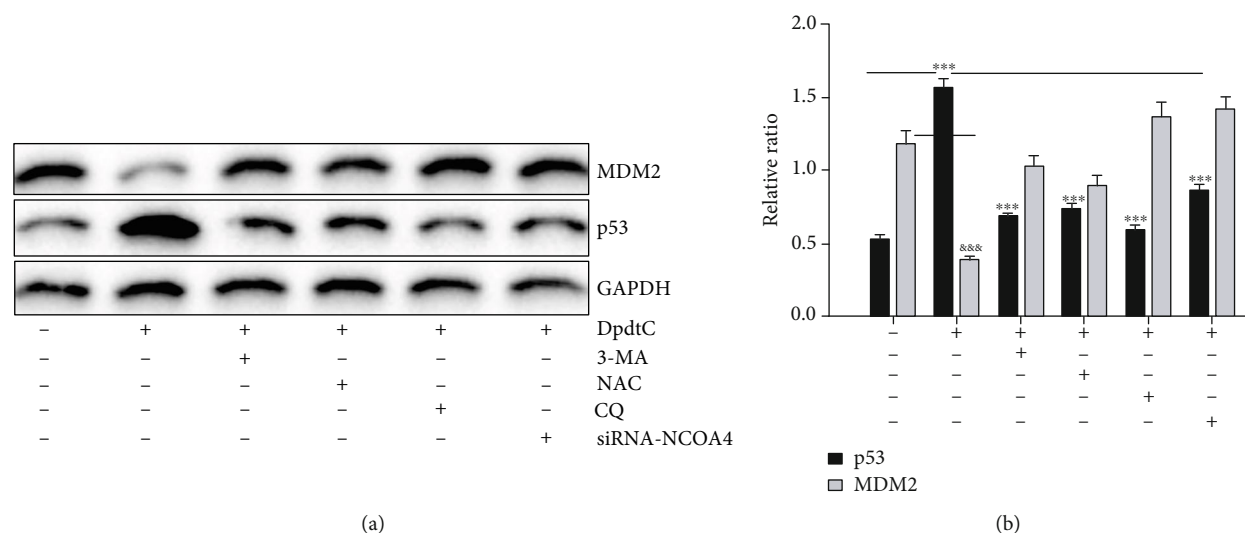


FIGURE 10: p53 responded to ROS production induced by DpdtC. (a) The upregulation of p53 could be attenuated by the addition of autophagy inhibitor, ROS scavenger, and the downregulation of NCOA4; (b) quantification of the changes of p53 and MDM2 from (a). The experiments were performed twice. ***,&&& $p < 0.01$.

4.6. Statistical Analysis. Results are presented as the mean \pm SEM. Comparisons between two groups were carried out using the two-tailed Student's *t*-test. Comparisons between multiple groups were performed by one-way ANOVA with Dunnett post hoc correction. A *p* value < 0.05 was considered statistically significant.

Data Availability

The data used to support the findings of this study are included within the article

Conflicts of Interest

The authors declare no conflict of interest.

Authors' Contributions

Jiankang Feng, Cuiping Li, and Ruifang Xu performed the experiments; they contributed equally to this work. Yongli Li and Changzheng Li conceived and designed the experiments; Qi Hou, an undergraduate student (2017) of academy of classical learning of RenZhi, and Yongli Li performed some immunofluorescent experiment. Rui Feng, Senye Wang, and Lei Zhang analyzed the data and generated figures. Changzheng Li prepared and wrote the paper.

Acknowledgments

The present study was supported by grants awarded by the Natural Science Foundation of China (No. 21571153), the Henan Science and Technology Agency (No. 152300410118), The Key Research Project Funding Program of Higher Educational Institutions of Henan Province (19A310021), and Innovation team awarded by Sanquan College of Xinxiang Medical University (SQTD201703 and SQTD201902).

Supplementary Materials

In the supplementary materials, we provided additional information that included the effects of ROS induced by DpdtC on cell growth, lower abundance of iron due to the occurrence of ferritinophagy, the knockdown of NCOA4 by small-interfering RNA resulted in enhancing EMT, and p53 involved the EMT inhibition and ferritinophagy induction, finally the occurrence of ferritinophagy contributed to ROS to support the conclusion that DpdtC-induced EMT inhibition was through ferritinophagy-mediated ROS/p53 pathway. (*Supplementary Materials*)

References

- [1] B. Vincenzi, M. Imperatori, M. Silletta, E. Marrucci, D. Santini, and G. Tonini, "Emerging kinase inhibitors of the treatment of gastric cancer," *Expert Opinion on Emerging Drugs*, vol. 20, no. 3, pp. 479–493, 2015.
- [2] X. Lin, Y. Zhao, W. M. Song, and B. Zhang, "Molecular classification and prediction in gastric cancer," *Computational and Structural Biotechnology Journal*, vol. 13, pp. 448–458, 2015.
- [3] W. Liu, Y. Lu, X. Chai et al., "Antitumor activity of TY-011 against gastric cancer by inhibiting Aurora A, Aurora B and VEGFR2 kinases," *Journal of Experimental & Clinical Cancer Research*, vol. 35, no. 1, p. 183, 2016.
- [4] M. Frezza, S. Hindo, D. Chen et al., "Novel metals and metal complexes as platforms for cancer therapy," *Current Pharmaceutical Design*, vol. 16, no. 16, pp. 1813–1825, 2010.
- [5] D. Buac, S. Schmitt, G. Ventro, F. R. Kona, and Q. P. Dou, "Dithiocarbamate-based coordination compounds as potent proteasome inhibitors in human cancer cells," *Mini Reviews in Medicinal Chemistry*, vol. 12, no. 12, pp. 1193–1201, 2012.
- [6] P. Savagner, "Epithelial-mesenchymal transitions: from cell plasticity to concept elasticity," *Current Topics in Developmental Biology*, vol. 112, pp. 273–300, 2015.
- [7] J. H. Tsai, J. L. Donaher, D. A. Murphy, S. Chau, and J. Yang, "Spatiotemporal regulation of epithelial-mesenchymal

- transition is essential for squamous cell carcinoma metastasis,” *Cancer Cell*, vol. 22, no. 6, pp. 725–736, 2012.
- [8] S. Lamouille, J. Xu, and R. Derynck, “Molecular mechanisms of epithelial–mesenchymal transition,” *Nature Reviews Molecular Cell Biology*, vol. 15, no. 3, pp. 178–196, 2014.
- [9] J. Massague, E. Battle, and R. R. Gomis, “Understanding the molecular mechanisms driving metastasis,” *Molecular Oncology*, vol. 11, no. 1, pp. 3–4, 2017.
- [10] D. Han, E. Williams, and E. Cadenas, “Mitochondrial respiratory chain-dependent generation of superoxide anion and its release into the intermembrane space,” *Biochemical Journal*, vol. 353, no. 2, pp. 411–416, 2001.
- [11] Y. M. Janssen-Heininger, B. T. Mossman, N. H. Heintz et al., “Redox-based regulation of signal transduction: principles, pitfalls, and promises,” *Free Radical Biology and Medicine*, vol. 45, no. 1, pp. 1–17, 2008.
- [12] M. P. Murphy, “How mitochondria produce reactive oxygen species,” *Biochemical Journal*, vol. 417, no. 1, pp. 1–13, 2009.
- [13] A. Terman and T. Kurz, “Lysosomal iron, iron chelation, and cell death,” *Antioxidants & Redox Signaling*, vol. 18, no. 8, pp. 888–898, 2013.
- [14] E. Giannoni, M. Parri, and P. Chiarugi, “EMT and oxidative stress: a bidirectional interplay affecting tumor malignancy,” *Antioxidants & Redox Signaling*, vol. 16, no. 11, pp. 1248–1263, 2012.
- [15] W. B. Zhu, Z. F. Zhao, and X. Zhou, “AMD3100 inhibits epithelial-mesenchymal transition, cell invasion, and metastasis in the liver and the lung through blocking the SDF-1 α /CXCR4 signaling pathway in prostate cancer,” *Journal of Cellular Physiology*, vol. 234, no. 7, pp. 11746–11759, 2019.
- [16] C. Zhang and Y. Wang, “Metformin attenuates cells stemness and epithelial-mesenchymal transition in colorectal cancer cells by inhibiting the Wnt3a/ β -catenin pathway,” *Molecular Medicine Reports*, vol. 19, no. 2, pp. 1203–1209, 2019.
- [17] T. J. Wu, B. Xu, G. H. Zhao, J. Luo, and C. Luo, “IL-37 suppresses migration and invasion of gallbladder cancer cells through inhibition of HIF-1 α induced epithelial-mesenchymal transition,” *European Review for Medical and Pharmacological Sciences*, vol. 22, no. 23, pp. 8179–8185, 2018.
- [18] C. Ricca, A. Aillon, M. Viano, L. Bergandi, E. Aldieri, and F. Silvagno, “Vitamin D inhibits the epithelial-mesenchymal transition by a negative feedback regulation of TGF- β activity,” *The Journal of Steroid Biochemistry and Molecular Biology*, vol. 187, pp. 97–105, 2019.
- [19] Y. Li, M.-C. Zhang, X.-K. Xu et al., “Functional Diversity of p53 in Human and Wild Animals,” *Frontiers in Endocrinology*, vol. 10, p. 152, 2019.
- [20] T. Stiewe and T. E. Haran, “How mutations shape p53 interactions with the genome to promote tumorigenesis and drug resistance,” *Drug Resistance Updates*, vol. 38, pp. 27–43, 2018.
- [21] A. C. Joerger and A. R. Fersht, “The p53 pathway: origins, inactivation in cancer, and emerging therapeutic approaches,” *Annual Review of Biochemistry*, vol. 85, pp. 375–404, 2016.
- [22] G. Stracquadanio, X. Wang, M. D. Wallace et al., “The importance of p53 pathway genetics in inherited and somatic cancer genomes,” *Nature Reviews Cancer*, vol. 16, no. 4, pp. 251–265, 2016.
- [23] The Cancer Genome Atlas Research Network, “Comprehensive and integrative genomic characterization of hepatocellular carcinoma,” *Cell*, vol. 169, no. 7, pp. 1327–1341.e23, 2017.
- [24] Y. Liu, X. Zhang, C. Han et al., “TP53 loss creates therapeutic vulnerability in colorectal cancer,” *Nature*, vol. 520, no. 7549, pp. 697–701, 2015.
- [25] A. Jethwa, M. Słabicki, J. Hüllelin et al., “TRRAP is essential for regulating the accumulation of mutant and wild-type p53 in lymphoma,” *Blood*, vol. 131, no. 25, pp. 2789–2802, 2018.
- [26] K. Wong, L. van der Weyden, C. R. Schott et al., “Cross-species genomic landscape comparison of human mucosal melanoma with canine oral and equine melanoma,” *Nature Communication*, vol. 10, no. 1, p. 353, 2019.
- [27] C. M. Fenoglio-Preiser, J. Wang, G. N. Stemmermann, and A. Noffsinger, “TP53 and gastric carcinoma: a review,” *Human Mutation*, vol. 21, no. 3, pp. 258–270, 2003.
- [28] L. C. Hofbauer, T. D. Rachner, R. E. Coleman, and F. Jakob, “Endocrine aspects of bone metastases,” *The Lancet Diabetes & Endocrinology*, vol. 2, no. 6, pp. 500–512, 2014.
- [29] M. A. Nieto, R. Y. Huang, R. A. Jackson, and J. P. Thiery, “Emt: 2016,” *Cell*, vol. 166, no. 1, pp. 21–45, 2016.
- [30] Y. Li, T. Wang, Y. Sun et al., “p53-mediated PI3K/AKT/mTOR pathway played a role in PtoxD^{Pt}-induced EMT inhibition in liver cancer cell lines,” *Oxidative Medicine and Cellular Longevity*, vol. 2019, Article ID 2531493, 15 pages, 2019, eCollection 2019.
- [31] M. Maan and U. Pati, “CHIP promotes autophagy-mediated degradation of aggregating mutant p53 in hypoxic conditions,” *FEBS Journal*, vol. 285, no. 17, pp. 3197–3214, 2018.
- [32] Y. Haupt, R. Maya, A. Kazaz, and M. Oren, “Mdm2 promotes the rapid degradation of p53,” *Nature*, vol. 387, no. 6630, pp. 296–299, 1997.
- [33] M. H. G. Kubbutat, S. N. Jones, and K. H. Vousden, “Regulation of p53 stability by Mdm2,” *Nature*, vol. 387, no. 6630, pp. 299–303, 1997.
- [34] S. R. Grossman, M. E. Deato, C. Brignone et al., “Polyubiquitination of p53 by a ubiquitin ligase activity of p300,” *Science*, vol. 300, no. 5617, pp. 342–344, 2003.
- [35] C. Esser, M. Scheffner, and J. Hohfeld, “The chaperone-associated ubiquitin ligase CHIP is able to target p53 for proteasomal degradation,” *The Journal of Biological Chemistry*, vol. 280, no. 29, pp. 27443–27448, 2005.
- [36] M. C. Linder, H. R. Kakavandi, P. Miller, P. L. Wirth, and G. M. Nagel, “Dissociation of ferritins,” *Archives of Biochemistry and Biophysics*, vol. 269, no. 2, pp. 485–496, 1989.
- [37] J. D. Mancias, X. Wang, S. P. Gygi, J. W. Harper, and A. C. Kimmelman, “Quantitative proteomics identifies NCOA4 as the cargo receptor mediating ferritinophagy,” *Nature*, vol. 509, no. 7498, pp. 105–109, 2014.
- [38] T. Huang, Y. Sun, Y. Li et al., “Growth inhibition of a novel iron chelator, DpdtC, against hepatoma carcinoma cell lines partly attributed to ferritinophagy-mediated lysosomal ROS generation,” *Oxidative Medicine and Cellular Longevity*, vol. 2018, Article ID 4928703, 13 pages, 2018.
- [39] Y. Sun, C. Li, J. Feng et al., “Ferritinophagic flux activation in CT26 cells contributed to EMT inhibition induced by a novel iron chelator, DpdtPA,” *Oxidative Medicine and Cellular Longevity*, vol. 2019, Article ID 8753413, 14 pages, 2019.
- [40] N. Gavert and A. Ben-Ze’ev, “Epithelial-mesenchymal transition and the invasive potential of tumors,” *Trends in Molecular Medicine*, vol. 14, no. 5, pp. 199–209, 2008.
- [41] T. R. Samatov, A. G. Tonevitsky, and U. Schumacher, “Epithelial-mesenchymal transition: focus on metastatic cascade,

- alternative splicing, non-coding RNAs and modulating compounds," *Molecular Cancer*, vol. 12, no. 1, p. 107, 2013.
- [42] K. Lee and C. M. Nelson, "New insights into the regulation of epithelial-mesenchymal transition and tissue fibrosis," *International Review of Cell and Molecular Biology*, vol. 294, pp. 171–221, 2012.
- [43] C. H. Jeong, H. Ryu, D. H. Kim et al., "Piperlongumine induces cell cycle arrest via reactive oxygen species accumulation and IKK β suppression in human breast cancer cells," *Antioxidants*, vol. 8, no. 11, p. 553, 2019.
- [44] J. P. Mazat, A. Devin, and S. Ransac, "Modelling mitochondrial ROS production by the respiratory chain," *Cellular and Molecular Life Sciences*, vol. 77, no. 3, pp. 455–465, 2020.
- [45] Y. Tsubakihara and A. Moustakas, "Epithelial-mesenchymal transition and metastasis under the control of transforming growth factor β ," *International Journal of Molecular Sciences*, vol. 19, no. 11, p. 3672, 2018.
- [46] Y. Y. Li, G. T. Jiang, L. J. Chen, Y. H. Jiang, and J. D. Jiao, "Formin mDial contributes to migration and epithelial-mesenchymal transition of tubular epithelial cells exposed to TGF- β 1," *Journal of Cellular Biochemistry*, 2019.
- [47] D. J. Lane, T. M. Mills, N. H. Shafie et al., "Expanding horizons in iron chelation and the treatment of cancer: role of iron in the regulation of ER stress and the epithelial-mesenchymal transition," *Biochimica et Biophysica Acta*, vol. 1845, no. 2, pp. 166–181, 2014.
- [48] R. Bellelli, M. D. Castellone, T. Guida et al., "NCOA4 transcriptional coactivator inhibits activation of DNA replication origins," *Molecular Cell*, vol. 55, no. 1, pp. 123–137, 2014.
- [49] K. H. Zhang, H. Y. Tian, X. Gao et al., "Ferritin heavy chain-mediated iron homeostasis and subsequent increased reactive oxygen species production are essential for epithelial-mesenchymal transition," *Cancer Research*, vol. 69, no. 13, pp. 5340–5348, 2009.
- [50] A. Sioutas, L. K. Vainikka, M. Kentson et al., "Oxidant-induced autophagy and ferritin degradation contribute to epithelial-mesenchymal transition through lysosomal iron," *Journal of Inflammation Research*, vol. 10, pp. 29–39, 2017.
- [51] I. Aversa, F. Zolea, C. Ieranò et al., "Epithelial-to-mesenchymal transition in FHC-silenced cells: the role of CXCR4/CXCL12 axis," *Journal of Experimental & Clinical Cancer Research*, vol. 36, no. 1, p. 104, 2017.
- [52] N. Bresgen and P. M. Eckl, "Oxidative stress and the homeodynamics of iron metabolism," *Biomolecules*, vol. 5, no. 2, pp. 808–847, 2015.
- [53] B. Vogelstein, D. Lane, and A. J. Levine, "Surfing the p53 network," *Nature*, vol. 408, no. 6810, pp. 307–310, 2000.
- [54] Z. Feng, H. Zhang, A. J. Levine, and S. Jin, "The coordinate regulation of the p53 and mTOR pathways in cells," *Proceedings of the National Academy of Sciences of the United States of America*, vol. 102, no. 23, pp. 8204–8209, 2005.
- [55] G. W. Verhaegh, M. J. Richard, and P. Hainaut, "Regulation of p53 by metal ions and by antioxidants: dithiocarbamate down-regulates p53 DNA-binding activity by increasing the intracellular level of copper," *Molecular and Cellular Biology*, vol. 17, no. 10, pp. 5699–5706, 1997.
- [56] P. Hainaut and J. Milner, "Redox modulation of p53 conformation and sequence specific DNA binding in vitro," *Cancer Research*, vol. 53, no. 19, pp. 4469–4473, 1993.
- [57] P. Hainaut, N. Rolley, M. Davies, and J. Milner, "Modulation by copper of p53 conformation and sequence-specific DNA binding: role for Cu(II)/Cu(I) redox mechanism," *Oncogene*, vol. 10, no. 1, pp. 27–32, 1995.
- [58] Z. Wang, C. Li, Y. Li et al., "DpdtbA-induced growth inhibition in human esophageal cancer cells involved inactivation of the p53/EGFR/AKT pathway," *Oxidative Medicine and Cellular Longevity*, vol. 2019, Article ID 5414670, 14 pages, 2019.

Review Article

Hydrogen Sulfide as a Potential Alternative for the Treatment of Myocardial Fibrosis

Se Chan Kang ¹, Eun-Hwa Sohn,² and Sung Ryul Lee ³

¹Department of Oriental Medicine Biotechnology, College of Life Sciences, Kyung Hee University, Yongin 17104, Republic of Korea

²Department of Herbal Medicine Resource, Kangwon National University, Samcheok 25949, Republic of Korea

³Department of Convergence Biomedical Science, Cardiovascular and Metabolic Disease Center, College of Medicine, Inje University, Busan 47392, Republic of Korea

Correspondence should be addressed to Sung Ryul Lee; lsr1113@inje.ac.kr

Received 4 November 2019; Accepted 10 December 2019; Published 23 January 2020

Guest Editor: Mario Fontana

Copyright © 2020 Se Chan Kang et al. This is an open access article distributed under the Creative Commons Attribution License, which permits unrestricted use, distribution, and reproduction in any medium, provided the original work is properly cited.

Harmful, stressful conditions or events in the cardiovascular system result in cellular damage, inflammation, and fibrosis. Currently, there is no targeted therapy for myocardial fibrosis, which is highly associated with a large number of cardiovascular diseases and can lead to fatal heart failure. Hydrogen sulfide (H_2S) is an endogenous gasotransmitter similar to nitric oxide and carbon monoxide. H_2S is involved in the suppression of oxidative stress, inflammation, and cellular death in the cardiovascular system. The level of H_2S in the body can be boosted by stimulating its synthesis or supplying it exogenously with a simple H_2S donor with a rapid- or slow-releasing mode, an organosulfur compound, or a hybrid with known drugs (e.g., aspirin). Hypertension, myocardial infarction, and inflammation are exaggerated when H_2S is reduced. In addition, the exogenous delivery of H_2S mitigates myocardial fibrosis caused by various pathological conditions, such as a myocardial infarct, hypertension, diabetes, or excessive β -adrenergic stimulation, via its involvement in a variety of signaling pathways. Numerous experimental findings suggest that H_2S may work as a potential alternative for the management of myocardial fibrosis. In this review, the antifibrosis role of H_2S is briefly addressed in order to gain insight into the development of novel strategies for the treatment of myocardial fibrosis.

1. Introduction

Although fibrosis is an essential process for the restoration and maintenance of organ integrity after injury or stress via the timely deposition of the extracellular matrix (ECM), the aberrant accumulation of stiff and disorganized ECM progressively disrupts tissue function and can ultimately cause organ failure [1–5]. Myocardial fibrosis is a hallmark feature of heart failure and is associated with hypertension, myocardial infarction (MI), and pathological hypertrophy followed by injury and stress [1, 2]. Systemic responses induced by the decline in systolic function, particularly neurohumoral activation (angiotensin–aldosterone system and β -adrenergic nervous system), are associated with the progression of heart failure (HF). Traditional therapies, such as β -blockers and renin-angiotensin-aldosterone system (RAAS) inhibitors, have been found to have beneficial effects in patients

with cardiac fibrosis in clinical trials [6, 7]. However, these conventional drugs do not aim at directly curing myocardial fibrosis but rather aim at alleviating the underlying cardiac dysfunction mechanisms indirectly [6]. Therefore, great effort is currently being devoted to research on the development of therapeutic interventions for decreasing the high morbidity and mortality associated with myocardial fibrosis, particularly on the identification and modulation of its core mechanisms [1–4].

Despite its previous characterization as a toxic gas with a rotten egg smell, H_2S is beginning to be associated with a growing family of gasotransmitters, with properties similar to nitric oxide (NO) and carbon monoxide (CO) [8–10]. As a gasotransmitter, H_2S is involved in both the physiology and pathophysiology of the nervous, cardiovascular, and gastrointestinal systems via its antioxidant, anti-inflammatory [11], antinociceptive, antihypertensive, neuromodulative,

and cytoprotective effects [9, 12–14]. The modulation of signals involved in myocardial fibrosis, and thereby the attenuation of pathological fibrosis, is an area of intense scientific interest due to its evident therapeutic implications for the treatment of HF [15]. Reduced levels of H₂S have been identified in patients with ischemia [16], diabetes [17, 18], high-fat diet-induced cardiomyopathy [19], hypertension [20], and heavy metal detoxifications, such as nickel detoxification [21].

The role of an exogenously delivered H₂S in antifibrosis has been identified in a variety of experimental settings (Table 1). In this review, myocardial fibrosis and the potential antifibrosis effects of H₂S are outlined. H₂S is not the sole gasotransmitter in the body and can interact with other gasotransmitters including NO and CO. In addition to direct chemical crosstalk, NO, CO, and H₂S compete in heme- or metal-containing proteins and at the posttranslational modification sites of proteins [9]. Thus, various types of crosstalk between CO, H₂S, and NO in the cardiovascular system exist [9]. For example, nitrosopersulfide, polysulfides, and dinitrosulfite can be formed by the interaction of NO and H₂S. These anionic intermediates modulate the bioavailability of NO/HNO or H₂S/sulfane sulfur and are thus responsible for distinct physiological consequences [22]. Although bioactive intermediates that form interactions with each other are an emerging research field, the modulatory role of H₂S intermediates in myocardial fibrosis is beyond our current review.

2. Hydrogen Sulfide

2.1. Synthesis of H₂S. H₂S is the simplest thiol, which are sulfur analogs of alcohol (R-SH); is associated with the smell of rotten eggs; and has a high redox potential [23]. As depicted in Figure 1, H₂S is endogenously synthesized from L-cysteine or L-homocysteine via cystathionine β -synthase (CBS) and cystathionine γ -lyase (CSE), which are pyridoxal 5'-phosphate-dependent cytosolic enzymes in the transsulfuration pathway [24]. CSE is involved in the cardiovascular system, especially in myocardial cells [25], vascular smooth muscle cells [26, 27], and endothelial cells [28], whereas CBS is predominantly found in the nervous system [29]. In the mitochondria, cysteine aminotransferase (CAT) catalyzes L-cysteine and glutamate to 3-mercaptopyruvate and α -ketoglutarate. Then, 3-mercaptopyruvate is metabolized to pyruvate and H₂S via 3-mercaptopyruvate sulfurtransferase (3-MST) [23]. Nonenzymatically, H₂S can also be released from preexisting intracellular sulfur stores (sulfane sulfur) through the activities of reducing agents [24, 30]. For example, the production of H₂S from sulfur-containing amino acids (e.g., cysteine) via iron and vitamin B₆ under physiological conditions has been found in red blood cells and tissues [31]. However, the exact biological roles of this nonenzymatic production of H₂S have not yet been established.

2.2. Exogenous H₂S. H₂S can be inhaled directly, and the regulated inhalation of H₂S is an effective method for the control of hemorrhages in preclinical studies [32]. Although the inhalation of H₂S gas produces few byproducts, controlling its dosage and handling the specialized equipment needed

for its delivery is difficult. There are a number of compounds that have been synthesized specifically to deliver therapeutic H₂S to tissues [9, 23, 33], including inorganic sulfide salts (e.g., NaHS), synthetic organic compounds with a slow H₂S-releasing mode, conventional drug molecules coupled with an H₂S-donating group, cysteine analogs, nucleoside phosphorothioates, and plant-derived polysulfides (Table 1).

2.3. Modulation of H₂S Level. The bioavailability of H₂S inside the cell is primarily regulated by H₂S-synthesizing enzymes (CSE, CBS, or 3-MST) and H₂S-oxidizing enzymes located in the mitochondria (e.g., sulfide quinone reductase, persulfide dioxygenase, and thiosulfate sulfurtransferase) [9]. Cysteine and its derivatives can be used to boost H₂S synthesis [33]. MicroRNA (miRNA) controls gene expression at the posttranscriptional level [34] and is one of the main factors involved in the upregulation of CSE expression [16]. Interestingly, currently used drugs, including angiotensin-converting enzyme (ACE) inhibitors (e.g., ramipril) [35], statins [36], calcium channel antagonists (e.g., amlodipine) [37], digoxin [38], vitamin D₃ [39], aspirin [40], metformin [40], and others [23], may increase the production of H₂S. For example, statins can increase H₂S synthesis via Akt-mediated upregulation of CSE [36] or suppress H₂S degradation by decreasing the concentration of coenzyme Q, which is a sulfide quinone reductase cofactor [41]. It is worth noting that either exogenously supplied or endogenously produced H₂S can be stored in the body in the form of bound sulfane, which is a reductant labile sulfur (e.g., persulfide (R-S-S-SH), polysulfide (RSS_nSR), and protein-associated sulfur, among others) [42]. With regard to the dietary supplementation of H₂S, garlic and garlic-derived organic polysulfides, such as diallyl trisulfide (DATS) and diallyl disulfide (DADS), behave as H₂S donors with the aid of a biological thiol (e.g., glutathione), maintained via pentose phosphate pathway-mediated NADPH production [43].

2.4. Functional Roles of H₂S in the Biological System. H₂S displays antioxidant effects through the direct quenching of reactive oxygen species (ROS) via a hydrosulfide anion (HS⁻), which is a powerful one-electron chemical reductant that is dissociated from H₂S in physiological fluid [12]. H₂S derivatives such as nitrosopersulfide, polysulfides, and dinitrosulfite may also be involved in redox switching in biological systems by generating redox congeners like nitroxyl, nitrous oxide, and sulfane sulfur [22]. NaHS may indirectly suppress ROS production through the H₂S-mediated activation of a copper/zinc superoxide [44, 45]. In addition, H₂S induces the suppression of oxidative stress through the activation of Nrf2 (transcription factor nuclear factor (erythroid-derived 2)-like 2) and NAD-dependent deacetylase sirtuin (SIRT)-3, resulting in increased expression of other antioxidant enzymes and proteins (e.g., GSH and thioredoxin-1) [46, 47]. The low concentration of H₂S may cause oxidative stress, resulting in the depletion of tetrahydrobiopterin, which determines the levels of endothelial nitric oxide synthase (eNOS) activity [48]. As latent matrix metalloproteinases (MMPs) can be activated by oxidative stress [49],

TABLE 1: H₂S donors and their involvement in myocardial fibrosis.

H ₂ S donor (characteristics)	Fibrosis model	Suggested mode of action
Sodium thiosulfate (Na ₂ O ₃ S) (Hydrophilic, fast H ₂ S release)	Hypertension	↓Oxidative stress and ↑endogenous H ₂ S production [126]
	Diabetes (type I)	↓Canonical Wnt pathway-TGF-β1/SMAD3 pathway [114] ↑PKC-ERK1/2/MAK signaling pathway [127] ↓ER stress [115]
	Diabetes (type II)	↓Autophagy via the upregulation of the PI3K/AKT1 pathway [116] ↓Cardiac muscle degradation via sulphydration of MuRF1 [128]
	Hypertension	↓Inflammatory response [103] ↓Extracellular matrix accumulation and ↑vascular density [129] ↓Nox4-ROS-ERK1/2 pathway and ↑HO-1 expression [130] ↑Akt/eNOS/NO pathway [105]
Sodium hydrosulfide (NaHS) (Hydrophilic, fast H ₂ S release)		↓Nitrotyrosine, ↓MMP-2 and MMP-9, and ↑TIMP-1 and TIMP-3 [131] ↑Opening of K _{ATP} channels and ↓oxidative stress [132] ↓Oxidative stress [133] ↓iNOS and ↑HO-1 expression [134] ↓mPTP opening in the aging cardiomyocytes [92] ↑Glycogen synthase kinase-3β/β-catenin pathway [85] ↑cGMP-dependent PKG/phospholamban pathway [135] ↑Angiogenesis [136] ↑Autophagy in the aged hearts [96]
	Metal toxicity (e.g., nickel)	↓Sp1 transactivation and ↓TGF-β1/SMAD1 pathway [21]
	Hypertension	↑Vasorelaxation [100, 101] ↑Trx1 [137]
	Myocardial infarction	↑Mitochondrial function [95] ↑Nrf2 signaling pathway [87] ↑miR-21 [91]
Sodium sulfide (Na ₂ S) (Hydrophilic, H ₂ S release for ~520 min <i>in vivo</i> ; ~5 min <i>in vitro</i>)		↓FoxO1 pathway [138]
GY4137 (Hydrolysis-triggered H ₂ S release; slow-release and 3–4 h lasting)	Diabetes (type I)	↑Autophagy via the AMPK/mTOR pathway [112] ↑Nrf2 pathway mediated by sulphydration of Keap1 [88] ↑PKG I [139]
	Myocardial infarction	↓Oxidative stress and ↓apoptosis [140, 141]
AP67/AP72 (Slow-releasing H ₂ S donors)	Atherosclerosis	↓Calcification effects in heart valves [142]
AP39 (Mitochondria-targeted H ₂ S)	Myocardial infarction	↓mPTP opening [93, 94]
	Hypertension	↓Cardiomyocyte death and ↓inflammatory response [143] ↑VEGF-Akt-eNOS-NO-cGMP signaling pathway [144]

TABLE 1: Continued.

H ₂ S donor (characteristics)	Fibrosis model	Suggested mode of action
SG-1002 (Orally active)	Myocardial dysfunction	↑Adiponectin-AMPK signaling and ↓ER stress [19] ↑NO bioavailability [145]
Diallyl disulfide (DAD) [146] (Organosulfur compound; insoluble in water; slow H ₂ S donor [146])	Myocardial infarction	↓ER stress via SIRT1 [147] ↑AMPK-mediated AKT/GSK-3β/HIF-1α activation [148]
Diallyl trisulfide (DAT) [146] (Organosulfur compound; fast H ₂ S donor)	Hyperglycemia	↑PI3K/Akt/Nrf2 pathway [89] ↓JNK/NF-κβ pathway [149]
ADT-OH (H ₂ S-aspirin hybrid molecule)	Myocardial infarction	↑Autophagic flux via activating AMPK [94]
ZYZ-803 (H ₂ S-NO hybrid molecule)	Adrenergic overload	↑Activation of VEGF/cGMP pathway [86]
ZYZ-802 (S-Propargyl-cysteine; cysteine derivatives)	Hypertension Myocardial infarction	↓Oxidative stress and ↓cardiomyocyte death [104] ↓miRNA-30 family [16]

Abbreviations: AMPK: AMP-activated protein kinase; Ang-II: angiotensin-II; cGMP: cyclic guanosine monophosphate; ECM: extracellular matrix; eNOS: endothelial nitric oxide synthase; ER: endoplasmic reticulum; ERK: extracellular-signal-regulated kinase; FoxO1: transcription factor Forkhead 1; GSK-3β: glycogen synthase kinase-3β; H₂S: hydrogen sulfide; HIF-1α: hypoxia-inducible factor-1α; HO-1: heme oxygenase-1; iNOS: inducible nitric oxide synthase; JNK: c-Jun N-terminal kinase; Keap1: Kelch-like ECH-associated protein 1; MAPK: mitogen-activated protein kinase; MI: myocardial infarction; miRNA: microRNA; MMP: matrix metalloproteinase; mPTP: mitochondrial permeability transition pore; NOX4: NADPH oxidase 4; MuRF1: muscle RING-finger protein-1; NF-κβ: nuclear factor kappa light chain enhancer of activated B cell; Nrf2: nuclear factor E2-related factor 2; PI3K: phosphoinositide 3-kinase; PKC: protein kinase C; PKG: protein kinase G; SIRT1: sirtuin 1; SMAD: mothers against decapentaplegic homolog; Sp1: specificity protein 1; TGF-β: transforming growth factor-β; TIMP: tissue inhibitor of metalloproteinase; Trx1: thioredoxin 1; VEGF: vascular endothelial growth factor. ↓ and ↑ denote inhibition or suppression and increase or activation, respectively.

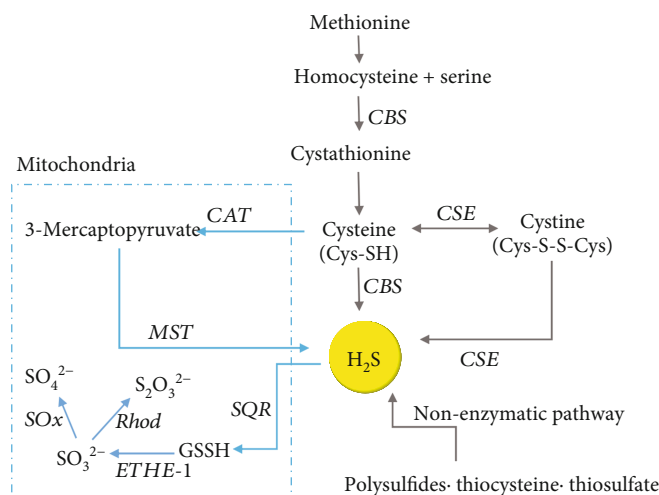


FIGURE 1: Endogenous H₂S production. Abbreviations: CAT: cysteine aminotransferase; CBS: cystathionine- β -synthase; CSE: cystathionine- γ -lyase; ETHE-1: persulfide dioxygenase; GSSH: oxidized glutathione; MST: 3-mercaptopyruvate sulfurtransferase; Rhod: rhodanase; SO_x: sulfur dioxide; SQR: sulfide quinone oxidoreductase.

the antioxidant capacity of H₂S may be involved, at least in part, in the suppression of MMP activation.

H₂S is able to modulate the functions of proteins containing prosthetic metal complexes in acceptor proteins due to its high reactivity with metal ions [50, 51]. For example, polysulfides bind to inactive ferric indoleamine 2,3-dioxygenase (IDO1), which strongly suppresses the immune response, thereby reducing it to its oxygen-binding ferrous state, thus activating IDO1 to maximal turnover [52]. As such, H₂S is able to elicit an anti-inflammatory response through the activation of IDO1. H₂S can lead to protein S-sulhydration (sulhydration or persulfidation) by covalently converting the -SH group of cysteine into an -SSH group in the protein [53], thereby altering the activities of various enzymes, including that of F₁F₀-ATPase [54], the ATP-sensitive potassium (K_{ATP}) channel [55], and the phosphatase and tensin homolog (PTEN) [56]. In addition, protein sulhydration changes the localization and stability of proteins inside cells and increases the resistance of proteins to oxidative stresses [54, 55]. H₂S can activate soluble guanylyl cyclase (sGC) via direct heme binding [57] or by the inhibition of the cGMP phosphodiesterase (PDE) activity [57], resulting in the activation of cyclic GMP (cGMP)-protein kinase G (PKG) pathways.

The bioavailability of H₂S may play an important role in the integrated stress response, that is, in coping with changes to the cellular environment [58, 59]. H₂S transiently increases the phosphorylation of eukaryotic initiation factor 2 (eIF2 α) via the inhibition of protein phosphatase-1 (PP1c) via H₂S-driven persulfidation [59], thereby inducing a transient adaptive reprogramming of global mRNA translation independent of upstream kinases [59]. As an epigenetic modulator, H₂S can modify the expression of Brahma-related gene 1 (Brg1) at the promoter region, thus suppressing the transcriptional activity of the ATP-dependent chromatin remodeling complex [60]. This suppressive activity of H₂S in the expression of Brg1 contributes to the inhibition of vascular smooth muscle cell proliferation [60]. H₂S may

be involved in the decrease of the lysine acetylation of enzymes involved in fatty acid β -oxidation and glucose oxidation in diabetic conditions, thereby exerting a beneficial effect on cardiac energy substrate utilization by favoring a switch from fatty acid oxidation to glucose oxidation [61].

Mitochondrial damage associated with cardiovascular pathological stimuli, including oxidative stress, the overactivation of the renin-angiotensin-aldosterone and adrenergic systems, and the dysfunction of growth hormones, plays a central role in the loss of ischemic, and even nonischemic, cardiomyocytes [62, 63]. The levels of mitochondrial DNA (mtDNA) content are dramatically reduced in CSE gene-knockout mice; however, this reduction can be reversed via the exogenous delivery of H₂S [64]. H₂S can induce the replication of mtDNA and mitochondrial biogenesis by suppressing the methylation of mitochondrial transcription factor A (TFAM) [64]. In a different way, H₂S may be involved in the stimulation of cardiac mitochondrial biogenesis through the activation of the 5' AMP-activated protein kinase (AMPK)-peroxisome proliferator-activated receptor gamma coactivator 1-alpha (PGC1 α) pathway [65]. The sulhydration of AMPK and protein phosphatase 2A (PP2A), which leads to the activation of AMPK and the inhibition of PP2A, respectively, has been suggested as a mechanism that may be involved in the H₂S-mediated stimulation of mitochondrial biogenesis under nonstressed conditions [65].

3. Myocardial Fibrosis and Antifibrosis Potential of H₂S

3.1. Myocardial Fibrosis. The heart is a highly organized structure composed of cardiomyocytes and noncardiomyocytes such as fibroblasts (nonexcitable cells of mesenchymal origin), endothelial cells, and vascular smooth muscle cells [66, 67]. Maladaptive crosstalk between cardiomyocytes and noncardiomyocytes responding to pathological stress may result in myocardial fibrosis, adverse remodeling, and

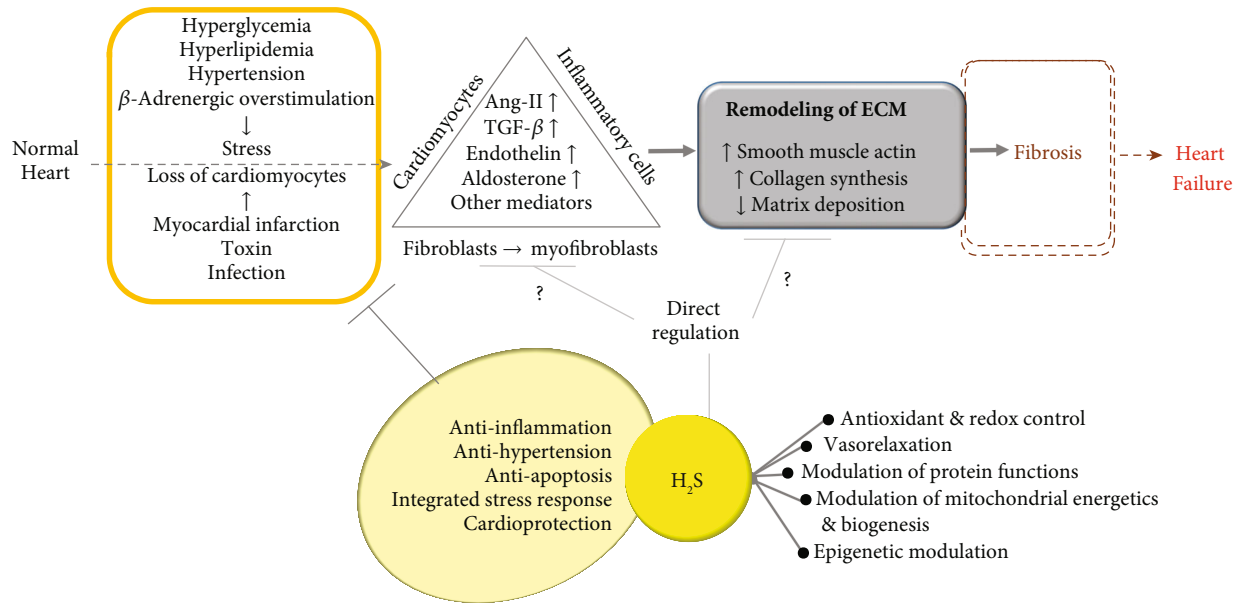


FIGURE 2: Simplified process of myocardial fibrosis and possible antifibrosis roles of H₂S. Abbreviations: Ang-II: angiotensin-II; ECM: extracellular matrix; H₂S: hydrogen sulfide; TGF- β : transforming growth factor- β .

arrhythmogenesis. Myocardial fibrosis is a reparative process involving the restoration of cardiomyocytes from cell death or sustained stress and is involved in maintaining the integrity of the heart, an action exerted mainly by the fibrillar, collagen-rich extracellular matrix (ECM), in the short term [68]. However, reactive fibrosis, such as interstitial and perivascular fibrosis [69], contributes to the progressive architectural remodeling of the heart as a result of the formation and deposition of excess fibrous connective tissue [70]. RAAS, transforming growth factor- β (TGF- β), and β -adrenergic systems are common contributors to cardiac remodeling. These systems are connected to each other in an auto-/paracrine manner as a part of a larger signaling network [71]. During the progression of myocardial fibrosis, various distinct immunological and molecular mechanisms are interconnected via interactions between various cells, including macrophages, myofibroblasts, and matrices [68, 70, 72, 73]. As depicted in Figure 2, the loss of cardiomyocytes driven by various injurious agents and stresses has a detrimental effect on the architecture and function of the heart due to the negligible regenerative capacity of the heart, especially with regard to cardiomyocytes [72, 74]. Inflammatory cells, such as macrophages, appear in damaged regions of the heart and are tasked with removing the necrotic cardiomyocyte debris. TGF- β is the best-known fibrogenic growth factor involved in cardiac fibrosis, even though a baseline level of TGF- β signaling or an early-responsive increase in TGF- β may protect the heart from acute injury [75]. It has been demonstrated that angiotensin-II (Ang-II) is an important mediator of cardiac fibrosis, working with the TGF- β in the fibrotic response, due to the coexistence of TGF- β receptors and Ang-II receptors in cardiomyocytes, inflammatory cells, and cardiac fibroblasts. TGF- β 1 triggers the appearance of inflammatory cells and myofibroblasts at the site of injury [75, 76] and stimulates the deposition of ECM, including

fibronectin, fibrillar collagen types I and III, and proteoglycans. During this initial stage, in addition to the production of inflammatory cytokines, inflammatory cells secrete Ang-I, which is converted to Ang-II via the action of ACE. Ang-II plays a pivotal role in stimulating TGF- β production, prompting the proliferation of circumambient fibroblasts and their transdifferentiation into myofibroblasts. The pool of fibroblasts can be enlarged by the transformation of either circulating bone marrow cells or endothelial/epithelial cells into fibroblasts [66, 77]. During the proliferative phase of cardiac repair, fibroblasts undergo transdifferentiation into contractile myofibroblasts, secreting large amounts of matrix proteins, such as collagens [66]. Then, the scar tissue matures with the formation of a collagen-based matrix [78], where the removal of myofibroblasts is controlled by unknown endogenous stop signals in order to restrain the fibrotic response [78]. However, a clear mechanistic view of phenotype and heterogeneity of cardiac fibroblasts in the process of fibrosis has yet to be fully established [77]. In terms of the underlying molecular mechanisms involved in the progression of fibrosis, several pathways, including the TGF- β , JNK/p38, PI3K/AKT, WNT/ β -catenin, and Ras-Raf- mitogen-activated protein kinase- (MEK-) extracellular signal-activated kinase (ERK) pathways, have been identified [79]. Involved in canonical fibrotic signaling, TGF- β induces the nuclear translocation of the complex known as “mothers against decapentaplegic homolog,” or SMAD complex promoting fibrosis. In noncanonical signaling, TGF- β signaling induces SMAD-independent pathways, including the PI3K/AKT and mitogen-activated protein kinase (MAPK) pathways, nuclear factor kappa light chain enhancer of activated B cell (NF- κ B), RHO/RAC1, and CDC42 [75]. Interestingly, it has been suggested that, if supplied in a timely manner, H₂S can suppress TGF- β 1-induced transdifferentiation from fibroblasts to

myofibroblasts via the inhibition of SMAD3 activation in human fibroblast cells [80].

3.2. Antifibrosis Potential of H₂S

3.2.1. Myocardial Infarction. Extensive necrosis of cardiomyocytes in infarcted hearts not only triggers a strong inflammatory response but also induces interstitial and perivascular fibrosis due to geometrical, biomechanical, and biochemical changes in the uninjured ventricular wall [69]. During cardiac injury and hypertrophic remodeling, the production of inflammatory signaling molecules, such as tumor necrosis factor- α (TNF- α), interleukin (IL)-1 β , and IL-6, can contribute to hypertrophic and fibrotic responses. Interestingly, ischemia causes a significant reduction in the levels of H₂S associated with decreased expression of CSE, which is an H₂S-synthesizing enzyme under the control of the miRNA-30 family [16]. Moreover, it has been suggested that reduced plasma H₂S levels are correlated with the severity of coronary heart disease [81]. Similar to the cardioprotective role of NO [82–84], various signaling pathways from different types of exogenous H₂S may be involved in the suppression of MI-associated fibrosis (Table 1). These pathways include GSK-3 β / β -catenin [85], cGMP-PKG [86], Nrf2 [87–89], miRNA signaling pathways [16, 90, 91], and the protection of mitochondria [92–95]. Although postconditioning only exerts cardioprotection in young hearts, exogenous H₂S restores postconditioning benefits by upregulating autophagy via the activation of the AMPK/mammalian target of rapamycin (mTOR) pathway in the aged hearts and cardiomyocytes [96]. It is unclear whether the signaling pathways identified share common contributors derived from H₂S, or whether this is simply the result of experimental settings targeting different signaling pathways. Therefore, the identification of a unique contributor of H₂S involved in the suppression of MI-mediated myocardial fibrosis is necessary.

3.2.2. Hypertension. Hypertension increases oxidative stress, vascular inflammation, and vascular remodeling, such as in the case of fibrosis [97]. The antihypertensive effects of H₂S, associated with its modulation of various levels of channel activity and cGMP-PKG pathways, may contribute to the suppression of fibrosis caused by hypertension [98–101]. As presented in Table 1, H₂S supplementation under hypertensive conditions may suppress myocardial fibrosis via the modulation of several different signaling pathways. It is worth noting that H₂S can inhibit ACE via the binding of zinc ions to the active center of ACE [102]. It has been postulated that the H₂S-mediated suppression of ACE may indirectly contribute to vasorelaxation and the suppression of the Ang-II-mediated transition of fibrosis. Alternatively, the suppression of inflammation [103] and the reduction of cardiomyocyte death from oxidative stress [104], as well as the activation of eNOS/NO pathway [105], are likely to have antifibrosis roles with regard to H₂S under hypertensive conditions. Interestingly, it has been noted that local delivery of H₂S

can lower systemic blood pressure. For example, the intra-cerebroventricular (ICV) infusion of NaHS in both spontaneous and Ang-II-induced hypertensive rat models was found to decrease the mean arterial blood pressure and heart rate during ICV infusions [106]. Moreover, H₂S secreted from periadventitial adipose tissue has been previously found to contribute to blood pressure homeostasis [107].

3.2.3. Diabetes. The metabolic environment of diabetes, including hyperglycemia, hyperlipidemia, and oxidative stress, causes cardiomyocyte cell death. The early stages of diabetic remodeling of the heart are usually asymptomatic, such that myocardial changes mostly occur at the molecular level. In the middle stage of remodeling, progressive cardiomyocyte hypertrophy and myocardial fibrosis result in impaired ejection fraction [108]. In patients with diabetes, as well as in streptozotocin- (STZ-) treated rats, lowered circulating levels of H₂S due to the downregulated expression of H₂S-synthesizing enzymes have been frequently found [109–111]. As depicted in Table 1, several underlying mechanisms of H₂S involve the suppression of myocardial fibrosis in diabetic rats via (1) the suppression of the TGF- β 1/SMAD3 pathway [110, 112, 113] and canonical Wnt pathway [114], (2) the suppression of endoplasmic reticulum stress [19, 115], (3) the downregulation of the JAK/STAT signaling pathway [110], and (4) the regulation of autophagy [112, 116]. Although it has not yet been clearly elucidated, there is a possibility that H₂S may be involved in the modulation of ECM remodeling via miRNA or other transcription machinery affecting the expression of ECM-processing enzymes in diabetes. For example, H₂S has been found to attenuate fibrotic changes in diabetic kidneys via the downregulation of miRNA-194, which plays an important role in the modulation of proteins involved in collagen realignment [117].

3.2.4. Neurohormonal Overstimulation. The activation of the β -adrenergic nervous system and RAAS has been commonly found in fibrotic HF patients, and β -blockers and RAAS inhibitors have been suggested as a first-line treatment to correct the underlying cardiac dysfunction and reduce morbidity [7, 118]. The overstimulation of β -adrenoceptor may result in the impairment of the negative modulation of H₂S on the β -adrenoceptor system, resulting in a calcium overload, leading to the impairment of cardiac contractility and, ultimately, to cardiomyocyte death [119]. Exogenous H₂S supplementation inhibits isoprenaline- (ISO-) induced cardiac hypertrophy depending on SIRT3, which is predominantly localized in the mitochondria, and may be associated with antioxidant properties [120]. Other signaling pathways, including reducing NADPH oxidase [121] or S-sulphydration of Ca²⁺/calmodulin-dependent protein kinase II [122], have been associated with the antifibrosis role of H₂S under conditions of β -adrenoceptor overstimulation. Mast cells will infiltrate into the heart at the site of inflammation and serve as a local source of renin in cardiovascular tissues. H₂S may benefit from the action of renin secreted from mast cells [123]. In view of hormone-associated myocardial fibrosis, the

excessive generation of thyroxine from thyroid induces thyrotoxicosis and affects the cardiovascular system, resulting in the symptoms of hypertension, arrhythmia, and cardiac hypertrophy [124]. Under conditions of excessive thyroxine, H₂S may bolster rat myocardial fibrosis through the activation of autophagy mediated by the PI3K/AKT signaling pathway and via the downregulation of miRNA-21, miRNA-34a, and miRNA-214 expression [125].

4. Summary and Perspectives

Currently, strategies for the treatment of established HF are focused on relieving the symptoms and signs of HF, such as treating edema, preventing hospital admission, and improving survival [6]. Myocardial fibrosis determines the clinical course of heart dysfunction and can eventually lead to heart failure. A substantial amount of research has been dedicated to the identification of HF target(s) to improve the diagnosis and treatment of fibrotic pathways with organ specificity. Myocardial fibrosis has many steps and usually involves several pathways. Complex networks of molecular signaling, including GSK-3 β , β -catenin, and TGF- β 1/SMAD3, have been implicated in the initiation, progression, and regression of myocardial fibrosis [1–5]. The targeting of collagen fibrillogenesis should be performed with caution as collagen turnover is a common process in most tissues whose effects can be detrimental [150]. Although TGF- β 1 is a central profibrogenic cytokine and a critical contributor during myocardial fibrosis, treatment with TGF- β antibody has been found to result in an increased mortality rate and poor MI-associated ventricular remodeling in a mouse model [151]. Although SMAD3 and TNF- α signaling play a fundamental role in fibrosis progression, the targeting of SMAD3 and TNF- α antagonism has not yet been found to provide a successful antifibrosis outcome [151]. Based on the important role of Ang-II in the initiation of myocardial fibrosis, the antagonism of the angiotensin pathway via ACE inhibitors and angiotensin receptor antagonists is considered to be a useful approach for the management of fibrotic diseases. Recently, AMPK α activators (e.g., metformin) have been found to be a promising therapeutic target for fibrosis [152]. Myocardial fibrosis is not caused by a single profibrotic pathway but is rather associated with the activation of several profibrotic pathways, including immunological and molecular mechanisms [70]. It is also worth noting that a combined antifibrotic strategy, including inflammatory mediators, profibrotic cytokines, and epigenetic and cell and/or tissue intrinsic changes, has been suggested as a possible method for the successful treatment of myocardial fibrosis [7, 70].

As briefly addressed in this review, H₂S possesses antioxidant capacities and modulates various signaling pathways, including the activation of cGMP-PKG pathways, the posttranslational modification of proteins, metal-binding (including heme), and mitochondrial respiratory control [9]. In addition, H₂S may serve as a fine-tuner of mitochondrial homeostasis and the autophagic process in the physiology and pathophysiology of the cardiovascular system [153]. Moreover, H₂S is involved in antiapoptosis of cardiomyocytes, anti-inflammation, antihypertension,

and other beneficial cardiovascular processes [154, 155]. As a timely response to energy stress, autophagy is a bulk degradation/recycling system that is tightly controlled by the homeostatic pathway in the cardiovascular system [153, 156]. Despite the existence of conflicting opinions on the beneficial and harmful effects of autophagy, disturbances in the autophagic process have been found in various forms of HF, including age-related cardiomyopathies [156]. H₂S may be involved in the regulation of autophagy by either suppressing or enhancing the signaling pathways that contribute to the attenuation of myocardial fibrosis, as reviewed in a previous paper [156, 157]. Although it is still currently under investigation, numerous findings have demonstrated that H₂S may be involved in the suppression of myocardial fibrosis caused by (1) myocardial infarction, (2) hypertension, (3) STZ-induced diabetes, and (4) the overstimulation of neurohormonal routes (Table 1). The signaling pathways mediated by H₂S may converge on the suppression of myocardial fibrosis that occurs as a result of various stresses, as shown in Figure 2 and Table 1. It is unclear whether target pathways modulated by the action of H₂S work independently of each other; however, it is most important to determine whether they allow for the merging of multiple pathways into a single antifibrosis signaling cascade. Versatile mechanisms and signaling pathways triggered by H₂S have already been identified, as briefly shown in this review. In this context, it appears that H₂S is emerging as a new type of myocardial fibrosis suppressor. However, it is necessary to identify the molecular target or specific signaling pathway that is under the control of H₂S in a direct and specific manner during myocardial fibrosis. It remains to be clearly established whether H₂S can directly control the cells involved in fibrosis (e.g., cardiomyocytes, fibroblasts, and inflammatory cells) and ECM deposition.

The advances being made in H₂S biology are a promising tool for the future development of medicines for the treatment of myocardial fibrosis based on H₂S, as well as multitarget molecules able to release H₂S [158]. There is currently a lack of fibrosis-specific biomarkers that can be used to determine the stage and grade of myocardial fibrosis, as well as for the identification of patients who may benefit from a specific type of therapy. In addition to the development of new techniques for evaluating the stage and/or severity of myocardial fibrosis [159], a new strategy for reversing preexisting fibrosis using H₂S could be a valuable approach. Moreover, the potential of H₂S in preventing or repairing cardiomyocyte loss via the stimulation of cardiac stem cells or transdifferentiation from noncardiomyocytes to cardiomyocytes needs to be critically evaluated in future studies [160]. It is worth mentioning that H₂S can have serious and toxic effects at high concentrations or high release rates, including sudden unconsciousness and death [14, 161]. Therefore, the optimal concentration or dose of H₂S for the desired antifibrosis effect needs to be critically examined. Additionally, for the therapeutic potential of H₂S, pharmacological agents that generate or release H₂S need to be adequately harnessed for the delivery of physiologically relevant concentrations in a safe manner. Considering that myocardial fibrosis is a long-

term consequence of heart disease, the study of dietary supplements that are able to supply H₂S safely or boost H₂S synthesis is needed for the management of myocardial fibrosis. The long-term consequences and clinical benefits of H₂S against myocardial fibrosis should also be investigated in the future. In addition, the study of the H₂S-mediated reversal of myocardial fibrosis could prove to be advantageous in clinical studies.

Conflicts of Interest

The authors declare that there are no conflicts of interest.

Authors' Contributions

Se Chan Kang and Eun-Hwa Sohn equally contributed to this work.

Acknowledgments

This work was supported by the Basic Science Research Program through the National Research Foundation of Korea (NRF) funded by the Ministry of Education, Science, and Technology (No. 2015R1D1A3A01015596). The authors apologize for the vast number of outstanding publications that could not be cited owing to space limitations.

References

- [1] A. Piek, R. A. de Boer, and H. H. W. Silljé, "The fibrosis-cell death axis in heart failure," *Heart Failure Reviews*, vol. 21, no. 2, pp. 199–211, 2016.
- [2] M. L. Urban, L. Manenti, and A. Vaglio, "Fibrosis—a common pathway to organ injury and failure," *The New England Journal of Medicine*, vol. 373, no. 1, pp. 95–96, 2015.
- [3] A. M. Segura, O. H. Frazier, and L. M. Buja, "Fibrosis and heart failure," *Heart Failure Reviews*, vol. 19, no. 2, pp. 173–185, 2014.
- [4] R. Weiskirchen, S. Weiskirchen, and F. Tacke, "Organ and tissue fibrosis: molecular signals, cellular mechanisms and translational implications," *Molecular Aspects of Medicine*, vol. 65, pp. 2–15, 2019.
- [5] J. Wu, W. Guo, S. Z. Lin et al., "Gp130-mediated STAT3 activation by S-propargyl-cysteine, an endogenous hydrogen sulfide initiator, prevents doxorubicin-induced cardiotoxicity," *Cell Death & Disease*, vol. 7, no. 8, pp. e2339–e2339, 2016.
- [6] J. J. McMurray, S. Adamopoulos, S. D. Anker et al., "ESC guidelines for the diagnosis and treatment of acute and chronic heart failure 2012: the task force for the diagnosis and treatment of acute and chronic heart failure 2012 of the European Society of Cardiology. Developed in collaboration with the heart failure association (HFA) of the ESC," *European Heart Journal*, vol. 33, no. 14, pp. 1787–1847, 2012.
- [7] M. N. Jameel and J. Zhang, "Heart failure management: the present and the future," *Antioxidants & Redox Signaling*, vol. 11, no. 8, pp. 1989–2010, 2009.
- [8] R. Wang, "Gasotransmitters: growing pains and joys," *Trends in Biochemical Sciences*, vol. 39, no. 5, pp. 227–232, 2014.
- [9] S. R. Lee, B. Nilius, and J. Han, "Gaseous signaling molecules in cardiovascular function: from mechanisms to clinical translation," *Reviews of Physiology, Biochemistry and Pharmacology*, vol. 174, pp. 81–156, 2018.
- [10] R. Wang, "Two's company, three's a crowd: can H₂S be the third endogenous gaseous transmitter?," *FASEB Journal*, vol. 16, no. 13, pp. 1792–1798, 2002.
- [11] L. L. Pan, M. Qin, X. H. Liu, and Y. Z. Zhu, "The role of hydrogen sulfide on cardiovascular homeostasis: an overview with update on immunomodulation," *Frontiers in Pharmacology*, vol. 8, 2017.
- [12] B. L. Predmore, D. J. Lefer, and G. Gojon, "Hydrogen sulfide in biochemistry and medicine," *Antioxidants & Redox Signaling*, vol. 17, no. 1, pp. 119–140, 2012.
- [13] J. W. Calvert, W. A. Coetzee, and D. J. Lefer, "Novel insights into hydrogen sulfide-mediated cytoprotection," *Antioxidants & Redox Signaling*, vol. 12, no. 10, pp. 1203–1217, 2010.
- [14] G. Szabó, G. Veres, T. Radovits et al., "Cardioprotective effects of hydrogen sulfide," *Nitric Oxide*, vol. 25, no. 2, pp. 201–210, 2011.
- [15] A. Deb and E. Ubil, "Cardiac fibroblast in development and wound healing," *Journal of Molecular and Cellular Cardiology*, vol. 70, pp. 47–55, 2014.
- [16] Y. Shen, Z. Shen, L. Miao et al., "miRNA-30 family inhibition protects against cardiac ischemic injury by regulating cystathionine-γ-lyase expression," *Antioxidants & Redox Signaling*, vol. 22, no. 3, pp. 224–240, 2015.
- [17] L. Zhang, Y. Wang, Y. Li et al., "Hydrogen sulfide (H₂S)-releasing compounds: therapeutic potential in cardiovascular diseases," *Frontiers in Pharmacology*, vol. 9, article 1066, 2018.
- [18] R. Guo, Z. Wu, J. Jiang et al., "New mechanism of lipotoxicity in diabetic cardiomyopathy: deficiency of endogenous H₂S production and ER stress," *Mechanisms of Ageing and Development*, vol. 162, pp. 46–52, 2017.
- [19] L. A. Barr, Y. Shimizu, J. P. Lambert, C. K. Nicholson, and J. W. Calvert, "Hydrogen sulfide attenuates high fat diet-induced cardiac dysfunction via the suppression of endoplasmic reticulum stress," *Nitric Oxide*, vol. 46, pp. 145–156, 2015.
- [20] U. Sen, P. K. Mishra, N. Tyagi, and S. C. Tyagi, "Homocysteine to hydrogen sulfide or hypertension," *Cell Biochemistry and Biophysics*, vol. 57, no. 2–3, pp. 49–58, 2010.
- [21] M. Racine, M. Fu, T. Shuang et al., "Reversal of Sp1 transactivation and TGFβ1/SMAD1 signaling by H₂S prevent nickel-induced fibroblast activation," *Toxicology and Applied Pharmacology*, vol. 356, pp. 25–35, 2018.
- [22] M. M. Cortese-Krott, G. G. C. Kuhnle, A. Dyson et al., "Key bioactive reaction products of the NO/H₂S interaction are S/N-hybrid species, polysulfides, and nitroxyl," *Proceedings of the National Academy of Sciences of the United States of America*, vol. 112, no. 34, pp. E4651–E4660, 2015.
- [23] J. Beltowski, "Hydrogen sulfide in pharmacology and medicine - An update," *Pharmacological Reports*, vol. 67, no. 3, pp. 647–658, 2015.
- [24] S. Yuan, S. Pardue, X. Shen, J. S. Alexander, A. W. Orr, and C. G. Kevil, "Hydrogen sulfide metabolism regulates endothelial solute barrier function," *Redox Biology*, vol. 9, pp. 157–166, 2016.
- [25] B. Geng, J. Yang, Y. Qi et al., "H₂S generated by heart in rat and its effects on cardiac function," *Biochemical and Biophysical Research Communications*, vol. 313, no. 2, pp. 362–368, 2004.

- [26] W. Zhao, J. Zhang, Y. Lu, and R. Wang, "The vasorelaxant effect of H₂S as a novel endogenous gaseous K_{ATP} channel opener," *EMBO Journal*, vol. 20, no. 21, pp. 6008–6016, 2001.
- [27] R. Hosoki, N. Matsuki, and H. Kimura, "The possible role of hydrogen sulfide as an endogenous smooth muscle relaxant in synergy with nitric oxide," *Biochemical and Biophysical Research Communications*, vol. 237, no. 3, pp. 527–531, 1997.
- [28] J. Beltowski and A. Jamroz-Wisniewska, "Hydrogen sulfide and endothelium-dependent vasorelaxation," *Molecules*, vol. 19, no. 12, pp. 21183–21199, 2014.
- [29] Y. Enokido, E. Suzuki, K. Iwasawa, K. Namekata, H. Okazawa, and H. Kimura, "Cystathionine beta-synthase, a key enzyme for homocysteine metabolism, is preferentially expressed in the radial glia/astrocyte lineage of developing mouse CNS," *FASEB Journal*, vol. 19, no. 13, pp. 1854–1856, 2005.
- [30] J. I. Toohey, "Sulfur signaling: is the agent sulfide or sulfane?," *Analytical Biochemistry*, vol. 413, no. 1, pp. 1–7, 2011.
- [31] J. Yang, P. Minkler, D. Grove et al., "Non-enzymatic hydrogen sulfide production from cysteine in blood is catalyzed by iron and vitamin B₆," *Communications Biology*, vol. 2, no. 1, article 194, 2019.
- [32] M. L. Morrison, J. E. Blackwood, S. L. Lockett, A. Iwata, R. K. Winn, and M. B. Roth, "Surviving blood loss using hydrogen sulfide," *The Journal of Trauma*, vol. 65, no. 1, pp. 183–188, 2008.
- [33] P. Dorsey, C. Keel, M. Klavens, and W. J. Hellstrom, "Phosphodiesterase type 5 (PDE5) inhibitors for the treatment of erectile dysfunction," *Expert Opinion on Pharmacotherapy*, vol. 11, no. 7, pp. 1109–1122, 2010.
- [34] K. U. Tüfekci, R. L. J. Meuwissen, and Ş. Genç, "The Role of Micro RNAs in Biological Processes," in *miRNomics: micro-RNA biology and computational analysis*, M. Yousef and J. Allmer, Eds., pp. 15–31, Humana Press, Totowa, NJ, USA, 2014.
- [35] J. Wilinski, E. Somogyi, M. Góralaska, B. Wiliński, and D. Czarnecka, "Ramipril enhances the endogenous hydrogen sulfide tissue concentration in mouse heart and brain," *Folia Medica Cracoviensia*, vol. 49, no. 3-4, pp. 123–130, 2008.
- [36] Y. Xu, H.-P. Du, J. Li et al., "Statins upregulate cystathionine γ -lyase transcription and H₂S generation via activating Akt signaling in macrophage," *Pharmacological Research*, vol. 87, pp. 18–25, 2014.
- [37] B. Wilinski, J. Wiliński, E. Somogyi, J. Piotrowska, and M. Góralaska, "Amlodipine affects endogenous hydrogen sulfide tissue concentrations in different mouse organs," *Folia Medica Cracoviensia*, vol. 51, no. 1-4, pp. 29–35, 2011.
- [38] W. Bogdan, W. Jerzy, S. Eugeniusz, P. Joanna, and G. Marta, "Digoxin increases hydrogen sulfide concentrations in brain, heart and kidney tissues in mice," *Pharmacological Reports*, vol. 63, no. 5, pp. 1243–1247, 2011.
- [39] B. Wilinski, J. Wilinski, E. Somogyi, J. Piotrowska, and W. Opoka, "Vitamin D3 (cholecalciferol) boosts hydrogen sulfide tissue concentrations in heart and other mouse organs," *Folia Biologica*, vol. 60, no. 3, pp. 243–247, 2012.
- [40] A. Bilska, M. Iciek, I. Kwiecień et al., "Effects of aspirin on the levels of hydrogen sulfide and sulfane sulfur in mouse tissues," *Pharmacological Reports*, vol. 62, no. 2, pp. 304–310, 2010.
- [41] J. Beltowski and A. Jamroz-Wisniewska, "Modulation of h(2)s metabolism by statins: a new aspect of cardiovascular pharmacology," *Antioxidants & Redox Signaling*, vol. 17, no. 1, pp. 81–94, 2012.
- [42] H. Kimura, "Hydrogen sulfide and polysulfides as biological mediators," *Molecules*, vol. 19, no. 10, pp. 16146–16157, 2014.
- [43] G. A. Benavides, G. L. Squadrito, R. W. Mills et al., "Hydrogen sulfide mediates the vasoactivity of garlic," *Proceedings of the National Academy of Sciences of the United States of America*, vol. 104, no. 46, pp. 17977–17982, 2007.
- [44] K. Okubo, M. Matsumura, Y. Kawaiishi et al., "Hydrogen sulfide-induced mechanical hyperalgesia and allodynia require activation of both Cav3.2 and TRPA1 channels in mice," *British Journal of Pharmacology*, vol. 166, no. 5, pp. 1738–1743, 2012.
- [45] D. J. Polhemus and D. J. Lefer, "Emergence of hydrogen sulfide as an endogenous gaseous signaling molecule in cardiovascular disease," *Circulation Research*, vol. 114, no. 4, pp. 730–737, 2014.
- [46] T. Corsello, N. Komaravelli, and A. Casola, "Role of hydrogen sulfide in NRF2- and sirutin-dependent maintenance of cellular redox balance," *Antioxidants*, vol. 7, no. 10, p. 129, 2018.
- [47] Y. Kimura and H. Kimura, "Hydrogen sulfide protects neurons from oxidative stress," *FASEB Journal*, vol. 18, no. 10, pp. 1165–1167, 2004.
- [48] N. J. Alp and K. M. Channon, "Regulation of endothelial nitric oxide synthase by tetrahydrobiopterin in vascular disease," *Arteriosclerosis, Thrombosis, and Vascular Biology*, vol. 24, no. 3, pp. 413–420, 2004.
- [49] J. D. Raffetto and R. A. Khalil, "Matrix metalloproteinases and their inhibitors in vascular remodeling and vascular disease," *Biochemical Pharmacology*, vol. 75, no. 2, pp. 346–359, 2008.
- [50] N. Takahashi, D. Kozai, and Y. Mori, "TRP channels: sensors and transducers of gasotransmitter signals," *Frontiers in Physiology*, vol. 3, p. 324, 2012.
- [51] A. K. Mustafa, M. M. Gadalla, and S. H. Snyder, "Signaling by gasotransmitters," *Science signaling*, vol. 2, no. 68, article re2, 2009.
- [52] M. T. Nelp, V. Zheng, K. M. Davis, K. J. E. Stiefel, and J. T. Groves, "Potent activation of indoleamine 2,3-dioxygenase by polysulfides," *Journal of the American Chemical Society*, vol. 141, no. 38, pp. 15288–15300, 2019.
- [53] A. K. Mustafa, M. M. Gadalla, N. Sen et al., "H₂S signals through protein S-sulfhydration," *Science signaling*, vol. 2, no. 96, article ra72, 2009.
- [54] K. Módis, Y. J. Ju, A. Ahmad et al., "S-Sulfhydration of ATP synthase by hydrogen sulfide stimulates mitochondrial bioenergetics," *Pharmacological Research*, vol. 113, Part A, pp. 116–124, 2016.
- [55] N. Sen, "Functional and molecular insights of hydrogen sulfide signaling and protein Sulfhydration," *Journal of Molecular Biology*, vol. 429, no. 4, pp. 543–561, 2017.
- [56] P. Manna and S. K. Jain, "Hydrogen sulfide and L-cysteine increase phosphatidylinositol 3,4,5-trisphosphate (PIP3) and glucose utilization by inhibiting phosphatase and tensin homolog (PTEN) protein and activating phosphoinositide 3-kinase (PI3K)/serine/threonine protein kinase (AKT)/protein kinase C ζ /lambda (PKC ζ /lambda) in 3T3L1 adipocytes," *The Journal of Biological Chemistry*, vol. 286, no. 46, pp. 39848–39859, 2011.
- [57] Y. Sun, Y. Huang, W. Yu et al., "Sulfhydration-associated phosphodiesterase 5A dimerization mediates vasorelaxant effect of hydrogen sulfide," *Oncotarget*, vol. 8, no. 19, pp. 31888–31900, 2017.

- [58] T. D. Baird and R. C. Wek, "Eukaryotic initiation factor 2 phosphorylation and translational control in metabolism," *Advances in Nutrition*, vol. 3, no. 3, pp. 307–321, 2012.
- [59] V. Yadav, X. H. Gao, B. Willard, M. Hatzoglou, R. Banerjee, and O. Kabil, "Hydrogen sulfide modulates eukaryotic translation initiation factor 2 α (eIF2 α) phosphorylation status in the integrated stress-response pathway," *Journal of Biological Chemistry*, vol. 292, no. 32, pp. 13143–13153, 2017.
- [60] L. Li, D. Liu, D. Bu et al., "Brg1-dependent epigenetic control of vascular smooth muscle cell proliferation by hydrogen sulfide," *Biochimica et Biophysica Acta (BBA) - Molecular Cell Research*, vol. 1833, no. 6, pp. 1347–1355, 2013.
- [61] Y. Sun, Z. Tian, N. Liu et al., "Exogenous H₂S switches cardiac energy substrate metabolism by regulating SIRT3 expression in db/db mice," *Journal of Molecular Medicine*, vol. 96, no. 3-4, pp. 281–299, 2018.
- [62] D. F. Dai, P. S. Rabinovitch, and Z. Ungvari, "Mitochondria and cardiovascular aging," *Circulation Research*, vol. 110, no. 8, pp. 1109–1124, 2012.
- [63] M. U. Khan, Y. Cheema, A. U. Shahbaz et al., "Mitochondria play a central role in nonischemic cardiomyocyte necrosis: common to acute and chronic stressor states," *Pflügers Archiv-European Journal of Physiology*, vol. 464, no. 1, pp. 123–131, 2012.
- [64] S. Li and G. Yang, "Hydrogen sulfide maintains mitochondrial DNA replication via demethylation of TFAM," *Antioxidants & Redox Signaling*, vol. 23, no. 7, pp. 630–642, 2015.
- [65] Y. Shimizu, R. Polavarapu, K. L. Eskla et al., "Hydrogen sulfide regulates cardiac mitochondrial biogenesis via the activation of AMPK," *Journal of Molecular and Cellular Cardiology*, vol. 116, pp. 29–40, 2018.
- [66] D. Fan, A. Takawale, J. Lee, and Z. Kassiri, "Cardiac fibroblasts, fibrosis and extracellular matrix remodeling in heart disease," *Fibrogenesis Tissue Repair*, vol. 5, no. 1, p. 15, 2012.
- [67] P. Zhou and W. T. Pu, "Recounting cardiac cellular composition," *Circulation Research*, vol. 118, no. 3, pp. 368–370, 2016.
- [68] P. Pakshir and B. Hinz, "The big five in fibrosis: macrophages, myofibroblasts, matrix, mechanics, and miscommunication," *Matrix Biology*, vol. 68–69, pp. 81–93, 2018.
- [69] V. Talman and H. Ruskoaho, "Cardiac fibrosis in myocardial infarction—from repair and remodeling to regeneration," *Cell and Tissue Research*, vol. 365, no. 3, pp. 563–581, 2016.
- [70] T. A. Wynn and T. R. Ramalingam, "Mechanisms of fibrosis: therapeutic translation for fibrotic disease," *Nature Medicine*, vol. 18, no. 7, pp. 1028–1040, 2012.
- [71] S. Rosenkranz, "TGF- β ₁ and angiotensin networking in cardiac remodeling," *Cardiovascular Research*, vol. 63, no. 3, pp. 423–432, 2004.
- [72] S. Psarras, D. Beis, S. Nikouli, M. Tsikitis, and Y. Capetanaki, "Three in a box: understanding cardiomyocyte, fibroblast, and innate immune cell interactions to orchestrate cardiac repair processes," *Frontiers in Cardiovascular Medicine*, vol. 6, p. 32, 2019.
- [73] J. G. Travers, F. A. Kamal, J. Robbins, K. E. Yutzey, and B. C. Blaxall, "Cardiac fibrosis: the fibroblast awakens," *Circulation Research*, vol. 118, no. 6, pp. 1021–1040, 2016.
- [74] P. Kong, P. Christia, and N. G. Frangogiannis, "The pathogenesis of cardiac fibrosis," *Cellular and Molecular Life Sciences*, vol. 71, no. 4, pp. 549–574, 2014.
- [75] Z. G. Ma, Y. P. Yuan, H. M. Wu, X. Zhang, and Q. Z. Tang, "Cardiac fibrosis: new insights into the pathogenesis," *International Journal of Biological Sciences*, vol. 14, no. 12, pp. 1645–1657, 2018.
- [76] K. C. Flanders, "Smad3 as a mediator of the fibrotic response," *International Journal of Experimental Pathology*, vol. 85, no. 2, pp. 47–64, 2004.
- [77] Y. Ma, R. P. Iyer, M. Jung, M. P. Czubyrt, and M. L. Lindsey, "Cardiac fibroblast activation post-myocardial infarction: current knowledge gaps," *Trends in Pharmacological Sciences*, vol. 38, no. 5, pp. 448–458, 2017.
- [78] A. V. Shinde and N. G. Frangogiannis, "Fibroblasts in myocardial infarction: a role in inflammation and repair," *Journal of Molecular and Cellular Cardiology*, vol. 70, pp. 74–82, 2014.
- [79] C. J. Li, C. S. Chen, G. T. Yiang, A. P.-Y. Tsai, W.-T. Liao, and M.-Y. Wu, "Advanced evolution of pathogenesis concepts in cardiomyopathies," *Journal of Clinical Medicine*, vol. 8, no. 4, p. 520, 2019.
- [80] Y. Zhang, J. Wang, H. Li et al., "Hydrogen sulfide suppresses transforming growth factor- β 1-induced differentiation of human cardiac fibroblasts into myofibroblasts," *Science China Life Sciences*, vol. 58, no. 11, pp. 1126–1134, 2015.
- [81] H. L. Jiang, H. C. Wu, Z. L. Li, B. Geng, and C. S. Tang, "Changes of the new gaseous transmitter H₂S in patients with coronary heart disease," *Di Yi Jun Yi Da Xue Xue Bao*, vol. 25, no. 8, pp. 951–954, 2005.
- [82] M. V. Cohen, X. M. Yang, and J. M. Downey, "Nitric oxide is a preconditioning mimetic and cardioprotectant and is the basis of many available infarct-sparing strategies," *Cardiovascular Research*, vol. 70, no. 2, pp. 231–239, 2006.
- [83] P. Pagliaro, D. Gattullo, R. Rastaldo, and G. Losano, "Involvement of nitric oxide in ischemic preconditioning," *Italian Heart Journal*, vol. 2, no. 9, pp. 660–668, 2001.
- [84] S. R. Lee and J. Han, "Mitochondrial metabolic inhibition and cardioprotection," *Korean Circulation Journal*, vol. 47, no. 2, pp. 168–170, 2017.
- [85] N. Ge, C. Liu, G. Li et al., "Hydrogen sulfide attenuates acute myocardial ischemic injury through the glycogen synthase kinase-3 β /catenin signaling pathway," *International Journal of Molecular Medicine*, vol. 37, no. 5, pp. 1281–1289, 2016.
- [86] D. Wu, Q. Hu, Y. Xiong, D. Zhu, Y. Mao, and Y. Z. Zhu, "Novel H₂S-NO hybrid molecule (ZYZ-803) promoted synergistic effects against heart failure," *Redox Biology*, vol. 15, pp. 243–252, 2018.
- [87] Y. Shimizu, C. K. Nicholson, J. P. Lambert et al., "Sodium sulfide attenuates ischemic-induced heart failure by enhancing proteasomal function in an Nrf2-dependent manner," *Circulation: Heart Failure*, vol. 9, no. 4, article e002368, 2016.
- [88] L. Xie, Y. Gu, M. Wen et al., "Hydrogen sulfide induces Keap1 S-sulphydration and suppresses diabetes-accelerated atherosclerosis via Nrf2 activation," *Diabetes*, vol. 65, no. 10, pp. 3171–3184, 2016.
- [89] C. Y. Tsai, C. C. Wang, T. Y. Lai et al., "Antioxidant effects of diallyl trisulfide on high glucose-induced apoptosis are mediated by the PI3K/Akt-dependent activation of Nrf2 in cardiomyocytes," *International Journal of Cardiology*, vol. 168, no. 2, pp. 1286–1297, 2013.
- [90] A. M. Rodriguez and V. P. Yin, "Emerging roles for immune cells and microRNAs in modulating the response to cardiac

- injury," *Journal of Cardiovascular Development and Disease*, vol. 6, no. 1, p. 5, 2019.
- [91] S. Toldo, A. Das, E. Mezzaroma et al., "Induction of microRNA-21 with exogenous hydrogen sulfide attenuates myocardial ischemic and inflammatory injury in mice," *Circulation: Cardiovascular Genetics*, vol. 7, no. 3, pp. 311–320, 2014.
- [92] H. Li, C. Zhang, W. Sun et al., "Exogenous hydrogen sulfide restores cardioprotection of ischemic post-conditioning via inhibition of mPTP opening in the aging cardiomyocytes," *Cell & Bioscience*, vol. 5, no. 1, p. 43, 2015.
- [93] A. Chatzianastasiou, S. I. Bibli, I. Andreadou et al., "Cardioprotection by H₂S donors: nitric oxide-dependent and independent mechanisms," *Journal of Pharmacology and Experimental Therapeutics*, vol. 358, no. 3, pp. 431–440, 2016.
- [94] Q. G. Karwi, J. Bornbaum, K. Boengler et al., "AP39, a mitochondria-targeting hydrogen sulfide (H₂S) donor, protects against myocardial reperfusion injury independently of salvage kinase signalling," *British Journal of Pharmacology*, vol. 174, no. 4, pp. 287–301, 2017.
- [95] J. W. Elrod, J. W. Calvert, J. Morrison et al., "Hydrogen sulfide attenuates myocardial ischemia-reperfusion injury by preservation of mitochondrial function," *Proceedings of the National Academy of Sciences of the United States of America*, vol. 104, no. 39, pp. 15560–15565, 2007.
- [96] J. Chen, J. Gao, W. Sun et al., "Involvement of exogenous H₂S in recovery of cardioprotection from ischemic post-conditioning via increase of autophagy in the aged hearts," *International Journal of Cardiology*, vol. 220, pp. 681–692, 2016.
- [97] L. Rochette, Y. Cottin, M. Zeller, and C. Vergely, "Carbon monoxide: mechanisms of action and potential clinical implications," *Pharmacology & Therapeutics*, vol. 137, no. 2, pp. 133–152, 2013.
- [98] G. Meng, Y. Ma, L. Xie, A. Ferro, and Y. Ji, "Emerging role of hydrogen sulfide in hypertension and related cardiovascular diseases," *British Journal of Pharmacology*, vol. 172, no. 23, pp. 5501–5511, 2015.
- [99] P. M. Snijder, A. R. Frenay, R. A. de Boer et al., "Exogenous administration of thiosulfate, a donor of hydrogen sulfide, attenuates angiotensin II-induced hypertensive heart disease in rats," *British Journal of Pharmacology*, vol. 172, no. 6, pp. 1494–1504, 2015.
- [100] S. Cacanyiova, A. Berenyiova, F. Kristek, M. Drobna, K. Ondrias, and M. Grman, "The adaptive role of nitric oxide and hydrogen sulphide in vasoactive responses of thoracic aorta is triggered already in young spontaneously hypertensive rats," *Journal of Physiology and Pharmacology*, vol. 67, no. 4, pp. 501–512, 2016.
- [101] L. Tomasova, L. Dobrowolski, H. Jurkowska et al., "Intracolonic hydrogen sulfide lowers blood pressure in rats," *Nitric Oxide*, vol. 60, pp. 50–58, 2016.
- [102] H. Laggner, M. Hermann, H. Esterbauer et al., "The novel gaseous vasorelaxant hydrogen sulfide inhibits angiotensin-converting enzyme activity of endothelial cells," *Journal of Hypertension*, vol. 25, no. 10, pp. 2100–2104, 2007.
- [103] T. Wu, H. Li, B. Wu et al., "Hydrogen sulfide reduces recruitment of CD11b⁺DG Gr-1⁺DG cells in mice with myocardial infarction," *Cell Transplantation*, vol. 26, no. 5, pp. 753–764, 2017.
- [104] C. Huang, J. Kan, X. Liu et al., "Cardioprotective effects of a novel hydrogen sulfide agent-controlled release formulation of S-propargyl-cysteine on heart failure rats and molecular mechanisms," *PLoS One*, vol. 8, no. 7, pp. e69205–e69205, 2013.
- [105] S. Jin, X. Teng, L. Xiao et al., "Hydrogen sulfide ameliorated L-NAME-induced hypertensive heart disease by the Akt/e-NOS/NO pathway," *Experimental Biology and Medicine*, vol. 242, no. 18, pp. 1831–1841, 2017.
- [106] M. Sikora, A. Drapala, and M. Ufnal, "Exogenous hydrogen sulfide causes different hemodynamic effects in normotensive and hypertensive rats via neurogenic mechanisms," *Pharmacological Reports*, vol. 66, no. 5, pp. 751–758, 2014.
- [107] L. Fang, J. Zhao, Y. Chen et al., "Hydrogen sulfide derived from periadventitial adipose tissue is a vasodilator," *Journal of Hypertension*, vol. 27, no. 11, pp. 2174–2185, 2009.
- [108] J. M. Pappachan, G. I. Varughese, R. Sriraman, and G. Arunagirinathan, "Diabetic cardiomyopathy: pathophysiology, diagnostic evaluation and management," *World Journal of Diabetes*, vol. 4, no. 5, pp. 177–189, 2013.
- [109] S. K. Jain, R. Bull, J. L. Rains et al., "Low levels of hydrogen sulfide in the blood of diabetes patients and streptozotocin-treated rats causes vascular inflammation?," *Antioxidants & Redox Signaling*, vol. 12, no. 11, pp. 1333–1337, 2010.
- [110] M. Liu, Y. Li, B. Liang et al., "Hydrogen sulfide attenuates myocardial fibrosis in diabetic rats through the JAK/STAT signaling pathway," *International Journal of Molecular Medicine*, vol. 41, no. 4, pp. 1867–1876, 2018.
- [111] S. Jin, S. X. Pu, C. L. Hou et al., "Cardiac H₂S generation is reduced in ageing diabetic mice," *Oxidative Medicine and Cellular Longevity*, vol. 2015, Article ID 758358, 14 pages, 2015.
- [112] F. Yang, L. Zhang, Z. Gao et al., "Exogenous H₂S protects against diabetic cardiomyopathy by activating autophagy via the AMPK/mTOR pathway," *Cellular Physiology and Biochemistry*, vol. 43, no. 3, pp. 1168–1187, 2017.
- [113] T. Xiao, O. Zeng, J. Luo, Z. Wu, F. Li, and J. Yang, "Effects of hydrogen sulfide on myocardial fibrosis in diabetic rats: changes in matrix metalloproteinases parameters," *Bio-Medical Materials and Engineering*, vol. 26, no. s1, pp. S2033–S2039, 2015.
- [114] R. Yang, Q. Jia, S. F. Ma, Y. Wang, S. Mehmood, and Y. Chen, "Exogenous H₂S mitigates myocardial fibrosis in diabetic rats through suppression of the canonical Wnt pathway," *International Journal of Molecular Medicine*, vol. 44, no. 2, pp. 549–558, 2019.
- [115] F. Li, J. Luo, Z. Wu et al., "Hydrogen sulfide exhibits cardioprotective effects by decreasing endoplasmic reticulum stress in a diabetic cardiomyopathy rat model," *Molecular Medicine Reports*, vol. 14, no. 1, pp. 865–873, 2016.
- [116] T. Xiao, J. Luo, Z. Wu, F. Li, O. Zeng, and J. Yang, "Effects of hydrogen sulfide on myocardial fibrosis and PI3K/AKT1-regulated autophagy in diabetic rats," *Molecular Medicine Reports*, vol. 13, no. 2, pp. 1765–1773, 2016.
- [117] A. John, S. Kundu, S. Pushpakumar et al., "GYY4137, a hydrogen sulfide donor modulates miR194-dependent collagen realignment in diabetic kidney," *Scientific Reports*, vol. 7, no. 1, article 10924, 2017.

- [118] N. Zhang, W. Y. Wei, L. L. Li, C. Hu, and Q.-Z. Tang, "Therapeutic potential of polyphenols in cardiac fibrosis," *Frontiers in Pharmacology*, vol. 9, p. 122, 2018.
- [119] Q. C. Yong, T. T. Pan, L. F. Hu, and J. S. Bian, "Negative regulation of β -adrenergic function by hydrogen sulphide in the rat hearts," *Journal of Molecular and Cellular Cardiology*, vol. 44, no. 4, pp. 701–710, 2008.
- [120] J. Zhang, J. Yu, Y. Chen et al., "Exogenous hydrogen sulfide supplement attenuates isoproterenol-induced myocardial hypertrophy in a sirtuin 3-dependent manner," *Oxidative Medicine and Cellular Longevity*, vol. 2018, 17 pages, 2018.
- [121] Z. Zhang, S. Jin, X. Teng, X. Duan, Y. Chen, and Y. Wu, "Hydrogen sulfide attenuates cardiac injury in takotsubo cardiomyopathy by alleviating oxidative stress," *Nitric Oxide*, vol. 67, pp. 10–25, 2017.
- [122] D. Wu, Q. Hu, B. Tan, P. Rose, D. Zhu, and Y. Z. Zhu, "Amelioration of mitochondrial dysfunction in heart failure through S-sulfhydration of Ca^{2+} /calmodulin-dependent protein kinase II," *Redox Biology*, vol. 19, pp. 250–262, 2018.
- [123] A. C. Reid, J. A. Brazin, C. Morrey, R. B. Silver, and R. Levi, "Targeting cardiac mast cells: pharmacological modulation of the local renin-angiotensin system," *Current Pharmaceutical Design*, vol. 17, no. 34, pp. 3744–3752, 2011.
- [124] F. Vargas, J. M. Moreno, I. Rodriguez-Gómez et al., "Vascular and renal function in experimental thyroid disorders," *European Journal of Endocrinology*, vol. 154, no. 2, pp. 197–212, 2006.
- [125] M. Liu, Z. Li, B. Liang et al., "Hydrogen sulfide ameliorates rat myocardial fibrosis induced by thyroxine through PI3K/AKT signaling pathway," *Endocrine Journal*, vol. 65, no. 7, pp. 769–781, 2018.
- [126] U. Sen, T. P. Vacek, W. M. Hughes et al., "Cardioprotective role of sodium thiosulfate on chronic heart failure by modulating endogenous H_2S generation," *Pharmacology*, vol. 82, no. 3, pp. 201–213, 2008.
- [127] J. Long, M. Liu, S. Liu et al., " H_2S attenuates the myocardial fibrosis in diabetic rats through modulating PKC-ERK1/2-MAPK signaling pathway," *Technology and Health Care*, vol. 27, no. S1, pp. 307–316, 2019.
- [128] X. Sun, D. Zhao, F. Lu et al., "Hydrogen sulfide regulates muscle RING finger-1 protein S-sulfhydration at Cys^{44} to prevent cardiac structural damage in diabetic cardiomyopathy," *British Journal of Pharmacology*, pp. 1–21, 2019.
- [129] L. L. Pan, X. L. Wang, X. L. Wang, and Y. Z. Zhu, "Sodium hydrosulfide prevents myocardial dysfunction through modulation of extracellular matrix accumulation and vascular density," *International Journal of Molecular Sciences*, vol. 15, no. 12, pp. 23212–23226, 2014.
- [130] L. L. Pan, X. H. Liu, Y. Q. Shen et al., "Inhibition of NADPH oxidase 4-related signaling by sodium hydrosulfide attenuates myocardial fibrotic response," *International Journal of Cardiology*, vol. 168, no. 4, pp. 3770–3778, 2013.
- [131] P. K. Mishra, N. Tyagi, U. Sen, S. Givvimani, and S. C. Tyagi, " H_2S ameliorates oxidative and proteolytic stresses and protects the heart against adverse remodeling in chronic heart failure," *American journal of physiology- Heart and circulatory physiology*, vol. 298, no. 2, pp. H451–H456, 2010.
- [132] Y. X. Shi, Y. Chen, Y. Z. Zhu et al., "Chronic sodium hydrosulfide treatment decreases medial thickening of intramyocardial coronary arterioles, interstitial fibrosis, and ROS production in spontaneously hypertensive rats," *American journal of physiology- Heart and circulatory physiology*, vol. 293, no. 4, pp. H2093–H2100, 2007.
- [133] B. Geng, L. Chang, C. Pan et al., "Endogenous hydrogen sulfide regulation of myocardial injury induced by isoproterenol," *Biochemical and Biophysical Research Communications*, vol. 318, no. 3, pp. 756–763, 2004.
- [134] W. Hua, Q. Chen, F. Gong, C. Xie, S. Zhou, and L. Gao, "Cardioprotection of H_2S by downregulating iNOS and upregulating HO-1 expression in mice with CVB3-induced myocarditis," *Life Sciences*, vol. 93, no. 24, pp. 949–954, 2013.
- [135] S. I. Bibli, I. Andreadou, A. Chatzianastasiou et al., "Cardioprotection by H_2S engages a cGMP-dependent protein kinase G/phospholamban pathway," *Cardiovascular Research*, vol. 106, no. 3, pp. 432–442, 2015.
- [136] N. Qipshidze, N. Metreveli, P. K. Mishra, D. Lominadze, and S. C. Tyagi, "Hydrogen sulfide mitigates cardiac remodeling during myocardial infarction via improvement of angiogenesis," *International Journal of Biological Sciences*, vol. 8, no. 4, pp. 430–441, 2012.
- [137] C. K. Nicholson, J. P. Lambert, J. D. Molkenin, J. Sadoshima, and J. W. Calvert, "Thioredoxin 1 is essential for sodium sulfide-mediated cardioprotection in the setting of heart failure," *Arteriosclerosis, Thrombosis, and Vascular Biology*, vol. 33, no. 4, pp. 744–751, 2013.
- [138] P. Ye, Y. Gu, Y. R. Zhu et al., "Exogenous hydrogen sulfide attenuates the development of diabetic cardiomyopathy via the FoxO1 pathway," *Journal of Cellular Physiology*, vol. 233, no. 12, pp. 9786–9798, 2018.
- [139] S. Lilyanna, M. T. Peh, O. W. Liew et al., "GYY4137 attenuates remodeling, preserves cardiac function and modulates the natriuretic peptide response to ischemia," *Journal of Molecular and Cellular Cardiology*, vol. 87, pp. 27–37, 2015.
- [140] G. Meng, J. Wang, Y. Xiao et al., "GYY4137 protects against myocardial ischemia and reperfusion injury by attenuating oxidative stress and apoptosis in rats," *Journal of Biomedical Research*, vol. 29, no. 3, pp. 203–213, 2015.
- [141] G. Meng, J. Zhu, Y. Xiao et al., "Hydrogen sulfide donor GYY4137 protects against myocardial fibrosis," *Oxidative Medicine and Cellular Longevity*, vol. 2015, Article ID 691070, 14 pages, 2015.
- [142] K. E. Sikura, L. Potor, T. Szerafin et al., "Hydrogen sulfide inhibits calcification of heart valves; implications for calcific aortic valve disease," *British Journal of Pharmacology*, pp. 1–17, 2019.
- [143] C. Zhu, Y. Su, S. Juriasingani et al., "Supplementing preservation solution with mitochondria-targeted H_2S donor AP39 protects cardiac grafts from prolonged cold ischemia-reperfusion injury in heart transplantation," *American Journal of Transplantation*, vol. 19, no. 11, pp. 3139–3148, 2019.
- [144] K. Kondo, S. Bhushan, A. L. King et al., " H_2S protects against pressure overload-induced heart failure via upregulation of endothelial nitric oxide synthase," *Circulation*, vol. 127, no. 10, pp. 1116–1127, 2013.
- [145] D. J. Polhemus, Z. Li, C. B. Pattillo et al., "A novel hydrogen sulfide Prodrug, SG1002, promotes hydrogen sulfide and nitric oxide bioavailability in heart failure patients," *Cardiovascular Therapeutics*, vol. 33, no. 4, pp. 216–226, 2015.

- [146] D. Liang, H. Wu, M. W. Wong, and D. Huang, "Diallyl trisulfide is a fast H₂S donor, but diallyl disulfide is a slow one: the reaction pathways and intermediates of glutathione with polysulfides," *Organic Letters*, vol. 17, no. 17, pp. 4196–4199, 2015.
- [147] L. Yu, S. Li, X. Tang et al., "Diallyl trisulfide ameliorates myocardial ischemia-reperfusion injury by reducing oxidative stress and endoplasmic reticulum stress-mediated apoptosis in type 1 diabetic rats: role of SIRT1 activation," *Apoptosis*, vol. 22, no. 7, pp. 942–954, 2017.
- [148] L. Yu, W. Di, X. Dong et al., "Diallyl trisulfide exerts cardioprotection against myocardial ischemia-reperfusion injury in diabetic state, role of AMPK-mediated AKT/GSK-3 β /HIF-1 α activation," *Oncotarget*, vol. 8, no. 43, pp. 74791–74805, 2017.
- [149] W. W. Kuo, W. J. Wang, C. Y. Tsai, C. L. Way, H. H. Hsu, and L. M. Chen, "Diallyl trisulfide (DATS) suppresses high glucose-induced cardiomyocyte apoptosis by inhibiting JNK/NF κ B signaling via attenuating ROS generation," *International Journal of Cardiology*, vol. 168, no. 1, pp. 270–280, 2013.
- [150] R. A. Frieler and R. M. Mortensen, "Immune cell and other noncardiomyocyte regulation of cardiac hypertrophy and remodeling," *Circulation*, vol. 131, no. 11, pp. 1019–1030, 2015.
- [151] S. Frantz, K. Hu, A. Adamek et al., "Transforming growth factor beta inhibition increases mortality and left ventricular dilatation after myocardial infarction," *Basic Research in Cardiology*, vol. 103, no. 5, pp. 485–492, 2008.
- [152] X. Zhang, Z.-G. Ma, Y.-P. Yuan et al., "Rosmarinic acid attenuates cardiac fibrosis following long-term pressure overload via AMPK α /Smad3 signaling," *Cell Death & Disease*, vol. 9, no. 2, pp. 102–102, 2018.
- [153] Q. Y. Zhang, H. F. Jin, S. Chen et al., "Hydrogen sulfide regulating myocardial structure and function by targeting cardiomyocyte autophagy," *Chinese Medical Journal*, vol. 131, no. 7, pp. 839–844, 2018.
- [154] K. Kashfi and K. R. Olson, "Biology and therapeutic potential of hydrogen sulfide and hydrogen sulfide-releasing chimeras," *Biochemical Pharmacology*, vol. 85, no. 5, pp. 689–703, 2013.
- [155] M. Bilban, A. Haschemi, B. Wegiel, B. Y. Chin, O. Wagner, and L. E. Otterbein, "Heme oxygenase and carbon monoxide initiate homeostatic signaling," *Journal of Molecular Medicine*, vol. 86, no. 3, pp. 267–279, 2008.
- [156] L. M. D. Delbridge, K. M. Mellor, D. J. Taylor, and R. A. Gottlieb, "Myocardial stress and autophagy: mechanisms and potential therapies," *Nature Reviews Cardiology*, vol. 14, no. 7, pp. 412–425, 2017.
- [157] D. Wu, H. Wang, T. Teng, S. Duan, A. Ji, and Y. Li, "Hydrogen sulfide and autophagy: a double edged sword," *Pharmacological Research*, vol. 131, pp. 120–127, 2018.
- [158] S. Sestito, G. Nesi, R. Pi, M. Macchia, and S. Rapposelli, "Hydrogen sulfide: a worthwhile tool in the design of new multitarget drugs," *Frontiers in Chemistry*, vol. 5, p. 72, 2017.
- [159] S. B. Montesi, P. Désogère, B. C. Fuchs, and P. Caravan, "Molecular imaging of fibrosis: recent advances and future directions," *The Journal of Clinical Investigation*, vol. 129, no. 1, pp. 24–33, 2019.
- [160] M. Abdelmonem, N. N. Shahin, L. A. Rashed, H. A. A. Amin, A. A. Shamaa, and A. A. Shaheen, "Hydrogen sulfide enhances the effectiveness of mesenchymal stem cell therapy in rats with heart failure: *In vitro* preconditioning versus *in vivo* co-delivery," *Biomedicine & pharmacotherapy*, vol. 112, article 108584, 2019.
- [161] T. L. Guidotti, "Chapter 8- Hydrogen Sulfide Intoxication," in *Handbook of Clinical Neurology*, M. Lotti and M. L. Bleeker, Eds., pp. 111–133, Elsevier, 2015.

Review Article

Oxidative Modifications in Advanced Atherosclerotic Plaques: A Focus on *In Situ* Protein Sulfhydryl Group Oxidation

Antonio Junior Lepedda  and Marilena Formato 

Dipartimento di Scienze Biomediche, University of Sassari, Sassari, Italy

Correspondence should be addressed to Antonio Junior Lepedda; ajlepedda@uniss.it

Received 2 October 2019; Revised 17 December 2019; Accepted 26 December 2019; Published 9 January 2020

Guest Editor: Alessia Baseggio Conrado

Copyright © 2020 Antonio Junior Lepedda and Marilena Formato. This is an open access article distributed under the Creative Commons Attribution License, which permits unrestricted use, distribution, and reproduction in any medium, provided the original work is properly cited.

Although oxidative stress has been long associated with the genesis and progression of the atherosclerotic plaque, scanty data on its *in situ* effects on protein sulfhydryl group modifications are available. Within the arterial wall, protein sulfhydryls and low-molecular-weight (LMW) thiols are involved in the cell regulation of both Reactive Oxygen Species (ROS) and Reactive Nitrogen Species (RNS) levels and are a target for several posttranslational oxidative modifications that take place inside the atherosclerotic plaque, probably contributing to both atherogenesis and atherosclerotic plaque progression towards complicated lesions. Advanced carotid plaques are characterized by very high intraplaque GSH levels, due to cell lysis during apoptotic and/or necrotic events, probably responsible for the altered equilibrium among protein sulfhydryls and LMW thiols. Some lines of evidence show that the prooxidant environment present in atherosclerotic tissue could modify filtered proteins also by protein-SH group oxidation, and demonstrate that particularly albumin, once filtered, represents a harmful source of homocysteine and cysteinylglycine inside the plaque. The oxidative modification of protein sulfhydryls, with particular emphasis to protein thiolation by LMW thiols and its association with atherosclerosis, is the main topic of this review.

1. Introduction

Cardiovascular diseases are the leading cause of death and illness in developed countries, being atherosclerosis a major contributor [1]. Cardiovascular risk factors such as hypertension, diabetes, and hyperlipidaemia play a key role in the onset and progression of atherosclerosis [2]. Atherosclerosis, a chronic inflammatory condition, develops and evolves in a site-specific and patient-specific manner, with a great heterogeneity in growth rate and pathologic features [3]. Atherosclerotic plaques are commonly characterized by accumulation of lipids and fibrous elements in the intimal layer of medium size and large arteries. Erosion of the atherosclerotic plaques could cause plaque ulceration leading to acute thrombosis and artery occlusion, driving major adverse clinical events. Indeed, plaque disruption is a common precipitating factor in the pathogenesis of both acute coronary occlusion and peripheral artery thrombosis. The mechanisms underlying plaque formation and progression towards advanced lesions potentially prone to rupture are not yet

completely understood. Despite current systemic application of therapies, such as statins and antiplatelet agents for prevention of both accelerated plaque growth and thrombotic consequences of its rupture, most of major adverse cardiovascular events cannot be averted [3].

Understanding the mechanisms that promote thin fibrous cap formation and stabilization, as opposed to lysis and disruption, would help to effectively counteract the release of prothrombogenic elements and prevent acute thrombotic occlusion. It is generally held that plaque instability is caused by a substantial increase in inflammatory and proteolytic activity [4]. Furthermore, some lines of evidence suggest that unstable plaques are also characterized by pronounced oxidative environment [5]. *In situ* oxidative events may determine lipid/protein metabolic fate, bioactivity, and antigenic properties.

This review will focus on oxidative modifications of protein sulfhydryl groups, with particular emphasis to protein thiolation by low-molecular-weight thiols (LMW thiols), and their association with atherosclerosis.

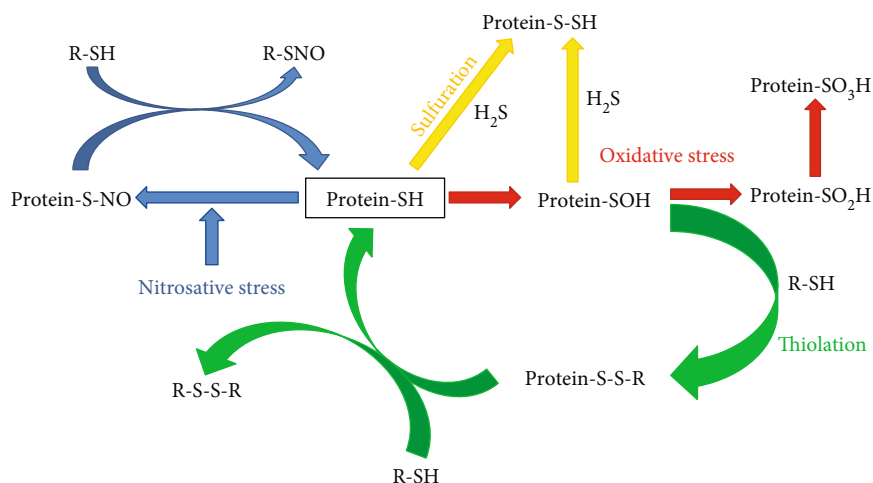


FIGURE 1: Overview of the wide variety of biochemical modifications that reduced protein sulfhydryl groups may potentially undergo. R-SH or LMW thiols: γ Glu-Cys-Gly (γ glutamyl-cysteinyl-glycine, glutathione), Cys (cysteine), HCy (homocysteine), Cys-Gly (cysteine-glycine), and Glu-Cys (glutamyl-cysteine).

2. Oxidative Stress and Atherosclerosis

A great deal of research has shown a contributory role of oxidative modifications of apolipoprotein B-100-containing lipoproteins (LDL and Lp(a)), within the arterial wall, in the early events of atherogenesis [1, 6, 7]. Oxidized LDL is readily internalized by macrophages through the so-called “scavenger receptor” pathway. These early modifications could initiate and/or contribute to atherogenesis, mainly when an imbalance between oxidant and antioxidant agents takes place [7]. Although several studies report that atherosclerotic plaques contain high concentrations of some amino acid oxidation products, caused mainly by carbonylation, ROS and RNS oxidation, or thiolation [8–10], limited information is available regarding the relationship between the accumulation of *in situ* oxidized proteins and atherosclerosis severity [11]. Furthermore, different oxidation-specific epitopes can be detected in blood and may reflect atherosclerosis manifestations [12]. At present, the mechanisms underlying the formation of these by-products and their relevance for disease progression are not completely understood and deserve further investigation.

ROS and RNS are highly reactive electrophiles that oxidize nucleophilic functional groups of proteins, polysaccharides, and nucleic acids such as -OH, -NH₂ and -SH, leading to cell damage and death, if not properly repaired. Due to its chemistry, -SH is more reactive than -OH and -NH₂ and, consequently, more prone to oxidation or conjugation [13, 14].

Within the arterial wall, several enzymes as well as non-enzymatic antioxidants take part in counteracting these oxidative modifications [7]. Among them, protein sulfhydryl groups (protein-SH (PSH) groups) and low-molecular-weight thiols (LMW thiols) are involved in the cell regulation of both ROS and RNS levels. Due to its high reducing power and its relatively high concentration, glutathione (GSH) represents the best intracellular reducing agent. In this respect, it has been reported that human atherosclerotic plaques display

lack of GSH-peroxidase (Px) activity and a deficient glutathione redox cycle status that may significantly weaken its antioxidant potential [15, 16], so corroborating the hypothesis that the prooxidant environment within the vascular wall might be involved in atherogenesis and complicated lesion formation. Further evidences come from differential proteomic analysis on advanced unstable and stable carotid plaques, where a reduced expression of superoxide dismutase 3 (major defence against the superoxide anion radical in the vascular extracellular matrix) and glutathione S-transferase (vessel protection against reactive species such as α,β -unsaturated carbonyls and 4-hydroxy-2-nonenal), in the former, suggests an even more impaired antioxidant/prooxidant balance in those plaques more prone to rupture [17].

3. Protein Sulfhydryls Oxidation and Atherosclerosis

The reactivity of LMW thiols, namely cysteine-glycine (Cys-Gly), homocysteine (HCy), cysteine (Cys), glutathione (GSH), and glutamylcysteine (Glu-Cys), due to their proton lability (pKa), is strictly dependent on their structure, whereas reactivity of protein-SH is affected also by the exposure to the milieu [18]. Some proteins, such as albumin and haemoglobin, have reactive cysteine residues susceptible to some reversible (thiolation, nitrosylation, and sulfenylation) or irreversible (sulfinylation and sulfonation) oxidative modifications (Figure 1). In the last years, it is becoming increasingly clear that also protein S-sulfuration [19] represents an important mechanism of regulation of protein activity mediated by hydrogen sulfide (H₂S) (Figure 1). In this respect, it has been reported that these modifications occur on enzymes, receptors, transcription factors, and ion channels and represent key regulatory events in maintaining the physiological function of proteins in the cardiovascular system [20].

Among the abovementioned reversible reactions, protein S-thiolation by LMW thiols is the most biologically

stable and important one [21]. The formation of S-thiolated proteins represents an antioxidant defence mechanism against such reactive molecules, and it has been suggested as a possible redox regulation mechanism of protein function [22, 23] and cell signalling [24, 25]. Indeed, the reversible covalent modification of some protein cysteine residues may be transitory and have critical modulatory effects as suggested for the activation of the latent elastolytic metalloproteinase-2 (pro-MMP-2) by homocysteinylation and S-glutathionylation of the propeptide via the so-called “cysteine switch” mechanism [26–29]. The activation of matrix metalloproteinases (MMPs) by LMW thiol adduction may have a key role in the extracellular matrix degradation and plaque rupture. Furthermore, reversible oxidative modifications, including sulfenylation, S-nitrosylation, and S-thiolation are thought to act as redox sensors in cell signalling pathways [30–32].

S-Glutathionylation is emerging as having a causative role in cardiovascular diseases by regulating numerous physiological processes involved in cardiovascular homeostasis, including myocyte contraction, oxidative phosphorylation, protein synthesis, vasodilation, glycolytic metabolism, and response to insulin [33]. With respect to atherogenesis, there are several *in vitro* evidences that GSH protects macrophages from OxLDL-induced cell injury [34–37]. Furthermore, Adachi et al. showed that S-glutathionylation of sarco/endoplasmic reticulum calcium (Ca^{2+}) ATPase (SERCA) induces NO-dependent relaxation that is impaired following irreversible oxidation of key thiol(s) during atherosclerosis, so preventing the activation of SERCA [38]. The same team described the mechanisms of redox-dependent p21ras activation induced by oxLDL in endothelial cells [39]. Actually, protein-S-glutathionylation/deglutathionylation in monocytes and macrophages is thought to be an important signalling mechanism that modulates cell response to oxidative stress in key events of plaque initiation (monocyte recruitment and differentiation) and progression (macrophage activation and death) [40]. Increased serum protein glutathionylation has been also correlated with peripheral atherosclerosis [41]. Furthermore, serum levels of glutathione, homocysteine, and cysteine have been independently associated with cardiovascular risk scores at a population level [42].

Elevated plasma levels of homocysteine are a known risk factor for cardiovascular disease and atherothrombosis [43]. Some of its effects include impaired relaxation of blood vessels mediated by the endothelium-derived NO, thiolation of plasma or endothelial proteins, low-density lipoprotein S-homocysteinylation [44, 45], activation of inflammatory pathways and apoptosis, vascular SMC activation and proliferation, and macrophage activation and differentiation [46–50]. Besides GSH, also homocysteine is involved in extracellular matrix remodelling through activation of latent metalloproteinases [26, 28, 29].

Attempting to investigate the relationship between oxidative stress and plaque progression, we studied sulfhydryl group oxidative modifications of extractable proteins from advanced human atherosclerotic plaques, by means of a differential proteomic approach [51]. The study provided evidence that in unstable carotid plaques, and to a lesser

extent in stable ones, there is a prooxidant microenvironment conducive to the formation of ROS- and RNS-mediated protein thiol oxidation products. The sulfhydryl group oxidation observed regarded both filtered (e.g., albumin and transferrin) and topically expressed (e.g., α -actin) proteins. Those findings were also corroborated by capillary electrophoresis analysis of LMW thiols bound to extractable proteins that showed higher levels of protein thiolation in unstable plaque extracts. Interestingly, such an increase in protein-bound thiol content was not associated with a concurrent increase in total LMW thiol content. Furthermore, the levels of plasma LMW thiols did not discriminate between patients with stable and unstable plaques, suggesting that the observed differences resulted from oxidative events which take place inside the atherosclerotic plaque [51].

4. Human Serum Albumin as a Carrier of Harmful LMW Thiols inside the Atherosclerotic Plaque

Human serum albumin (HSA) is the most abundant plasma multifunctional protein and the major antioxidant in plasma with a concentration (0.8 mM) higher than the other antioxidants by an exponential factor [52]. Its plasma levels have been strongly inversely correlated with both incident coronary heart disease [53, 54] and some carotid plaque oxidation markers (i.e., TBARS and AOPP) detected in advanced lesions [55]. Recently, its redox state has been associated with some indices of atherosclerosis [56]. Furthermore, a positive correlation between serum total homocysteine and HSA-bound homocysteine in hyperlipidaemic patients has been reported [57]. Interestingly, S-thiolation of HSA occurred not only at Cys³⁴ but also at other cysteine residues, such as Cys⁹⁰ and Cys¹⁰¹ [57].

Albumin accounts for ROS/RNS scavenging, metal ion binding [58], and transport functions for fatty acids [59, 60], nitric oxide, hemin, and drugs [61–63]. It displays also pseudoenzymatic hydrolytic activity of several endogenous and exogenous compounds [64]. Most of the abovementioned functions are due to its unique redox active free cysteine residue (Cys³⁴) [65]. Thiol concentration in plasma are lower than in the cells, mostly represented by albumin Cys³⁴ residue, which accounts for 80% (500 $\mu\text{mol/L}$) of total plasma thiols. Due to its reactivity (unexpectedly low Cys³⁴ pKa) and its relatively high concentration, it is the preferential target for oxidants and electrophiles. In fact, in blood as well as in extravascular fluids, albumin is susceptible to different oxidative modifications, especially thiol oxidation and carbonylation [66, 67]. Although albumin circulates primarily in its reduced form, about 30–40% of its reactive Cys³⁴ residues could be variably oxidized, either reversibly as mixed disulphide with low-molecular-weight thiols [68], S-nitroso Cys [69], or sulfenic acid [70] or irreversibly as sulfinic or sulfonic acid [52] (Figure 1). Furthermore, it has been described that albumin, through its nucleophilic Cys³⁴ residue, acts as scavenger for proatherogenic species such as 4-hydroxytrans-2-nonenal [71].

S-Thiolation of circulating albumin by LMW thiols is the most prevalent Cys³⁴ oxidative modification. Although the

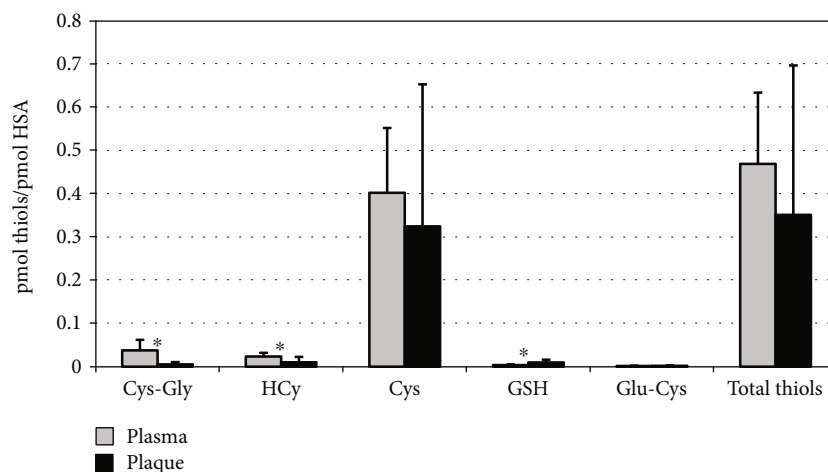


FIGURE 2: Levels of LMW thiols extracted from both circulating and plaque-filtered HSA, expressed as pmoles/pmoles of albumin, obtained by CE-LIF analysis (from [75]). *Significant differences between the two HSA forms ($P < 0.001$). Cys-Gly: cysteine-glycine; HCy: homocysteine; Cys: cysteine; GSH: glutathione; Glu-Cys: glutamylcysteine.

proinflammatory mechanisms mediated by LMW thiols are not yet completely understood, it was suggested that albumin could act as homocysteine carrier inside the cells where it could exert its noxious effects by altering the redox potential or modifying intracellular proteins resulting in cellular dysfunction [72].

Starting from this interesting assumption, we have hypothesized that circulating albumin may filter into the atherosclerotic plaque where it may release harmful LMW thiols. Some previous results obtained on advanced human carotid plaques extracts showed that about 70% of extractable proteins were of plasma origin, being albumin the most represented [17], and intraplaque LMW thiol content and distribution deeply differed from plasma [73]. In particular, the high intraplaque glutathione levels, probably consequent to red blood cell lysis, a frequently observed event in atherosclerotic lesions, could contribute to plaque fate by perturbing the physiological LMW thiol redox state.

To assess a possible role for albumin as a carrier of LMW thiols inside the plaque, we set up a very sensitive method for the thiolation analysis of both circulating and intraplaque albumin [74]. The method, which allows for the separation and quantitation of all five LMW thiols starting from $3 \mu\text{g}$ of albumin, consisted of (1) a preanalytical albumin purification from both plasma and plaque extracts by nonreducing SDS-PAGE, (2) in-gel extraction of LMW thiols, and (3) capillary electrophoresis laser induced fluorescence analysis (CE-LIF).

This method was applied to the analysis of HSA Cys³⁴ thiolation/oxidation on twenty-seven atherosclerotic plaque specimens and the corresponding plasma samples collected from patients undergoing carotid endarterectomy [75]. By this way, we evidenced distinct patterns of thiolation for the two HSA forms with a significant reduction of Cys-Gly (~7-fold) and HCy (~2-fold), as well as an increase of GSH (~2.8-fold) in intraplaque HSA (Figure 2). Overall, following infiltration, albumin releases $16.2 \pm 11.2 \text{ nmol HCy/g proteins}$ and $32.8 \pm 23.9 \text{ nmol Cys-Gly/g proteins}$, which represent the bulk of free HCy and Cys-Gly inside the plaque

environment [44]. In this regard, carotid plaques are characterized by very high intraplaque GSH levels, with respect to plasma ($225 \pm 177 \text{ nmol/g proteins}$ vs. $59 \pm 15 \text{ nmol/g proteins}$, 23.9% vs. 1.72%), probably due to cell lysis during apoptotic and/or necrotic events, responsible for the different equilibrium among protein-bound LMW thiols and the higher Cys³⁴ glutathionylation of the intraplaque form.

These *in situ* evidences have been further supported by recent *in vitro* data [76] showing equilibria among protein-bound LMW thiols and free LMW thiols released in a thiol-free medium. In particular, the Authors, by using commercial HSA with or without previous incubation with HCy and HCy thiolactone, have evidenced that (1) albumin spontaneously releases HCy in a thiol-free medium (and likely in a thiol-poor medium such as the plaque environment) and such event (2) is positively correlated with the levels of albumin homocysteinylation and (3) could be further increased by the presence in the medium of other LMW thiols, such as Cys and GSH.

5. Conclusions

Understanding the mechanisms that regulate either plaque stabilization or its evolution towards complication and rupture is essential to prevent the clinical events related to acute artery atherothrombosis.

Within the arterial wall, oxidative modifications could initiate and/or contribute to atherogenesis and plaque development. Among them, the formation of mixed disulfides between protein sulfhydryls and LMW thiols may represent an antioxidant defence mechanism, and it has been suggested as a possible redox regulation mechanism of protein function and cell signalling.

Although several *in vitro* and *in vivo* evidences show a link between protein thiolation and cardiovascular diseases, only scanty data on these oxidative modifications *in situ* (inside atherosclerotic plaque) have been reported so far, leaving the issue at a speculative perspective.

In these respect, in the last years, a step forward has been made by reporting the different sulfhydryl oxidation/thiolation of plaque proteins in relation to stable/unstable advanced atherosclerotic lesions and demonstrating that serum albumin, the main plasma protein filtered in plaque, represents a carrier of LMW thiols inside the atherosclerotic lesions, where it releases harmful quantities of homocysteine, probably contributing to plaque progression. However, some aspects, including the equilibria between LMW thiols and protein sulfhydryls, and the effects of specific protein thiolation on their functions remain to be elucidated. They could provide further insight into the relevance of oxidative modifications in atherosclerotic plaque development and progression towards advanced lesions and, surely, deserve further studies.

Conflicts of Interest

The authors declare that they have no conflicts of interest.

Acknowledgments

AJ Lepedda thanks Regione Autonoma della Sardegna for its financial support (POR-FSE 2014-2020-Asse Prioritario 3 “Istruzione e Formazione”-Obiettivo Tematico: 10, Priorità d’investimento: 10ii, Obiettivo Specifico: 10.5, Azione dell’Accordo di Partenariato 10.5.12-C.U.P. J86C18000270002). The authors thank the University of Sassari for its financial support (Fondo di Ateneo per la Ricerca 2019).

References

- [1] P. Libby, J. E. Buring, L. Badimon et al., “Atherosclerosis,” *Nature Reviews Disease Primers*, vol. 5, no. 1, p. 56, 2019.
- [2] W. Herrington, B. Lacey, P. Sherliker, J. Armitage, and S. Lewington, “Epidemiology of atherosclerosis and the potential to reduce the global burden of atherothrombotic disease,” *Circulation Research*, vol. 118, no. 4, pp. 535–546, 2016.
- [3] G. K. Hansson, P. Libby, and I. Tabas, “Inflammation and plaque vulnerability,” *Journal of Internal Medicine*, vol. 278, no. 5, pp. 483–493, 2015.
- [4] G. R. Geovanini and P. Libby, “Atherosclerosis and inflammation: overview and updates,” *Clinical Science*, vol. 132, no. 12, pp. 1243–1252, 2018.
- [5] N. R. Madamanchi, A. Vendrov, and M. S. Runge, “Oxidative stress and vascular disease,” *Arteriosclerosis, Thrombosis, and Vascular Biology*, vol. 25, no. 1, pp. 29–38, 2005.
- [6] D. Steinberg and J. L. Witztum, “Oxidized low-density lipoprotein and atherosclerosis,” *Arteriosclerosis, Thrombosis, and Vascular Biology*, vol. 30, no. 12, pp. 2311–2316, 2010.
- [7] R. Stocker and J. F. Kearney Jr., “Role of oxidative modifications in atherosclerosis,” *Physiological Reviews*, vol. 84, no. 4, pp. 1381–1478, 2004.
- [8] R. L. Charles and P. Eaton, “Redox signalling in cardiovascular disease,” *Proteomics Clinical Applications*, vol. 2, no. 6, pp. 823–836, 2008.
- [9] A. Gödecke, J. Schrader, and M. Reinartz, “Nitric oxide-mediated protein modification in cardiovascular physiology and pathology,” *Proteomics Clinical Applications*, vol. 2, no. 6, pp. 811–822, 2008.
- [10] K. Sugamura and J. F. Kearney Jr., “Reactive oxygen species in cardiovascular disease,” *Free Radical Biology & Medicine*, vol. 51, no. 5, pp. 978–992, 2011.
- [11] A. J. Lepedda, *Journal Biomedical and Biopharmaceutical Research*, vol. 2, no. 14, p. 296, 2017.
- [12] H. Ou, Z. Huang, Z. Mo, and J. Xiao, “The characteristics and roles of advanced oxidation protein products in atherosclerosis,” *Cardiovascular Toxicology*, vol. 17, no. 1, pp. 1–12, 2017.
- [13] P. Di Simplicio, F. Franconi, S. Frosali, and D. Di Giuseppe, “Thiolation and nitrosation of cysteines in biological fluids and cells,” *Amino Acids*, vol. 25, no. 3–4, pp. 323–339, 2003.
- [14] K. K. Griendling, R. M. Touyz, J. L. Zweier et al., “Measurement of reactive oxygen species, reactive nitrogen species, and redox-dependent signaling in the cardiovascular system: a scientific statement from the American Heart Association,” *Circulation Research*, vol. 119, no. 5, pp. e39–e75, 2016.
- [15] D. Lapenna, S. de Gioia, G. Ciofani et al., “Glutathione-related antioxidant defenses in human atherosclerotic plaques,” *Circulation*, vol. 97, no. 19, pp. 1930–1934, 1998.
- [16] D. Lapenna, G. Ciofani, A. M. Calafiore, F. Cipollone, and E. Porreca, “Impaired glutathione-related antioxidant defenses in the arterial tissue of diabetic patients,” *Free Radical Biology & Medicine*, vol. 124, pp. 525–531, 2018.
- [17] A. J. Lepedda, A. Cigliano, G. M. Cherchi et al., “A proteomic approach to differentiate histologically classified stable and unstable plaques from human carotid arteries,” *Atherosclerosis*, vol. 203, no. 1, pp. 112–118, 2009.
- [18] O. Spiga, D. Summa, S. Cirri et al., “A structurally driven analysis of thiol reactivity in mammalian albumins,” *Biopolymers*, vol. 95, no. 4, pp. 278–285, 2011.
- [19] J. I. Toohey, “The conversion of H₂S to sulfane sulfur,” *Nature Reviews Molecular Cell Biology*, vol. 13, no. 12, p. 803, 2012.
- [20] G. Meng, S. Zhao, L. Xie, Y. Han, and Y. Ji, “Protein S-sulfhydration by hydrogen sulfide in cardiovascular system,” *British Journal of Pharmacology*, vol. 175, no. 8, pp. 1146–1156, 2018.
- [21] P. Eaton, “Protein thiol oxidation in health and disease: techniques for measuring disulfides and related modifications in complex protein mixtures,” *Free Radical Biology & Medicine*, vol. 40, no. 11, pp. 1889–1899, 2006.
- [22] P. J. Hogg, “Disulfide bonds as switches for protein function,” *Trends in Biochemical Sciences*, vol. 28, no. 4, pp. 210–214, 2003.
- [23] P. Klatt and S. Lamas, “Regulation of protein function by S-glutathiolation in response to oxidative and nitrosative stress,” *European Journal of Biochemistry*, vol. 267, no. 16, pp. 4928–4944, 2000.
- [24] S. Biswas, A. S. Chida, and I. Rahman, “Redox modifications of protein-thiols: emerging roles in cell signaling,” *Biochemical Pharmacology*, vol. 71, no. 5, pp. 551–564, 2006.
- [25] I. Dalle-Donne, R. Rossi, G. Colombo, D. Giustarini, and A. Milzani, “Protein S-glutathionylation: a regulatory device from bacteria to humans,” *Trends in Biochemical Sciences*, vol. 34, no. 2, pp. 85–96, 2009.
- [26] A. Bescond, T. Augier, C. Chareyre, D. Garçon, W. Hornebeck, and P. Charpiot, “Influence of homocysteine on matrix metalloproteinase-2: activation and activity,” *Biochemical and Biophysical Research Communications*, vol. 263, no. 2, pp. 498–503, 1999.

- [27] T. Okamoto, T. Akaike, T. Sawa, Y. Miyamoto, A. van der Vliet, and H. Maeda, "Activation of matrix metalloproteinases by peroxynitrite-induced protein S-glutathiolation via disulfide S-oxide formation," *The Journal of Biological Chemistry*, vol. 276, no. 31, pp. 29596–29602, 2001.
- [28] S. C. Tyagi, L. M. Smiley, V. S. Mujumdar, B. Clonts, and J. L. Parker, "Reduction-oxidation (redox) and vascular tissue level of homocyst(e)ine in human coronary atherosclerotic lesions and role in extracellular matrix remodeling and vascular tone," *Molecular and Cellular Biochemistry*, vol. 181, no. 1-2, pp. 107–116, 1998.
- [29] Z. S. Wang, H. Jin, and D. M. Wang, "Influence of hydrogen sulfide on zymogen activation of homocysteine-induced matrix metalloproteinase-2 in H9C2 cardiocytes," *Asian Pacific Journal of Tropical Medicine*, vol. 9, no. 5, pp. 489–493, 2016.
- [30] R. L. Charles, E. Schröder, G. May et al., "Protein sulfenation as a redox sensor: proteomics studies using a novel biotinylated dimedone analogue," *Molecular & Cellular Proteomics*, vol. 6, no. 9, pp. 1473–1484, 2007.
- [31] L. B. Poole and K. J. Nelson, "Discovering mechanisms of signaling-mediated cysteine oxidation," *Current Opinion in Chemical Biology*, vol. 12, no. 1, pp. 18–24, 2008.
- [32] J. Ying, N. Clavreul, M. Sethuraman, T. Adachi, and R. A. Cohen, "Thiol oxidation in signaling and response to stress: detection and quantification of physiological and pathophysiological thiol modifications," *Free Radical Biology & Medicine*, vol. 43, no. 8, pp. 1099–1108, 2007.
- [33] A. Pastore and F. Piemonte, "Protein glutathionylation in cardiovascular diseases," *International Journal of Molecular Sciences*, vol. 14, no. 10, pp. 20845–20876, 2013.
- [34] F. Bea, F. N. Hudson, A. Chait, T. J. Kavanagh, and M. E. Rosenfeld, "Induction of glutathione synthesis in macrophages by oxidized low-density lipoproteins is mediated by consensus antioxidant response elements," *Circulation Research*, vol. 92, no. 4, pp. 386–393, 2003.
- [35] V. M. Darley-Usmar, A. Severn, V. J. O'Leary, and M. Rogers, "Treatment of macrophages with oxidized low-density lipoprotein increases their intracellular glutathione content," *The Biochemical Journal*, vol. 278, no. 2, pp. 429–434, 1991.
- [36] N. Gotoh, A. Graham, E. Nikl, and V. M. Darley-Usmar, "Inhibition of glutathione synthesis increases the toxicity of oxidized low-density lipoprotein to human monocytes and macrophages," *The Biochemical Journal*, vol. 296, no. 1, pp. 151–154, 1993.
- [37] Y. Wang, M. Qiao, J. J. Mieyal, L. M. Asmis, and R. Asmis, "Molecular mechanism of glutathione-mediated protection from oxidized low-density lipoprotein-induced cell injury in human macrophages: role of glutathione reductase and glutaredoxin," *Free Radical Biology & Medicine*, vol. 41, no. 5, pp. 775–785, 2006.
- [38] T. Adachi, R. M. Weisbrod, D. R. Pimentel et al., "S-Glutathiolation by peroxynitrite activates SERCA during arterial relaxation by nitric oxide," *Nature Medicine*, vol. 10, no. 11, pp. 1200–1207, 2004.
- [39] N. Clavreul, T. Adachi, D. R. Pimental, Y. Ido, C. Schöneich, and R. A. Cohen, "S-Glutathiolation by peroxynitrite of p21ras at cysteine-118 mediates its direct activation and downstream signaling in endothelial cells," *The FASEB Journal*, vol. 20, no. 3, pp. 518–520, 2006.
- [40] J. D. Short, K. Downs, S. Tavakoli, and R. Asmis, "Protein thiol redox signaling in monocytes and macrophages," *Antioxidants & Redox Signaling*, vol. 25, no. 15, pp. 816–835, 2016.
- [41] K. Nonaka, N. Kume, Y. Urata et al., "Serum levels of S-glutathionylated proteins as a risk-marker for arteriosclerosis obliterans," *Circulation Journal*, vol. 71, no. 1, pp. 100–105, 2007.
- [42] A. A. Mangoni, A. Zinellu, C. Carru, J. R. Attia, and M. McEvoy, "Serum thiols and cardiovascular risk scores: a combined assessment of transsulfuration pathway components and substrate/product ratios," *Journal of Translational Medicine*, vol. 11, no. 1, p. 99, 2013.
- [43] D. Djuric, V. Jakovljevic, V. Zivkovic, and I. Srejsovic, "Homocysteine and homocysteine-related compounds: an overview of the roles in the pathology of the cardiovascular and nervous systems," *Canadian Journal of Physiology and Pharmacology*, vol. 96, no. 10, pp. 991–1003, 2018.
- [44] A. Zinellu, A. Lepedda Jr., S. Sotgia et al., "Evaluation of low molecular mass thiols content in carotid atherosclerotic plaques," *Clinical Biochemistry*, vol. 42, no. 9, pp. 796–801, 2009.
- [45] A. Zinellu, S. Sotgia, B. Scanu et al., "Low density lipoprotein S-homocysteinylation is increased in acute myocardial infarction patients," *Clinical Biochemistry*, vol. 45, no. 4-5, pp. 359–362, 2012.
- [46] R. C. Austin, S. R. Lentz, and G. H. Werstuck, "Role of hyperhomocysteinemia in endothelial dysfunction and atherothrombotic disease," *Cell Death and Differentiation*, vol. 11, Supplement 1, pp. S56–S64, 2004.
- [47] I. Chernyavskiy, S. Veeranki, U. Sen, and S. C. Tyagi, "Atherogenesis: hyperhomocysteinemia interactions with LDL, macrophage function, paraoxonase 1, and exercise," *Annals of the New York Academy of Sciences*, vol. 1363, no. 1, pp. 138–154, 2016.
- [48] R. Esse, M. Barroso, I. Tavares de Almeida, and R. Castro, "The contribution of homocysteine metabolism disruption to endothelial dysfunction: state-of-the-art," *International Journal of Molecular Sciences*, vol. 20, no. 4, p. 867, 2019.
- [49] S. R. Lentz, "Mechanisms of homocysteine-induced atherothrombosis," *Journal of Thrombosis and Haemostasis*, vol. 3, no. 8, pp. 1646–1654, 2005.
- [50] J. C. Tsai, M. A. Perrella, M. Yoshizumi et al., "Promotion of vascular smooth muscle cell growth by homocysteine: a link to atherosclerosis," *Proceedings of the National Academy of Sciences of the United States of America*, vol. 91, no. 14, pp. 6369–6373, 1994.
- [51] A. J. Lepedda, A. Zinellu, G. Nieddu et al., "Protein sulfhydryl group oxidation and mixed-disulfide modifications in stable and unstable human carotid plaques," *Oxidative Medicine and Cellular Longevity*, vol. 2013, Article ID 403973, 8 pages, 2013.
- [52] M. Bruschi, G. Candiano, L. Santucci, and G. M. Ghiggeri, "Oxidized albumin. The long way of a protein of uncertain function," *Biochimica et Biophysica Acta*, vol. 1830, no. 12, pp. 5473–5479, 2013.
- [53] J. J. Nelson, D. Liao, A. R. Sharrett et al., "Serum albumin level as a predictor of incident coronary heart disease: the atherosclerosis risk in communities (ARIC) study," *American Journal of Epidemiology*, vol. 151, no. 5, pp. 468–477, 2000.
- [54] P. Pignatelli, A. Farcomeni, D. Menichelli, D. Pastori, and F. Violi, "Serum albumin and risk of cardiovascular events in primary and secondary prevention: a systematic review of observational studies and Bayesian meta-regression analysis," *Internal and Emergency Medicine*, pp. 1–9, 2019.

- [55] D. Lapenna, G. Ciofani, S. Uchino et al., "Serum albumin and biomolecular oxidative damage of human atherosclerotic plaques," *Clinical Biochemistry*, vol. 43, no. 18, pp. 1458–1460, 2010.
- [56] R. Fujii, J. Ueyama, A. Aoi et al., "Oxidized human serum albumin as a possible correlation factor for atherosclerosis in a rural Japanese population: the results of the Yakumo study," *Environmental Health and Preventive Medicine*, vol. 23, no. 1, p. 1, 2018.
- [57] F. Nakashima, T. Shibata, K. Kamiya et al., "Structural and functional insights into S-thiolation of human serum albumins," *Scientific Reports*, vol. 8, no. 1, p. 932, 2018.
- [58] W. Bal, M. Sokołowska, E. Kurowska, and P. Faller, "Binding of transition metal ions to albumin: sites, affinities and rates," *Biochimica et Biophysica Acta*, vol. 1830, no. 12, pp. 5444–5455, 2013.
- [59] S. Fujiwara and T. Amisaki, "Fatty acid binding to serum albumin: molecular simulation approaches," *Biochimica et Biophysica Acta*, vol. 1830, no. 12, pp. 5427–5434, 2013.
- [60] J. A. Hamilton, "NMR reveals molecular interactions and dynamics of fatty acid binding to albumin," *Biochimica et Biophysica Acta*, vol. 1830, no. 12, pp. 5418–5426, 2013.
- [61] U. Anand and S. Mukherjee, "Binding, unfolding and refolding dynamics of serum albumins," *Biochimica et Biophysica Acta*, vol. 1830, no. 12, pp. 5394–5404, 2013.
- [62] Z. M. Wang, J. X. Ho, J. R. Ruble et al., "Structural studies of several clinically important oncology drugs in complex with human serum albumin," *Biochimica et Biophysica Acta*, vol. 1830, no. 12, pp. 5356–5374, 2013.
- [63] K. Yamasaki, V. T. Chuang, T. Maruyama, and M. Otagiri, "Albumin-drug interaction and its clinical implication," *Biochimica et Biophysica Acta*, vol. 1830, no. 12, pp. 5435–5443, 2013.
- [64] U. Kragh-Hansen, "Molecular and practical aspects of the enzymatic properties of human serum albumin and of albumin-ligand complexes," *Biochimica et Biophysica Acta*, vol. 1830, no. 12, pp. 5535–5544, 2013.
- [65] M. Anraku, V. T. Chuang, T. Maruyama, and M. Otagiri, "Redox properties of serum albumin," *Biochimica et Biophysica Acta*, vol. 1830, no. 12, pp. 5465–5472, 2013.
- [66] G. Colombo, M. Clerici, D. Giustarini, R. Rossi, A. Milzani, and I. Dalle-Donne, "Redox albuminomics: oxidized albumin in human diseases," *Antioxidants & Redox Signaling*, vol. 17, no. 11, pp. 1515–1527, 2012.
- [67] L. Turell, R. Radi, and B. Alvarez, "The thiol pool in human plasma: the central contribution of albumin to redox processes," *Free Radical Biology & Medicine*, vol. 65, pp. 244–253, 2013.
- [68] Y. Ogasawara, Y. Mukai, T. Togawa, T. Suzuki, S. Tanabe, and K. Ishii, "Determination of plasma thiol bound to albumin using affinity chromatography and high-performance liquid chromatography with fluorescence detection: ratio of cysteinyl albumin as a possible biomarker of oxidative stress," *Journal of Chromatography B, Analytical Technologies in the Biomedical and Life Sciences*, vol. 845, no. 1, pp. 157–163, 2007.
- [69] J. S. Stamler, O. Jaraki, J. Osborne et al., "Nitric oxide circulates in mammalian plasma primarily as an S-nitroso adduct of serum albumin," *Proceedings of the National Academy of Sciences of the United States of America*, vol. 89, no. 16, pp. 7674–7677, 1992.
- [70] J. Bonanata, L. Turell, L. Antmann et al., "The thiol of human serum albumin: acidity, microenvironment and mechanistic insights on its oxidation to sulfenic acid," *Free Radical Biology & Medicine*, vol. 108, pp. 952–962, 2017.
- [71] M. Mol, L. Regazzoni, A. Altomare et al., "Enzymatic and non-enzymatic detoxification of 4-hydroxynonenal: methodological aspects and biological consequences," *Free Radical Biology & Medicine*, vol. 111, pp. 328–344, 2017.
- [72] S. Sengupta, H. Chen, T. Togawa et al., "Albumin thiolate anion is an intermediate in the formation of albumin-S-S-homocysteine," *The Journal of Biological Chemistry*, vol. 276, no. 32, pp. 30111–30117, 2001.
- [73] A. Zinellu, S. Sotgia, B. Scanu et al., "S-homocysteinylated LDL apolipoprotein B adversely affects human endothelial cells in vitro," *Atherosclerosis*, vol. 206, no. 1, pp. 40–46, 2009.
- [74] A. Zinellu, A. Lepedda Jr., S. Sotgia et al., "Albumin-bound low molecular weight thiols analysis in plasma and carotid plaques by CE," *Journal of Separation Science*, vol. 33, no. 1, pp. 126–131, 2010.
- [75] A. J. Lepedda, A. Zinellu, G. Nieddu et al., "Human Serum Albumin Cys³⁴ Oxidative Modifications following Infiltration in the Carotid Atherosclerotic Plaque," *Oxidative Medicine and Cellular Longevity*, vol. 2014, Article ID 690953, 7 pages, 2014.
- [76] A. Zinellu, S. Sotgia, A. A. Mangoni et al., "Spontaneous release of human serum albumin S-bound homocysteine in a thiol-free physiological medium," *International Journal of Peptide Research and Therapeutics*, vol. 25, no. 1, pp. 187–194, 2019.

Research Article

Products of Sulfide/Selenite Interaction Possess Antioxidant Properties, Scavenge Superoxide-Derived Radicals, React with DNA, and Modulate Blood Pressure and Tension of Isolated Thoracic Aorta

Marian Grman,¹ Anton Misak,¹ Lucia Kurakova,² Vlasta Brezova,³ Sona Cacanyiova ⁴,
Andrea Berenyiova,⁴ Peter Balis ⁴, Lenka Tomasova,¹ Ammar Kharma,¹
Enrique Domínguez-Álvarez,⁵ Miroslav Chovanec ⁶, and Karol Ondrias ¹

¹Institute of Clinical and Translational Research, Biomedical Research Center, Slovak Academy of Sciences, Dubravská cesta 9, 845 05 Bratislava, Slovakia

²Department of Pharmacology and Toxicology, Faculty of Pharmacy, Comenius University, Odbojarov 10, 832 32 Bratislava, Slovakia

³Faculty of Chemical and Food Technology, Slovak University of Technology, Radlinského 9, 812 37 Bratislava, Slovakia

⁴Institute of Normal and Pathological Physiology, Centre of Experimental Medicine, Slovak Academy of Sciences, Dubravská cesta 9, 841 04 Bratislava, Slovakia

⁵Instituto de Química Orgánica General, Consejo Superior de Investigaciones Científicas (IQOG-CSIC), 28006 Madrid, Spain

⁶Cancer Research Institute, Biomedical Research Center, Slovak Academy of Sciences, Dubravská cesta 9, 845 05 Bratislava, Slovakia

Correspondence should be addressed to Miroslav Chovanec; miroslav.chovanec@savba.sk
and Karol Ondrias; karol.ondrias@savba.sk

Received 27 June 2019; Accepted 12 September 2019; Published 25 November 2019

Guest Editor: Kyoung Soo Kim

Copyright © 2019 Marian Grman et al. This is an open access article distributed under the Creative Commons Attribution License, which permits unrestricted use, distribution, and reproduction in any medium, provided the original work is properly cited.

Selenium (Se), an essential trace element, and hydrogen sulfide (H₂S), an endogenously produced signalling molecule, affect many physiological and pathological processes. However, the biological effects of their mutual interaction have not yet been investigated. Herein, we have studied the biological and antioxidant effects of the products of the H₂S (Na₂S)/selenite (Na₂SeO₃) interaction. As detected by the UV-VIS and EPR spectroscopy, the product(s) of the H₂S-Na₂SeO₃ and H₂S-SeCl₄ interaction scavenged superoxide-derived radicals and reduced [•]cPTIO radical depending on the molar ratio and the preincubation time of the applied interaction mixture. The results confirmed that the transient species are formed rapidly during the interaction and exhibit a noteworthy biological activity. In contrast to H₂S or selenite acting on their own, the H₂S/selenite mixture cleaved DNA in a bell-shaped manner. Interestingly, selenite protected DNA from the cleavage induced by the products of H₂S/H₂O₂ interaction. The relaxation effect of H₂S on isolated thoracic aorta was eliminated when the H₂S/selenite mixture was applied. The mixture inhibited the H₂S biphasic effect on rat systolic and pulse blood pressure. The results point to the antioxidant properties of products of the H₂S/selenite interaction and their effect to react with DNA and influence cardiovascular homeostasis. The effects of the products may contribute to explain some of the biological effects of H₂S and/or selenite, and they may imply that a suitable H₂S/selenite supplement might have a beneficial effect in pathological conditions arisen, e.g., from oxidative stress.

1. Introduction

Exogenously added and endogenously produced H₂S affects many physiological and pathological processes [1–3]. Accumulating evidence supports the involvement of H₂S in the regulation of cardiovascular homeostasis [4]. It has mostly beneficial effects during oxidative stress by reacting with reactive oxygen and nitrogen species, i.e., hydrogen peroxide (H₂O₂), superoxide anion radical (O₂^{•-}), hypochlorite (HOCl), or peroxyxynitrite (ONOO⁻) [5–8]. However, several effects of H₂S on cells are toxic [9–11].

Selenium (Se) is a relatively rare but an essential trace element for humans, plants, and microorganisms. Se, which exerts multiple and complex effects on human health, is known as an antioxidant due to its presence in 25 selenoproteins in the form of selenocysteine amino acid. Both beneficial and detrimental effects of Se deficiency and/or supplementation are well known. The biological effects of Se compounds (selenite, selenate, selenocysteine, and selenomethionine) on cardiac oxidative damage, heart disease, cancer prevention, immunity, diabetes, neuroregeneration, or dementia have been reported [12–17]. However, the beneficial effect of Se supplementation for men's health is still a controversial issue [18–23]. Selenite, which is a common Se supplement, is considered as a promising anticarcinogen [24–26]. It can induce apoptosis in cancer cells through the production of reactive oxygen species (ROS) leading to oxidative stress [27, 28]. However, Se compounds were also found to damage DNA in healthy cells [29] and therefore may not be considered as a suitable protective agent against cancer and/or other chronic diseases. Actually, they can cause or advance some kinds of cancers [30, 31]. The exact mechanisms of the beneficial and toxic effects of Se are not yet fully understood, giving rise to further uncertainty about its potential use in nutrition supplements and/or clinical treatment.

Se and H₂S are present in living organisms, and each one has beneficial and/or toxic effects through its interaction mostly with ROS [1, 2, 30–33]. However, the biological effects of products of the H₂S/selenite interaction are not yet known, namely, their involvement in the production and/or inhibition of ROS, reaction with DNA, or influence on cardiovascular system. Therefore, we have studied the effects of products of the H₂S/selenite interaction on O₂^{•-} and [•]cPTIO radicals, DNA cleavage, tension of isolated aortic rings, and rat blood pressure (BP). We found that the products have significant biological effects that differ from those caused by H₂S or by selenite on their own. These results may contribute to the understanding of possible coupled biological effects of H₂S and Se.

2. Material and Methods

2.1. Chemicals

2.1.1. Selenium Compounds. Stock solutions of sodium selenite (Na₂SeO₃, 10 or 40 mmol L⁻¹, Merck K34993707-542 or Sigma 214485), selenium tetrachloride (SeCl₄, 10 mmol L⁻¹, Aldrich 323527), and sodium selenate (Na₂SeO₄,

10 mmol L⁻¹, Sigma S0882) were prepared freshly in deionized H₂O, stored at 23°C, and used within 5 h. Na₂SeO₃ dissociates in solution to yield mostly H₂SeO₃ at acidic pH, HSeO₃⁻ at neutral pH, and SeO₃²⁻ at alkaline pH. For simplicity, the term SeO₃²⁻ is employed as representative expression to encompass the total mixture of these different (de)protonation states.

2.1.2. Hydrogen Peroxide. Hydrogen peroxide (H₂O₂) (14.7 mol L⁻¹; Sigma-Aldrich 85321), according to a particular experiment, was diluted in H₂O or in 100 mmol L⁻¹ sodium phosphate buffer, supplemented with 200 or 50 μmol L⁻¹ DTPA, pH 7.4, 37°C before application.

2.1.3. Radicals. 5-*tert*-butoxycarbonyl-5-methyl-1-pyrroline-*N*-oxide (BMPO, 100 mmol L⁻¹, Dojindo B568-10, Japan) was dissolved in deionized H₂O, stored at -80°C, and used after thawing. 2-(4-Carboxyphenyl)-4,4,5,5-tetramethylimidazole-1-oxyl-3-oxide ([•]cPTIO, 10 mmol L⁻¹, Cayman 81540 or Sigma C221) was dissolved in deionized H₂O and was stored at -20°C for several weeks.

2.1.4. Sulfide. Na₂S (100 mmol L⁻¹ stock solution, Dojindo SB01, Japan) was dissolved in argon degassed deionized H₂O, stored at -80°C, and used immediately after thawing. Na₂S dissociates in aqueous solution and reacts with H⁺ to yield H₂S, HS⁻, and a trace of S²⁻. We use the term H₂S to describe the total mixture of H₂S, HS⁻, and S²⁻ forms. The stock concentration was checked by UV-VIS spectroscopy: by the absorbance of 1000x diluted stock solution at 230 nm ($\epsilon_{230\text{nm}} = 7700 \text{ mol}^{-1} \text{ L cm}^{-1}$, diluted by deionized water) and also by the reduction of 100 μmol L⁻¹ DTNB by 2000x diluted stock solution (1 H₂S molecule generates 2 TNB⁻ equivalents, $\epsilon_{412\text{nm}} = 14,100 \text{ mol}^{-1} \text{ L cm}^{-1}$, measured in 1 mmol L⁻¹ phosphate buffer), according to Nagy et al. [34].

2.1.5. Buffers. 100 mmol L⁻¹ sodium phosphate buffer supplemented with 100 μmol L⁻¹ diethylenetriaminepentaacetic acid (DTPA), pH 6.5, 7.0, 7.4, 8.0, and 9.0, 37°C, was employed for UV-VIS experiments. 50 and 25 mmol L⁻¹ sodium phosphate buffer, supplemented with 100 and 50 μmol L⁻¹ DTPA, pH 7.4, 37°C, was used for electron paramagnetic resonance (EPR) and plasmid DNA (pDNA) cleavage studies, respectively.

2.2. UV-VIS of [•]cPTIO. To obtain 1 mL of the working solution, 10 or 100 μL of stock solution of the compounds studied was added to the appropriate volume (990 or 900 μL, respectively) of 100 mmol L⁻¹ sodium phosphate buffer (at given pH, 37°C) containing the final concentrations of 100 μmol L⁻¹ [•]cPTIO and 100 μmol L⁻¹ DTPA. UV-VIS absorption spectra (900–190 nm) were recorded every 30 s for 20 to 40 min with a Shimadzu 1800 (Kyoto, Japan) spectrometer at 37°C. The [•]cPTIO extinction coefficient of 920 mol⁻¹ L cm⁻¹ at 560 nm was used. The reduction of the [•]cPTIO radical was determined as the decrease of the absorbance at 560 nm (absorption maximum of [•]cPTIO in VIS range) or at 358 nm after subtracting the absorbances at 730 or at 420 nm, respectively [5, 35].

To study the involvement of O_2 in the H_2S/SeO_3^{2-} -induced reduction of the $\cdot cPTIO$ radical, 10 mmolL^{-1} Na_2S in H_2O , 10 mmolL^{-1} Na_2SeO_3 in H_2O , and $102\ \mu\text{molL}^{-1}$ $\cdot cPTIO$ in the 100 mmolL^{-1} sodium phosphate buffer, supplemented with $100\ \mu\text{molL}^{-1}$ DTPA (pH 7.4; 37°C), were deaerated with argon for 10 min at 37°C . The compounds were mixed in a closed UV-cuvette, and the UV-VIS spectra were recorded. The O_2 concentration in the deaerated samples was 3-5%, confirmed with an oxygen electrode (OXELP, SYS-ISO2, WPI, USA). In all UV-VIS experiments, H_2O was used as a blank.

2.3. EPR of the $\cdot BMPO$ Adducts. To study the ability of H_2S/SeO_3^{2-} to scavenge the $O_2^{\cdot -}$ radical or its derivatives produced in DMSO/ KO_2 solution, sample preparation and EPR measurements were conducted in accordance with previously reported protocols [5]. The solution (final concentrations) of $\cdot BMPO$ (20 mmolL^{-1}), DTPA ($100\ \mu\text{molL}^{-1}$) in sodium phosphate buffer (50 mmolL^{-1} , pH 7.4) was incubated for 1 min at 37°C ; an aliquot of the compound was added, followed by saturated KO_2 /DMSO solution (10% v/v DMSO/final buffer) 3 s later. The sample was mixed for 5 s and transferred to a standard cavity aqueous EPR flat cell. The first EPR spectrum was recorded 2 min after the addition of KO_2 /DMSO solution at 37°C . The sets of individual EPR spectra of the $\cdot BMPO$ spin adducts were recorded as 15 sequential scans, each 42 s, with a total time of 11 min. Each experiment was repeated at least twice. EPR spectra of the $\cdot BMPO$ spin adducts were measured on a Bruker EMX spectrometer, X-band $\sim 9.4\text{ GHz}$, 335.15 mT central field, 8 mT scan range, 20 mW microwave power, 0.1 or 0.15 mT modulation amplitude, 42 s sweep time, 20.48 ms time constant, and 20.48 ms conversion time at 37°C . Intensities of the $\cdot BMPO$ adducts in the EPR spectra were reproducible, when the KO_2 /DMSO stock solution was stored at 5°C for 1 day or at $23 \pm 1^\circ\text{C}$ for 4 h.

2.4. Plasmid DNA Cleavage. pDNA cleavage assay with the use of pBR322 plasmid (New England BioLabs Inc., N3033L) was performed as reported previously [5, 36]. In this assay, all samples contained $0.2\ \mu\text{g}$ pDNA in sodium phosphate buffer (25 mmolL^{-1} sodium phosphate, $50\ \mu\text{molL}^{-1}$ DTPA, pH 7.4, 37°C). After addition of compounds, the resulting mixtures were incubated for 30 min at 37°C . All concentrations listed in the section were final in the samples. After incubation, the reaction mixtures were subjected to 0.6% agarose gel electrophoresis. Samples were electrophoresed in TBE buffer (89 mmolL^{-1} Tris, 89 mmolL^{-1} boric acid, and 2 mmolL^{-1} EDTA) at 5.5 V cm^{-1} for 2 h; gels were stained with GelRed™ Nucleic Acid Gel Stain and photographed using a UV transilluminator. Integrated densities of all pBR322 forms in each lane were quantified using the TotalLab TL100 image analysis software to estimate pDNA cleavage efficiency (Nonlinear Dynamic Ltd., USA).

2.5. Guide for the Use and Care of Laboratory Animals

2.5.1. Isolated Thoracic Aorta. Procedures were performed in accordance with the Institutional Guidelines of the Eth-

ical Committee on the Ethics of Procedures in Animal, Clinical and other Biomedical Experiments (permit number: EC/CEM/2017/4) of the Institute of Normal and Pathological Physiology, Centre of Experimental Medicine and were approved by the State Veterinary and Food Administration of the Slovak Republic and by an Ethical Committee according to the European Convention for the Protection of Vertebrate Animals used for Experimental and other Scientific Purposes, Directive 2010/63/EU of the European Parliament. The Institute of Normal and Pathological Physiology provided veterinary care.

2.5.2. Rat Blood Pressure. All procedures were approved by the State Veterinary and Food Administration of the Slovak Republic (No.: Ro-1545/15-221) according to the guidelines from Directive 2010/63/EU of the European Parliament. Experiments were carried out according to the guidelines laid down by the animal welfare committee of the Institute of Normal and Pathological Physiology of the Slovak Academy of Sciences and conformed to the principles and regulations, as described in the editorial by Grundy [37].

2.6. Functional Study of Isolated Thoracic Aorta. Normotensive Wistar Kyoto (WKY) rats ($307 \pm 4.3\text{ g}$) were killed by decapitation after a brief anesthetization with CO_2 , and the thoracic aorta was isolated as described in our previous study [38]. The changes in isometric tension were measured by the electromechanical transducers (FSG-01, MDE, Budapest, Hungary). The resting tension of 1 g was applied to each ring and maintained throughout a 45 to 60 min of equilibration period until stress relaxation no longer occurred. Changes in thoracic aorta tension were followed by noradrenaline (NA; $1\ \mu\text{molL}^{-1}$) precontracted arterial rings after a stable plateau was achieved.

2.7. Functional Study of Rat Blood Pressure. Male Wistar rats ($n = 10$; $350 \pm 40\text{ g}$) were from the Department of Toxicology and Laboratory Animal Breeding at Dobra Voda, Slovak Academy of Sciences, Slovakia. The rats were housed under a 12 h light-12 h dark cycle, at a constant humidity (45-65%) and temperature ($20\text{-}22^\circ\text{C}$), with free access to standard laboratory rat chow and drinking water. The *Institute of Experimental Pharmacology and Toxicology*, Centre of Experimental Medicine, Slovak Academy of Sciences, provided veterinary care. The tranquilizer xylazine (Rometar) was purchased from Zentiva (Czech Republic), and the anesthetic combination of tiletamine+zolazepam (Zoletil 100) was acquired from Virbac (France). All other chemicals were purchased from Sigma-Aldrich. Experiments were carried out as previously described [39]. Rats were anesthetized with Zoletil 100 (tiletamine+zolazepam, 80 mg kg^{-1} , i.p.) and Rometar (xylazine, 5 mg kg^{-1} , i.p.). During the anesthesia, BP, heart rate, and reflex responses to mechanical stimuli were monitored. The animals were under anesthesia during the whole experiment and were euthanized with an overdose of Zoletil *via* jugular vein at the end of the surgical procedure. All experiments were supervised and performed under the same experimental conditions.

2.8. Blood Pressure Measurement. The right jugular vein was cannulated to administer compounds under anesthesia as described above. The left arteria carotis communis was cannulated for inserting the fiber optic microcatheter pressure transducers (FISO LS 2F Harvard Apparatus, USA). The analog signal was digitalized at 10 kHz, filtered at 1 kHz, and recorded by DEWEsoft 6.6.7 (GmbH, Austria). The signal was evaluated 5 s before and 10 min after compound administration. After stabilization of BP (10–20 min), the compounds were administered into the right jugular vein as a bolus of 500 $\mu\text{L kg}^{-1}$ over 15 s period. The solution of the $\text{H}_2\text{S}/\text{SeO}_3^{2-}$ mixture (10/5 in mmol L^{-1}) was prepared as follows: to 123.5 μL of 100 mmol L^{-1} phosphate buffer, 100 $\mu\text{mol L}^{-1}$ DTPA, 14 μL of 1 mol L^{-1} HCl was added, followed by 62.5 μL of 40 mmol L^{-1} Na_2SeO_3 in 0.9% NaCl, and finally 50 μL of 100 mmol L^{-1} Na_2S in H_2O was added. The pH of the buffered mixture was 7.4. The mixture was incubated for 40 ± 10 s at 23°C before i.v. administration. Unbuffered $\text{H}_2\text{S}/\text{SeO}_3^{2-}$ mixture (10/5 in mmol L^{-1}) was prepared, when 0.9% NaCl was used instead of phosphate buffer and HCl. The pH of the unbuffered mixture was ~ 11 measured by a pH paper indicator.

2.9. Statistical Analysis. Unless otherwise stated, data are represented as the means \pm S.E.M. Statistical significance was determined by Student's *t*-test or one-way ANOVA followed by the multiple comparison test. Differences between means were considered significant at $*P \leq 0.05$. Data analysis and plot construction were carried out using SigmaPlot 12 (Systat Software GmbH).

3. Results

3.1. H_2S Interacts with Na_2SeO_3 and SeCl_4 , but Not with Na_2SeO_4 , to Form Initial Reactive Intermediate(s), which Reduce the $\cdot\text{cPTIO}$ Radical. Since the antioxidant properties of $\text{H}_2\text{S}/\text{SeO}_3^{2-}$ products are unknown, we have used the $\cdot\text{cPTIO}$ radical to study the reducing properties of the products of $\text{H}_2\text{S}/\text{SeO}_3^{2-}$ interaction. The $\cdot\text{cPTIO}$ radical is stable in aqueous solution, and its formation and reduction can be monitored by the UV-VIS spectrophotometry at 358 or 560 nm. Even in the presence of up to 100 $\mu\text{mol L}^{-1}$ H_2S or 100–400 $\mu\text{mol L}^{-1}$ SeO_3^{2-} , the absorbance (ABS) of the radical at 358 and 560 nm decreases only by $<7\%$ after 40 min, indicating that neither H_2S nor SeO_3^{2-} on its own reduces this radical (Figure 1). In contrast, once H_2S (25–100 $\mu\text{mol L}^{-1}$) was added to the $\cdot\text{cPTIO}/\text{SeO}_3^{2-}$ (100/2.5–400 $\mu\text{mol L}^{-1}$) mixture, or SeO_3^{2-} was added to $\cdot\text{cPTIO}/\text{H}_2\text{S}$, the absorbances at 358 and 560 nm decreased rapidly over the time (≤ 30 s), indicating a possible formation of strong reducing agent(s) which fastly and efficiently reduced the $\cdot\text{cPTIO}$ radical (Figures 1 and 2). Similar results were obtained when SeCl_4 , but not Na_2SeO_4 , was used instead of SeO_3^{2-} (Figures S1 and S2a).

The reduction of $\cdot\text{cPTIO}$ followed a bell-shaped dependence on the concentration of SeO_3^{2-} at a constant $\cdot\text{cPTIO}/\text{H}_2\text{S}$ concentration (Figure 2(a)), with a maximum radical scavenging activity at an $\text{H}_2\text{S}:\text{SeO}_3^{2-}$ ratio of roughly 4:1. The ability of H_2S to reduce $\cdot\text{cPTIO}$ in the presence of

SeO_3^{2-} increased with the increasing H_2S concentration (Figure 2(b)) and followed also a bell-shaped dependence on pH (Figures 3 and S3).

If H_2S and SeO_3^{2-} were preincubated for different periods of time before the addition to $\cdot\text{cPTIO}$, it clearly resulted in the highest radical scavenging activity, which was subsequently lost over the time (Figure 4). An $\text{H}_2\text{S}/\text{SeO}_3^{2-}$ (100/100 in $\mu\text{mol L}^{-1}$) mixture preincubated for ≥ 1 min prior to $\cdot\text{cPTIO}$ addition did not reduce $\cdot\text{cPTIO}$, demonstrating that later products of the reaction of sulfide with SeO_3^{2-} could not be responsible for the reduction of the radical and that the relevant active species were formed swiftly, in less than 1 min and have a short lifetime, as recently suggested [40]. Notably, formation of these active early intermediates to reduce $\cdot\text{cPTIO}$ was prolonged with the increase of the $\text{H}_2\text{S}/\text{SeO}_3^{2-}$ ratio (Figure 4(e)). At $\text{H}_2\text{S}/\text{SeO}_3^{2-}$ concentration of 100/25 in $\mu\text{mol L}^{-1}$ and 5 min preincubation time, the mixture still possessed around 50% potency to reduce $\cdot\text{cPTIO}$ (Figure 4(e)). This timing, once more, accounts for a rapidly formed selenosulfide intermediate as being the ultimate responsible for this radical scavenging activity, a species also possibly being sensitive to oxidation over prolonged time periods (Figure 4).

While the available evidence is in accordance with the formation of HSSeSH as the main reactive species, there are other chalcogen-based candidates which are good reducing agents, namely, hydrogen selenide (H_2Se), hydroselenide anion (HSe^-), selenide (Se^{2-}), persulfides, and polysulfides (S_x^{2-}) [41–43]. Interestingly, O_2 does not seem to play a major role in the $\text{H}_2\text{S}/\text{SeO}_3^{2-}$ -induced reduction of the $\cdot\text{cPTIO}$ radical probably due to slower kinetics of interaction of reactants and/or intermediates with O_2 in comparison to the rate of $\cdot\text{cPTIO}$ reduction [44–48]. Under argon flushed conditions, reduction of the $\cdot\text{cPTIO}$ radical was neither enhanced nor suppressed significantly, hence ruling out any major involvement of H_2Se , as this selenium compound is highly sensitive to O_2 (Figure S2b).

3.2. EPR of $\cdot\text{BMPO-OOH}$: The Initial Products of the $\text{H}_2\text{S}/\text{SeO}_3^{2-}$ Interaction Also Scavenge Derivatives of Superoxide Anion ($\text{O}_2^{\cdot-}$) Radical. We aimed to ascertain whether the initial products of the $\text{H}_2\text{S}/\text{SeO}_3^{2-}$ interaction are able to scavenge other radicals, i.e., $\text{O}_2^{\cdot-}$ or its derivatives. The interactions with $\text{O}_2^{\cdot-}$ were studied with the EPR spin trap method based on the reaction of this dioxygen radical with BMPO to form the $\cdot\text{BMPO-OOH}$ adduct [49]. This assay was chosen due to biological and mechanistical reason; $\text{O}_2^{\cdot-}$ is a simple radical reduced by one-electron transfer.

$\text{O}_2^{\cdot-}$ was dissolved in phosphate buffer (pH 7.4, 37°C) and trapped by BMPO. Under these conditions, the relative intensity of the $\cdot\text{BMPO-OOH}$ adduct decreased slowly over the time and was comparable to the values reported under physiological conditions (Figures 5(a1)–5(a3)) [49]. The addition of SeO_3^{2-} (25 and 50 $\mu\text{mol L}^{-1}$) did not significantly interfere with the $\cdot\text{BMPO-OOH}$ adduct formation, its concentration, and rate of decay (Figures 5(b1)–5(b3), S4b1–b3). In contrast, H_2S (25 and 50 $\mu\text{mol L}^{-1}$) decreased the $\cdot\text{BMPO-OOH}$ concentration and increased the rate of the decay, and this “antioxidant” activity of H_2S was

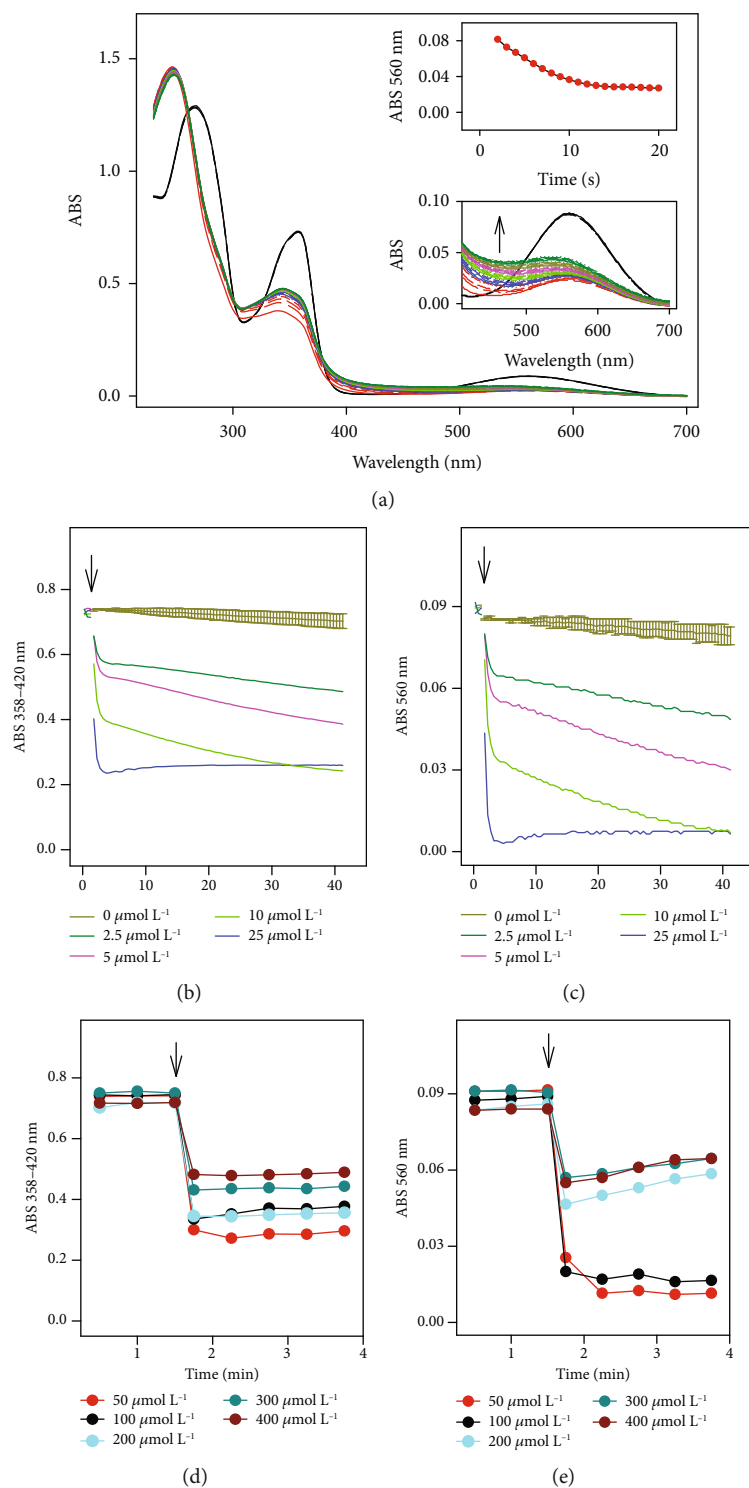


FIGURE 1: Interaction of cPTIO/SeO₃²⁻ with H₂S. (a) Time resolved UV-VIS spectra of the interaction of 100 μmol L⁻¹ cPTIO with 100 μM SeO₃²⁻ (3 times repeated every 30 s, black) and subsequent addition of 100 μmol L⁻¹ H₂S. Spectra were collected every 30 s for 15 min; the first spectrum, indicated by the solid red line, was measured 15 s after addition of H₂S. Top inset: kinetics of changes in absorbance at 560 nm after addition of 100 μmol L⁻¹ H₂S into cPTIO/SeO₃²⁻ (100/100 in μmol L⁻¹) solution at time 0 s. Bottom inset: details of the time resolved spectra of the cPTIO/SeO₃²⁻ (100/100 in μmol L⁻¹) interaction before (black) and after addition of H₂S (100 μmol L⁻¹, the first spectrum is indicated by the solid red line, which is followed each 30 s by: long dash red, medium dash red, short dash red, dotted red, solid blue line, long dash blue, medium dash blue, etc.). (b, c, d, e) H₂S (100 μmol L⁻¹) was added to 100 μmol L⁻¹ solution of cPTIO containing different concentrations of SeO₃²⁻ (0-400 μmol L⁻¹, see legend). The kinetics of the reduction of 100 μmol L⁻¹ cPTIO before and after addition of 100 μmol L⁻¹ H₂S (marked by arrow) was monitored as a decrease of the absorbance at 358 nm minus the absorbance at 420 nm (b, d) and also as a decrease of the absorbance at 560 nm (c, e).

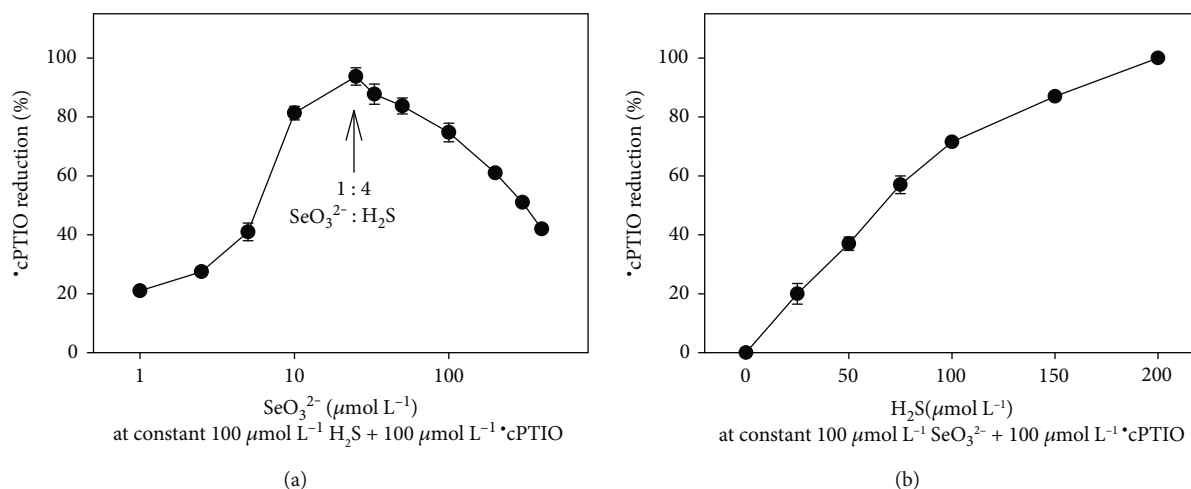


FIGURE 2: Effect of the SeO_3^{2-} and H_2S concentration on the reduction of \cdot cPTIO. (a) Effect of the SeO_3^{2-} concentration (1-400 $\mu\text{mol L}^{-1}$) on the reduction of \cdot cPTIO (100 $\mu\text{mol L}^{-1}$) in the presence of H_2S (100 $\mu\text{mol L}^{-1}$). Arrow indicates the 1 : 4 molar ratio of $\text{SeO}_3^{2-} : \text{H}_2\text{S}$. (b) Effect of the H_2S concentration (0-200 $\mu\text{mol L}^{-1}$) on the reduction of \cdot cPTIO (100 $\mu\text{mol L}^{-1}$) in the presence of SeO_3^{2-} (100 $\mu\text{mol L}^{-1}$). The reduction of \cdot cPTIO was evaluated as the decrease of the absorbance at 560 nm after 2.25 min of the reaction (pH 7.4, 37°C). All values represent the means \pm S.E.M., $n = 2-4$.

increased further in the presence of SeO_3^{2-} (more than three times at a 50/25 in $\mu\text{mol L}^{-1}$ $\text{H}_2\text{S}/\text{SeO}_3^{2-}$ ratio). This indicates that $\text{H}_2\text{S}/\text{SeO}_3^{2-}$ products scavenge $\text{O}_2^{\cdot -}$ and/or its derivatives. The effects of $\text{H}_2\text{S}/\text{SeO}_3^{2-}$ were less pronounced when KO_2/DMSO was added 5 min after addition of $\text{H}_2\text{S}/\text{SeO}_3^{2-}$, suggesting that the reducing intermediate had already decomposed at this stage (Figure 5, S4). Similar results were obtained when H_2S was incubated with SeCl_4 (Figure S5). This indicates that the production of highly active species, products of the $\text{H}_2\text{S}/\text{SeO}_3^{2-}$ interaction, was time-dependent: they appeared within a few seconds after addition of SeO_3^{2-} to the H_2S solution and their effects diminished after few minutes of interaction.

From our previous studies of $\text{O}_2^{\cdot -}$ reaction with BMPO [5], we assumed that the EPR spectra of the BMPO adducts were superposed on the BMPO-OOH/OH radicals with minor contribution from the BMPO-C radical. Therefore, we simulated the spectra using hyperfine coupling constants for BMPO-OOH, BMPO-OH, and BMPO-C (derived from DMSO) radicals. The means of hyperfine coupling constants used were as follows: BMPO-OOH1 (black) $a_N = 13.30 \pm 0.03$ G, $a_H = 11.7 \pm 0.1$ G; BMPO-OOH2 (red) $a_N = 13.24 \pm 0.03$ G, $a_H = 9.4 \pm 0.1$ G; BMPO-OH1 (green) $a_N = 13.7 \pm 0.3$ G, $a_H = 12.3 \pm 0.4$ G; BMPO-OH2 (yellow) $a_N = 13.6 \pm 0.2$ G, $a_H = 15.3 \pm 0.1$ G; and BMPO-C (blue) $a_N = 15.2 \pm 0.1$ G, $a_H = 21.5 \pm 0.1$ G. The constants are similar to those reported by Zhao et al. [49]. The simulation revealed that $\text{O}_2^{\cdot -}$ was trapped in the control and in the presence of SeO_3^{2-} (Figures 5(a) and 5(b)), since the EPR spectra of BMPO-OOH were only observed. However, BMPO-OH component was present in the samples containing H_2S alone or with SeO_3^{2-} (Figures 5(c)–5(h)). The results may indicate that H_2S alone or with SeO_3^{2-} decomposed BMPO-OOH to BMPO-OH and/or \cdot OH was formed as a result of compound presence. Since the first spectrum was recorded 110 ± 15 s after sample preparation, we cannot exclude a possibility of trapping of other radicals with lifetimes shorter than 110 s.

3.3. $\text{H}_2\text{S}/\text{SeO}_3^{2-}$ Cleaves pDNA. It was of interest to know if the products of the $\text{H}_2\text{S}/\text{SeO}_3^{2-}$ interaction have biological effects *in vitro*. Therefore, we investigated the direct effects of H_2S and SeO_3^{2-} on the cleavage of pDNA *in vitro* using the Fenton reaction as a positive benchmark control (Figure 6) [5].

Interestingly, neither H_2S (1 mmol L^{-1}) nor SeO_3^{2-} (0-1 mmol L^{-1}) alone significantly cleaved pDNA. In contrast, SeO_3^{2-} in a concentration-dependent manner caused damage to DNA in the presence of 1 mmol L^{-1} H_2S (Figures 6(a1) and 6(a2)). The observed cleavage of DNA caused by SeO_3^{2-} and H_2S showed a bell-shaped concentration ratio dependence similar to the one observed in the reduction of the \cdot cPTIO radical. We can suggest that the intermediate responsibility of the action can be a selenopolysulfide with a $\text{H}_2\text{S} : \text{SeO}_3^{2-}$ ratio of 4 : 1. In the presence of H_2O_2 , damage to pDNA by H_2S occurs also without SeO_3^{2-} , since H_2O_2 now takes on the role of SeO_3^{2-} as an oxidant, with the simultaneous formation of the \cdot OH radicals (Figures 6(b1) and 6(b2)). Further evidence for the involvement of radicals may come from the fact that dimethylsulfoxide (DMSO), a known \cdot OH scavenger [50, 51] frequently employed as solvent in biology, is able to interfere with the damage to DNA (Figures 6(c1) and 6(c2)).

3.4. $\text{H}_2\text{S}/\text{SeO}_3^{2-}$ Modulates Tension of Isolated Thoracic Aorta. As some of our *in vitro* assays indicated an antioxidant activity of the $\text{H}_2\text{S}/\text{SeO}_3^{2-}$ mixture, and H_2S is known to promote relaxation of blood vessels [52], the impact of the $\text{H}_2\text{S}/\text{SeO}_3^{2-}$ mixture on the isolated thoracic aorta was examined. The thoracic aorta was precontracted by noradrenaline (NA) (1 $\mu\text{mol L}^{-1}$). After a stable plateau of the contraction was reached (Figure 7(a)), SeO_3^{2-} (100 $\mu\text{mol L}^{-1}$) showed only negligible activity, while Na_2S (200 $\mu\text{mol L}^{-1}$) significantly relaxed the aortic rings, in agreement with our previous studies [38]. A simultaneous addition of SeO_3^{2-} (100 $\mu\text{mol L}^{-1}$) and H_2S (200 $\mu\text{mol L}^{-1}$) resulted once more in a biphasic activity profile, where a minor

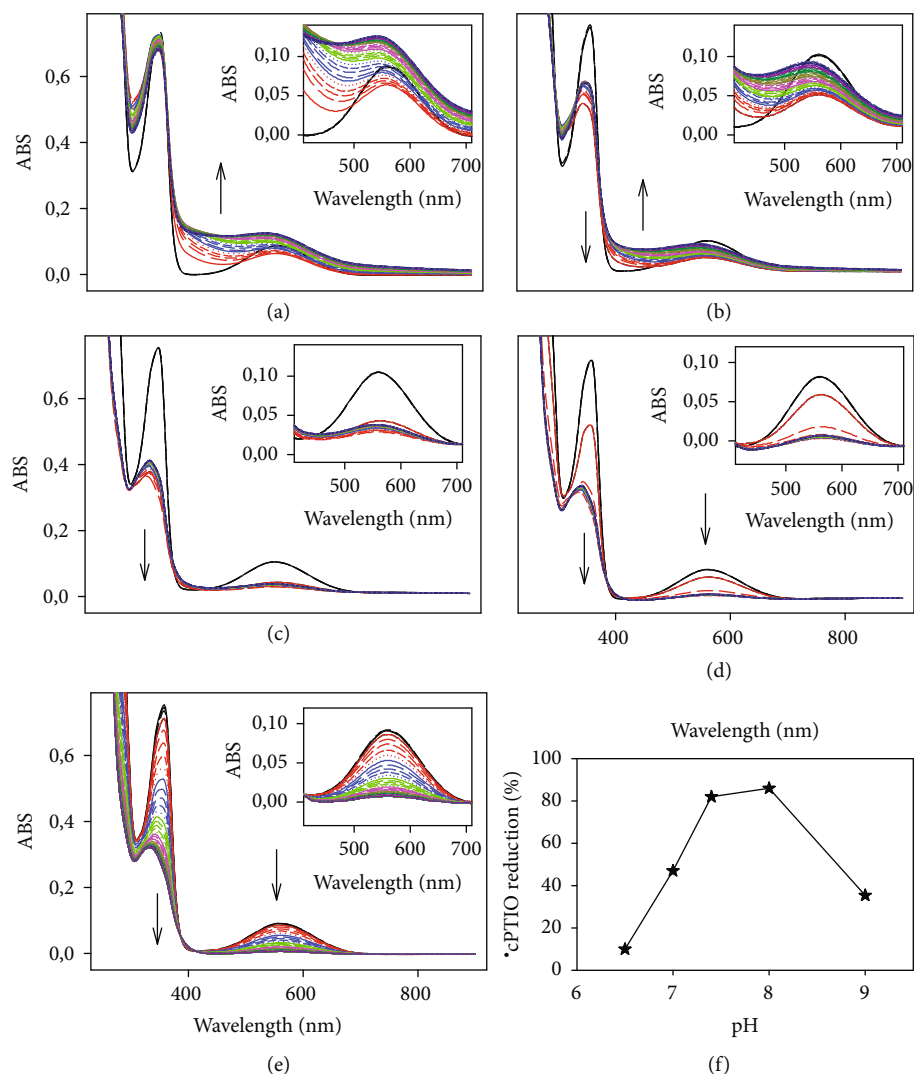


FIGURE 3: Effect of pH on the reduction of cPTIO in the presence of SeO_3^{2-} induced by H_2S . Time resolved UV-VIS spectra of the interaction of H_2S ($100 \mu\text{mol L}^{-1}$ final) with cPTIO/ SeO_3^{2-} ($100/50$ in $\mu\text{mol L}^{-1}$ final) at pH 6.5 (a), 7.0 (b), 7.4 (c), 8.0 (d), and 9.0 (e). The first spectrum was recorded 15 s after H_2S addition (solid red line) followed each 30 s by: long dash red, medium dash red, short dash red, dotted red, solid blue line, long dash blue, medium dash blue, etc. Samples were measured every 30 s for 20 min. The black line represents the spectrum of cPTIO/ SeO_3^{2-} before the H_2S addition. (f) Dependence of cPTIO ($100 \mu\text{mol L}^{-1}$) reduction by $\text{H}_2\text{S}/\text{SeO}_3^{2-}$ ($100/50$ in $\mu\text{mol L}^{-1}$) on pH. Data were taken from the spectra shown in (a), (b), (c), (d), and (e) as a minimum of A_{560} in the range of 0-4 min. The buffers consisted of 100 mmol L^{-1} sodium phosphate, $100 \mu\text{M}$ DTPA, 37°C , and pH values were adjusted to desired pH.

relaxation was noticed first, followed by a pronounced contraction (Figure 7). It is supposed that the contraction effect may result also from the antioxidant properties of the mixture, similarly as it has been reported for ascorbate [53].

3.5. $\text{H}_2\text{S}/\text{SeO}_3^{2-}$ Modulates Rat Systolic and Pulse Blood Pressure. Since the products of the $\text{H}_2\text{S}/\text{SeO}_3^{2-}$ interaction modulated the tension of the thoracic aorta, we subsequently studied whether the products influence blood pressure (BP). Intravenous (i.v.) administration of $5 \mu\text{mol kg}^{-1}$ SeO_3^{2-} had only minor effects on BP (Figure 8(g)). The administration of $10 \mu\text{mol kg}^{-1}$ of Na_2S transiently decreased and increased BP (Figures 8(a) and 8(g)), as observed in our previous study [54]. The stock solution of the $\text{H}_2\text{S}/\text{SeO}_3^{2-}$ mixture

($20/10$ in mmol L^{-1}) prepared in 0.9% NaCl was colorless and had pH ~ 11 . However, when the mixture was prepared in solution with pH 7.4, it had orange color with an absorption maximum at 570 nm (Figure S6), indicating formation of the sulfur-selenium complexes [40]. The i.v. administration of the mixture $\text{H}_2\text{S}/\text{SeO}_3^{2-}$ ($10/5 \mu\text{mol kg}^{-1}$, pH ~ 7.4), in comparison to H_2S alone, inhibited both BP decrease and increase (Figures 8(b) and 8(g)). The effects of the mixture were less pronounced at pH ~ 11 , being the effects at this pH similar to those observed for H_2S alone (Figures 8(c) and 8(g)).

The studied compounds influenced pulse BP, as an important parameter of cardiovascular system reflecting arterial stiffness [55, 56]. The administration of $5 \mu\text{mol kg}^{-1}$

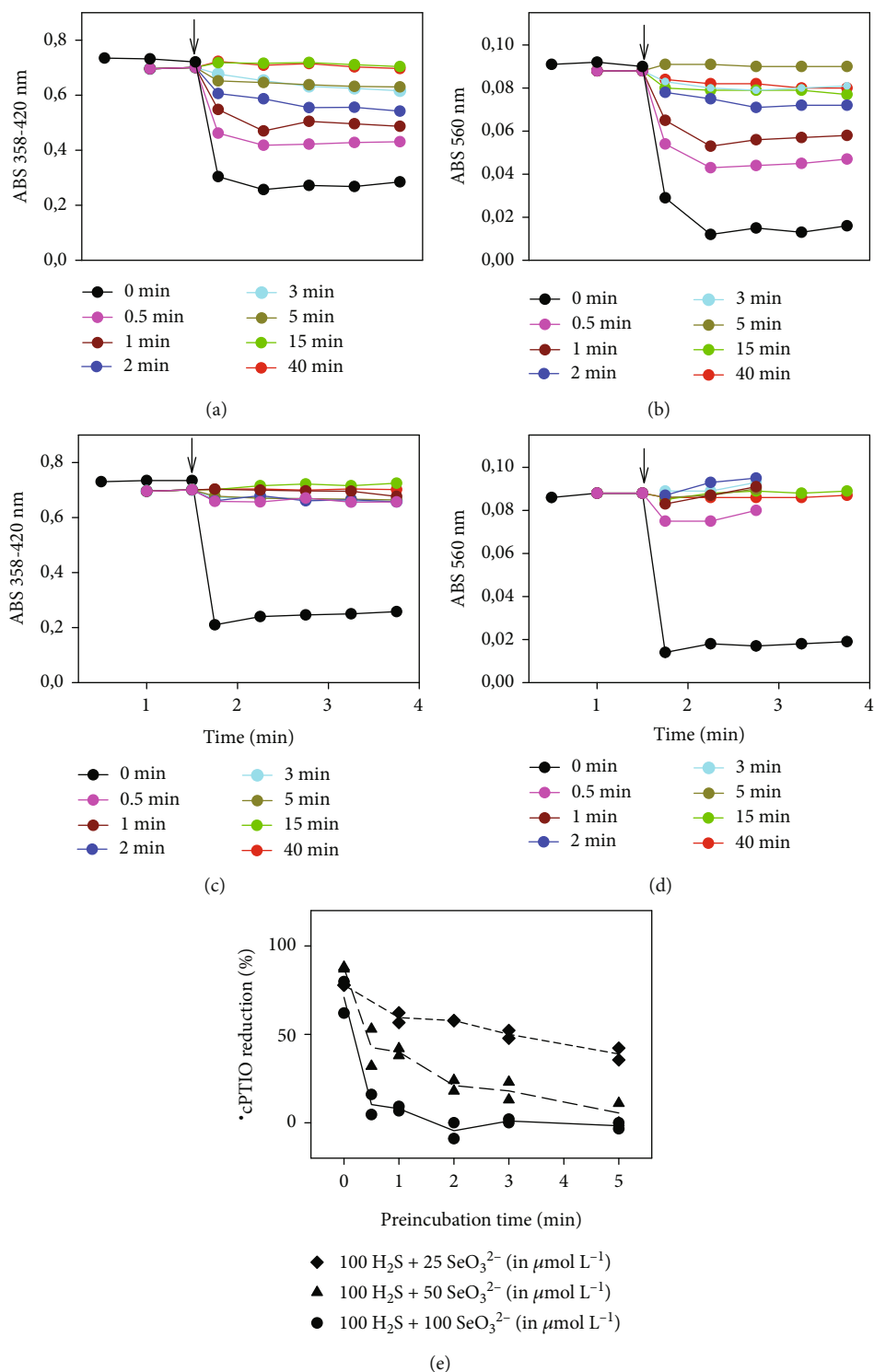


FIGURE 4: Influence of the preincubation time of the $\text{H}_2\text{S}/\text{SeO}_3^{2-}$ mixture on the time-dependent reduction of cPTIO . The reduction of cPTIO ($100 \mu\text{mol L}^{-1}$) once added into the preincubated $\text{H}_2\text{S}/\text{SeO}_3^{2-}$ mixture ($100/50$ in $\mu\text{mol L}^{-1}$, (a, b); $100/100$ in $\mu\text{mol L}^{-1}$ (c, d)) was evaluated as the decrease of absorbance at 358 nm minus 420 nm (a, c) and the decrease of absorbance at 560 nm (b, d), respectively. The preincubation time of the $\text{H}_2\text{S}/\text{SeO}_3^{2-}$ mixture was 0-40 min (see legend). (e) Impact of the preincubation time of the $\text{H}_2\text{S}/\text{SeO}_3^{2-}$ mixture on the reduction of cPTIO . cPTIO ($100 \mu\text{M}$) was added into preincubated $\text{H}_2\text{S}/\text{SeO}_3^{2-}$ (in $\mu\text{mol L}^{-1}$, $100/100$, circles; $100/50$, triangles; $100/25$, diamonds) at pH 7.4, 37°C . Data represent the reduction of cPTIO in 1st minute after addition of cPTIO .

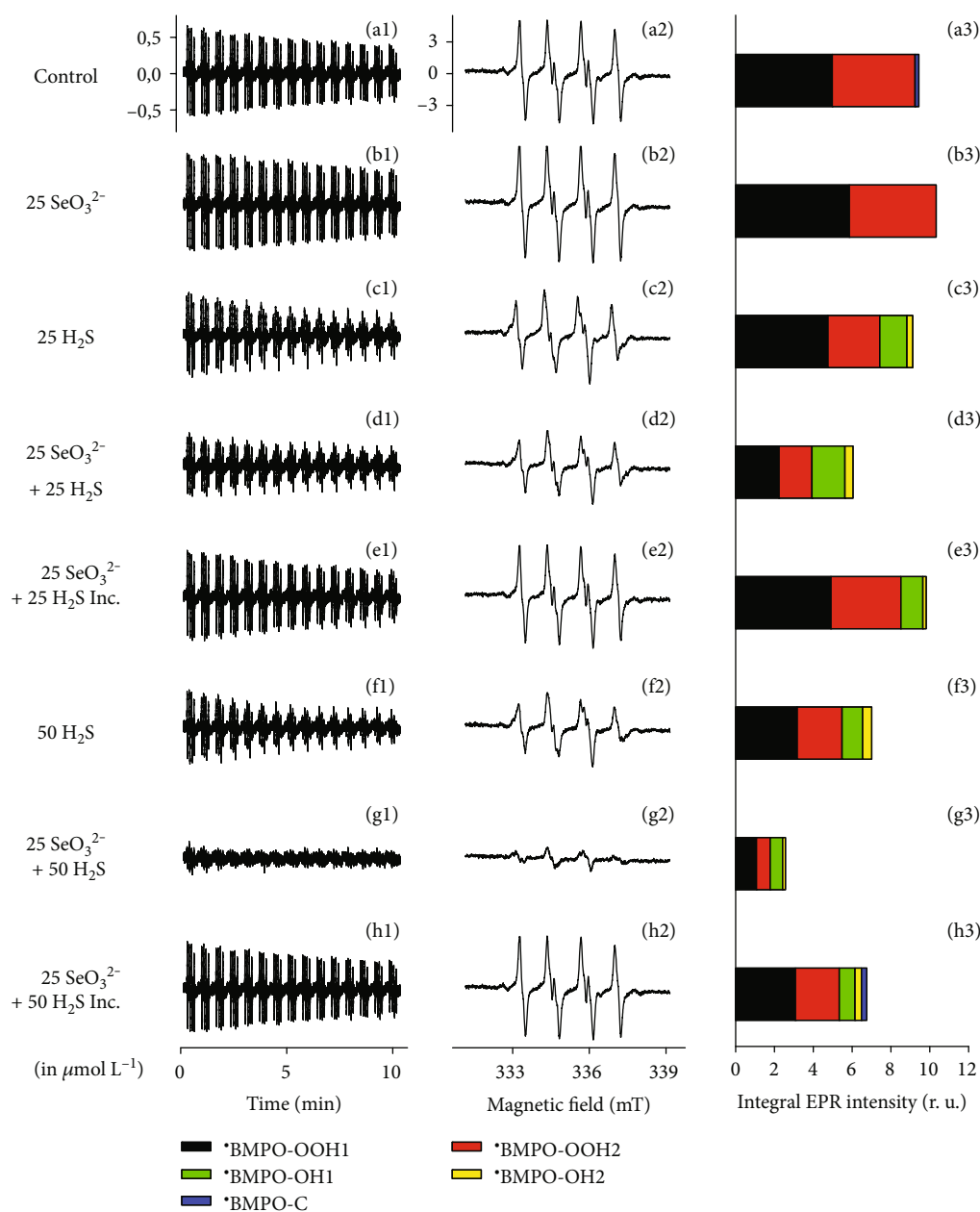


FIGURE 5: EPR spectra of \cdot BMPO in the presence of $O_2^{\cdot -}$ are modulated by H_2S/SeO_3^{2-} . Representative EPR spectra of the \cdot BMPO adducts were monitored in 10% v/v saturated $KO_2/DMSO$ solution in 50 mmol L^{-1} sodium phosphate buffer, 0.1 mmol L^{-1} DTPA, pH 7.4, 37°C in the presence of the various investigated chalcogen species and 20 mmol L^{-1} BMPO. Sets of individual EPR spectra of the \cdot BMPO adducts monitored upon 15 sequential scans, each 42 s (a1-h1), starting acquisition 2 min after sample preparation in: control 10% v/v $KO_2/DMSO$ in the buffer (a1), the $KO_2/DMSO$ in the presence of 25 μ mol L^{-1} SeO_3^{2-} (b1), 25 μ mol L^{-1} H_2S (c1), mixture of 25/25 in μ mol L^{-1} H_2S/SeO_3^{2-} (d1), 25/25 in μ mol L^{-1} H_2S/SeO_3^{2-} preincubated 5 min before $KO_2/DMSO$ stock solution addition (e1), 50 μ mol L^{-1} H_2S (f1), mixture of 50/25 in μ mol L^{-1} H_2S/SeO_3^{2-} (g1), and 50/25 in μ mol L^{-1} H_2S/SeO_3^{2-} preincubated 5 min before addition of $KO_2/DMSO$ stock solution (h1). The spectra (a2-h2) show details of the accumulated first ten spectra of the (a1-h1) sets. The intensities of the time-dependent EPR spectra (a1-h1) and detailed spectra (a2-h2) are comparable; they were measured under identical EPR settings. EPR modulation amplitude 0.15 mT. (a3-h3) Comparison of the integral intensity of individual components of simulated BMPO+ $O_2^{\cdot -}$ without (control) and with chalcogen species shown in (a1-h1). The first five EPR spectra were accumulated and used for simulation. The data represent the means of $n = 2$; standard error was $\leq 10\%$ of the mean value. Simulated relative intensities of the two conformers of the radicals: \cdot BMPO-OOH1 (black), \cdot BMPO-OOH2 (red), \cdot BMPO-OH1 (green), \cdot BMPO-OH2 (yellow), and \cdot BMPO-C (blue).

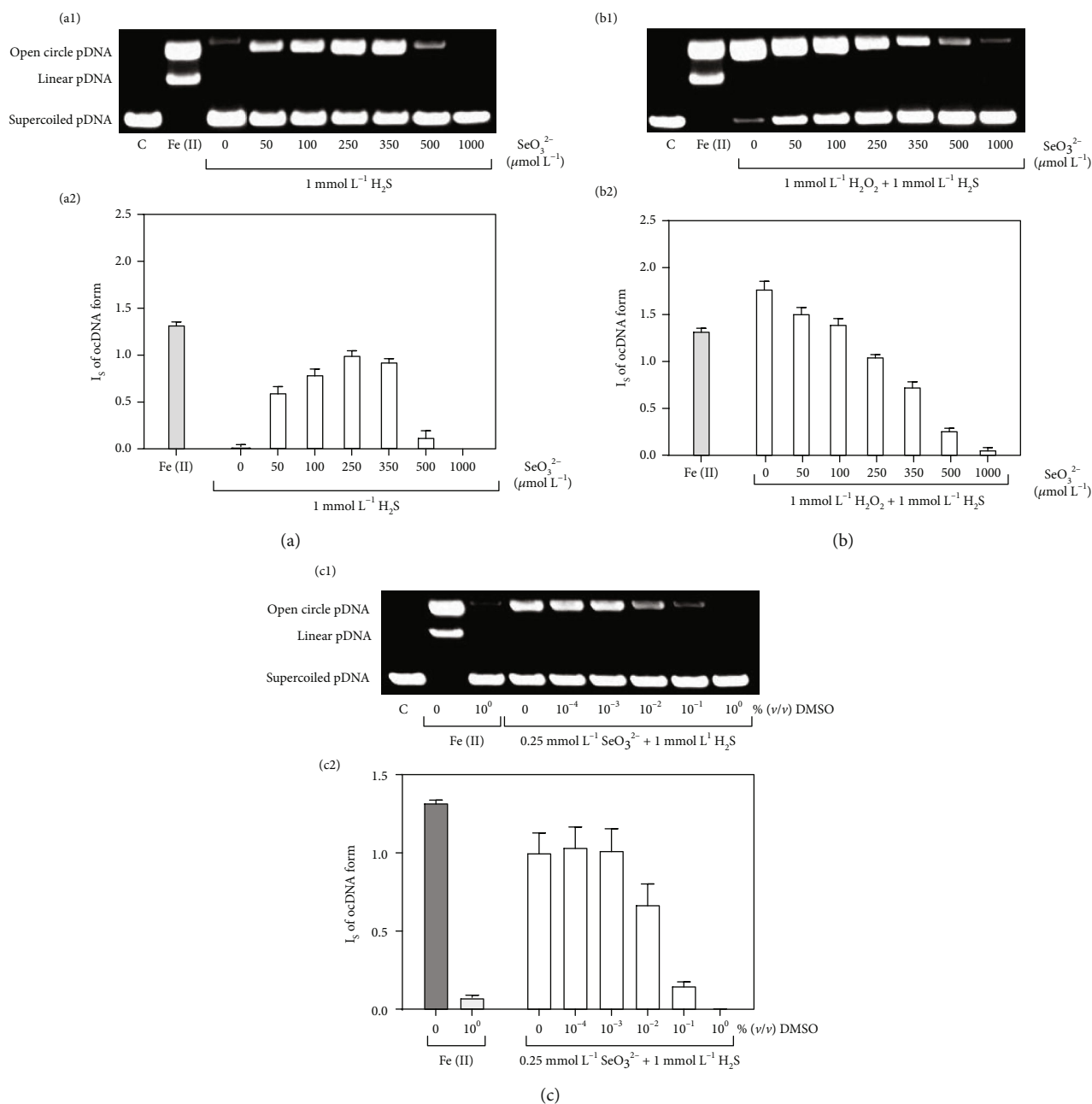


FIGURE 6: The influence of $\text{H}_2\text{S}/\text{SeO}_3^{2-}$ on pDNA cleavage in the absence and presence of H_2O_2 and DMSO. Representative gels (a1, b1) and column graphs (a2, b2) indicating the effects of increasing concentrations of SeO_3^{2-} (0–1 mmol L^{-1}) on pDNA cleavage in the presence of $1 \text{ mmol L}^{-1} \text{H}_2\text{S}$, without (a1, a2) and with $1 \text{ mmol L}^{-1} \text{H}_2\text{O}_2$ (b1, b2). The band at the bottom corresponds to the circular supercoiled form of pDNA, and the less intense band appearing above, in the case of $\text{Fe}^{2+}\text{-H}_2\text{O}_2$, represents the linear form of pDNA. The top band corresponds to the nicked circular form of pDNA. The effects of $150 \mu\text{mol L}^{-1} \text{FeCl}_2 + 1 \text{ mmol L}^{-1} \text{H}_2\text{O}_2$ (full column) are shown for comparison. Values are the means \pm S.E.M., $n = 3$. Representative gels (c1) and column graph (c2) showing the effects of increasing concentrations of DMSO on $\text{H}_2\text{S}/\text{SeO}_3^{2-}$ (0.25/1 in mmol L^{-1})-induced pDNA cleavage. DMSO concentrations: $1 \times 10^{-4}\%$ (v/v) DMSO = $14.1 \mu\text{mol L}^{-1}$ DMSO; $1 \times 10^{-3}\%$ = $141 \mu\text{mol L}^{-1}$; $1 \times 10^{-2}\%$ = 1.41 mmol L^{-1} ; $1 \times 10^{-1}\%$ = 14.1 mmol L^{-1} ; $1 \times 10^0\%$ = 141 mmol L^{-1} . Values represent means \pm S.E.M., $n = 4$.

SeO_3^{2-} intravenously had minor effects on pulse BP (Figure 8(h)). The administration of $10 \mu\text{mol kg}^{-1}$ of Na_2S transiently increased and later decreased pulse BP (Figures 8(d) and 8(h)) [54]. The i.v. administration of the mixture $\text{H}_2\text{S}/\text{SeO}_3^{2-}$ (10/5 in $\mu\text{mol kg}^{-1}$, pH ~ 7.4), with

comparison to H_2S alone, eliminated pulse BP increase, but did not affect pulse BP decrease (Figures 8(e) and 8(h)). The effects of the mixture were less pronounced at pH ~ 11 and were similar to those observed for H_2S alone (Figures 8(f) and 8(h)). The inefficiency of the

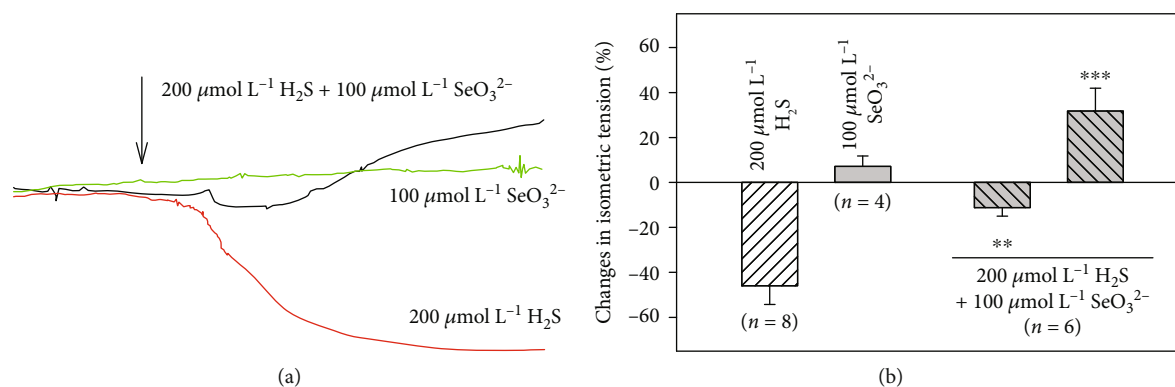


FIGURE 7: Time-dependent tonus of isolated thoracic aorta. The original records of changes in NA ($1 \mu\text{mol L}^{-1}$)-increased arterial tone of isolated rat thoracic aorta after addition of SeO_3^{2-} ($100 \mu\text{mol L}^{-1}$), H_2S ($200 \mu\text{mol L}^{-1}$), and $\text{H}_2\text{S}/\text{SeO}_3^{2-}$ ($200/100$ in $\mu\text{mol L}^{-1}$) mixture. The arrow indicates the compound application (a). The effects of SeO_3^{2-} , H_2S , and $\text{H}_2\text{S}/\text{SeO}_3^{2-}$ on NA ($1 \mu\text{mol L}^{-1}$)-precontracted rings of rat thoracic aorta. The rings were exposed to bolus dose of H_2S ($200 \mu\text{mol L}^{-1}$, relaxation), SeO_3^{2-} ($100 \mu\text{mol L}^{-1}$, nonsignificant contraction), and that of the mixture $\text{H}_2\text{S}/\text{SeO}_3^{2-}$ ($100 \mu\text{mol L}^{-1}$ of SeO_3^{2-} immediately followed by $200 \mu\text{mol L}^{-1}$ H_2S). The $\text{SeO}_3^{2-}/\text{H}_2\text{S}$ mixture had a biphasic activity; firstly, it significantly relaxed the aorta, which was followed by significant contraction (b). Asterisks mark the statistical significance of $\text{H}_2\text{S}/\text{SeO}_3^{2-}$ mixture vs. H_2S (** $P < 0.01$, *** $P < 0.001$).

$\text{H}_2\text{S}/\text{SeO}_3^{2-}$ products at pH ~ 11 may be connected with the minor effect of the mixture on the cPTIO radical reduction at high pH (Figures 3(e) and 3(f)). This may imply that the reduction properties of the mixture could be responsible for their effects on systolic and pulse BP. The results confirm that the products of the $\text{H}_2\text{S}/\text{SeO}_3^{2-}$ interaction depend on pH and influence differently the cardiovascular system. In conclusion, the reactivity and biological activity of the $\text{H}_2\text{S}/\text{SeO}_3^{2-}$ interaction products prepared at pH 7.4 differ from those of Na_2S alone.

4. Discussion and Conclusions

Overall, our studies demonstrate that the two suspected and commonly used “antioxidants,” H_2S and SeO_3^{2-} , are not necessarily typical reducing agents, such as ascorbic acid or tocopherol, when employed on their own. Interestingly, these two chalcogen agents, when added together, rapidly activate each other and form a cascade of considerably more reactive, often reducing species, supposing the involvement of inorganic HSSeSH and polysulfides S_x^{2-} , which may account for some of the observed biological actions. The nature of some of these intermediate reactive sulfur and/or selenium species was suggested in a recently published review [40].

The fast and efficient reduction of the cPTIO radical by $\text{H}_2\text{S}/\text{SeO}_3^{2-}$ products (Figures 1 and 4) supports the notion that the initial intermediate(s) formed by the reaction of H_2S with SeO_3^{2-} are responsible for this kind of action. The bell shape and the maximum radical scavenging activity of $\text{H}_2\text{S}:\text{SeO}_3^{2-}$ at a ratio of $\sim 4:1$ (Figure 2) may indicate the suggested formation of $(\text{HSS})_2\text{Se}$ [40]. The kinetics and efficiency of the $\text{H}_2\text{S}/\text{SeO}_3^{2-}$ products to reduce cPTIO (Figure 3) point out to complex pH-dependent chemical and radical reactions of the species.

Reactions of H_2S or polysulfides with SeO_3^{2-} and/or SeCl_4 were reported [40, 57–59]. They point towards a rapid

conversion of SeO_3^{2-} and SeCl_4 to an intermediate, probably HSSeSH, and a subsequent, slower reductive elimination of this intermediate to elemental (mixed) chalcogen particles and disulfides [40]. However, to our knowledge, there is no information about the formation and detection of HSSeSH in cells or its cytoprotective or other biological effect. The first synthesis of H-S-Se-S-H (1,3-dithiatriselane) was reported by Hahn and Klünsch in 1994, but the stability and reactivity in aqueous solution were not investigated. Solid HSSeSH has a melting point at -40°C . It was one component of a mixture of $\text{H}_2\text{S}_2\text{Se}_n$, prepared by the interaction of 2 H_2S with Se_2Cl_2 [60].

The EPR data (Figure 5) once more confirm that SeO_3^{2-} on its own is not an antioxidant; it becomes activated by reduction, for instance, by H_2S , which concurrently is activated by oxidation. The mutual redox activation is fast, and, as in the case of the cPTIO radical scavenging, the pristine mixture of H_2S and SeO_3^{2-} is most active, with a decrease of activity over the time, pointing once more at simple H_2S_x or $\text{H}_2\text{S}_x\text{Se}$, and notably HSSeSH, but not an S_xSe_y , as being responsible for this kind of activity.

We found that the products of this described $\text{H}_2\text{S}/\text{SeO}_3^{2-}$ interaction have several noteworthy biological effects, involving ROS scavenging, modulation of the redox state, reaction with DNA, tensing isolated aorta, and influencing BP and pulse BP (Figures 6–8). These effects obviously need to be investigated further and in considerably more detail and were not present or were less pronounced when H_2S or selenite acted alone. The properties of the products of the $\text{H}_2\text{S}/\text{SeO}_3^{2-}$ interactions significantly depended on the $\text{H}_2\text{S}/\text{SeO}_3^{2-}$ molar ratio, pH, and preincubation time. The combination of these variables makes the work with $\text{H}_2\text{S}/\text{SeO}_3^{2-}$ very complicated, and these facts should be taken into account at the time of designing *in vitro* and *in vivo* experiments. These properties of the products may explain the previously published beneficial and contrasting toxic Se

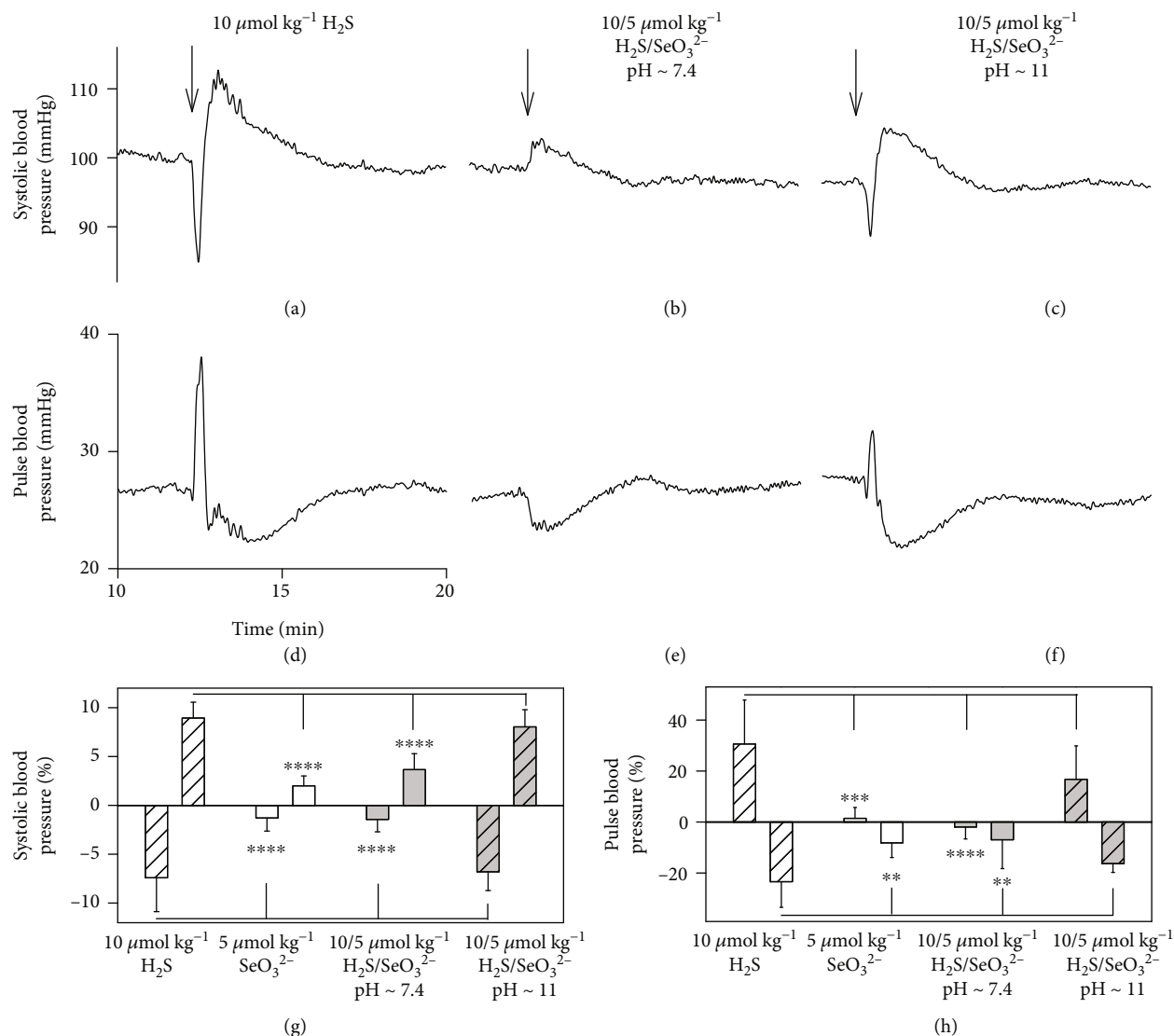


FIGURE 8: The time-dependent effects of SeO_3^{2-} , H_2S , and $\text{H}_2\text{S}/\text{SeO}_3^{2-}$ on rat BP and pulse BP. Representative traces of the time-dependent effect of i.v. bolus administration of H_2S ($10 \mu\text{mol kg}^{-1}$; (a, d)) and its mixture with $5 \mu\text{mol kg}^{-1} \text{SeO}_3^{2-}$ prepared at $\text{pH} \sim 7.4$ (b, e) and $\text{pH} \sim 11$ (c, f) solution on BP (a, b, c) and pulse BP (d, e, f). Transient changes of rat BP (g) and pulse BP (h) after i.v. bolus administration of SeO_3^{2-} ($5 \mu\text{mol kg}^{-1}$, empty column), H_2S ($10 \mu\text{mol kg}^{-1}$, empty coarse column) and their mixture ($\text{SeO}_3^{2-}/\text{H}_2\text{S}$, 5/10 in $\mu\text{mol kg}^{-1}$) prepared at $\text{pH} \sim 7.4$ (grey column) and $\text{pH} \sim 11$ (grey coarse column). Data are presented as means \pm SD; $n = 5-10$. To test a statistical significance between group differences, we used one-way ANOVA followed by Dunnett's test for multiple comparisons. Hence, we also observed the biphasic effect of Na_2S in our previous study [54]; we compared a set of "first part" and "second part" effects of SeO_3^{2-} , $\text{H}_2\text{S}/\text{SeO}_3^{2-}$ at $\text{pH} \sim 7.4$, and $\text{H}_2\text{S}/\text{SeO}_3^{2-}$ at $\text{pH} \sim 11.0$ to the corresponding effect of Na_2S on systolic or pulse blood pressure. Only the mixture of $\text{H}_2\text{S}/\text{SeO}_3^{2-}$ prepared at $\text{pH} \sim 11.0$ was able to generate similar decrease and subsequent increase or *vice versa* in systolic blood pressure or pulse blood pressure as the H_2S , respectively. Asterisks mark the statistical significance as follows: ** $P < 0.01$, *** $P < 0.001$, and **** $P < 0.0001$.

effects, for example, in conditions of oxidative stress and cancer [12–14, 18, 20, 22, 23, 30].

H_2S is endogenously produced *in vivo* in most, if not in all, cells, and H_2S donors are commonly used in biological experiments, and they are considered to be applied in medicine. Our results suggest that in biological experiments with selenite, in its nutrition supplement and clinical use, effects of the $\text{H}_2\text{S}/\text{SeO}_3^{2-}$ interaction should be considered. While SeO_3^{2-} is used widely as a nutritional supplement already,

one may, in the future, wish to spice it up with some reduced sulfur. Natural spices such as garlic and onions contain suitable sulfide releasing agents, such as diallyltrisulfide (DATS) and diallyltetrasulfide (DATTS), which both occur naturally in garlic, or dipropyltrisulfide and dipropyltetrasulfide, both present in onions [61]. Our results imply that application research of suitable $\text{H}_2\text{S}/\text{SeO}_3^{2-}$ supplements may lead to the beneficial effects in pathological conditions arising, e.g., from ROS overproduction.

Abbreviations

ABS:	Absorbance
BMPO:	5- <i>tert</i> -butoxycarbonyl-5-methyl-1-pyrroline- <i>N</i> -oxide
BP:	Blood pressure
¹³ CPTIO:	2-(4-Carboxyphenyl)-4,4,5,5-tetramethylimidazo- line-1-oxyl-3-oxide
DTPA:	Diethylenetriaminepentaacetic acid
EPR:	Electron paramagnetic resonance
H ₂ S:	Hydrogen sulfide
H ₂ O ₂ :	Hydrogen peroxide
i.p.:	Intraperitoneal
i.v.:	Intravenous
NA:	Noradrenaline
pDNA:	Plasmid DNA
SeCl ₄ :	Selenium tetrachloride
SeO ₃ ²⁻ :	Selenite
UV/VIS:	Ultraviolet-visible.

Data Availability

All findings and conclusions are based on the presented figures in the main text or in the supplementary information. Original source files (UV-VIS spectra, EPR spectra, DNA gels, rat blood pressure records, and aorta relaxation records) can be sent from the corresponding author, Dr. Karol Ondrias, upon request.

Conflicts of Interest

The authors declare no conflict of interest.

Authors' Contributions

K.O. and M.C. conceived, initiated, and coordinated the study; K.O., M.C. and V.B. designed research; K.O., M.G., A.M., and A.K. performed UV-VIS experiments and analyzed data; V.B., K.O., M.G., and A.M. performed EPR experiments and analyzed data; M.C. and A.M. performed pDNA cleavage experiments and analyzed data; L.T., A.M, K.O., S.C., A.B., and P.B. performed aorta experiments and analyzed data; L.K., A.M., S.C., A.B., and K.O. performed rat *in vivo* experiments. K.O. wrote the paper; K.O., M.C., V.B., A.K., and E.A-D contributed to analyze data and manuscript writing. Marian Grman and Anton Misak contributed equally to this work. Miroslav Chovanec and Karol Ondrias shared senior authorship.

Acknowledgments

This research was funded by the Slovak Research and Development Agency (grant numbers APVV-15-0371 to A.M., M.G., and K.O.; APVV-17-0384 to M.C.; and APVV-15-0565 to A.M, S.C., A.B., and P.B.), the VEGA Grant Agency of the Slovak Republic (grant numbers 2/0079/19 to M.G.; 1/0026/18 to V.B.; 2/0053/19 to M.C.; and 2/0014/17 to K.O.), and University Science Park for Biomedicine (ITMS 26240220087).

Supplementary Materials

The supplementary information's file (PDF) contains only additional figures with legends to the main manuscript text. (*Supplementary Materials*)

References

- [1] R. Wang, "Physiological implications of hydrogen sulfide: a whiff exploration that blossomed," *Physiological Reviews*, vol. 92, no. 2, pp. 791–896, 2012.
- [2] C. Szabo and A. Papapetropoulos, "International union of basic and clinical pharmacology. CII: pharmacological modulation of H₂S levels: H₂S donors and H₂S biosynthesis inhibitors," *Pharmacological Reviews*, vol. 69, no. 4, pp. 497–564, 2017.
- [3] L. Tomasova, P. Konopelski, and M. Ufnal, "Gut bacteria and hydrogen sulfide: the new old players in circulatory system homeostasis," *Molecules*, vol. 21, no. 11, p. 1558, 2016.
- [4] Y.-H. Liu, M. Lu, L.-F. Hu, P. T.-H. Wong, G. D. Webb, and J.-S. Bian, "Hydrogen sulfide in the mammalian cardiovascular system," *Antioxidants and Redox Signaling*, vol. 17, no. 1, pp. 141–185, 2012.
- [5] A. Misak, M. Grman, Z. Bacova et al., "Polysulfides and products of H₂S/S-nitrosoglutathione in comparison to H₂S, glutathione and antioxidant Trolox are potent scavengers of superoxide anion radical and produce hydroxyl radical by decomposition of H₂O₂," *Nitric Oxide*, vol. 76, pp. 136–151, 2018.
- [6] A. Staško, V. Brezová, M. Zalibera, S. Biskupič, and K. Ondriaš, "Electron transfer: a primary step in the reactions of sodium hydrosulphide, an H₂S/HS⁻ donor," *Free Radical Research*, vol. 43, no. 6, pp. 581–593, 2009.
- [7] M. Whiteman, J. S. Armstrong, S. H. Chu et al., "The novel neuromodulator hydrogen sulfide: an endogenous peroxynitrite 'scavenger?'," *Journal of Neurochemistry*, vol. 90, no. 3, pp. 765–768, 2004.
- [8] M. Whiteman, N. S. Cheung, Y.-Z. Zhu et al., "Hydrogen sulphide: a novel inhibitor of hypochlorous acid-mediated oxidative damage in the brain?," *Biochemical and Biophysical Research Communications*, vol. 326, no. 4, pp. 794–798, 2005.
- [9] M. A. Eghbal, P. S. Pennefather, and P. J. O'Brien, "H₂S cytotoxicity mechanism involves reactive oxygen species formation and mitochondrial depolarisation," *Toxicology*, vol. 203, no. 1–3, pp. 69–76, 2004.
- [10] D. H. Truong, M. A. Eghbal, W. Hindmarsh, S. H. Roth, and P. J. O'Brien, "Molecular mechanisms of hydrogen sulfide toxicity," *Drug Metabolism Reviews*, vol. 38, no. 4, pp. 733–744, 2006.
- [11] J. Jiang, A. Chan, S. Ali et al., "Hydrogen sulfide—mechanisms of toxicity and development of an antidote," *Scientific Reports*, vol. 6, no. 1, 2016.
- [12] S. Miller, S. W. Walker, J. R. Arthur et al., "Selenite protects human endothelial cells from oxidative damage and induces thioredoxin reductase," *Clinical Science*, vol. 100, no. 5, pp. 543–550, 2001.
- [13] R. S. Lymbury, M. J. Marino, and A. V. Perkins, "Effect of dietary selenium on the progression of heart failure in the ageing spontaneously hypertensive rat," *Molecular Nutrition & Food Research*, vol. 54, no. 10, pp. 1436–1444, 2010.

- [14] S. J. Fairweather-Tait, Y. Bao, M. R. Broadley et al., "Selenium in human health and disease," *Antioxidants and Redox Signaling*, vol. 14, no. 7, pp. 1337–1383, 2011.
- [15] J. Bleys, A. Navas-Acien, and E. Guallar, "Serum selenium and diabetes in U.S. adults," *Diabetes Care*, vol. 30, no. 4, pp. 829–834, 2007.
- [16] G. Deyab, I. Hokstad, J. Aaseth et al., "Effect of anti-rheumatic treatment on selenium levels in inflammatory arthritis," *Journal of Trace Elements in Medicine and Biology*, vol. 49, pp. 91–97, 2018.
- [17] R. A. Heller, J. Seelig, T. Bock et al., "Relation of selenium status to neuro-regeneration after traumatic spinal cord injury," *Journal of Trace Elements in Medicine and Biology*, vol. 51, pp. 141–149, 2019.
- [18] Clark, Dalkin, Krongrad et al., "Decreased incidence of prostate cancer with selenium supplementation: results of a double-blind cancer prevention trial," *British Journal of Urology*, vol. 81, no. 5, pp. 730–734, 1998.
- [19] S. M. Lippman, E. A. Klein, P. J. Goodman et al., "Effect of selenium and vitamin E on risk of prostate cancer and other cancers," *JAMA*, vol. 301, no. 1, pp. 39–51, 2009.
- [20] M. Vinceti, T. Filippini, C. Del Giovane et al., "Selenium for preventing cancer," *Cochrane Database of Systematic Reviews*, no. 3, Article CD005195, 2014.
- [21] N. Karunasinghe, S. Zhu, and L. R. Ferguson, "Benefits of selenium supplementation on leukocyte DNA integrity interact with dietary micronutrients: a short communication," *Nutrients*, vol. 8, no. 5, p. 249, 2016.
- [22] J. Lü, J. Zhang, C. Jiang, Y. Deng, N. Özten, and M. C. Bosland, "Cancer chemoprevention research with selenium in the post-SELECT era: promises and challenges," *Nutrition and Cancer*, vol. 68, no. 1, pp. 1–17, 2016.
- [23] J. K. Wrobel, R. Power, and M. Toborek, "Biological activity of selenium: revisited," *IUBMB Life*, vol. 68, no. 2, pp. 97–105, 2016.
- [24] R. R. Ramoutar and J. L. Brumaghim, "Effects of inorganic selenium compounds on oxidative DNA damage," *Journal of Inorganic Biochemistry*, vol. 101, no. 7, pp. 1028–1035, 2007.
- [25] C. Jiang, H. Hu, B. Malewicz, Z. Wang, and J. Lü, "Selenite-induced p53 ser-15 phosphorylation and caspase-mediated apoptosis in LNCaP human prostate cancer cells," *Molecular Cancer Therapeutics*, vol. 3, no. 7, pp. 877–884, 2004.
- [26] J. Lu, M. Kaeck, C. Jiang, A. C. Wilson, and H. J. Thompson, "Selenite induction of DNA strand breaks and apoptosis in mouse leukemic L1210 cells," *Biochemical Pharmacology*, vol. 47, no. 9, pp. 1531–1535, 1994.
- [27] J. J. An, K. J. Shi, W. Wei et al., "The ROS/JNK/ATF2 pathway mediates selenite-induced leukemia NB4 cell cycle arrest and apoptosis *in vitro* and *in vivo*," *Cell Death and Disease*, vol. 4, no. 12, 2013.
- [28] G. Nilsson, X. Sun, C. Nyström et al., "Selenite induces apoptosis in sarcomatoid malignant mesothelioma cells through oxidative stress," *Free Radical Biology and Medicine*, vol. 41, no. 6, pp. 874–885, 2006.
- [29] S. Biswas, G. Talukder, and A. Sharma, "Chromosome damage induced by selenium salts in human peripheral lymphocytes," *Toxicology In Vitro*, vol. 14, no. 5, pp. 405–408, 2000.
- [30] J. Brozmanová, D. Mániková, V. Vlčková, and M. Chovanec, "Selenium: a double-edged sword for defense and offence in cancer," *Archives of Toxicology*, vol. 84, no. 12, pp. 919–938, 2010.
- [31] E. Jablonska and M. Vinceti, "Selenium and human health: witnessing a Copernican revolution?," *Journal of Environmental Science and Health, Part C*, vol. 33, no. 3, pp. 328–368, 2015.
- [32] S. Koike, Y. Ogasawara, N. Shibuya, H. Kimura, and K. Ishii, "Polysulfide exerts a protective effect against cytotoxicity caused by *t*-butylhydroperoxide through Nrf2 signaling in neuroblastoma cells," *FEBS Letters*, vol. 587, no. 21, pp. 3548–3555, 2013.
- [33] W. H. Sun, F. Liu, Y. Chen, and Y. C. Zhu, "Hydrogen sulfide decreases the levels of ROS by inhibiting mitochondrial complex IV and increasing SOD activities in cardiomyocytes under ischemia/reperfusion," *Biochemical and Biophysical Research Communications*, vol. 421, no. 2, pp. 164–169, 2012.
- [34] P. Nagy, Z. Pálinkás, A. Nagy, B. Budai, I. Tóth, and A. Vasas, "Chemical aspects of hydrogen sulfide measurements in physiological samples," *Biochimica et Biophysica Acta (BBA) - General Subjects*, vol. 1840, no. 2, pp. 876–891, 2014.
- [35] U. Samuni, Y. Samuni, and S. Goldstein, "On the distinction between nitroxyl and nitric oxide using nitronyl nitroxides," *Journal of the American Chemical Society*, vol. 132, no. 24, pp. 8428–8432, 2010.
- [36] A. Misak, L. Kurakova, E. Goffa et al., "Sulfide (Na₂S) and polysulfide (Na₂S₂) interacting with doxycycline produce/scavenge superoxide and hydroxyl radicals and induce/inhibit DNA cleavage," *Molecules*, vol. 24, no. 6, p. 1148, 2019.
- [37] D. Grundy, "Principles and standards for reporting animal experiments in *The Journal of Physiology and Experimental Physiology*," *Journal of Physiology*, vol. 593, no. 12, pp. 2547–2549, 2015.
- [38] S. Cacanyiova, A. Berenyiova, F. Kristek, M. Drobna, K. Ondrias, and M. Grman, "The adaptive role of nitric oxide and hydrogen sulphide in vasoactive responses of thoracic aorta is triggered already in young spontaneously hypertensive rats," *Journal of Physiology and Pharmacology*, vol. 67, no. 4, pp. 501–512, 2016.
- [39] L. Tomasova, M. Pavlovicova, L. Malekova et al., "Effects of AP39, a novel triphenylphosphonium derivatised anethole dithiolethione hydrogen sulfide donor, on rat haemodynamic parameters and chloride and calcium Ca_v3 and RyR2 channels," *Nitric Oxide*, vol. 46, pp. 131–144, 2015.
- [40] A. Kharm, M. Grman, A. Misak et al., "Inorganic polysulfides and related reactive sulfur-selenium species from the perspective of chemistry," *Molecules*, vol. 24, no. 7, 2019.
- [41] K. A. Cupp-Sutton and M. T. Ashby, "Biological chemistry of hydrogen selenide," *Antioxidants*, vol. 5, no. 4, 2016.
- [42] X. Pan, X. Song, C. Wang et al., "H₂Se induces reductive stress in HepG2 cells and activates cell autophagy by regulating the redox of HMGB1 protein under hypoxia," *Theranostics*, vol. 9, no. 6, pp. 1794–1808, 2019.
- [43] C. L. Bianco, T. A. Chavez, V. Sosa et al., "The chemical biology of the persulfide (RSSH)/perthiyl (RSS[•]) redox couple and possible role in biological redox signaling," *Free Radical Biology and Medicine*, vol. 101, pp. 20–31, 2016.
- [44] D. J. O'Brien and F. B. Birkner, "Kinetics of oxygenation of reduced sulfur species in aqueous solution," *Environmental Science & Technology*, vol. 11, no. 12, pp. 1114–1120, 1977.
- [45] K. L. Nuttall and F. S. Allen, "Kinetics of the reaction between hydrogen selenide ion and oxygen," *Inorganica Chimica Acta*, vol. 91, no. 4, pp. 243–246, 1984.

- [46] G. W. Luther, A. J. Findlay, D. J. MacDonald et al., "Thermodynamics and kinetics of sulfide oxidation by oxygen: a look at inorganically controlled reactions and biologically mediated processes in the environment," *Frontiers in Microbiology*, vol. 2, 2011.
- [47] J. M. Fukuto, S. J. Carrington, D. J. Tantillo et al., "Small molecule signaling agents: the integrated chemistry and biochemistry of nitrogen oxides, oxides of carbon, dioxygen, hydrogen sulfide, and their derived species," *Chemical Research in Toxicology*, vol. 25, no. 4, pp. 769–793, 2012.
- [48] S. S. Saund, V. Sosa, S. Henriquez et al., "The chemical biology of hydropersulfides (RSSH): chemical stability, reactivity and redox roles," *Archives of Biochemistry and Biophysics*, vol. 588, pp. 15–24, 2015.
- [49] H. Zhao, J. Joseph, H. Zhang, H. Karoui, and B. Kalyanaraman, "Synthesis and biochemical applications of a solid cyclic nitron spin trap: a relatively superior trap for detecting superoxide anions and glutathyl radicals," *Free Radical Biology and Medicine*, vol. 31, no. 5, pp. 599–606, 2001.
- [50] J. E. Repine, O. W. Pfenninger, D. W. Talmage, E. M. Berger, and D. E. Pettijohn, "Dimethyl sulfoxide prevents DNA nicking mediated by ionizing radiation or iron/hydrogen peroxide-generated hydroxyl radical," *Proceedings of the National Academy of Sciences*, vol. 78, no. 2, pp. 1001–1003, 1981.
- [51] M. Noda, Y. Ma, Y. Yoshikawa et al., "A single-molecule assessment of the protective effect of DMSO against DNA double-strand breaks induced by photo- and γ -ray-irradiation, and freezing," *Scientific Reports*, vol. 7, no. 1, 2017.
- [52] S. Cacanyiova, A. Berenyiova, P. Balis et al., "Nitroso-sulfide coupled signaling triggers specific vasoactive effects in the intrarenal arteries of patients with arterial hypertension," *Journal of Physiology and Pharmacology*, vol. 68, no. 4, pp. 527–538, 2017.
- [53] P. F. Dillon, R. S. Root-Bernstein, and C. M. Lieder, "Antioxidant-independent ascorbate enhancement of catecholamine-induced contractions of vascular smooth muscle," *American Journal of Physiology-Heart and Circulatory Physiology*, vol. 286, 2004.
- [54] M. Drobná, A. Misak, T. Holland et al., "Captopril partially decreases the effect of H_2S on rat blood pressure and inhibits H_2S -induced nitric oxide release from S-nitrosoglutathione," *Physiological Research*, vol. 64, no. 4, pp. 479–486, 2015.
- [55] S. S. Franklin, S. A. Khan, N. D. Wong, M. G. Larson, and D. Levy, "Is pulse pressure useful in predicting risk for coronary heart disease?," *Circulation*, vol. 100, no. 4, pp. 354–360, 1999.
- [56] P. M. Mottram, B. A. Haluska, R. Leano, S. Carlier, C. Case, and T. H. Marwick, "Relation of arterial stiffness to diastolic dysfunction in hypertensive heart disease," *Heart*, vol. 91, no. 12, pp. 1551–1556, 2005.
- [57] N. Geoffroy and G. P. Demopoulos, "The elimination of selenium(IV) from aqueous solution by precipitation with sodium sulfide," *Journal of Hazardous Materials*, vol. 185, no. 1, pp. 148–154, 2011.
- [58] B. Jung, A. Safan, B. Batchelor, and A. Abdel-Wahab, "Spectroscopic study of Se(IV) removal from water by reductive precipitation using sulfide," *Chemosphere*, vol. 163, pp. 351–358, 2016.
- [59] M. Pettine, F. Gennari, L. Campanella, B. Casentini, and D. Marani, "The reduction of selenium(IV) by hydrogen sulfide in aqueous solutions," *Geochimica et Cosmochimica Acta*, vol. 83, pp. 37–47, 2012.
- [60] J. Hahn and R. Klüsch, "Synthesis and characterization of the first thiaselanes," *Angewandte Chemie International Edition in English*, vol. 33, no. 17, pp. 1770–1772, 1994.
- [61] M. Grman, M. Nasim, R. Leontiev et al., "Inorganic reactive sulfur-nitrogen species: intricate release mechanisms or cacophony in yellow, blue and red?," *Antioxidants*, vol. 6, no. 1, 2017.

Research Article

L-Cystathionine Protects against Homocysteine-Induced Mitochondria-Dependent Apoptosis of Vascular Endothelial Cells

Xiuli Wang,^{1,2} Yi Wang,¹ Lulu Zhang,¹ Da Zhang,¹ Lu Bai,¹ Wei Kong,³ Yaqian Huang ¹,
Chaoshu Tang,^{3,4} Junbao Du ¹, and Hongfang Jin ¹

¹Department of Pediatrics, Peking University First Hospital, Beijing 100034, China

²Research Unit of Clinical Diagnosis and Treatment of Pediatric Syncope and Cardiovascular Diseases, Chinese Academy of Medical Sciences, Beijing, China

³Department of Physiology and Pathophysiology, Peking University Health Science Center, Beijing 100191, China

⁴Key Lab. of Ministry of Education of China, Beijing 100191, China

Correspondence should be addressed to Hongfang Jin; jinhongfang51@126.com

Received 11 June 2019; Accepted 9 October 2019; Published 25 November 2019

Guest Editor: Mario Fontana

Copyright © 2019 Xiuli Wang et al. This is an open access article distributed under the Creative Commons Attribution License, which permits unrestricted use, distribution, and reproduction in any medium, provided the original work is properly cited.

The study was aimed at investigating the effects of L-cystathionine on vascular endothelial cell apoptosis and its mechanisms. Cultured human umbilical vein endothelial cells (HUVECs) were used in the study. Apoptosis of vascular endothelial cells was induced by homocysteine. Apoptosis, mitochondrial superoxide anion, mitochondrial membrane potential, mitochondrial permeability transition pore (MPTP) opening, and caspase-9 and caspase-3 activities were examined. Expression of Bax, Bcl-2, and cleaved caspase-3 was tested and BTSA1, a Bax agonist, and HUVEC Bax overexpression was used in the study. Results showed that homocysteine obviously induced the apoptosis of HUVECs, and this effect was significantly attenuated by the pretreatment with L-cystathionine. Furthermore, L-cystathionine decreased the production of mitochondrial superoxide anion and the expression of Bax and restrained its translocation to mitochondria, increased mitochondrial membrane potential, inhibited mitochondrial permeability transition pore (MPTP) opening, suppressed the leakage of cytochrome c from mitochondria into the cytoplasm, and downregulated activities of caspase-9 and caspase-3. However, BTSA1, a Bax agonist, or Bax overexpression successfully abolished the inhibitory effect of L-cystathionine on Hcy-induced MPTP opening, caspase-9 and caspase-3 activation, and HUVEC apoptosis. Taken together, our results indicated that L-cystathionine could protect against homocysteine-induced mitochondria-dependent apoptosis of HUVECs.

1. Introduction

Homocysteine (Hcy) is an important sulfur-containing amino acid. The concentration of Hcy over 15 $\mu\text{mol/L}$ in plasma is defined as hyperhomocysteinemia [1]. Hcy is an independent risk factor for cardiovascular disease and can cause the damage to vascular endothelial cells (VECs), thus participating in the pathogenesis of a variety of diseases including atherosclerosis, hypertension, and coronary artery disease [2–5]. Previous studies showed that high homocysteine accentuated the production of reactive oxygen species, thereby activating the mitochondrial apoptotic pathway resulting in an apoptosis of VECs, which is regarded as an important cause of vascular dysfunction [6].

In order to treat hyperhomocysteinemia and reduce the incidence of cardiovascular disease, many studies have been conducted in this field. In the past, it was considered that the deficiency of vitamin B complex was an important factor in the formation of hyperhomocysteinemia. Therefore, the method of supplementing folic acid, vitamin B6, and vitamin B12 was used to reduce the concentration of homocysteine in the body, but clinical studies have shown that although vitamin B complex reduces homocysteine concentration in plasma, it cannot significantly inhibit Hcy-induced endothelial dysfunction [7–9]. Thus, it is necessary to develop new modalities of medication to prevent endothelial dysfunction and cardiovascular events caused by Hcy.

L-cystathionine is a nonprotein thioether containing amino acids and is mainly produced in the metabolic transformation process of methionine to cysteine in the body [10]. Previous studies on L-cystathionine have focused on it as a key amino acid associated with the metabolic state of sulfur-containing amino acids [11]. In recent years, studies have shown that it plays an important role in cardiovascular protection other than merely a metabolite in the methionine metabolic pathway. For example, L-cystathionine can antagonize vascular injury through the inhibition of ox-LDL-induced inflammatory response in macrophages [12]. Nevertheless, how L-cystathionine regulates Hcy-induced vascular endothelial cell injury remains unknown.

Therefore, this present study was undertaken to investigate the protective effect of L-cystathionine on Hcy-induced VEC apoptosis and reveal the significance and mechanism by which L-cystathionine maintains VEC homeostasis.

2. Materials and Methods

2.1. Cell Culture and Processing. Human umbilical VECs (HUVECs) were purchased from the China Infrastructure of Cell Line Resources Centre. The cells were grown in DMEM containing 10% FBS, 1% penicillin, 1% streptomycin, and 1% glutathione and maintained in an incubator at 37°C with 5% CO₂. When the cell confluence reached 80%, the experiments were started. Before each experiment, the cells were placed in synchronization buffer for 12 h. Cells were divided into the control group, Hcy group, Hcy+0.1 mmol/L L-Cth group, Hcy+0.3 mmol/L L-Cth group, and Hcy+1.0 mmol/L L-Cth group. According to the manufacturer's instructions, L-cystathionine was dissolved in 0.5 mol/L hydrochloric acid to a stock concentration of 5 mg/mL (22.5 mmol/L) in this study. Cells in the Hcy+0.1 mmol/L L-Cth group, Hcy+0.3 mmol/L L-Cth group and Hcy+1.0 mmol/L L-Cth group were pretreated with L-cystathionine for 30 min and then stimulated with 500 μmol/L Hcy for 24 h. Cells in the Hcy group were treated with 500 μmol/L Hcy for 24 h [13]. For the purpose of Bax manipulation, cells were preadministered with 0.625 μmol/L BTSA1 for 2.5 h [14], followed by 0.3 mmol/L L-cystathionine and 500 μmol/L homocysteine treatment. To further understand the role of Bax expression in the protection of cell apoptosis by L-cystathionine, the cells were transfected with 1 μg of vehicle plasmid or bax-overexpressed plasmid. Freshly completed culture medium was replaced after 6 h of transfection, and synchronization was performed after another 24 h, and then L-cystathionine and homocysteine were sequentially added.

2.2. In Situ and Quantitative Detection of Apoptosis in HUVECs by Using TdT-Mediated dUTP Nick End Labeling (TUNEL) Assay and ELISA. *In situ* cell apoptosis was determined with an *in situ* cell death detection kit and fluorescein (R&D Systems, USA) in accordance with the instructions of the manufacturer. Briefly, the cells on slides were fixed in 4% paraformaldehyde for 15 min after washing three times with PBS. Then, the cells were incubated with permeabilization solution at 37°C for 30 min. After washing with

PBS, the cells were incubated with TUNEL reaction mixture for 60 min at 37°C in the dark. The antifade solution was used to mount the slides after washing three times with PBS, and the slides were analyzed under a confocal laser scanning microscope (Olympus, Japan).

Moreover, the quantitative detection of DNA fragments in HUVECs was measured with a Cell Death Detection ELISA^{PLUS} Kit (Roche, Mannheim, Germany). According to the manufacturer's instructions, an appropriate volume of cell lysis buffer was added to lyse the cells. The cell lysate was added into a streptavidin-coated microplate. A mixture of anti-histone-biotin and anti-DNA-POD was added and incubated. The microplate was vortexed at room temperature for 2 h. The unbound components were removed after washing three times with incubation buffer, and an appropriate volume of substrate solution was added to each well. The microplate was vortexed at room temperature for 20 min, and the reaction was stopped by the addition of a stop solution. A microplate reader was used to obtain an absorbance value of each well, and the apoptosis level was calculated [15].

2.3. Detection of Mitochondrial Superoxide Anion by the MitoSOX Reagent in HUVECs. A MitoSOX Red Mitochondrial Superoxide Indicator (Life Technologies, USA) was used to measure mitochondrial ROS production. The indicator was applied to incubate the treated cells at 37°C for 10 min, protected from light. After washing with PBS, the cells were fixed in prewarmed 4% paraformaldehyde at room temperature for 15 min after washing with warm PBS for three times. The slides were mounted with an antifluorescence quencher (Beijing Zhongshan Golden Bridge Biotechnology Company, Beijing, China) after washing with PBS. Then, the cells on slides were detected with a laser scanning confocal microscope (Olympus, Japan).

2.4. Assessment of Cell Viability in HUVECs. The CCK8 assay was used to evaluate the cell viability in HUVECs (Beyotime, Shanghai, China). The cells were seeded in a 96-well plate. After the treatment with Hcy alone or Hcy plus L-cystathionine, CCK8 solution was added and incubated with cells for 2 h at 37°C. A microplate reader (Thermo, Finland) was used to detect the absorbance at a wavelength of 450 nm.

2.5. Measurement of Lactate Dehydrogenase (LDH) Activity in the Culture Media. LDH activity in the culture media of the HUVECs was measured with an LDH cytotoxicity assay kit (Beyotime, Shanghai, China). The cells were seeded in a 96-well plate. After the treatment with Hcy alone or Hcy plus L-cystathionine, LDH activity analysis was carried out according to the manufacturer's instructions. The absorbance of each well was read at 490 nm with a microplate reader.

2.6. Measurement of Mitochondrial Membrane Potential in HUVECs. Mitochondrial membrane potential changes in HUVECs were detected with a JC-1 mitochondrial membrane potential detection kit (Beyotime, Shanghai, China). When the mitochondrial membrane potential is at a high level, JC-1 accumulates within the mitochondria and becomes fluorescent red. When the mitochondrial membrane potential is at a low level, JC-1 cannot accumulate

within the mitochondria and remains in the cytoplasm in a green fluorescent monomeric form. A 1:1 mixture of JC-1 staining working solution and cell culture medium was added to cover the cell culture slides and incubated at 37°C in the dark for 20 min. The slides were washed twice with JC-1 assay buffer and fixed with 4% paraformaldehyde at room temperature for 20 min. Then, the slides were washed three times with PBS and mounted with antifade mounting media. The cells were analyzed with a confocal laser scanning microscope (Olympus, Japan).

2.7. Detection of Mitochondrial Permeability Transition Pore (MPTP) Opening in HUVECs. The MPTP opening in HUVECs was determined with a Cell MPTP Assay Kit (Genmed Scientific Inc., Arlington, TX, USA). Calcein AM, as a fluorescent probe, enters the mitochondria to form a green fluorescent compound. Once the mitochondrial permeability transition pore is opened, calcein AM is released, and accordingly, the fluorescence is quenched. First, culture medium was discarded and slides were rinsed gently with cleaning solution. Slides were subsequently incubated with the staining working solution at 37°C in the dark for 30 min. 4% paraformaldehyde was used to fix the cells for 15 min after rinsing for three times with cleaning solution. Finally, the slides were washed 3 times with PBS and mounted with antifade mounting media. A laser scanning confocal microscope was used for the analysis.

2.8. Immunofluorescence Microscopy. To determine the localization of cytochrome c or Bax, the cells were incubated in prewarmed medium containing 200 nmol/L of MitoTracker (Life Technologies, USA) at 37°C for 30 min after washing twice with PBS, and then, 4% paraformaldehyde was used to fix the cells at room temperature for 15 min. After washing three times with PBS, the cells were permeabilized with 0.1% Triton X-100 and then stained with anti-cytochrome c or anti-Bax at room temperature for 1 h and at 4°C overnight. After the incubation, an Alexa 594-conjugated secondary antibody (Life Technologies, USA) was added and incubated at 37°C for 90 min. Then, the antifade mounting media were used to mount the slides, and the cells were imaged with a confocal laser scanning microscope (Olympus, Japan) [16].

2.9. Measurement of Caspase-9 Activities in Human Macrophages by a Fluorescence and Colorimetric Assay. Change of *in situ* caspase-9 activity in HUVECs was detected with a living cell caspase-9 Fluo-staining kit (Genmed Scientific Inc., Arlington, TX, USA). The cell culture slides were rinsed with wash buffer and incubated with the staining working solution at 37°C in the dark for 20 min. After washing three times with wash buffer, fixation buffer was used to fix the cells at room temperature for 30 min. Then, antifade mounting media were used to mount the slides and the cells were analyzed with a confocal laser scanning microscope (Olympus, Japan).

Caspase-9 activity in HUVECs was detected with a cell caspase-9 activity colorimetric kit (Appligen, Beijing, China). Briefly, after washing twice with the wash buffer, the cells were incubated with Appligen lysis buffer at 4°C

for 30 min and then harvested into a centrifuge tube by scraping. The tubes were centrifuged (12,000 × *g*) at 4°C for 5 min. The supernatant was collected in a fresh tube on ice. The Bradford method was used for protein quantification. Then, 50 μg of sample and a reaction reagent were added to each well of a 96-well plate in order and incubated at 37°C in the dark for 2 h. A microplate reader at 405 nm was used to obtain an absorbance value of each well, and the caspase-9 activity level was calculated.

2.10. Measurement of Caspase-3 Activities in Human Macrophages by a Colorimetric Assay. Caspase-3 activity in HUVECs was quantified using a cell caspase-3 activity colorimetric kit (Appligen, Beijing, China). The cells were scraped on ice with Appligen lysis solution after washing twice with PBS. The supernatant was transferred into tubes after centrifugation (12,000 × *g*) at 4°C for 5 min. The Bradford method was used to measure protein concentration. The protein and reagent were added in a 96-well plate in order and incubated for 2 h at 37°C in the dark. Finally, the 96-well plate was read in a microplate reader.

2.11. Preparation of Mitochondrial Protein. A mitochondria isolation kit (Beyotime, Shanghai, China) was used to extract mitochondrial and cytosolic protein. The HUVECs were mixed thoroughly with Mito solution after centrifugation (600 × *g*) at 4°C for 5 min. After incubating on ice for 30 min with Mito solution, grinding pestles were used to grind the cells. Then, the cells were transferred to centrifuge tubes. The supernatant was moved into precooled tubes after centrifugation (1000 × *g*) at 4°C for 10 min. The supernatant was moved into new precooled tubes after centrifugation (3500 × *g*) at 4°C for 10 min. The supernatant containing the cytoplasm was then collected after centrifugation (12,000 × *g*) at 4°C for 10 min, while the precipitate containing mitochondria was resuspended with Mito lysate. Mitochondrial and cytosolic protein concentration was measured by Bradford methods.

2.12. Western Blotting Analysis. Western blotting was used to determine the expression of Bcl-2, Bax, cytc, flag, and cleaved caspase-3 and caspase-3 in HUVECs. The cells were lysed with an appropriate volume of protein lysis buffer at 4°C for 20 min after washing twice with precooled PBS. The lysate was transferred to an Eppendorf tube after fully scraping the cells. The tubes were centrifuged (12,000 × *g*) for 10 min, and the supernatant was collected. A small volume of supernatant was used for protein quantification (Bradford method). The remaining supernatant was boiled in equal volume of 2× sample buffer at 100°C for 10 min. Protein samples (30 μg) were separated in 10% SDS-PAGE and then electrically transferred onto a nitrocellulose membrane with a constant current of 200 mA for 2 h. After the transfer, the nitrocellulose membrane was blocked with 5% skim milk for 1 h. Then, the membrane was incubated with the following primary antibodies: β-actin (Santa Cruz, USA), Bcl-2 (Cell Signaling Technology, USA), Bax (Cell Signaling Technology, USA), cytc (Santa Cruz, USA), caspase-3 (Beyotime, Shanghai, China), cleaved caspase-3 (Beyotime, Shanghai, China),

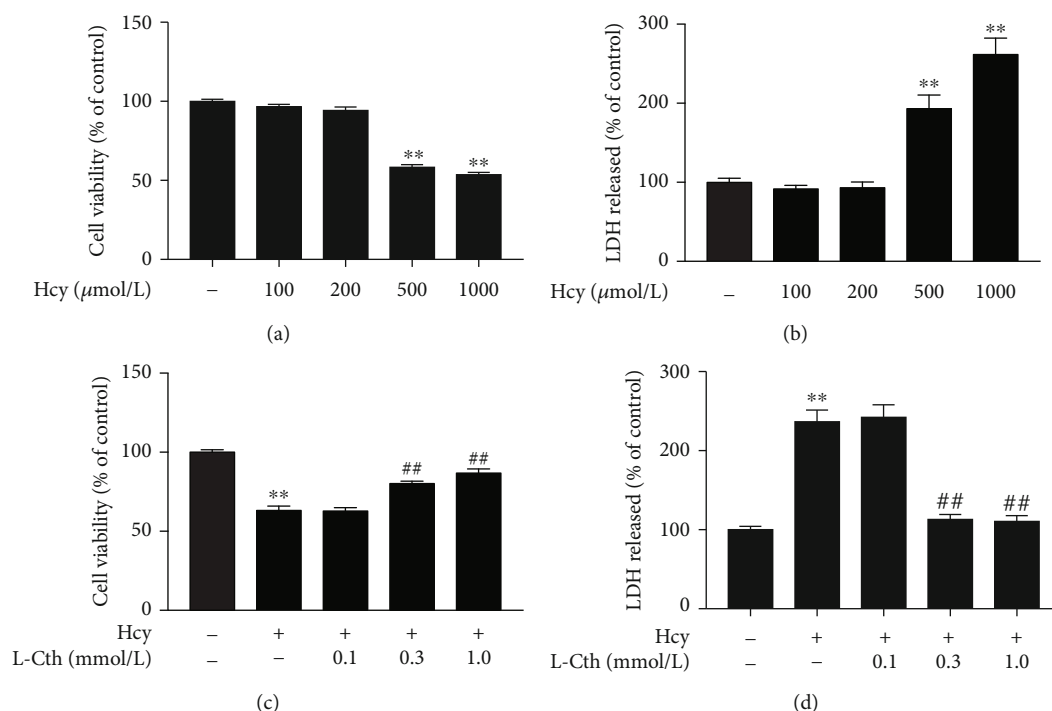


FIGURE 1: Effects of L-Cth on Hcy-induced cytotoxicity in HUVECs. (a) Cell viability in HUVECs treated with different concentrations of Hcy was measured by the CCK8 assay. (b) The LDH release from HUVECs treated with different concentrations of Hcy was analyzed. (c) Cell viability in HUVECs treated with 500 μmol Hcy alone or Hcy plus different concentrations of L-Cth was measured by the CCK8 assay. (d) The LDH release from HUVECs treated with 500 μmol Hcy alone or Hcy plus different concentrations of L-Cth was analyzed. Data are presented as mean \pm SEM. ** $P < 0.01$ versus control group; ## $P < 0.01$ versus Hcy group. L-Cth: L-cystathionine; LDH: lactate dehydrogenase.

cytochrome c oxidase IV (Cell Signaling Technology, USA), and flag (ZSbio, China) at room temperature for 2 h and at 4°C overnight. Cytochrome c oxidase IV (COX IV) and β -tubulin were used as the markers of mitochondrial and cytosolic protein, respectively. After the incubation, a horseradish peroxidase- (HRP-) conjugated secondary antibody was added and incubated at room temperature for 1 h. The protein band images were developed with FluorChem M (Protein Simple, USA) and quantitatively analyzed with the AlphaImager graphical analysis software (Alpha Innotech Corporation, USA).

2.13. Statistical Analysis. The quantitative data are expressed as the mean \pm SEM. SPSS 23.0 was used for data analysis. The mean among the three groups was compared by ANOVA. If the homogeneity of the variance test showed equal variance, the Bonferroni test was used to compare the differences between two groups. Otherwise, Dunnett's T3 test was used to compare the differences between two groups. $P < 0.05$ was considered statistically significant.

3. Results

3.1. L-Cystathionine Inhibited Hcy-Induced Cytotoxicity in HUVECs. The CCK8 assay and LDH leakage assay were used to evaluate the cytotoxicity of Hcy on HUVECs. As shown in Figures 1(a) and 1(b), the treatment of HUVECs with 500 and 1000 $\mu\text{mol/L}$ Hcy significantly suppressed the cell viability

and increased the LDH activity in the culture medium. In contrast, pretreatment of HUVECs with 0.3 and 1.0 mmol/L L-cystathionine significantly increased cell viability and blocked the LDH release in the HUVECs treated with 500 $\mu\text{mol/L}$ Hcy (Figures 1(c) and 1(d)). These results suggested that L-cystathionine could inhibit Hcy-induced cytotoxicity in HUVECs.

3.2. L-Cystathionine Suppressed Cell Apoptosis Induced by Hcy in HUVECs. To study whether L-cystathionine could inhibit cell apoptosis induced by 500 $\mu\text{mol/L}$ Hcy in HUVECs, we used the TUNEL assay to detect cell apoptosis. Results showed that the green fluorescence intensity was significantly higher in the Hcy group than in the control group, indicating that Hcy could significantly increase the apoptosis of the cells. After the treatment with 0.1 mmol/L L-cystathionine, no significant change in apoptosis was observed. However, the treatment with 0.3 and 1.0 mmol/L L-cystathionine significantly inhibited Hcy-induced apoptosis, respectively (Figure 2(a)).

Western blotting was used to analyze the cleavage of caspase-3 protein. Data showed that 500 $\mu\text{mol/L}$ Hcy significantly promoted caspase-3 cleavage. Pretreatment with 0.1 mmol/L L-cystathionine did not alter the expression of cleaved caspase-3 protein, while 0.3 and 1.0 mmol/L L-cystathionine significantly inhibited the cleavage of caspase-3, respectively. These results demonstrated that

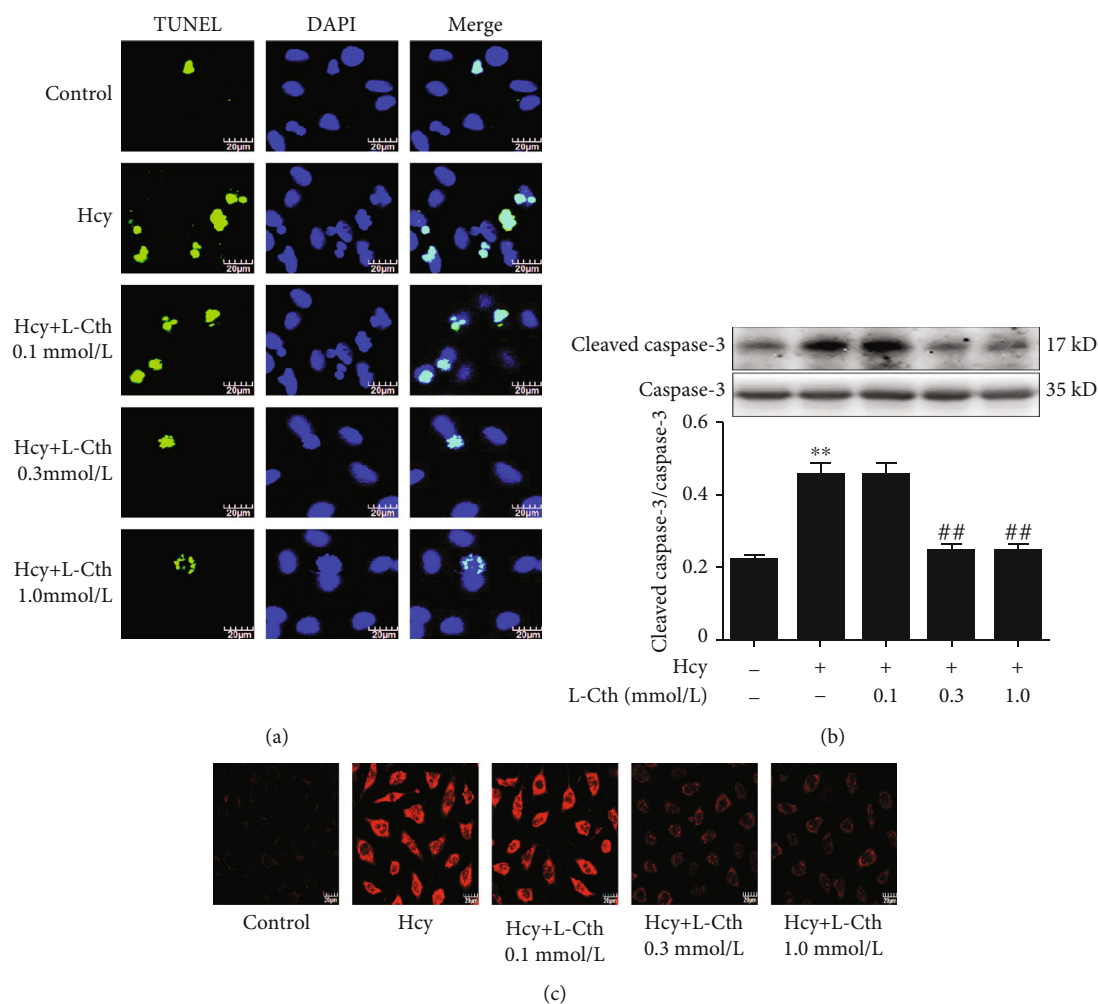


FIGURE 2: Effects of L-Cth on apoptosis, caspase-3 activities, and mitochondrial superoxide generation in Hcy-treated HUVECs. (a) HUVEC apoptosis detected by TdT-mediated dUTP nick end labeling (TUNEL) methods (magnification, $\times 600$; scale bar: $20 \mu\text{m}$). (b) Cleavage of caspase-3 analyzed by western blotting. (c) Mitochondrial superoxide generation in HUVECs detected with MitoSOX. Data are presented as mean \pm SEM. ** $P < 0.01$ versus control group; ## $P < 0.01$ versus Hcy group. L-Cth: L-cystathionine.

L-cystathionine antagonized apoptosis induced by Hcy in HUVECs (Figure 2(b)).

3.3. L-Cystathionine Inhibits Mitochondrial Superoxide Anion Generation Induced by Hcy in HUVECs. Results showed that the red fluorescence intensity was significantly higher in the Hcy group than in the control group, indicating that mitochondrial superoxide generation in the Hcy group was significantly increased compared with that in the control group. Pretreatment with 0.1 mmol/L L-cystathionine did not change mitochondrial superoxide generation. However, when pretreated with 0.3 and 1.0 mmol/L L-cystathionine, the generation of mitochondrial superoxide dramatically declined (Figure 2(c)).

3.4. L-Cystathionine Inhibits the Expression of Bax Induced by Hcy in HUVECs. Western blotting results showed that $500 \mu\text{mol/L}$ Hcy significantly increased Bax protein expression but did not impact on Bcl-2 protein expression, resulting in a decrease in the ratio of Bcl-2/Bax, which activated the

mitochondrial pathway to cause apoptosis. However, pretreatment with 0.3 and 1.0 mmol/L L-cystathionine significantly inhibited the increased Bax protein expression, respectively, while the Bcl-2 protein expression was unaffected, which increased the ratio of Bcl-2/Bax and antagonized apoptosis. Pretreatment with 0.1 mmol/L L-cystathionine had no impact on Bax and Bcl-2 protein expressions (Figure 3(a)). Moreover, immunofluorescence microscopy was used to determine the localization of Bax. Results showed that 0.3 and 1.0 mmol/L L-cystathionine not only reduced the expression of Bax but also inhibited its translocation to mitochondria, respectively (Figure 3(b)).

3.5. L-Cystathionine Reversed the Decline of Mitochondrial Membrane Potential Induced by Hcy in HUVECs. The green fluorescence intensity was significantly higher in the Hcy group than in the control group, indicating that $500 \mu\text{mol/L}$ Hcy could reduce the mitochondrial membrane potential. After the addition of 0.1 mmol/L L-cystathionine, there was no significant change in the mitochondrial membrane

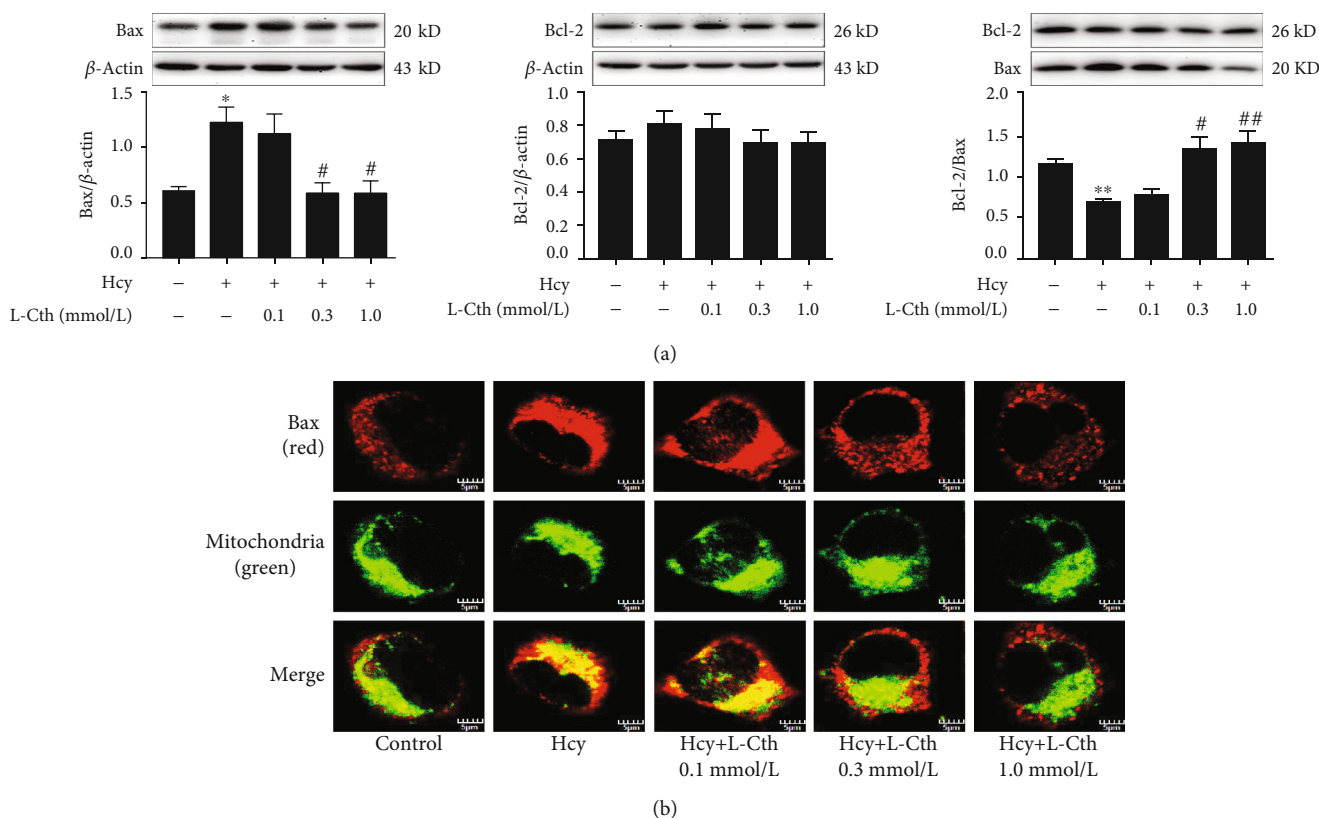


FIGURE 3: Effect of L-Cth on Bax and Bcl-2 expression as well as Bax distribution in Hcy-treated HUVECs. (a) Bax and Bcl-2 expression analyzed by western blotting. Data are presented as mean \pm SEM. * $P < 0.05$ versus control group; ** $P < 0.01$ versus control group; # $P < 0.05$ versus Hcy group; ## $P < 0.01$ versus Hcy group. (b) The localization of Bax in HUVECs detected by immunofluorescence microscopy, with red fluorescence indicating Bax and green fluorescence indicating mitochondria (magnification, $\times 600$; scale bar: $5 \mu\text{m}$). L-Cth: L-cystathionine.

potential. However, the red fluorescence intensity was significantly enhanced after the addition of 0.3 and 1.0 mmol/L L-cystathionine, respectively. These results indicated that 0.3 and 1.0 mmol/L L-cystathionine could reverse the decline of mitochondrial membrane potential induced by Hcy (Figure 4(a)).

3.6. L-Cystathionine Antagonized Mitochondrial Permeability Transition Pore (MPTP) Opening Induced by Hcy in HUVECs. Compared with the control group, fluorescence intensity was significantly weakened in the Hcy group, suggesting an increased MPTP opening. However, a significantly enhanced fluorescence intensity was observed when pretreated with 0.3 and 1.0 mmol/L L-cystathionine, respectively, implying the inhibition of MPTP opening. When HUVECs were pretreated with 0.1 mmol/L L-cystathionine, however, fluorescence intensity did not alter (Figure 4(b)).

3.7. L-Cystathionine Inhibited the Release of Cytc from the Mitochondrion into the Cytoplasm Induced by Hcy in HUVECs. To investigate whether MPTP opening had an effect on cytc release, the immunofluorescence method was used to detect the leakage of cytc from the mitochondrion into the cytoplasm in HUVECs. Compared with the control group, 500 $\mu\text{mol/L}$ Hcy treatment significantly downregulated cytc protein expression in mitochondria of HUVECs

and markedly increased cytoplasmic cytc. The pretreatment with 0.1 mmol/L L-cystathionine had no effect on the cytc expression in the mitochondrion and cytoplasm. Interestingly, 0.3 and 1.0 mmol/L L-cystathionine significantly upregulated cytc expression in the mitochondrion, respectively, but downregulated cytc expression in the cytoplasm, demonstrating the inhibiting effect on the leakage of cytc from the mitochondrion into the cytoplasm (Figure 5).

3.8. L-Cystathionine Inhibits Caspase-9 Activation Induced by Hcy in HUVECs. The colorimetry results showed that 500 $\mu\text{mol/L}$ Hcy significantly increased the caspase-9 activity, whereas the pretreatment with 0.3 and 1.0 mmol/L L-cystathionine significantly inhibited the caspase-9 activity, respectively (Figure 6(a)). The fluorescence results showed that the green fluorescence intensity was significantly strengthened in the Hcy group compared with the control group. However, the fluorescence intensity was significantly weakened with the pretreatment of 0.3 and 1.0 mmol/L L-cystathionine, respectively, suggesting the inhibition of caspase-9 activities (Figure 6(b)). Both methods indicated that 0.1 mmol/L L-Cth has no effect on the caspase-9 activation (Figure 6).

3.9. BSA1 Abolished the Inhibitory Effect of L-Cystathionine on Apoptosis Induced by Hcy in HUVECs. To further

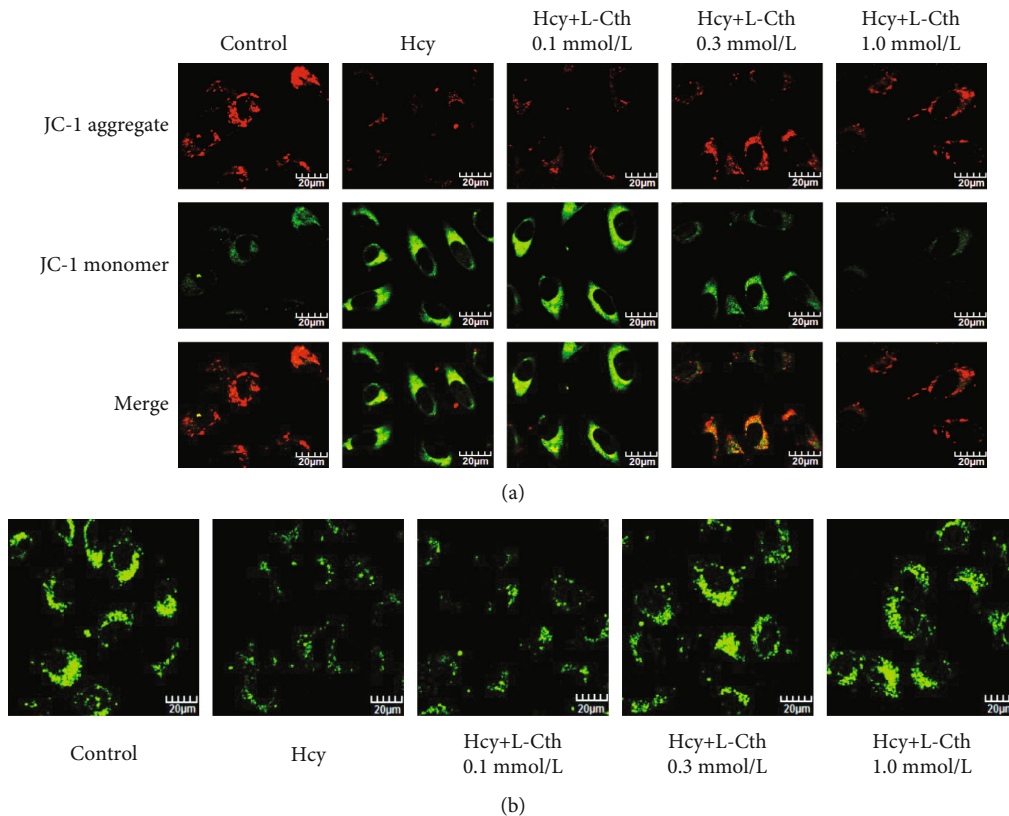


FIGURE 4: Effect of L-Cth on mitochondrial membrane potential and mitochondrial permeability transition pore (MPTP) opening in Hcy-treated HUVECs. (a) Change of mitochondrial membrane potential detected by a JC-1 fluorescent probe, with red fluorescence indicating high mitochondrial membrane potential and green indicating low mitochondrial membrane potential (magnification, $\times 600$; scale bar: $20 \mu\text{m}$). (b) Changes of MPTP opening in HUVECs detected with calcein AM. The green fluorescence quenching represented MPTP opening (magnification, $\times 600$; scale bar: $20 \mu\text{m}$). L-Cth: L-cystathionine.

demonstrate that L-cystathionine exerted antiapoptotic effects through the Bax pathway, the HUVECs were pretreated with BTSA1, a Bax agonist that promotes Bax translocation to mitochondria but has no effect on its expression [14]. Results showed that in the absence of BTSA1, 0.3 mmol/L L-cystathionine inhibited the translocation of Bax to mitochondria (Figure 7(a)), the opening of MPTP, and the activation of caspase-9 and caspase-3 (Figures 7(b)–7(e)), thereby antagonizing apoptosis induced by Hcy in HUVECs. However, after the pretreatment with $0.625 \mu\text{mol/L}$ BTSA1, L-cystathionine could no longer inhibit the translocation of Bax to mitochondria (Figure 7(a)), the opening of MPTP, and the activation of caspase-9 and caspase-3 induced by Hcy (Figures 7(b)–7(e)), suggesting that the protective effect of L-cystathionine on the Hcy-induced apoptosis in HUVECs was abolished.

3.10. Overexpression of Bax Abolished the Inhibitory Effect of L-Cystathionine on Apoptosis Induced by Hcy in HUVECs. In order to prove if L-cystathionine plays an antiapoptotic role by inhibiting the expression of Bax, we overexpressed Bax protein with the transfection of plasmid (Figure 8(a)). Results showed that in the vehicle group, the administration of 0.3 mmol/L L-cystathionine significantly inhibited caspase-3

activation induced by Hcy, whereas in the overexpression group, L-cystathionine failed to inhibit caspase-3 activation (Figure 8(b)). The ELISA results also showed that 0.3 mmol/L L-Cth in the vehicle group could inhibit the apoptosis of endothelial cells induced by Hcy, while in the Bax overexpression group, the antiapoptotic effect of L-cystathionine was abolished (Figure 8(c)).

4. Discussion

Our results demonstrated for the first time that L-cystathionine could inhibit Hcy-induced mitochondria-mediated apoptosis of HUVECs via restraining the expression and translocation of Bax, increasing mitochondrial membrane potential, inhibiting MPTP opening, suppressing cytc release from mitochondria into the cytoplasm, and reducing caspase-9 activities and protein expression.

The maintenance of homeostasis in the cardiovascular system is a complex process, and VECs are critical in this process. VECs regulate vascular tone by secreting nitric oxide synthase, endothelin-1, etc., and when they are damaged, they can secrete various inflammatory mediators such as $\text{TNF-}\alpha$, IL-1, and IL-6 [17–20]. Many studies have been conducted to explore the mechanism of VEC damage caused by Hcy. The discovery of circulating endothelial cells in the

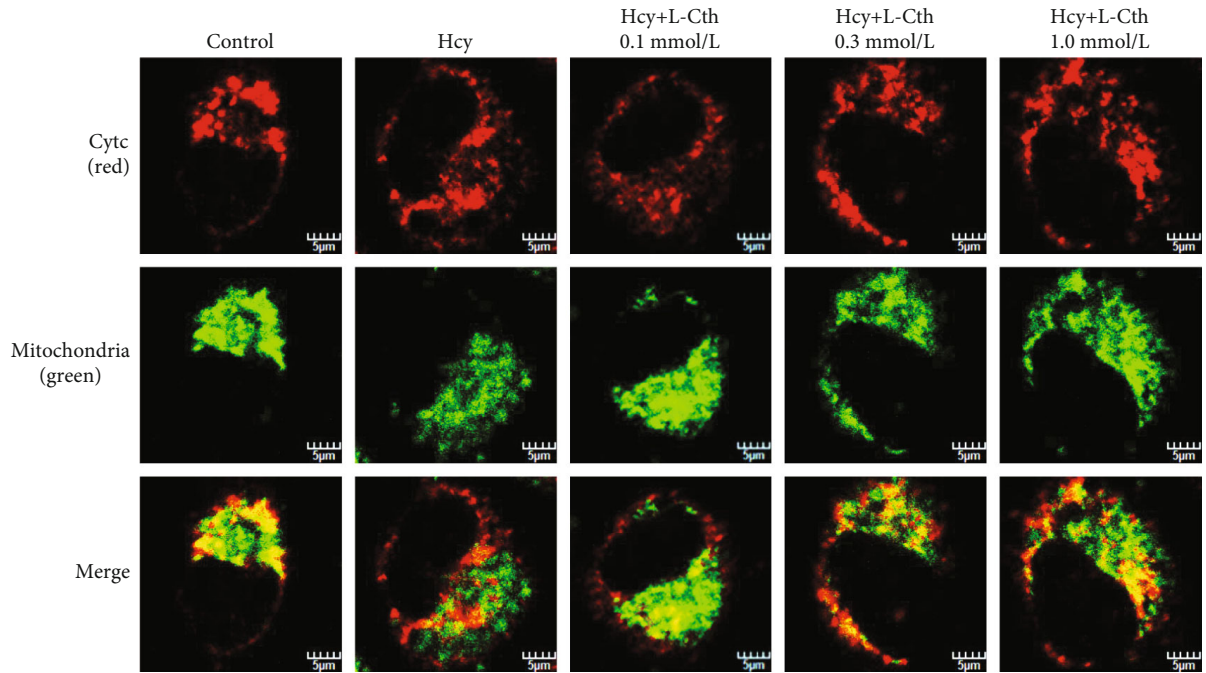


FIGURE 5: Effect of L-Cth on cytochrome c (cytc) protein expression and distribution in Hcy-treated HUVECs detected by immunofluorescence microscopy, with red fluorescence indicating cytc and green indicating mitochondria (magnification, $\times 600$; scale bar: $5 \mu\text{m}$). L-Cth: L-cystathionine.

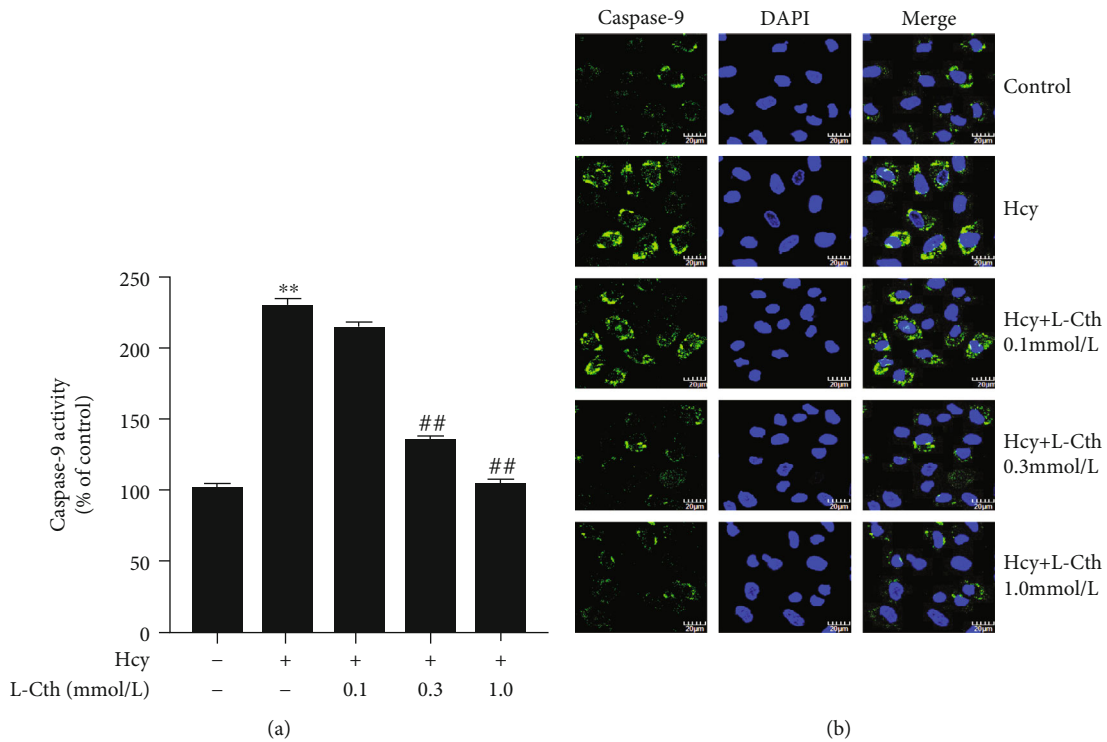


FIGURE 6: Effect of L-Cth on caspase-9 activities in Hcy-treated HUVECs. (a) Quantitative analysis of caspase-9 activities measured with a caspase-9 activity colorimetric kit. (b) Caspase-9 activity detected with living cell caspase-9 Fluo-staining kit (magnification, $\times 600$; scale bar: $20 \mu\text{m}$). Data are presented as mean \pm SEM. ** $P < 0.01$ versus control group; ## $P < 0.01$ versus Hcy group. L-Cth: L-cystathionine.

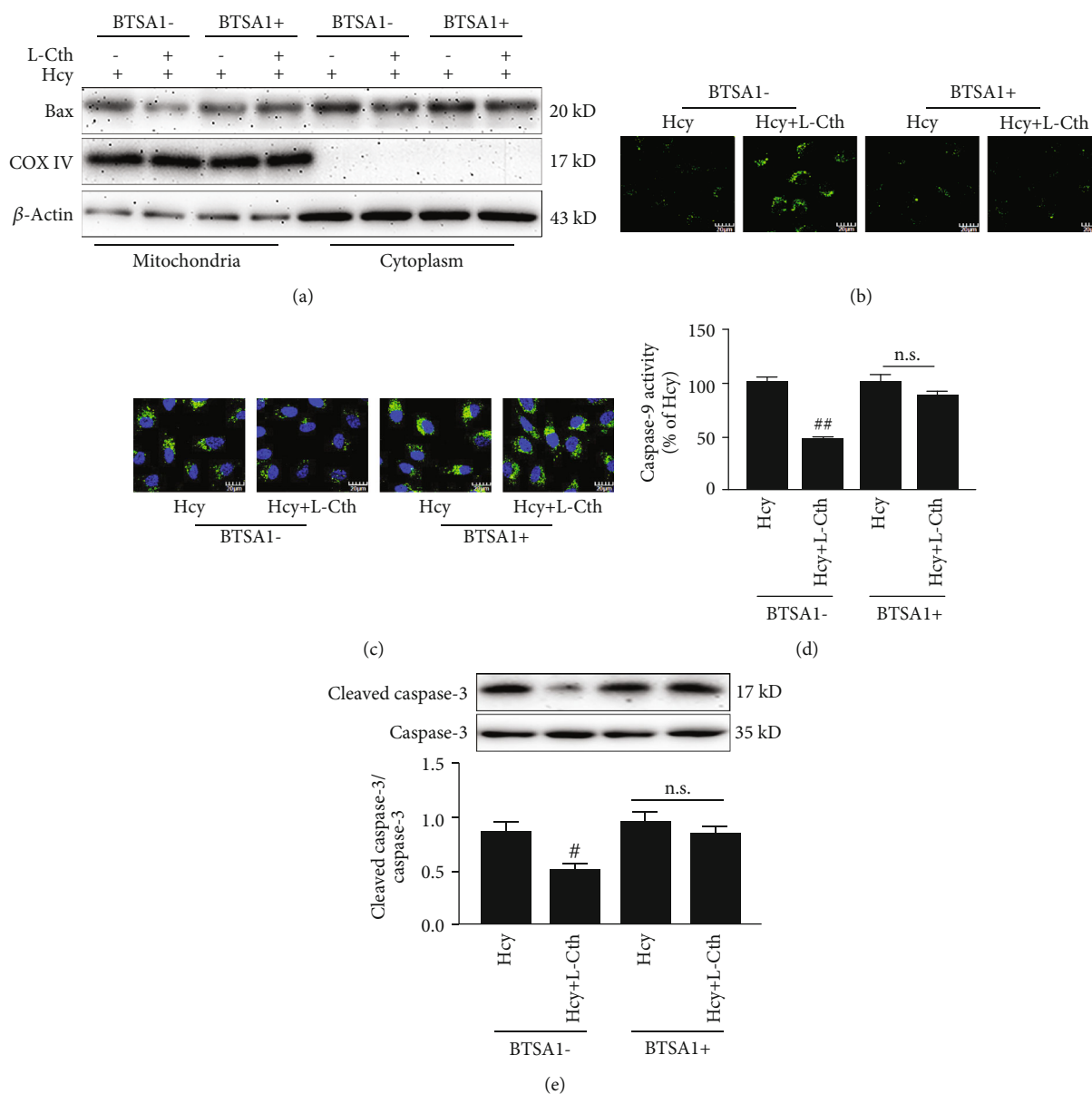


FIGURE 7: Effect of L-Cth on Bax expression, MPTP opening, caspase-9 activity, and cleaved-caspase3 expression in Hcy-treated HUVECs when administering BTS1 in advance. (a) Bax expression analyzed by western blotting. (b) Changes of MPTP opening in HUVECs (magnification, $\times 600$; scale bar: $20\ \mu\text{m}$). (c) Caspase-9 activity detected with the living cell caspase-9 Fluoro-staining kit (magnification, $\times 600$; scale bar: $20\ \mu\text{m}$). (d) Quantitative analysis of caspase-9 activities measured with the caspase-9 activity colorimetric kit. (e) Cleavage of caspase-3 analyzed by western blotting. Data are presented as mean \pm SEM. [#] $P < 0.05$ versus Hcy group; ^{##} $P < 0.01$ versus Hcy group; n.s.: no significance; L-Cth: L-cystathionine.

plasma of patients with severe hyperhomocysteinemia suggests that the abnormal vascular function caused by high homocysteine level is not only due to the loss of NO bioavailability but also associated with VEC apoptosis. Studies have shown that pathologically relevant levels of homocysteine can induce apoptosis of cultured endothelial cells by regulating endoplasmic reticulum stress and unfolded protein responses [21]. In order to treat hyperhomocysteinemia, in addition to supplementing group B vitamins, a large number of studies have been carried out. Wei et al. found that hydrogen sulfide attenuated Hcy-induced cardiomyocytic endoplasmic reticulum stress

in rats [22]. Liu et al. found that epigallocatechin gallate (EGCG) inhibited vascular endothelial cell apoptosis by regulating the PI3K/Akt/eNOS signaling pathway [23]. Jin et al. found that paclitaxel inhibited endoplasmic reticulum stress and endothelial cell apoptosis by regulating Nrf2-dependent HO-1 expression [24]. However, up to now, there has no effective medication for vascular damage caused by hyperhomocysteinemia. L-cystathionine is a key intermediate in the sulfur transformation process [25]. So far, we know little about the biological effects of L-cystathionine. Preliminary studies suggested that L-cystathionine might have protective effects in many aspects,

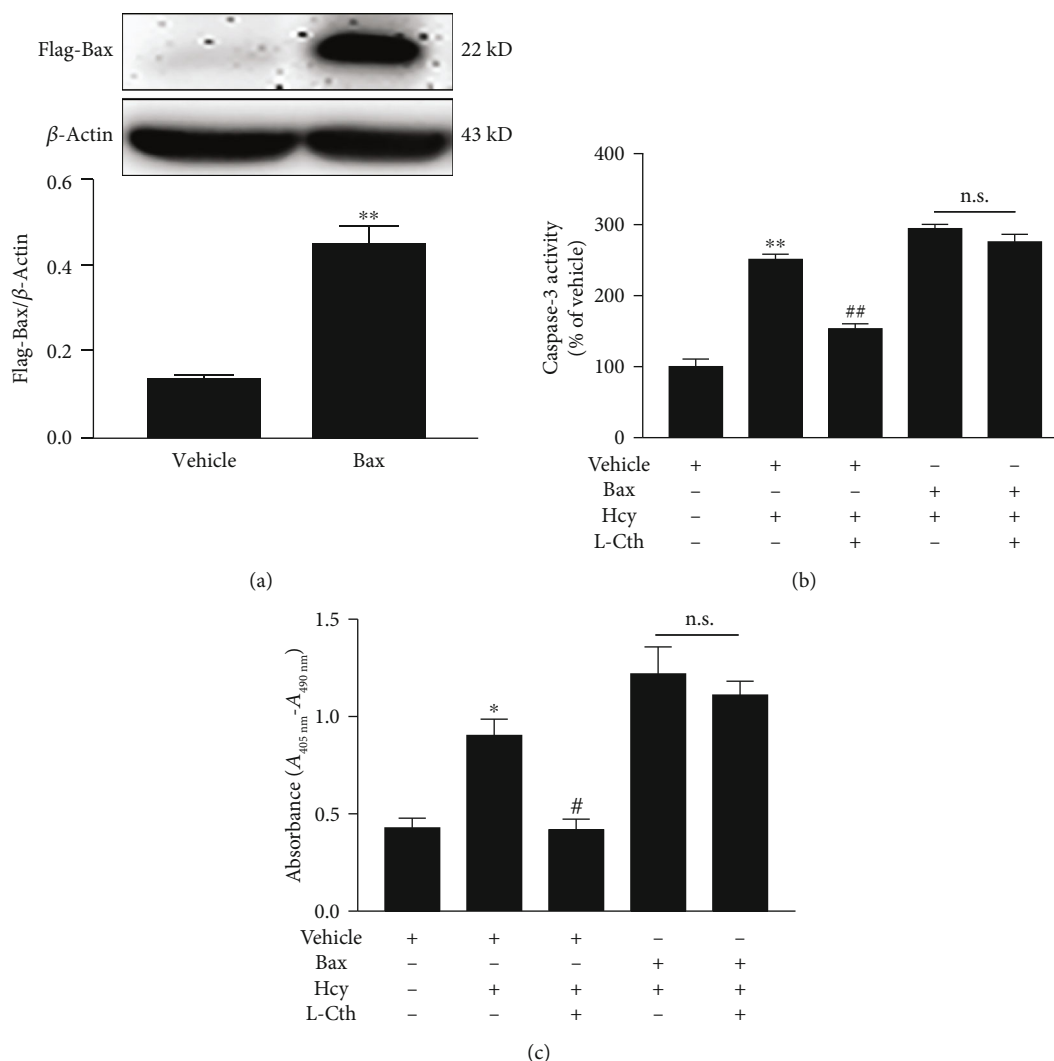


FIGURE 8: Effect of L-Cth on caspase-3 activity and apoptosis in Hcy-treated HUVECs when Bax is overexpressed. (a) Bax overexpression in HUVECs detected by western blotting. (b) Quantitative analysis of caspase-3 activities measured with the caspase-3 activity colorimetric kit. (c) Apoptosis of HUVECs measured with the Cell Death Detection ELISA^{PLUS} Kit. Data are presented as mean \pm SEM. * $P < 0.05$ versus control group; ** $P < 0.01$ versus control group; # $P < 0.05$ versus Hcy group; ## $P < 0.01$ versus Hcy group; n.s.: no significance; L-Cth: L-cystathionine.

including significantly reducing superoxide anion produced by human leukocytes and preventing hepatic steatosis and acute tubular necrosis caused by endoplasmic reticulum stress [26, 27]. It can also reduce the apoptosis of U937 cells and HepG2 cells by inhibiting the excretion of glutathione [28]. It is noteworthy that L-cystathionine inhibits the macrophage apoptosis induced by ox-LDL [29]. Therefore, we speculated that L-cystathionine may protect against vascular damage caused by Hcy. In our studies, we first found that L-cystathionine antagonized homocysteine-induced mitochondria-dependent apoptosis of vascular endothelial cells. It is of great significance in the understanding of the interaction among the metabolites in the methionine metabolic pathway in keeping the vascular homeostasis and providing a novel approach for the prevention and therapy of apoptosis-related cardiovascular diseases.

Firstly, we evaluated the cytotoxicity of Hcy in HUVECs by measuring cell viability and LDH release. Results showed that the treatment of HUVECs with 500 and 1000 $\mu\text{mol/L}$ Hcy significantly suppressed the cell viability and increased the leakage of LDH. Therefore, we selected 500 $\mu\text{mol/L}$ Hcy as a working concentration to investigate whether L-cystathionine has protective effects on Hcy-induced HUVEC injury. We used the concentrations of L-cystathionine with reference to the previous studies [12, 26–29]. We found that 0.3 mM and 1 mM L-cystathionine significantly increased cell viability and inhibited LDH leakage and apoptosis induced by Hcy in HUVECs. Caspase-3 is an apoptosis performer in cells [30]. When cells are exposed to apoptotic stimuli, caspase-3 can be activated by the mitochondria-mediated caspase activation pathway to form cleaved caspase-3 which in turn causes apoptosis. Our experiments showed that Hcy

treatment increased cleaved caspase-3 expression, while L-cystathionine reduced cleaved caspase-3 expression. All of the above results demonstrated that L-cystathionine antagonized Hcy-induced apoptosis in HUVECs.

There are many ways mediating apoptosis, and the mitochondria-mediated apoptotic pathway is the classical one. However, it is still unclear whether L-cystathionine acts through the mitochondrial apoptotic pathway. Considering that mitochondria are one of the main sites producing oxygen free radicals, abnormalities in the structure and function of mitochondria would lead to an increase in oxygen free radical generation and a decrease in removal. Previous studies have shown that Hcy increases mitochondrial oxygen free radical production, while excessive oxygen free radicals can activate mitochondria-mediated apoptosis. Therefore, we designed experiments to study the impact of L-cystathionine on the production of mitochondrial oxygen free radicals. The results indicated that L-cystathionine inhibited the production of mitochondrial oxygen free radicals caused by Hcy. Studies have shown that caspase-9 is an apoptotic promoter on the mitochondrial apoptotic pathway, which can activate caspase-3 [31]. Therefore, we detected the activation of caspase-9 by colorimetry and the fluorescence assay. The results showed that L-cystathionine inhibited the activation of caspase-9 induced by Hcy. Previous studies have shown that DNA-damaging agents activate the mitochondrial apoptotic pathway by inducing the release of cytc. Cytc, a peripheral protein of the mitochondrial inner membrane, functions as an electron shuttle. Once released into the cytosol, cytc would cause the activation of caspase-9 [32]. We used immunofluorescence to detect the leakage of cytc. The results showed that the release of cytc to the cytoplasm was increased under the exposure to Hcy, and interestingly, the leakage of cytc to the cytoplasm was significantly reduced after the administration of L-cystathionine.

The mechanism by which L-cystathionine inhibits the leakage of cytc is unclear. Stabilization of mitochondrial membrane potential is essential for maintaining mitochondrial function. A decrease in mitochondrial membrane potential implies that the cell is in the early stages of apoptosis, meanwhile cytc in the mitochondria leaks out into the cytoplasm [33]. Thus, we examined the changes in mitochondrial membrane potential and found that L-cystathionine antagonized the decrease in mitochondrial membrane potential induced by Hcy and maintained the stability of mitochondrial membrane potential. Studies showed that in association with a decrease in mitochondrial transmembrane potential, excessive reactive oxygen species-(ROS-) triggered apoptosis is mediated by MPTP [34]. MPTP is composed of a variety of protein molecules existing between the mitochondrial inner and outer membranes and is a nonspecific channel whose molecular composition has not been fully studied [35]. Under physiological conditions, MPTP is periodically opened, nonselectively allowing water and small molecules to pass through, maintaining the electrochemical balance in the mitochondria, while protons can freely pass through the mitochondrial inner membrane, causing a potential difference inside and outside the mitochondria to form a stable mitochondrial membrane potential

[36]. Therefore, we examined the opening of MPTP and found that Hcy did increase the opening of MPTP, while L-cystathionine inhibited the opening of MPTP.

Studies have shown that the opening and closing of MPTP are closely related to the concentration ratio of Bcl-2 and Bax on the outer membrane of the mitochondria. Both Bcl-2 and Bax belong to the Bcl-2 family and are often expressed in tissue cells. Bcl-2 is an antiapoptotic protein. Bax is a proapoptotic protein, and some scientists even refer to the ratio of the two as an “apoptosis switch” [37]. The decreased Bcl-2/Bax ratio promotes MPTP opening, leading to apoptosis [38]. We examined the effects of L-cystathionine on Bcl-2 and Bax. Results showed that L-cystathionine inhibited the expression of Bax protein, increased the ratio of Bcl-2/Bax, and inhibited the translocation of Bax to mitochondria, thereby antagonizing apoptosis. These results demonstrated that L-cystathionine antagonized the apoptosis of vascular endothelial cells induced by Hcy by regulating the mitochondrial apoptosis pathway.

To examine if L-cystathionine inhibited Hcy-induced apoptosis of vascular endothelial cells by targeting the Bax pathway, we used Bax agonist and Bax overexpression, respectively, in the experiment. Results showed that BTSA1 or overexpression of Bax successfully prevented the inhibitory effect of L-cystathionine on the Hcy-induced opening of MPTP and the activation of caspase-3 and caspase-9. Bax agonist or Bax overexpression subsequently blocked the inhibition of L-cystathionine on Hcy-induced apoptosis in HUVECs as well. The above facts demonstrated that L-cystathionine antagonized vascular endothelial cell apoptosis by inhibiting the expression of Bax and its translocation to mitochondria.

This study still has some limitations. The molecular mechanism for L-cystathionine-mediated antiapoptosis via the mitochondrial pathway requires further study. In particular, it is necessary to explore the biologic protective role of cystathionine in endothelial injury induced by hyperhomocysteinemia in animal models. However, our present studies for the first time showed that L-cystathionine inhibited homocysteine-induced mitochondria-dependent apoptosis of vascular endothelial cells by inhibiting the expression and translocation of Bax, which would be of great value in further exploration of the potential therapeutic targets to protect vascular injury.

Data Availability

The data used to support the findings of this study are available from the corresponding author upon request.

Conflicts of Interest

The authors declare that they have no conflict of interest.

Authors' Contributions

Xiuli Wang conducted most of the experiments, analyzed data, and participated in manuscript writing. Yi Wang, Lulu Zhang, Da Zhang, and Lu Bai performed the experiments.

Wei Kong, Yaqian Huang, Junbao Du, and Chaoshu Tang designed the research, interpreted the results of the experiment, and edited the manuscript. Hongfang Jin designed the experiments, provided the overall guidance, and contributed to manuscript writing.

Acknowledgments

This study was supported by the National Natural Science Foundation of China (81622004, 81921001), Beijing Natural Science Foundation (7171010), the Peking University Clinical Scientist Program (BMU2019LCKXJ001, Beijing), and the Fundamental Research Funds for the Central Universities.

References

- [1] G. J. Hankey and J. W. Eikelboom, "Homocysteine and vascular disease," *The Lancet*, vol. 354, no. 9176, pp. 407–413, 1999.
- [2] L. E. Bautista, I. A. Arenas, A. Peñuela, and L. X. Martínez, "Total plasma homocysteine level and risk of cardiovascular disease: a meta-analysis of prospective cohort studies," *Journal of Clinical Epidemiology*, vol. 55, no. 9, pp. 882–887, 2002.
- [3] C. S. Kim, Y. R. Kim, A. Naqvi et al., "Homocysteine promotes human endothelial cell dysfunction via site-specific epigenetic regulation of p66shc," *Cardiovascular Research*, vol. 92, no. 3, pp. 466–475, 2011.
- [4] A. B. L. de Koning, G. H. Werstuck, J. Zhou, and R. C. Austin, "Hyperhomocysteinemia and its role in the development of atherosclerosis," *Clinical Biochemistry*, vol. 36, no. 6, pp. 431–441, 2003.
- [5] F. Shakerian, M. Hajilooi, B. Naghshtabrizi, and F. Emami, "Plasma homocysteine level and its genotypes as a risk factor for coronary artery disease in patients undergoing coronary angiography," *Journal of Cardiovascular Disease Research*, vol. 3, no. 4, pp. 276–279, 2012.
- [6] Z. Zhang, C. Wei, Y. Zhou et al., "Homocysteine induces apoptosis of human umbilical vein endothelial cells via mitochondrial dysfunction and endoplasmic reticulum stress," *Oxidative Medicine and Cellular Longevity*, vol. 2017, Article ID 5736506, 13 pages, 2017.
- [7] C. M. Albert, N. R. Cook, J. M. Gaziano et al., "Effect of folic acid and B vitamins on risk of cardiovascular events and total mortality among women at high risk for cardiovascular disease: a randomized trial," *JAMA*, vol. 299, no. 17, pp. 2027–2036, 2008.
- [8] M. Ebbing, Ø. Bleie, P. M. Ueland et al., "Mortality and cardiovascular events in patients treated with homocysteine-lowering B vitamins after coronary angiography: a randomized controlled trial," *JAMA*, vol. 300, no. 7, pp. 795–804, 2008.
- [9] E. Lonn, S. Yusuf, M. J. Arnold et al., "Homocysteine lowering with folic acid and B vitamins in vascular disease," *The New England Journal of Medicine*, vol. 354, no. 15, pp. 1567–1577, 2006.
- [10] G. Gaull, J. A. Sturman, and N. C. R. Räihä, "Development of mammalian sulfur metabolism: absence of cystathionase in human fetal tissues," *Pediatric Research*, vol. 6, no. 6, pp. 538–547, 1972.
- [11] Y. Amino and Y. Suzuki, "Synthesis and evaluation of L-cystathionine as a standard for amino acid analysis," *Bioscience, Biotechnology, and Biochemistry*, vol. 81, no. 1, pp. 95–101, 2017.
- [12] M. Zhu, J. du, A. D. Liu et al., "L-Cystathionine inhibits oxidized low density lipoprotein-induced THP-1-derived macrophage inflammatory cytokine monocyte chemoattractant protein-1 generation via the NF- κ B pathway," *Scientific Reports*, vol. 5, no. 1, article 10453, 2015.
- [13] W. Wang, Y. Sun, J. Liu et al., "Protective effect of theaflavins on homocysteine-induced injury in HUVEC cells in vitro," *Journal of Cardiovascular Pharmacology*, vol. 59, no. 5, pp. 434–440, 2012.
- [14] D. E. Reyna, T. P. Garner, A. Lopez et al., "Direct activation of BAX by BTSA1 overcomes apoptosis resistance in acute myeloid leukemia," *Cancer Cell*, vol. 32, no. 4, pp. 490–505.e10, 2017.
- [15] Y. Zong, Y. Huang, S. Chen et al., "Downregulation of endogenous hydrogen sulfide pathway is involved in mitochondrion-related endothelial cell apoptosis induced by high salt," *Oxidative Medicine and Cellular Longevity*, vol. 2015, Article ID 754670, 11 pages, 2015.
- [16] H. Sohn, J. S. Kim, S. J. Shin et al., "Targeting of Mycobacterium tuberculosis heparin-binding hemagglutinin to mitochondria in macrophages," *PLoS Pathogens*, vol. 7, no. 12, article e1002435, 2011.
- [17] A. B. Levine, D. Punihale, and T. B. Levine, "Characterization of the role of nitric oxide and its clinical applications," *Cardiology*, vol. 122, no. 1, pp. 55–68, 2012.
- [18] J. Noireaud and R. Andriantsitohaina, "Recent insights in the paracrine modulation of cardiomyocyte contractility by cardiac endothelial cells," *BioMed Research International*, vol. 2014, Article ID 923805, 10 pages, 2014.
- [19] N. D. Brunetti, G. Salvemini, A. Cuculo et al., "Coronary artery ectasia is related to coronary slow flow and inflammatory activation," *Atherosclerosis*, vol. 233, no. 2, pp. 636–640, 2014.
- [20] G. Luc, J. M. Bard, I. Juhan-Vague et al., "C-reactive protein, interleukin-6, and fibrinogen as predictors of coronary heart disease," *Arteriosclerosis, Thrombosis, and Vascular Biology*, vol. 23, no. 7, pp. 1255–1261, 2003.
- [21] R. C. Austin, S. R. Lentz, and G. H. Werstuck, "Role of hyperhomocysteinemia in endothelial dysfunction and atherothrombotic disease," *Cell Death and Differentiation*, vol. 11, Supplement 1, pp. S56–S64, 2004.
- [22] H. Wei, R. Zhang, H. Jin et al., "Hydrogen sulfide attenuates hyperhomocysteinemia-induced cardiomyocytic endoplasmic reticulum stress in rats," *Antioxidants & Redox Signaling*, vol. 12, no. 9, pp. 1079–1091, 2010.
- [23] S. Liu, Z. Sun, P. Chu et al., "EGCG protects against homocysteine-induced human umbilical vein endothelial cells apoptosis by modulating mitochondrial-dependent apoptotic signaling and PI3K/Akt/eNOS signaling pathways," *Apoptosis*, vol. 22, no. 5, pp. 672–680, 2017.
- [24] J. S. Kil, S. O. Jeong, H. T. Chung, and H. O. Pae, "Piceatannol attenuates homocysteine-induced endoplasmic reticulum stress and endothelial cell damage via heme oxygenase-1 expression," *Amino Acids*, vol. 49, no. 4, pp. 735–745, 2017.
- [25] J. D. Finkelstein and J. J. Martin, "Homocysteine," *The International Journal of Biochemistry & Cell Biology*, vol. 32, no. 4, pp. 385–389, 2000.
- [26] K. Wada, Y. Kamisaki, K. Nakamoto, and T. Itoh, "Effect of cystathionine as a scavenger of superoxide generated from human leukocytes or derived from xanthine oxidase

- in vitro," *European Journal of Pharmacology*, vol. 296, no. 3, pp. 335–340, 1996.
- [27] K. N. Maclean, L. S. Greiner, J. R. Evans et al., "Cystathionine protects against endoplasmic reticulum stress-induced lipid accumulation, tissue injury, and apoptotic cell death," *The Journal of Biological Chemistry*, vol. 287, no. 38, pp. 31994–32005, 2012.
- [28] L. Ghibelli, C. Fanelli, G. Rotilio et al., "Rescue of cells from apoptosis by inhibition of active GSH extrusion," *The FASEB Journal*, vol. 12, no. 6, pp. 479–486, 1998.
- [29] M. Zhu, J. Du, S. Chen et al., "L-Cystathionine inhibits the mitochondria-mediated macrophage apoptosis induced by oxidized low density lipoprotein," *International Journal of Molecular Sciences*, vol. 15, no. 12, pp. 23059–23073, 2014.
- [30] H. H. Park, "Structural features of caspase-activating complexes," *International Journal of Molecular Sciences*, vol. 13, no. 4, pp. 4807–4818, 2012.
- [31] M. L. Wurstle, M. A. Laussmann, and M. Rehm, "The central role of initiator caspase-9 in apoptosis signal transduction and the regulation of its activation and activity on the apoptosome," *Experimental Cell Research*, vol. 318, no. 11, pp. 1213–1220, 2012.
- [32] R. Beesoo, V. Neergheen-Bhujun, R. Bhagooli, and T. Bahorun, "Apoptosis inducing lead compounds isolated from marine organisms of potential relevance in cancer treatment," *Mutation Research*, vol. 768, pp. 84–97, 2014.
- [33] Z. Zhang, L. Zhao, Y. Zhou et al., "Taurine ameliorated homocysteine-induced H9C2 cardiomyocyte apoptosis by modulating endoplasmic reticulum stress," *Apoptosis*, vol. 22, no. 5, pp. 647–661, 2017.
- [34] J. W. Elrod and J. D. Molkenin, "Physiologic functions of cyclophilin D and the mitochondrial permeability transition pore," *Circulation Journal*, vol. 77, no. 5, pp. 1111–1122, 2013.
- [35] N. Mnatsakanyan, G. Beutner, G. A. Porter, K. N. Alavian, and E. A. Jonas, "Physiological roles of the mitochondrial permeability transition pore," *Journal of Bioenergetics and Biomembranes*, vol. 49, no. 1, pp. 13–25, 2017.
- [36] D. R. Green and G. Kroemer, "The pathophysiology of mitochondrial cell death," *Science*, vol. 305, no. 5684, pp. 626–629, 2004.
- [37] J. G. Pastorino, M. Tafani, R. J. Rothman, A. Marcineviciute, J. B. Hoek, and J. L. Farber, "Functional consequences of the sustained or transient activation by Bax of the mitochondrial permeability transition pore," *Journal of Biological Chemistry*, vol. 274, no. 44, pp. 31734–31739, 1999.
- [38] W. R. Schäbitz, C. Sommer, W. Zoder, M. Kiessling, M. Schwaninger, and S. Schwab, "Intravenous brain-derived neurotrophic factor reduces infarct size and counterregulates Bax and bcl-2 expression after temporary focal cerebral ischemia," *Stroke*, vol. 31, no. 9, pp. 2212–2217, 2000.